PERFORMANCE-ORIENTED SYNTAX-DIRECTED SYNTHESIS OF ASYNCHRONOUS CIRCUITS

A thesis submitted to the University of Manchester
for the degree of Doctor of Philosophy
in the Faculty of Engineering and Physical Sciences

2010

By
Luis Tarazona Duarte
School of Computer Science

Contents

Word Count 38592

List of Tables

List of Figures

Abstract

This thesis evaluates the capabilities and limitations of the syntax-directed approach to synthesise high-performance asynchronous systems and proposes a number of optimisations to improve the performance of the synthesised circuits.

The first part of this work explores new methods for improving the performance of asynchronous circuits synthesised from syntax-directed descriptions, targeting handshake circuits and using the Balsa synthesis system as the research framework. This includes investigating description styles and the use of language constructs that result in faster circuits. A number of new peephole optimisations based on the previous observations are also presented.

The second part investigates the performance of a new, token-flow based synthesiser for the Balsa language called *Teak*. A set of optimisations based in circuit transformations and buffering strategies are proposed in order to improve the performance of Teak circuits. These optimisations have been automated and incorporated into the Teak synthesiser.

All optimisations target dual-rail, quasi-delay-insensitive implementations as this is a robust approach that helps to reduce the impact of the timing closure problem within modern fabrication processes variability. The techniques and optimisations presented here has been tested in a set of non-trivial examples including a 32-bit RISC processor.

The use of the proposed techniques result in optimised compositions of handshake circuits and Teak components that generally synthesise into faster circuits.

Declaration

No portion of the work referred to in this thesis has been submitted in support of an application for another degree or qualification of this or any other university or other institute of learning.

Copyright

i. The author of this thesis (including any appendices and/or schedules to this thesis) owns any copyright in it (the "Copyright") and s/he has given The University of Manchester the right to use such Copyright for any administrative, promotional, educational and/or teaching purposes.

ii. Copies of this thesis, either in full or in extracts, may be made only in accordance with the regulations of the John Rylands University Library of Manchester. Details of these regulations may be obtained from the Librarian. This page must form part of any such copies made.

iii. The ownership of any patents, designs, trade marks and any and all other intellectual property rights except for the Copyright (the "Intellectual Property Rights") and any reproductions of copyright works, for example graphs and tables ("Reproductions"), which may be described in this thesis, may not be owned by the author and may be owned by third parties. Such Intellectual Property Rights and Reproductions cannot and must not be made available for use without the prior written permission of the owner(s) of the relevant Intellectual Property Rights and/or Reproductions.

iv. Further information on the conditions under which disclosure, publication and exploitation of this thesis, the Copyright and any Intellectual Property Rights and/or Reproductions described in it may take place is available from the Head of School of Computer Science (or the Vice-President).

Acknowledgements

I would like to express my deep gratitude to my parents Nelly and Luis for all the love and support they have always given me. My life has been blessed by having them as my parents. Thanks to all my brothers and sisters, nieces and nephews for their support and their love. I have been missing you all a lot.

Thanks to my supervisor Doug Edwards who gave me the opportunity of doing this PhD under his supervision. Thanks to my fine proof readers Andrew Bardsley and Will Toms for all the careful reading and comments done on my writing. I must thank Andrew twice for giving me the opportunity of working with him on his Teak system and having introduced me to the beauties of the Haskell language. Many thanks to Charlie Brej for all his support, nice food, friendship and for doing the final proof read of my thesis. Thanks to Wei Song for kindly allowing me to use his router design. Thanks to Mikel Luján for his advice and support.

My special gratitude to Luis Plana for all his support, advice and encouragement. Many thanks "Luis One". Thanks to the whole Plana Oteiza family for being my family here in Manchester. Thanks to all my friends and families from Barquisimeto, Venezuela, specially to my brother José Ortiz and his family: ¡Gracias José! Thank you dear Emilia for giving me your love and support during all these years.

Thanks to the people I have met in the APT group. I have learnt many things from them. I am sure I will forget many names if I try to list them.

Finally, thanks to the School of Computer Science and EPSRC for the financial support I have received during my PhD.

To my Parents, my nieces and nephews, my brotheres and sisters, and my families from Barquisimeto.

A mis Padres, mis sobrinas y sobrinos, mis hermanas y hermanos, y a mis familias de Barquisimeto.

Chapter 1

Introduction

1.1 Motivation

Asynchronous design has regained interest in recent years due to its potential advantages over its synchronous (clocked) counterpart. Synchronous digital systems, which are the basis of most of today's digital designs, are based on two major assumptions: all signals are binary and time is discrete, defined by the system's clock signal which controls all communication and event sequencing. These assumptions simplify greatly the task of design but also lead to clock distribution and clock skew problems, increased power consumption, coherent electromagnetic emissions and forcing all parts of the circuit to work at the same (worst-case) rate.

Unlike synchronous systems, asynchronous systems do not rely on a global clock signal. Instead, these systems use a form of local communication that comprises *handshake signals* to request (initiate) the start of an operation and acknowledge (indicate) to determine its completion.

Asynchronous circuits have some potential advantages over their synchronous counterparts that make them attractive to use in large VLSI designs. These include: no clock distribution or clock skew problems, better modularity and composability, less coherent electromagnetic emissions, automatic power management, average-case performance and robustness towards variations in supply voltage, temperature and fabrication process parameters [91, 107, 35, 48, 37, 39].

Synchronous design has the advantage of being a mature technology supported

by many commercially available Computer-Aided Design (CAD) tools and implementation alternatives, which cannot be used or provide little support for asynchronous design. The increased interest in asynchronous design has led to the development of several methodologies and CAD tools targeted specifically at asynchronous design. Among these, *Balsa* [5] and *TiDE*™(formerly *Tangram*) [23, 83] are fully-automated systems that have successfully synthesised large-scale circuits using a process called *syntax-directed synthesis*. Although these tools greatly improve the design time for a complex system, there is evidence that shows that this is done at the cost of reduced performance when compared to manual, full-custom design approaches [36, 84, 11]. If the performance penalty imposed by the syntax-directed synthesis could be reduced, then this asynchronous design methodology could be used in performance-demanding, real-world applications. These applications could then benefit from some of the potential advantages of asynchronous circuits.

This thesis explores new methods for improving the performance of asynchronous circuits synthesised using the syntax-directed approach. In this work, the Balsa synthesis system has been used as the research framework. The work includes investigating description styles and language constructs that result in faster circuits, new peephole optimisations based on these observations, and the analysis and optimisation of a novel token-flow implementation for the Balsa language, using a new system called *Teak*, introduced initially in [6]. The synthesis targets dual-rail, quasi-delay-insensitive implementation (QDI – see section 2.5.3) as this is a robust approach that helps to reduce the impact of increasingly difficult timing closure within modern fabrication processes variability.

1.2 Syntax-directed synthesis

The syntax-directed approach to synthesise asynchronous circuits is based in the compilation of descriptions written in a high-level language into a communicating network of pre-designed modules. The compilation process performs a mapping of each language construct into the network of modules that implements it. This mapping gives a high degree of transparency in the design as incremental changes to the specification generates predictable changes in the resulting circuit. This transparency allows the designer to optimise the circuit, in terms of performance,

power or area, at the language level. The compiled network of components constitutes an intermediate representation that can subsequently be expanded into gate netlists.

Currently there exists two fully automated CAD systems that use this approach for the synthesis of asynchronous systems: *Timeless Design Environment* (*TiDE* [23] formerly *Tangram* [10, 8]) a proprietary system developed at Philips Research Laboratories, and *Balsa* [5, 29], an open-source system developed at the University of Manchester that closely follows the Tangram philosophy.

1.2.1 Tangram and TiDE

Tangram uses a CSP-like description language (the language is also called Tangram), but with a syntax more similar to traditional programming languages than CSP. Tangram has been used to successfully develop complex asynchronous chips [39, 105, 58]. The Tangram synthesis system has evolved into *TiDE*, and the new version of the Tangram language is now called *Haste* since the Tangram system began to form part of the product portfolio of *Handshake Solutions* [23].

1.2.2 Balsa

Balsa is an open-source package and is freely available from [4]. The Balsa system is still under development and, from version 3.5.1, incorporates a GUI user interface with facilities such as project management, editor and behavioural graphical simulator. Balsa is the name for both the framework for synthesising asynchronous circuits and the language used to describe such systems. The Balsa language has support for parameterisation and recursive procedures, records and symbolic enumerated types, has greater expressiveness than Tangram and is also more "human readable".

In both Tangram and Balsa approach to syntax-directed synthesis, the resulting communicating network of components interact using *handshake signals*. These networks of *handshake components* are called *handshake circuits*.

1.2.3 Handshake circuits and handshake components

A handshake circuit is a communicating network of handshake components (handshake modules) connected point-to-point using handshake channels (see section 2.3). Each channel connects exactly one *passive port* of a handshake component to an

active port of another handshake component. An *active port* is a port that initiates the communication by sending a request signal to a *passive port*. When ready, the passive port will respond with the acknowledge signal. The handshake can involve the transfer of data or control to synchronise two processes.

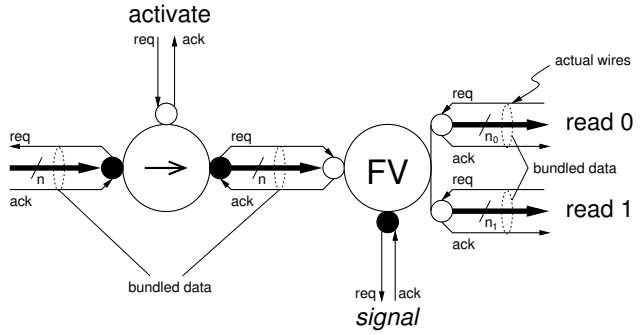

(a) detailed

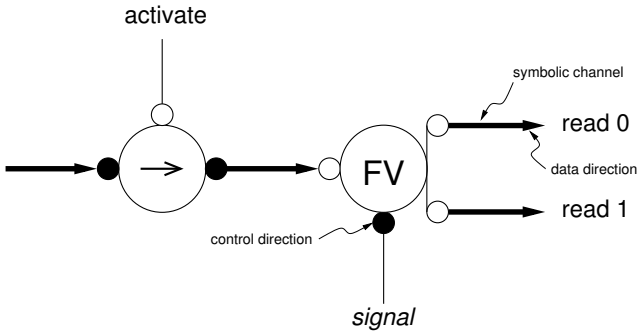

(b) simplified

Figure 1.1: A Handshake Circuit composed of a *Transferrer* ($\rightarrow$) and a *False-Variable* (FV) handshake components.

Figure 1.1(a) shows details of a handshake circuit composed of two handshake components: a *Transferrer* ($\rightarrow$) and a *FalseVariable* (`FV`) component with two read ports. In the figure, the components are represented by larger circles, passive ports by small unfilled circles, and active ports by small filled circles. Data-less control channels are composed of a *req*uest and an *ack*nowledge pair of wires. Data are represented by thick arrows signalling the direction of data. In figure 1.1(a), data wires using binary signalling are bundled together with the *req* and *ack* pair to form a *bundled-data* channel.

Handshake circuits are not normally represented at the level of detail in figure 1.1(a). A simplified diagram as shown in 1.1(b) is preferred, where the channels carrying data are represented as a single arc with an arrowhead signalling the direction of data; the control (synchronisation) channels are represented by single arcs. Control direction is implied by the type of port involved.

The circuit operation is as follows:

i. The circuit starts its operation when a request is made to the *Transferrer* component on its upper (activate) passive port. Upon receiving this, the *Transferrer* issues a request to its environment connected to its active, left port. This left port is an example of a *pull* data channel (data flows from the passive port to the active port). The right port of the *Transferrer* is an example of a *push* data channel (data flows from the active port to the passive port).

ii. Eventually, the environment will respond with the data and the acknowledgement. The *Transferrer* in turn passes it as a request to the *FalseVariable* component at its right.

iii. The *FalseVariable* receives this request and issues a request on its synchronisation *signal* port, indicating that another process can safely read data from the *read* ports until the handshake in the *signal* port has been acknowledged.

iv. The environment connected to the *read* and *signal* ports may read the data zero or more times and when done, sends an acknowledgement on *signal*.

v. After receiving the acknowledgement on *signal*, the *FalseVariable* sends back an acknowledgement to the *Transferrer* which in turn passes it to the *activate* channel.

vi. The environment connected to the activate will eventually remove the request, which in turn causes the *Transferrer* to finish the handshake in its left channel, terminating the transfer. Note that the handshake on the activation port of the *Transferrer encloses* full handshakes on its input and output ports.

As an example of syntax-directed translation into handshake circuits, consider the Balsa specification for a simple 1-place buffer (register) shown in figure 1.2(a).

The specification is parameterised in the type of data the register can hold. The register has an input channel `inp` and an output channel `out`. The variable `v` stores the data and the operation consists of an infinite repetition (`loop`) of two actions: transfer of data (`<-`) from channel `inp` into `v` sequenced (`;`) with the transfer (`->`) of data stored in `v` to the channel `out`.

```
procedure buffer
(
  parameter DataType : type;
  input inp  : DataType;
  output out : DataType
) is
  variable v : Datatype
begin
    loop
        inp -> v
        ;
        out <- v
    end
end
```

(a)

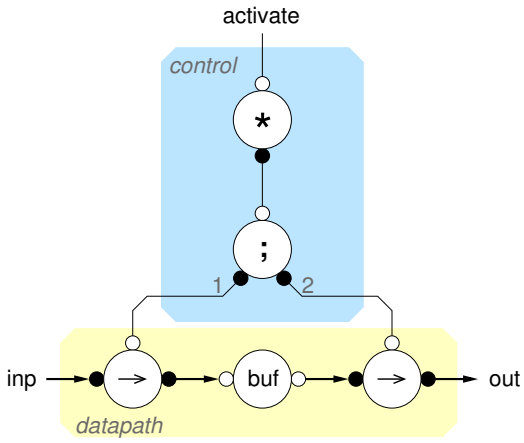

(b)

Figure 1.2: 1-place buffer: (*a*) Balsa description, (*b*) handshake circuit.

Figure 1.2(b) shows the handshake circuit generated by Balsa from the code in 1.2(a). A *Transferrer* component (→) connects the input channel to the write port of the *Variable* component (`v`) that acts as the variable `v` of the description. The read port of `v` is connected to the output using a second *Transferrer*. A *Sequencer* (`;`) is used to sequence the writing to and the reading from `v`, and a *Loop* (∗)component activates the *Sequencer* repeatedly. Given that many handshake components have simple implementations (for instance, a *Transferrer* can be implemented using only wires and the *Loop* using a NOR gate), the resulting synthesised circuit is not complex.

1.3 Optimising handshake circuits

As stated before, the syntax-directed syntax paradigm is attractive in terms of flexibility and compilation simplicity, but these come at the cost of low to moderate performance. In general, Balsa/Tangram translation generates a datapath section together with a control tree which mirrors the control flow of the language description as shown in figure 1.2(a). For this reason, the translation is

also described as *control-driven*. The overhead of this control-driven approach has been identified as one of the major causes of performance penalty in handshake circuits.

Previous work in handshake circuits optimisation include peephole optimisations [83], more concurrent designs for handshake components [85] and control resynthesis [19, 33]. The following sections introduce recent work on the optimisation of handshake circuits.

1.3.1 *Push* data-driven handshake circuits

In an attempt to reduce this penalty, Taylor [100] introduced a novel *data-driven* circuit style, together with a new description language and compiler, which produced significant performance increases in the synthesised circuits compared to those generated by conventional Balsa/Tangram. This approach is based on reducing the control overhead by using the following techniques:

- all control is activated in parallel.
- sequencing is localised to storage elements (variables). This ensures that storage elements are not concurrently read and written and allows the read and write sections of control to operate in parallel.
- data processing makes use of push-only structures and operations are speculatively executed to allow control and data sections to operate in parallel.

The techniques above are enforced by a more restrictive description language syntax. In particular, variables have a write-once, read-once behaviour, which means that they must be read every time they are written and they must be written before they can be read. Also, conditional multicasting of a channel value is replaced by speculative broadcasting to all possible destinations together with a rejection mechanism to discard unwanted data at the places where the condition states that data is not required. These and other restrictions make the generation of very small, localised control trees, possibly reducing the control overhead and improving performance. However, this is done at the expense of significantly larger area, energy use and reduced flexibility at the description level.

1.3.2 Automated source-to-source transformations

In [47] Hansen and Singh describe a series of automated "source-to-source" transformations that optimises syntax-directed descriptions using a variety of concurrency enhancing optimisations. Although considerable speed-ups are claimed, some of the examples used start with extremely naïve code sequences, so it is easy to obtain significant improvements. Also, their proposed approach is limited to *slack elastic* [64] systems descriptions only (a slack elastic system preserves correct operation even if extra pipeline buffer stages are introduced in any channel). This limitation reduces the usefulness of an "automated" approach as it is frequently necessary for the designer to understand the nature of the transformations to ensure they are safe, which may represent a considerable extra design effort to the user.

1.3.3 Behavioural synthesis of asynchronous circuits

In another recent work, Nielsen et al. [75, 76] presented a method for automatic behavioural synthesis of asynchronous circuits using syntax-directed translation as backend. The initial development was based on the Balsa framework but the final automated tool targets the Haste/TiDE design flow. Input to the tool is a behavioural description in the Haste language (both Haste and Balsa are behavioural languages). From this description, the tool extracts a *Control Data Flow Graph*, *CDFG* [1] (a directed graph that does not contain cycles and in which a node can be either an operation node or a control node and edges carry data and reflect dependencies between computations).

The CDFG representation of the original description is then used as the input to the behavioural synthesis which performs *scheduling* (time slot allocation), *allocation* (finding the minimum required hardware resources) and *binding* (mapping of operators and variables into the different resources available). The behavioural synthesis targets an architecture consisting of a datapath and a controller, similar to that used in synchronous synthesis but the architecture is constructed entirely from asynchronous handshake components. The final step is the mapping of the generated architecture into a new optimised Haste description. The overall effect is a source-to-source translation of the original description guided by either minimum area (by limiting the available resources) or minimum latency constraints. An interesting feature of this approach is the possibility of

performing constraint-driven automated design-space exploration.

Average area reductions of 30% and average speed-ups of 40% are reported when applied to a series of digital filter designs. However, it is also reported in [75] that "the origin of this large improvement lies in the fact that the source code is written for *code maintainability*, which is usually far from the optimal execution of operations". In common with the previous approach, the quality of the input description will influence the results of the optimisations.

1.4 Teak

Teak[6] is a data-driven implementation for the Balsa language, which uses a new target component set and synthesis scheme. Teak replaces the data-less activation channel (used to enclose the behaviour of description fragments in handshake circuits synthesis) with separate *go* and *done* channels. Control/datapath interactions using components which exploit signal-level event interleaving are replaced by the forking/rendezvous of control and data channels with local handshaking to complete control interactions. This separation of *go* and *done* makes Teak much more like the Macromodules system [93] than Handshake Circuits, albeit with more flexibility in the elimination of control channels through merging with data channels. Explicit buffering is used to decouple one component from another and to introduce the desired degree of token storage to enable the circuit to function and, looking beyond this work, to allow more transforming synthesis methods to increase circuit parallelism.

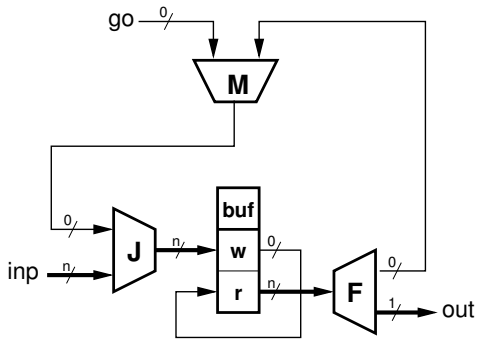

Figure 1.3: Teak circuit for the 1-place buffer.

Figure 1.3 shows the *buffer* example in 1.2 constructed from Teak components. Notice that, rather than a composition of enclosing control components the *Loop*

... *end* construct has become a loop comprised of a *Merge* (M) to introduce the 'go' token, a *Join* (J) to meet incoming data, and a *Fork* (F) to return a token back around the loop after the output command. The aim of Teak is to provide a path for future performance increases in Balsa by exploiting high performance pipelined asynchronous circuit styles. More details on the Teak system will be introduced in chapter 5.

1.5 Aims of this research

The aim of this research is to explore new alternatives to increase the performance of synthesised circuits using the syntax-directed synthesis paradigm. This work targets dual-rail, quasi-delay-insensitive implementation as this is a robust approach that helps to reduce the impact of increasingly difficult timing closure within modern fabrication processes variability [14, 52].

Having a highly expressive, high-level description language like Balsa or Haste can result in naïve, poor performance descriptions for a novice or even a medium-experienced designer due to the directness of the synthesis method. Furthermore, it is always claimed that in this approach, an experienced designer could make performance/power/area trade-offs. This task would be easier if the designer could have some insight of the impact of a particular construct or coding style.

In contrast with other optimisation approaches, the approach used in the first part of this work is to help the designer select a coding style that results in more concurrent, faster implementations, while providing insight about the trade-offs made. The coding techniques presented here could also serve as a source for future optimising compilers. This work also explores further optimisations on circuits synthesised from highly optimised Balsa code and proposes some circuit transformations and new peephole optimisations that help to increase further the benefits of the performance-oriented coding style.

The second part of this work analyses the circuits generated by the new data-driven based Teak synthesis scheme as a more flexible alternative to implement data-driven circuits. A set of optimisations based on circuit transformations and buffering strategies are proposed in order to improve the performance of Teak circuits. These optimisations have been automated and incorporated into the Teak synthesiser.

The increase on performance of the above mentioned techniques and optimisations are demonstrated using substantial Balsa designs written by both novice and experienced users. The examples include a 32-bit RISC processor, a forwarding unit for this processor, a 32-bit Booth's multiplier, a Viterbi decoder and a wormhole router. Although area and power are not considered as an optimisation target, area/power savings or penalties are shown for the evaluated examples and proposed optimisations.

1.6 Contribution of this research

The research work presented in this thesis contributes to the field of synthesis of asynchronous circuits in several aspects, including:

- An evaluation of the synthesis of high-performance asynchronous systems using the syntax-directed synthesis approach targeting handshake circuits.
- Performance-oriented language techniques that can be used to describe asynchronous systems within a syntax-directed synthesis framework and their evaluation. These techniques can also serve as the basis for developing optimising syntax-directed compilers targeting handshake circuits.
- New performance-oriented handshake circuits peephole optimisations and their evaluation.
- An evaluation of the performance of the new Teak synthesis system and a set of automated circuit optimisation rules that increase the performance of the Teak-generated circuits.
- An automated set of rules to implement latch insertion in the Teak synthesis system.
- The evaluation of a number of substantial examples using the techniques developed during the course of this research and that can be used as reference for future research.

1.7 Thesis organisation

This thesis is organised as follows:

Chapter 2 presents an overview of the asynchronous design methodologies including commonly used handshake protocols, synthesis of QDI datapaths, synthesis of control circuits and major asynchronous synthesis tools.

Chapter 3 presents an introduction to the Balsa Synthesis System and the Balsa language.

Chapter 4 introduces and analyses a set of description-level performance-oriented techniques for the Balsa language, which target handshake circuits synthesis. A number of new peephole optimisations that increase the performance of the synthesised circuits are presented.

Chapter 5 introduces the Teak synthesis system and component set, together with a number of circuit-level optimisations that have been incorporated in the Teak synthesis tools. This chapter also discusses the impact of description-level styles in the performance of the Teak-synthesised circuits.

Chapter 6 introduces a range of latching strategies currently implemented in the Teak system. An analysis on the complexity of the latching strategies and resulting performance is also presented.

Chapter 7 describes a number of design examples that have been developed to evaluate the impact on performance of the techniques proposed in this research. Simulation results of these examples for both Balsa an Teak styles are presented and discussed.

Chapter 8 present the conclusions and summary of this research work and discusses future work.

1.8 Publications

During the course of this research, the author has contributed to the following papers:

[97] Luis Tarazona, Doug Edwards, Andrew Bardsley and Luis Plana. Description-level optimisation of synthesisable asynchronous circuits. To be published in *Proceedings of 13 Euromicro Conference on Digital System Design (DSD)*, September 2010.

[96] Luis Tarazona, Doug Edwards and Luis Plana. A Synthesisable quasi-delay insensitive result forwarding unit for an asynchronous processor. *In Proceedings of 12 Euromicro Conference on Digital System Design (DSD)*, pages

627–634, August 2009.

[6] Andrew Bardsley, Luis Tarazona and Doug Edwards. Teak: a token flow implementation for the Balsa language. In: *Proceedings of International Conference on Application of Concurrency to System Design (ACSD)*, pages 23–31, July 2009.

Luis Tarazona and Doug Edwards. Performance-oriented peephole optimisation of Balsa dual-rail circuits. In *Twentieth UK Asynchronous Forum*, September 2008.

[102] Sam Taylor, Doug Edwards, Luis A. Plana and Luis A. Tarazona D. Asynchronous data-driven circuit synthesis. In IEEE Transactions on Very Large Scale Integration (VLSI) Systems, Volume 18, number 7, pages 1093–1106, July 2010.

L. A. Tarazona and D. A. Edwards. A result forwarding unit for a synthesisable asynchronous processor. In *Twentieth UK Asynchronous Forum*, September 2008.

L. A. Tarazona, L. A. Plana, and D. A. Edwards. Architecture enhancements for a synthesised self-timed processor. In *Nineteenth UK Asynchronous Forum*, pages September 2007.

[85] L.A. Plana, D. Edwards, S. Taylor, L. Tarazona, and A. Bardsley. Performance-driven syntax directed synthesis of asynchronous processors. In *Proceedings of International Conference on Compilers,Architecture & Synthesis for Embedded Systems (CASES)*, pages 43–47, September 2007.

Chapter 2

Background

2.1 Introduction

This chapter presents an overview of basic concepts of asynchronous digital circuits and the most common handshake protocols used in asynchronous design. The chapter also introduces the various delay models used in the design of asynchronous circuits and the concepts of indication, speed-independency, delay insensitivity and quasi-delay insensitivity (QDI). Finally, the chapter presents an overview of the tools and methodologies most commonly used for the synthesis of asynchronous circuits.

2.2 Asynchronous Circuits

Asynchronous systems do not rely on a global clock signal to control communications and event sequencing. Instead, communication between two asynchronous components is implemented as a *handshake protocol* using *handshake signals* to request (initiate) the start of an operation and acknowledge (indicate) to determine its completion.

There are several properties of asynchronous circuits that make them attractive to use in large VLSI designs, including:

- *No clock distribution or clock skew problems:* It is well known that distributing a clock across the chip whilst both minimising the area, power used and the skew between clock arrival at different points of the system is one of the major problems in synchronous design. Eliminating the global

clock signal, automatically eliminates these problems.

- *Better modularity and composability:* As communication between modules depends only on the handshake interface compatibility and not on global timing constraints, modules can be reused and composed as long as their interfaces are compatible [66, 71, 8]. This can be very attractive to modern System On Chip (SoC) and reconfigurable processors.

- *Lower electromagnetic interference (EMI):* Synchronous circuits switch at fixed frequencies, generating a spectrum with relatively higher localised energy at multiples of the clock. Asynchronous circuits only switch during information exchange and the local switching frequency is less coherent, generating a broader emissions spectrum [11, 79, 9].

- *Lower power consumption:* In synchronous circuits, the clock global clock forces to switch all latching stages, unless complex clock gating circuitry is added to enable clocking only to stages where useful work is done. In asynchronous circuits, switching occurs only where the circuits are computing, there is no power wastage in unnecessary switching if the circuits are idle [9, 74].

- *Average-case performance:* In a clocked system, the clock period of the system is dictated by the slowest unit, hence the system operates at worst-case. In asynchronous circuits each unit operates at its own speed, giving the possibility of average-case operation [69, 113].

- *Robustness towards variations in supply voltage, temperature and fabrication process parameters:* In asynchronous circuits, the circuit can be insensitive to wires and gates delays, apart from some localised and easy to meet delay assumptions, reducing the effect of variations on the correct operation of the circuit [68, 74]. Variability has become a major issue in modern fabrication technologies and quasi-delay insensitive asynchronous circuits (see section 2.5.3) are being seen as an attractive solution to this problem.

However, asynchronous design has also some disadvantages, which include:

- *Increased area and circuit complexity:* In order to provide the local handshaking, it is necessary to add circuitry to each asynchronous module. The

solutions to this problem translate into area, power and performance overheads. In contrast, synchronous circuits just use the global clock as the communications control.

- *Lack of design tools:* Modern VLSI circuits cannot be designed without the support of CAD tools for the synthesis, simulation, testing and validation processes. Synchronous design is a mature methodology fully supported by industry CAD tools which have little or no support for asynchronous methodologies. Only recently has TiDE™ [23], a fully-automated commercial tool for asynchronous design with capabilities similar to those present in synchronous tools, been made available. There are also some academic tools like Balsa (freely available) and CAST (not available outside Caltech), but in general they are still far from the maturity and industrial acceptance of today's synchronous tools.

- *Learning curve:* Designers used to thinking "synchronously" will need to learn an arguably more difficult design methodology in order to exploit the benefits of asynchronous design. The lockstep, deterministic behaviour of synchronous designs is simpler to understand than the concurrent, non-deterministic behaviour of true asynchronous circuits.

2.3 Handshake protocols and data encoding

In circuits that communicate using handshake channels (composed of handshake signals), the unit that initiates (requests) the communication is called the *active* party and the unit that responds is referred to as the *passive* party. If, as in figure 2.1(a), the sender of data is the active party the channel is called a *push channel*. In figure 2.1(b) it is the receiver who initiates the communication and this channel is called a *pull channel*. In abstract diagrams, it is common to identify the active end of a channel using a black dot.

There are several common asynchronous handshake protocols named according to the encoding used for handshake and data signals. This section describes the most common of them.

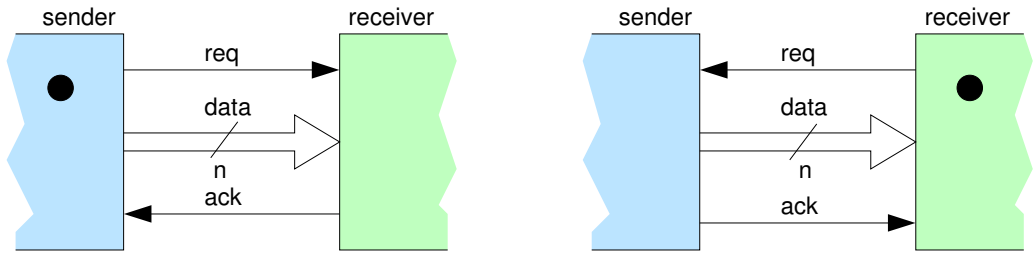

(a) push channel *(b) pull channel*

Figure 2.1: Bundled-data channels.

2.3.1 Bundled-data protocols

In bundled-data protocols there are separate wires for *req* and *ack* signals which are *bundled* with binary data wires to form the channel, as shown in figure 2.1. Because in this protocol data is encoded using one wire per bit, it is also called *single-rail*.

Two-phase bundled-data

Figure 2.2 shows a timing diagram of a two-phase bundled-data handshake protocol. The active party initiates the *handshaking* phase by transitioning the *req* signal. The other party terminates the handshake by transitioning the *ack* signal and takes the channel to the *quiescent* (idle) phase and data becomes invalid until a new request is generated by the active party. In the figure, invalid data is shown as hashed lines and implicit signal causality is shown with dashed lines. This implicit signal ordering must be enforced in bundled-data circuits by using *delay matching*. Two-phase protocols are also known as Non-Return-to-Zero (NRZ) protocols.

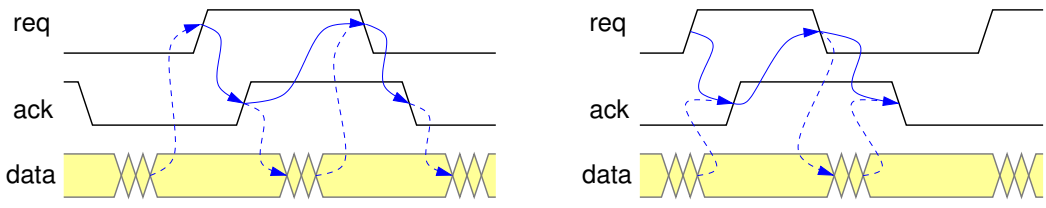

(a) push channel *(b) pull channel*

Figure 2.2: Two-phase bundled-data protocol.

Two-phase protocols are very efficient in time because there are no redundant phases, but normally require more complex circuits to implement than the four-phase protocol described in next section. The overhead due to the circuits' complexity often reduces the advantages of not having redundant phases.

Four-phase bundled-data

In four-phase protocols, the request and acknowledge signals are level-encoded. Figure 2.3(a) shows a timing diagram for a push channel using a four-phase protocol. In this example, the active party first issues the data and then initiates the handshake by setting the *req* signal high. The passive acknowledge the data by setting *ack* high. Upon receiving the acknowledge, the active party returns the *req* signal to zero. finally, the receiver detects the return to zero of *req* and acknowledges this by taking *ack* low, allowing a new handshake to start.

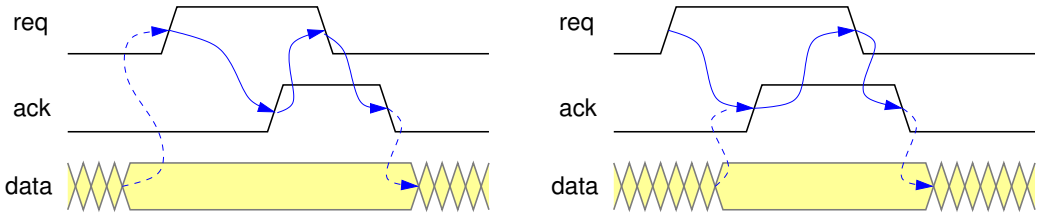

(a) push channel *(b) pull channel*

Figure 2.3: Four-phase bundled-data protocol.

Due to presence of the return to zero phases these protocols are also known as Return-To-Zero (RTZ) protocols. Depending on the interval that valid data is available there are a number of different data-valid conventions for this protocol [83]. Figure 2.4 shows the data-valid schemes for a push channel. In the figure, the *early* data scheme uses $req \uparrow$ as the data validity event and $ack \uparrow$ as the data release event. The *broad* scheme uses $req \uparrow$ as data-valid and $ack \downarrow$ as data-release. In the *late* scheme, $req \downarrow$ is the data-valid signal and $ack \downarrow$ is the data-release.

For a pull channel, figure 2.5 shows that the *early* data scheme uses $ack \uparrow$ as the data validity signal and $req \downarrow$ as the data release signal. The *broad* scheme uses $ack \uparrow$ as data-valid and $req \uparrow$ (of the next handshake) as data-release. In the *late* scheme, $ack \downarrow$ is the data-valid signal and $req \uparrow$ of the next handshake is the data-release. Analysis and comments on the advantages and disadvantages of each of these schemes when used in real systems can be found in [83, 5, 17].

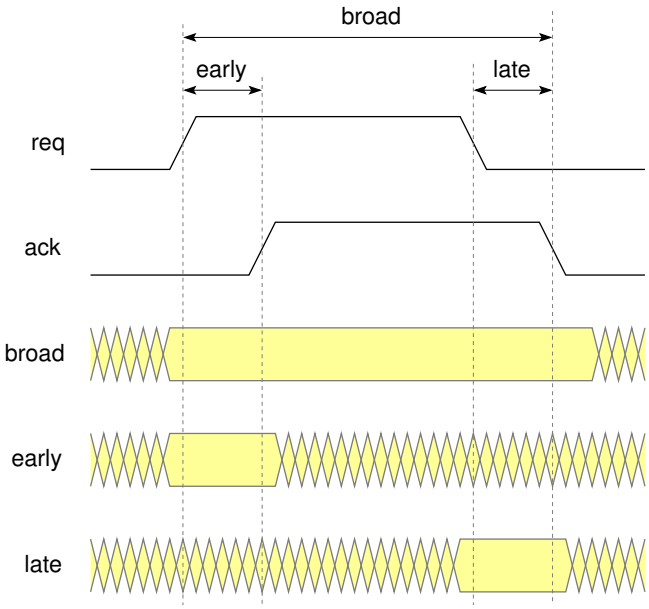

Figure 2.4: Four-phase data-validity schemes for a *push* channel.

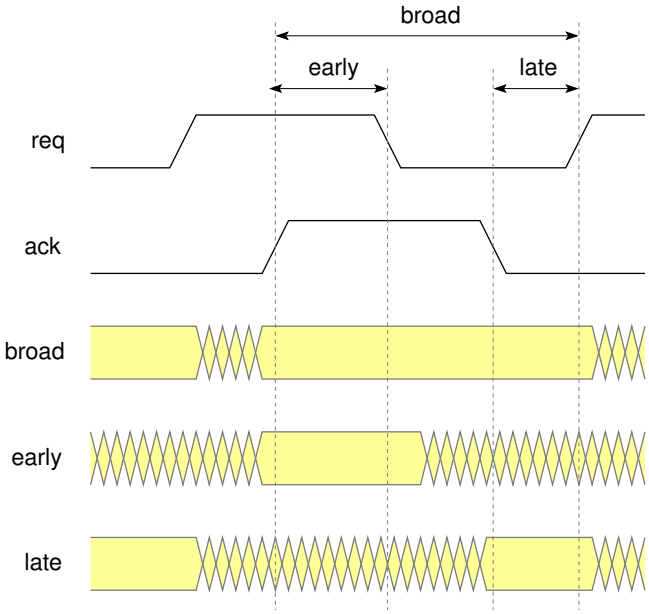

Figure 2.5: Four-phase data-validity schemes for a *pull* channel.

Compared to two-phase bundle-data protocols, four-phase bundled-data protocols have the advantage of using simpler circuits which result in smaller and faster designs, despite requiring more transitions per handshake (which results in more energy consumption).

Delay matching

Bundled-data protocols rely on the timing assumption that the order of events in the sender is preserved at the receiver. For instance, in a push channel data must always be valid before $req \uparrow$. Delays in control and data wires must be matched adequately to make sure that the order of events is preserved at the sender and receiver ends. For instance, in the protocol diagram of figure 2.3, valid data must precede the *req* signal in order to guarantee correct operation. This implicit causality is showed with dotted lines in figures 2.2 and 2.3.

A physical implementation of a circuit that uses these protocols must take this into account to avoid operational failures. Controlled placement and routing of wires, buffer insertion to adjust delays, and use of safety margins at the receiver's end, are possible solutions to this problem. These timing closure problems are similar to those in synchronous circuits, making bundled-data protocols unattractive to use with deep sub-micron fabrication processes affected by large variability in the parameters of the transistors. An alternative to these is to use a more robust class of protocols that are insensitive to wire delays, such as the *dual-rail protocols*.

2.3.2 Dual-rail protocols

These protocols make use of the *dual-rail* code to transmit both data and data validity indication on the same set of wires, eliminating the timing assumptions. The dual-rail code is a member of the family of *delay-insensitive codes* [110]. This encoding method allows a reliable communication between two parties regardless of the delay in the wires.

Dual-rail code

In a dual-rail code the data is encoded using two wires per bit, $d.t$ for signalling a logic 1 (*true*) and $d.f$ for signalling a logic 0 (*false*). The pair of wires $\{d.t, d.f\}$ form a code whose codewords are shown in table 2.1.

$d.t$	$d.f$	meaning
0	0	Empty
0	1	Valid "0"
1	0	Valid "1"
1	1	Not used

Table 2.1: Dual-rail encoding for 1-bit

This encoding scheme can be easily extended to an n-bit channel. An n-bit channel is formed by concatenating n bits coded in dual-rail as above. For a codeword to be valid, *every* pair of wires must hold a valid code. Similarly, the *empty* codeword (also referred to as *spacer* or *NULL*) occurs when all bit pairs contain the empty code. In this way, when data changes from empty to valid (or vice versa) no intermediate value is valid. This property makes dual-rail encoding a more robust option that helps to reduce the impact of the timing closure problem caused by process variability, despite the fact of using more wires. The price to be paid for this advantage is some extra complexity, area, energy and performance penalties (see section 2.5.3).

The four-phase dual-rail protocol

In this protocol either the request signal and data (push channel) or the acknowledge signal and data (pull channel) are encoded together using the dual-rail code. Figure 2.6 shows a 1-bit push channel using the four-phase dual-rail protocol.

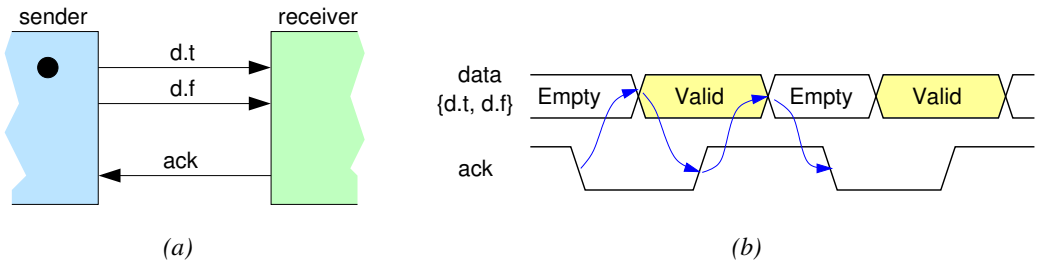

Figure 2.6: Four-phase dual-rail protocol. (a) *push* channel, (b) timing diagram.

Assuming that initially all signals are *low*, request is indicated by issuing a valid codeword on the data wires. Before another request can be made, the data wires must assume the empty value. The receiver identifies that data is valid when *all* bit pairs have become valid, then reads the data and issues *ack* $\uparrow$. The sender detects the acknowledgement and changes the bits to the empty state .

The receiver then identifies when all the bits have become empty and responds with $ack \downarrow$, allowing the sender initiate a new handshake. Figure 2.7 shows a simplified timing diagram of this operation for an n-bit push channel.

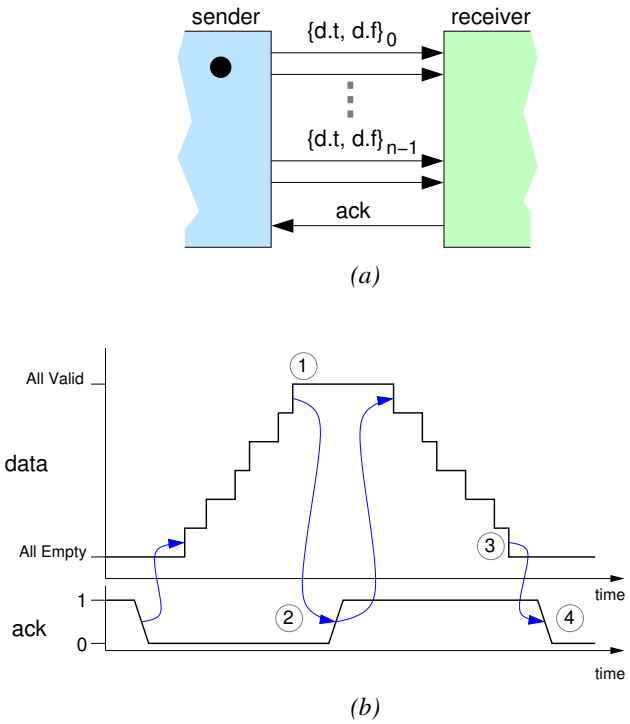

Figure 2.7: n-bit four-phase dual-rail protocol in a push channel.

The Two-phase dual-rail protocol

This protocol also uses two wires per bit but the information is encoded as transitions instead of logic levels. On an n-bit channel, a new codeword is received when exactly one wire per bit has made a transition. In this case there is no empty value: a valid codeword is acknowledged and the sender can change one wire per bit again to send another codeword. Figure 2.8(b) shows a timing diagram of a 2-bit push channel using this protocol.

2.4 Operation modes

Operation modes specify the restrictions the circuit is subject to when communicating with the environment in order to operate correctly. The most common operation modes for asynchronous circuits are described below.

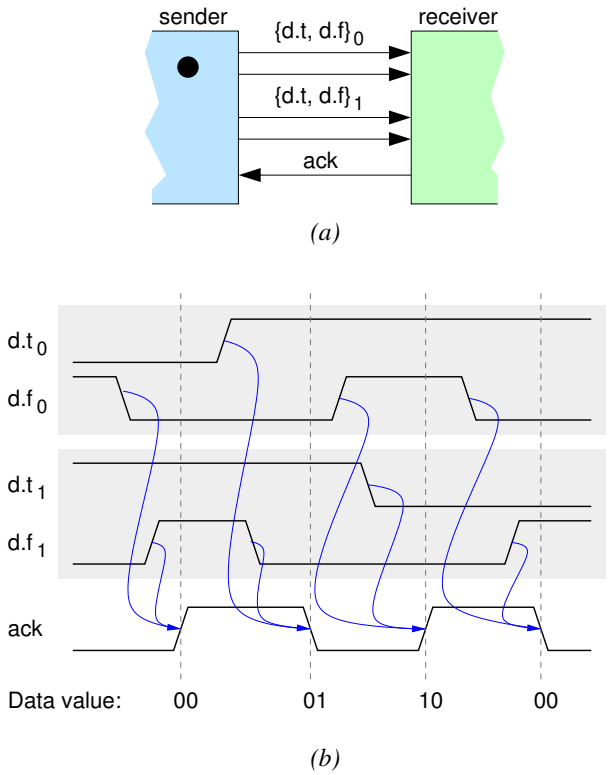

Figure 2.8: Two-phase dual-rail protocol in a 2-bit *push* channel.

2.4.1 Fundamental Mode Circuits

Circuits having this model are also called *Huffman circuits* after D.A. Huffman, who was the developer of many theoretical concepts about these circuits. The design method of fundamental mode circuits is similar to the method used for designing synchronous circuits (finite state machine approach). However, as there is no clock to indicate when the signals are valid, the following constraints to the environment apply:

i. only one external input can change at a time.

ii. the environment must wait until the whole circuit settles into a stable state (as a result of a previous input change) before changing one of the inputs.

These strong restrictions help to make the design process easier at the expense of increasing the response time. This method is not practical for complex designs with a large number of state variables due to the exponential increase in the number of possible states.

2.4.2 Burst-Mode circuits

This model was developed by Nowick, Youn and Dill [77, 78, 117]. The model relaxes the restriction of fundamental mode by allowing a group of inputs (*input burst*) to change in order to move from one state into another. The following are the restrictions used in the burst-mode model:

i. the inputs in a burst are allowed to change in any order but the machine will not react until the entire group of inputs has changed.

ii. after the burst has occurred, the machine generates the specified output burst.

iii. new burst is allowed only after the machine has completely stabilised after reacting to the previous input burst.

Several tools exist to synthesise circuits using burst-mode. *Minimalist*[34], developed at Columbia University, is one of the more sophisticated examples. Chelcea et al. [19] developed a burst-mode oriented back-end for the Balsa Synthesis System.

2.4.3 Input-output mode

In this model, the environment cannot excite a circuit until it has responded to the previous excitation by changing the value of the output. Note that no assumption is made with respect to the settling of the internal signals. The environment is also allowed to change at any time the values of inputs that do not excite the circuit. The implied causality of the input and output transitions results in more relaxed constraints on the environment connected to input-output mode circuits, but also in more complex interfaces. Different synthesis tools are based on input-output mode, making use of *Petri-nets*(see section 2.6.1) techniques to facilitate the modelling of circuit interfaces.

2.5 Delay models

Together with the operation mode, in the design of asynchronous circuits some timing assumptions are used, generating a number of delay models. These assumptions allow simplifications to the modelling of the systems. Delay models fall into two main categories: *bounded-delay* and *unbounded-delay*.

In a bounded-delay model, the propagation delay of circuit components and wires is bounded. Bounded-delay models are used in the datapath of bundled-data handshaking, and in fundamental mode and burst-mode circuits. Synchronous circuits also make use of a bounded-delay assumption because the maximum delay cannot exceed the length of the clock period.

An unbounded-delay model circuit, the propagation delay of all or some of the circuit components is unbounded. The most common unbounded-delay models include *Speed-Independent*, Delay-Insensitive and Quasi-Delay-Insensitive.

2.5.1 Speed-independent (SI) circuits

The *speed-independent* model is based on the theory developed by David Muller [71]. A circuit that is speed-independent assumes positive, unbounded delays for the elements of the circuit (gates) and zero or negligible delay in the wires. In this model, gates are modelled as Boolean operators and, at any given time, each gate of the circuit can be in one of two states:

- stable: The output of the gate is consistent with the value implied by the values of its inputs; its "next output" is the same as its "current output".
- excited: The inputs of the gate have changed but the corresponding output change is about to occur; its "next output" is different from its "current output"

When an excited gate finally changes its output after some arbitrary delay and becomes stable, the gate "fires". This in turn may excite other gates which will eventually fire and so on. The requirements for a circuit designed in this way are that once excited, a gate must fire and remain in that state until its inputs change again. This removes any hazards and guarantees monotonic transitions. Modelling SI circuits requires a state variable for each node of the circuit making the space state very large even for small circuits. Some of the synthesis techniques for SI make use of Signal Transition Graphs (STGs – see section 2.6.1) as an efficient way of representing all possible firing sequences.

2.5.2 Delay-insensitive (DI) circuits

In *delay-insensitive* circuits all wires and circuit elements can have positive, unbounded delay. With this assumption, an element that receives an input signal is

forced to *indicate* (acknowledge) to the sender when it has received the information. This is known as the *principle of acknowledgement* [91]. No new changes can occur at the input before receiving the acknowledge signal.

Consider for instance a two-input AND gate: If both inputs are high, the output is high and, in this case, a change in any of the inputs will generate a change in the output (the output acknowledges (or *indicates*) the change at the input). In the case when both inputs were low, a change in any input would not be indicated by the output. A similar situation will occur with other input combinations or by using a different basic gate. This analysis can be easily extended to any basic gate with n-inputs and a single output ($n \geq 2$).

The DI model is a very robust model, however, it has limitations if applied to general circuit design due to its heavy restrictions. It is trivial to show that the basic single output gates AND, NAND, OR, NOR or XOR cannot indicate all the possible transitions that can occur at their inputs. For this reason, they cannot be used to build a DI circuit.

The only n-input, single-output gate that can be safely used in DI circuit must be one that only allows transitions on all of its inputs before generating a new transition on its output. This class of gate is called the *Muller C-element* [71]. Due to this restriction, the class of delay-insensitive circuits happens to be very limited. It has been demonstrated that only circuits composed of C-elements and inverters can be delay insensitive [67]. Figure 2.9 shows the symbol and the specification for a two-input C-element.

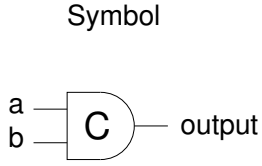

Function Table

a	b	output
0	0	0
0	1	no change
1	0	no change
1	1	1

Figure 2.9: The Muller C-element.

2.5.3 Quasi-delay insensitive (QDI) circuits

This model uses the DI assumptions with the addition of *isochronic forks* [65]. Isochronic forks are forking wires where the difference in delays between the destinations is negligible. This allows a signal that is routed to different places to be safely acknowledged by only one of the ends, simplifying the design of the

circuits. Using this restriction, a QDI circuit is equivalent to an SI circuit if the wire delays are lumped into the unbounded-delay gates.

It is possible to extend the isochronic fork assumption to the output of the gates driven by the fork (*extended isochronic fork*) [109]. This assumption can be extended through more than one level of gates at the cost of making the circuit less robust. The type of circuits that uses the extended isochronic fork are referred to as Q^nDI.

2.6 Asynchronous synthesis

With the level of complexity in today's designs, high-level modelling and synthesis is a necessary requirement. The use of of a high-level based synthesis can also reduce the design time compared to full-custom, hand-made designs. Asynchronous designers have today a set of automated and partially-automated synthesis tools available that allow the description and synthesis of complete systems including control and datapath elements (also referred to as `functional blocks`). This section briefly introduces some of the most popular approaches and synthesis tools available for the design of asynchronous circuits.

2.6.1 Synthesis of SI control circuits

Control circuits are required within an asynchronous environment in order to generate the events that guarantee the correct sequence of operation for other components. In the SI approach the designer must specify all possible sequences of input and output signal transitions that describe the restrictions on the circuit environment. This specification can be done using *Signal Transition Graphs* (STGs) [20], [21]. STGs belong to the family of models called *Petri Nets* [72]. A brief introduction to Petri Nets and STGs are given below, followed by an introduction to the STG-based synthesis tool Petrify [25].

Petri nets

A Petri net is a graph composed of directed *arcs* and two types of nodes: *transitions* and *places*. Arcs can only run between places and transitions. The places from which an arc runs to a transition are called the *input places* of the transition; the places to which arcs run from a transition are called the *output places*

of the transition. Places may contain any number of *tokens*. A distribution of tokens over the places of a net is called a *marking*. A Petri Net model can be "executed by" *firing* transitions. A transition is enabled to fire if there are tokens in all of its input places. When a transition fires, it consumes the tokens from its input places, performs some processing task, and places a specified number of tokens into each of its output places. This is done atomically, in one single non-pre-emptive step. During the execution, multiple transitions can be enabled and they will fire at any time, and it is also possible for an enabled transition not to fire at all. This non-deterministic behaviour makes Petri nets to be well suited for modelling the concurrent behaviour of distributed systems.

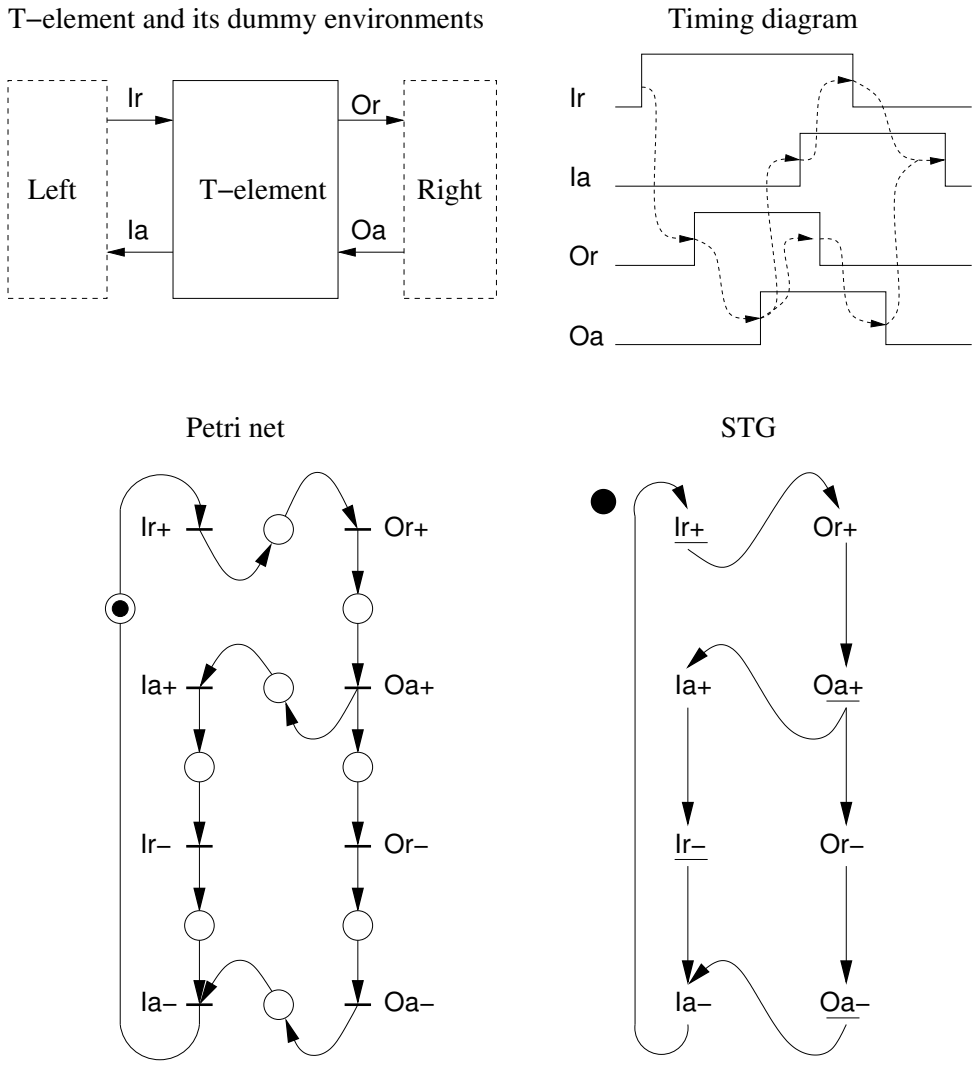

Figure 2.10: A T-element connected to left and right "well behaved" environments and its specification in the form of a timing diagram, a Petri net and an STG.

As an example of Petri-nets usage, consider the specification of an *auto-sweeping module* [73], (most commonly called a *T-element*) shown in figure 2.10. T-elements are used in handshake control circuits that implement *handshake enclosure* (the handshake of the right side is enclosed within the handshake of the left side), parallelisation and sequencing of operations, with concurrent RTZ phases [73, 89, 57, 82].

In the Petri net of figure 2.10, signal transitions are represented by horizontal bars and places with circles. Tokens are represented by black dots inside a place. A transition from 0 to 1 in signal x is represented by $x+$; similarly, a transition from 1 to 0 is represented by $x-$. The graph is marked with a token in the input place of the $Ir+$ transition. The T-element is connected to a "well behaved" dummy environments on the left and right hand sides that allow changes on the inputs only after the T-element has changed its output responding to a previous request. In this situation, the $Ir+$, $Or+$ $Oa+$ transitions must fire in sequence.

After the firing of $Oa+$, a token is placed in the input place of $Ia+$ transition and another token is placed in the input place of the $Or-$ transition, allowing these transitions to fire and so on. Note that the execution of $Ia+$ followed by $Ir-$ is allowed to occur concurrently with the execution of $Or-$ followed by $Oa-$.

Signal Transition Graphs

An STG is a Petri net with the following characteristics [91], [48]:

i. *Input free choice*: The selection among alternatives must only be controlled by mutually exclusive inputs.

ii. *1-bounded*: There must never be more than one token on an arc.

iii. *Liveness*: the STG must be free from deadlocks. That means that from every reachable marking, every transition can eventually be fired.

iv. *Consistent state assignment*: The transitions of a signal must strictly alternate between + and −.

v. *Persistence*: For all arcs $a* \rightarrow b*$ in the STG (where $t*$ means transition $t+$ or $t-$), there must be other arcs that insure that $b*$ fires before the opposite transition of $a*$ occurs.

vi. *Complete state coding (CSC)*: Two or more different markings of the STG must not have the same signal values (i.e., correspond to the same state). If this is not the case, it is necessary to introduce extra variables such that different markings corresponds to different states.

STGs represent synthesisable circuit implementations. Figure 2.10 shows the STG specification of a T-element equivalent to the Petri-net at its left. Compared to a Petri net diagram, in an STG, labelled transitions are replaced with its label, and places with a single input and output are omitted. As shown in the figure, the tokens in these omitted places are placed on the corresponding arcs. Transitions corresponding to inputs are distinguished by underlines. In the example, the original Petri-net is 1-bounded with no choice, hence a circuit implementation may be synthesised.

Petrify

Petrify [25] is a public domain synthesis tool for manipulating Petri nets and for synthesising SI control circuits from STG specifications. STG descriptions for Petrify are written in plain text. Petrify can solve CSC violations by automatically inserting state variables. From the STG specification Petrify can produce either a complex-gate circuit, a generalised C-element circuit or map the circuit onto a gate library supplied by the user.

2.6.2 Communicating Hardware Processes (CHP) and the Caltech Asynchronous Synthesis Tool (CAST)

The CHP synthesis system was developed at Caltech by A.J. Martin[66]. CHP language has a syntax similar to the concurrent programming language Communicating Sequential Processes (CSP) [50], using various special symbols. Design flow in CHP starts with a specification of the system in the CHP language. The first step is to reduce complex control structures found in the specification into combinations of simple processes. In a second step, these processes are then expanded into four-phase handshake protocols (handshake expansion - HSE) to convert them into sets of transitions. In order to distinguish ambiguous states, reshuffling and variable insertion is performed and, finally, production rule sets (PRS) are generated, which can be mapped into a physical circuit realisation, targeting a specific building block called PHCB (precharge half-buffer). Many

of the above steps require user intervention and guidance and this may have a significant impact in the performance and area of the synthesised circuit.

The Caltech Asynchronous Synthesis Tool (CAST) is a suite of design tools based in CHP that provides modules to refine CHP descriptions, translate CHP descriptions into HSE, HSE into PRS and mapping PRS into PHCB circuit networks. CAST has been used to synthesise complex chips, including the MIPS R3000 [69] and the Luthonium 18 (a 8051 clone) [70], but these rely on significant manual intervention in the synthesis flow to achieve the most effective program transformations. Another issue is that the automatic program transformations used in CAST are not behaviour preserving and are only correct for designs that meet particular requirements, which may not be straightforward to an inexperienced designer. CAST tools are currently only available internally at Caltech.

TIMA Asynchronous digital systems Synthesis Tool (TAST)

TAST (Tool for Asynchronous circuits SynThesis)[104] is a compiler/synthesis tool that synthesises asynchronous systems from a specification written in CHP. The compiler analyses the given specification and transforms it into an internal format based on Petri Nets and Data Flow Graphs. From this intermediate form the user can generate:

- a functional VHDL description of the model for simulation purposes.
- an RTL VHDL description, which can be used to target ASICs or FPGAs technologies by means of standard CAD tools.
- an asynchronous circuit. However, in this case, CHP descriptions must be written using the *Data Transfer Level* (DTL) style subject to certain rules to ensure a correct mapping [28]. If the mapping is possible, a gate netlist is produced. The gate netlist can either be simulated using standard CAD tools or used to implement the circuit through a technology mapping process that requires a specialised TAST cell library.

2.6.3 Macromodular based synthesis

The *Macromodular* methodologies make use of pre-designed blocks (the *macromodules*)that communicate asynchronously using handshake channels. Macromodules were first proposed by Clark in Washington University [22] during the late 1960's. More recently, Brunvand introduced a macromodular synthesis system [18], making use of the channel-based, CSP-like programming language Occam [63] to describe circuits. Descriptions are automatically synthesised into compositions of control, variable read/write and datapath macrocells implemented with 2-phase signalling with bundled data. Plana [87] describes a system of macromodules to construct asynchronous circuits that communicates using pulse-mode [56] handshaking. The macromodules are described using petri-nets with signal pulse labelled transitions. The examples of pulse-mode circuits given by Plana were constructed by hand but they are specified using a pseudo-code that could be the basis for a synthesis system.

The handshake circuits paradigm proposed by van Berkel for use in the Tangram tool is another approach to macromodular synthesis. Tangram TiDE and Balsa synthesis tools are all based in the transparent compilation and the handshake circuits paradigm (c.f 1). They use CSP-like description language but with a syntax more similar to traditional programming languages than CHP. TiDE and Balsa are currently the major fully-automated synthesis systems for asynchronous design.

Due to its relevance to the work in this thesis, a more complete introduction to the Balsa synthesis system will be presented in chapter 3. Details of Teak[6], a novel data-flow implementation for the Balsa language, will be introduced in chapter 5.

2.6.4 Desynchronisation methods

Desynchronisation methods rely on the use of a synchronous design methodology and commercial CAD tools and then convert the resulting circuits into asynchronous designs. The flow described in [26] targets bundled data implementation whereas the one presented in [61] targets QDI circuits and uses the *NCL_X* approach. In these approaches, synchronous CAD tools are used for datapath synthesis and asynchronous control synthesis tools are used to produce controllers that replace the global clock.

The advantages of this approach are that designers need little specialist knowledge of asynchronous techniques and the synthesis uses well-known commercial tools. However, as the design is targeted at a synchronous implementation, some potential advantages of asynchronous techniques are not exploited, such as: (a) the fine-grained concurrency that can be possible in asynchronous design, (b) the possibility for asynchronous designs to use data-dependent delays instead of the worst-case delays used in synchronous design. Two popular approaches used in the desynchronisation method are briefly described below.

Null convention logic (NCL)

In order to reduce the complexity in QDI functional blocks, Theseus Logic Inc. [32] proposed the Null Convention Logic approach. In NCL data is DI encoded (using dual-rail encoding or other 1 of N code) and uses a 4-phase protocol. Data changes from the empty (NULL) value to a valid codeword (Data) in the set phase and then back to NULL in the reset (RTZ) phase. To implement this operation, NCL makes use of m-of-n threshold gates with hysteresis. An hysteresis threshold gate is a logic gate which will set its output high when the sum of the weights on the inputs exceeds a fixed gate threshold (m inputs for an m-of-n threshold gate). The output of the gate will return to low when *all* inputs become low. Notice that, in applying this idea, a C-element is an n-of-n hysteresis threshold gate and an OR gate is a 1-of-n threshold gate.

Synthesis of NCL circuits from logical descriptions can be performed by mapping two level Boolean implementations of those functions into minterms implemented with C-elements and OR gates to implement the AND and OR levels using *Delay Insensitive Minterm Synthesis* (DIMS) [71]. The C-elements and OR gates of DIMS can then be mapped onto their threshold gate analogues. Simple hysteresis threshold gates can then be optimised into threshold gates with more complicated input weightings. This is the key part of the synthesis process, however, these optimisations are not easily automated.

Figure 2.11 shows an optimised NCL implementation of a dual-rail 1-bit adder. In this figure, the number inside the gate corresponds to the value of the threshold.

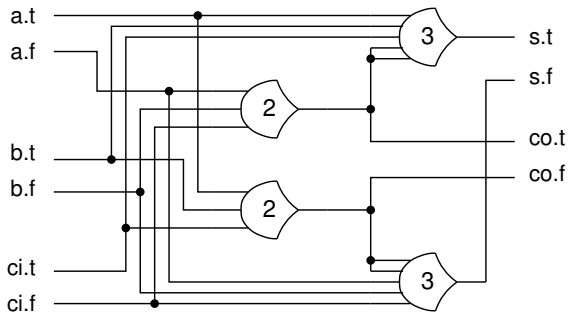

Figure 2.11: A dual-rail full adder using NCL gates.

NCL with explicit completeness (NCL_X)

In order to reduce the area and energy of NCL circuits, Kondratyev and Lwin [61] proposed NCL_X, a different approach based on the idea of "separate implementations for functionality and delay insensitivity" allowing independent optimisations of each. In NCL_X, after obtaining the optimised Boolean implementation of the functional block, the circuit is mapped into *unate gates* (gates that implement a *positively unate function* - all inputs in such functions are used without inversions). This is done by using two different variables, $x.t$ and $x.f$ for direct and inverse signals of x. The obtained network implements rail "1" (t) of a dual-rail circuit for the functional block. The dual-rail expansion is completed by creating a corresponding dual gate in the rail "0" (f) network for each gate in the rail "1" network. Finally, delay insensitivity is achieved by providing local completion detectors (OR gates) on each pair of dual gates and connecting them into a multi-input C-element to generate the *done* signal. In NCL_X for each dual-rail primary input of a block, there must be a signal *go* that indicates the state of the input ($go = 0 \rightarrow$ NULL, $go = 1 \rightarrow$ Valid).

The claimed benefits of both NCL and NCL_X methodology is that they can make use of existing electronic design automation (EDA) tools developed for synchronous synthesis. In [61] it was reported that, compared to NCL, NCL_X circuits reduce significantly the area overhead, are faster and have a similar power consumption. It was also noted there that compared to synchronous circuits, NCL_X are 2 to 2.5 times larger and consume more energy, with the benefits being on lower EMI and improved security and reliability.

2.7 Summary

Asynchronous circuits have some attractive advantages over their synchronous counterparts. By eliminating the clock, some major problems associated with it could be alleviated. In particular, reduced EMI and robustness towards fabrication process variability are nowadays their most attractive characteristics.

Delay-insensitive encoding and quasi-delay insensitive asynchronous circuits have been proposed as an alternative to alleviate the complex problem of timing closure in modern sub-micron fabrication technologies. However, their robustness comes at the price of more complex, slower and expensive circuits when compared to synchronous implementation. Some approaches towards the synthesis of QDI datapath circuits have been proposed with different complexity/robustness tradeoffs to reduce the inherent penalties of the QDI approach.

Research in asynchronous synthesis has resulted in the development of various synthesis techniques and tools available for the design of large scale asynchronous circuits, some based in pure asynchronous methodologies such as the various macromodular methods (including the handshake circuits approach used in Balsa) and other recent approaches based in synchronous methodologies plus a "desynchronisation" process.

Chapter 3

The Balsa synthesis system and language

3.1 Introduction

This chapter presents a brief introduction to the Balsa synthesis system and the Balsa language, which is also the input language for the Teak synthesis system described in chapter 5. Some small examples are included to highlight the directness of the compilation scheme and the most common input and control structures used in Balsa circuits.

3.2 The Balsa synthesis system

Balsa is the name for both the framework for synthesising asynchronous circuits and the language used to describe such systems. Balsa uses the syntax-directed compilation approach to generate *handshake circuits* from a description written in the Balsa language.

Originally introduced by van Berkel [108], a handshake circuit is a communicating network of handshake components connected point-to-point using *handshake channels* (see 2.3). Each channel connects exactly one passive port of a handshake component to an active port of another handshake component. As mentioned in section 2.3, an *active port* is a port that initiates the communication by sending a request signal to a *passive port*. When ready, the passive port will respond with the acknowledge signal. The handshake can involve the transfer of data or simply synchronisation (control) using a dataless *sync* channel

(a channel conveying the request and acknowledge signals only).

3.2.1 Balsa design flow

As shown in figure 3.1, in order to synthesise a circuit from its description the Balsa system uses a compiler (`balsa-c`) that generates a handshake circuit described in an intermediate netlist format (*Breeze*). A Breeze description can be processed using `balsa-netlist` to produce a structural Verilog netlist of the circuit for a chosen target cell library, asynchronous protocol implementation style and data encoding described in the selected back-end library. This file can then be processed using commercial layout tools for simulation, validation, and fabrication.

The system also features a behavioural simulation tool, `breeze-sim`, that works at the handshake component level, and an area cost estimator: `breeze-cost`. From version 3.5, Balsa includes `balsa-mgr`, a graphical front-end that provides project management facilities. More detailed information on Balsa and the Balsa language can be found in the Balsa Manual [30].

The Balsa synthesis system has been used successfully to synthesise the 32-channel DMA controller for the DRACO chip [40], an asynchronous MIPS processor [118], and the G3Card smartcard System-on-Chip. Those designs together with more recent work [89, 85] have demonstrated the potential of Balsa and its synthesis approach to generate efficient asynchronous systems for complex, real world applications.

3.3 The Balsa language

This section briefly introduces the Balsa language. Details of the language and compilation scheme not relevant to this work have been omitted. Detailed information on the language features and a complete language syntax reference can be found in the Balsa Manual [30]. Extensive details on the compilation process and handshake circuits used with Balsa can be found in [108, 29, 89, 82]. The description of the language features are accompanied with example code and, where relevant, the resulting handshake circuit generated by the compiler.

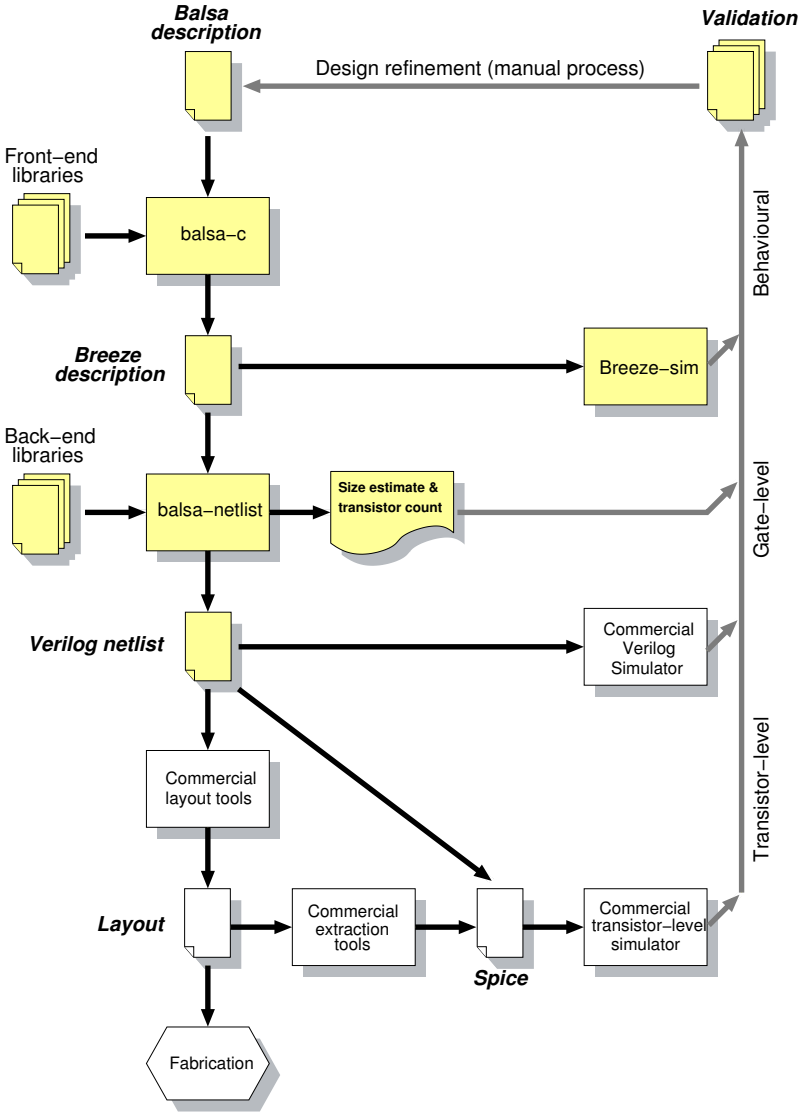

Figure 3.1: Balsa design flow.

3.3.1 The structure of a Balsa description

A description in Balsa is composed of one or more files that have a structure similar to the example shown in figure 3.2. In this figure the main parts of a Balsa description are indicated. Balsa descriptions are divided into a number of procedures. Each procedure has an implicit activation port (that activates the circuits within the procedure) and any number of input, output or sync (dataless) ports that must be explicitly declared. Within the procedure, *channels* and *variables* can be declared with local scope. Channels are used to communicate between procedures or between concurrent actions (commands). Each channel

must have at least one source (producer) and one sink (consumer). Variables are used as temporary storage for values. Writes and reads on the same variable must be sequenced.

```
1  -- This is a comment in Balsa.
2  -- Block comments use the (-- COMMENT --) pair
3  -- imports (dotted notation to specify path.
4  -- Extension '.breeze' assumed
5  import [Path.And.Name]
6  -- Global declarations (types, constants & procedures)
7  -- Examples of type declarations
8  type word is 16 bits          -- unsigned type
9  type sword is 16 signed bits -- signed type
10 --
11 -- Other global declarations ...
12
13 -- A procedure declaration
14 procedure exampleProc
15 -- port declarations are separated by ';'
16 (
17   -- 'someType' must have been declared previously
18   input a    : someType;
19   output out : sword;
20   sync z
21 ) is
22     -- local declarations (types, constants, procedures)
23     -- local declarations (variables & internal channels)
24     variable var : someType
25     channel c : otherType
26
27 begin -- exampleProc body
28   (--
29   Commands and procedures composed with "||"  or ";" operators
30   --)
31 end -- end of exampleProc body
```

Figure 3.2: The structure of a Balsa description.

Procedures consist of one or more commands composed using control operators. A command may consist of:

- a basic read or write action on a channel or variable.
- an iteration construct.
- a conditional construct.
- another instantiation of a procedure.
- a sequential or parallel composition of commands.

A command makes used of channels to communicate internally with other local commands using the declared channels or externally using the procedure's ports. Channels and variables can be read or write, input ports are read-only channels and output ports are write-only channels.

Balsa supports modular compilation: a description can be divided into multiple files which are included using `import` statements. These must always be located at the beginning of the file preceding any other declaration. The files to be imported must be pre-compiled handshake circuits in Breeze format. Constants and user-defined data types can be declared afterwards inside or outside the procedures. In order to use any type/constant/procedure in Balsa, this has to be declared previously within the file or imported files, as Balsa follows the same "declare before use" rule of C and Modula [30].

3.3.2 Data Types

Balsa is a strongly typed language with data types based on bit vectors. Results of expressions must be guaranteed to fit within the range of the underlying vector representation [30]. Balsa supports global and local type and constant declarations. Balsa supports the following data types:

Numeric types

Bit vectors of *width* bits that can be signed or unsigned. Examples:

```
type word is 16 bits
```
(unsigned type with range $[0, 2^{16} - 1]$)

```
type sword is 16 signed bits
```
(unsigned type with range $[-2^{15}, 2^{15} - 1]$)

Enumerated types

This type consists of named numeric values. The numeric values are given incrementally starting at zero, with explicit values resetting the counter, for example:

```
type MyEnum is enumeration
    ZERO, ONE, FIVE=5, OTHER
end
```

In the above example the following values are assigned: `ZERO=0, ONE=1, FIVE=5, OTHER=6`. The values require 3 bits, hence this type is 3 bits wide. Note that values 2,3,4 and 7 are not bound to names.

Record types

Bit-wise composition of named elements of possibly different (pre-declared) types. for example:

```
type SignMagnitude is record
    Magnitude :  MyEnum;
    Sign :  bit;
end
```

In this example, a value of type `SignMagnitude` will have a width of 4 bits with the `Magnitude` field occupying the first three least significant positions and `Sign` occupying the most significant position. Referring to a field within a record is accomplished with the usual dot notation.

Array types

Numerically (or enumerated) indexed compositions of values of the same type. For example:

```
type RegisterBank :  array 0..15 of word
```

3.3.3 Basic transfer commands

Balsa provides two basic commands to transfer information: channel read and channel write; these generate handshake data transfers within the involved channels.

`a -> b` reads channel `a` and writes channel to `b`. `a` can be either an input port or an internal channel. `b` can be either a variable, an internal channel or an output port.

`d <- c` transfers the value of variable/expression `c` to the output port or internal channel named `d`.

3.3.4 Dataless handshakes

`sync a` generate a handshake in the dataless channel `a`. Further actions can only occur after the handshake on `a` completes.

3.3.5 Variable assignment

`var := expression` transfers the result of `expression` to the variable `var`. Balsa allows variable auto-assignment, where an expression includes the target variable. However, the resulting circuit will contain an invisible auxiliary variable, whose contents will be written back to the programmer's variable after being assigned the result of `f(x)`. The type of a result must agree with that of the variable to be assigned. In cases when these types may differ, the user can truncate/expand the width of the result by explicit casting. For instance, if `x` is a variable of type byte, the following statement is invalid:

```
x := x + 1  -- invalid, result may require an extra bit
```

The correct statement should look like:

```
x := (x + 1 as byte)  -- the result is truncated to 1 byte.
```

3.3.6 Control operators

Balsa has two control operators to form composed commands: *Concur* `||` and *Sequence* `;` .

`<command1> || <command2>` composes the two commands so that they operate concurrently. However, both commands must terminate before the composed command is completed. *Concur* generates a *rendezvous* point when both commands complete.

`<command1> ; <command2>` sequences the execution of the two commands: the first must terminate before the second can proceed.

The `||` operator has a higher precedence than `;` . This precedence can be overridden by creating groups of commands using either square brackets (`[ ]`) or the pair of keywords `begin ... end` to enclose a command. For instance:

```
-- 'x' is written first, sequenced by the concurrent write
-- of variable 'y' and channel 'z'
x := 10 ; y := 20 || z <- 30
-- here, 'x' is written first sequenced by the writing of 'y'.
-- These two actions are concurrent with the writing of 'z'
[ x := 10 ; y := 20 ] || z <- 30
```

When composing commands, care must be taken to avoid introducing dependencies that may lead to a deadlock. As a very simple example, consider the program in figure 3.3. The program consist of an infinite repetition of two compound commands (lines 9 and 11), which in turn are composed with the `||` operator, effectively creating two execution threads.

```
1  procedure deadlock
2  (
3    output out : byte
4  ) is
5      channel a, b  : byte
6      variable v1, v2 : byte
7  begin
8      loop
9          [ a -> v1 ; out <- v1 || b <- v1 ]   -- command 2
10         ||
11         [b -> v2 ;  a <- (v2 + v2 as byte) ]  -- command 1
12     end
13 end
```

Figure 3.3: Example of deadlocking code.

Upon activation, a transfer from channel `a` into variable `v1` is activated (first action in line 9). Concurrently, in the second group, a transfer from channel `b` into variable `v2` is also activated. However, the circuit deadlocks because the read from channel `a` can complete only after the write to channel `a` completes but this last action can only start after the read from channel `b` completes (and that requires the completion of the read from channel `a`). In this simple example deadlock is eliminated by swapping the sequenced actions in one of the composed commands.

Invalid compositions

In order to avoid some potential deadlock situations or unsafe operations, the Balsa compiler will fail (and the user will get the relevant feedback on the error) when it encounters the following compositions within a description:

- A write sequenced with a read on the same channel or a read sequenced

with a write on the same channel. These will result in a deadlock because the first action cannot complete until the second action completes and the second action cannot start until the first completes.

- Commands composed with the *Concur* operator that: (*i*) write and read from the same variable, (*ii*) write to the same channel, (*iii*) write to the same variable. Concurrent occurrence of these actions are unsafe and causes malfunction. When any of these conditions occur in a description, the compilation will fail. However, from version 3.5.1 Balsa introduced the experimental "permissive" *Concur* (`|||!`) which leaves to the user the responsibility of making sure that those conditions will not actually occur during operation. This operator can be used (with care!) to exploit the designer's knowledge on the operation of the circuit, as will be described below.

`Continue` and `halt` commands

The `continue` command is used to implement "no operation" (always acknowledges any activation request it receives). When the execution of a process thread reaches a `halt` command, this thread deadlocks (no further actions occur).

3.3.7 Iteration and conditional constructs

An unbounded repetition in Balsa uses the `loop <command> end` construct as shown in the example in figure 1.2(a). Bounded repetitions use the construct:

```
loop (<command0>) -- command0 is optional
while guard1 then <command1>
     |guard2 then <command2>
     |.
     |.
     |guardN then <commandN>
end
```

This construct allows the specification of repetitive loops equivalent to `for`, `repeat ... until` and `do ... while` found in other languages. However, Balsa allows the specification of multiple guard conditions. If multiple guards are used, they are evaluated in order. If more than one guard is satisfied, only the command associated with the guard that appears earlier in the list will be activated.

The following are code examples of `loop` constructs:

```
variable x : byte
channel inp, out : byte
-- infinite loop
loop
    inp -> x ;
    out <- x
end
--


-- for (x=0; x<10; x++) <command> equivalent
x := 0 ; -- initialisation
loop
while x < 10 then
    print "value of x is: ", x ;
    x := (x + 1 as byte) -- autoassignment
end
--


-- repeat <command> until x<10 equivalent
loop
    print "value of x is: ", x ;
    x := (x + 1 as byte) -- autoassignment
while x < 10
end
--


-- multiple guards: 0 to 9 counter with autowrap
-- Note 1: guards are evaluated in order.
-- Note 2: the loop is infinite unless initially x > 9
loop while
  x <  9 then x := (x + 1 as byte)
| x = 9 then  x := 0
end
```

Balsa features the `if ... then ... else` and the `case ... of ... else` constructs for conditional execution. The former can have multiple guards which makes it equivalent to nested `if ... else` statements found in other languages and, similarly, the `else` clause is optional. Multiple guard evaluation is similar to that of the `loop ... while` construct. The syntax of the `if ... then ... else` and the `case ... of ... else` constructs is as follows:

```
if condition1 then <command1>
| condition2 then   <command2>
|.
|.
| conditionN then <commandN>
else <commandDefault> -- optional clause
end

case expression of
  guardList1 then <command1>
| guardList2 then <command2>
|.
|.
| guardListN then <commandN>
else <commandDefault> -- optional clause
end
```

The `guardList` can be either a single expression of a comma-separated list of expressions whose values must be resolvable at compile time. All guard values must be disjoint from one another. As the reader could easily prove, the `if` and `case` constructs can be used to implement equivalent conditional behaviours. The `if` construct is more flexible as it allows the use of expressions for guards and guards do not need to be disjoint. In the `case` construct, guards must be disjoint and either explicitly given or written as expressions resolvable at compile time. However, in general, the `case` construct generates faster circuits (see section 4.5).

3.3.8 Data processing operators

Balsa provides basic unary and binary bit-wise logic (`not, and, or, xor`) and arithmetic operators (`+, -`), as well as Boolean and comparison operators (`=, /=, >, <, >=, <=`) to construct expressions. There are not shift operators but these can be implemented with the contatenation (`@`) and smash (`#`) operators. A complete table can be found in Appendix A. Other operators like multiply, divide and remainder (`*, /, %`), `log` and exponentiation (`^`) can only be used in constant expressions.

3.3.9 Input enclosure

Balsa features two constructs that allow the handshake of one or more input channels to be held open until a command or a group of composed commands complete: (*i*) passive-input enclosure with choice with the `select` command and (*ii*) active-input enclosure with the `<channels> -> then <command> end`

construct. The "enclosed" commands can read the value of the channels as many times as required (or even not read at all) without the need of variables to hold those values. Within the enclosure construct, enclosed channels act like variables for reading purposes.

Input enclosure can generate area benefits and help to produce simpler descriptions. However, there are performance implications: the tree of handshakes connected to the enclosing inputs cannot themselves complete until the enclosed actions complete. These implications will be discussed in section 4.4.2.

Passive-input enclosure

The syntax for this type of enclosure is as follows:

```
select
  groupOfChannels1 then command1
| groupOfChannels2 then command2
.
.
.
| groupOfChannelsN then commandN
end --select
```

The `select` statement allows selection between groups of input channels by waiting for data on any of the groups to arrive. The arrival of data among each group must be guaranteed to be mutually exclusive. This also means that a channel can only be part of exactly one group. The enclosed commands are activated only after all the inputs involved arrive. This type of enclosure generates passive ports for the inputs as opposed to the active-ported circuits that Balsa normally generates.

It is recommended that the use of `select` is restricted to only cases where input choice is genuinely required and that the faster active-input enclosure is used instead in other cases. Another reason for using passive-input enclosure is if the interface of a design requires passive (*push*) inputs.

Active-input enclosure

This enclosure has the following syntax:

```
groupOfChannels -> then
    command
end
```

Similar to the `select` construct, the enclosed commands are activated only after the arrival of all input channels. In contrast, this type of enclosure does not allow choice and generates active (*pull*) inputs.

Eager input enclosures

Balsa also features *eager* variations of the passive and active enclosures using their "banged" variants:

```
select!  channels then command end
channels ->!  then command end.
```

In its eager variant, the `select` cannot be used with input choice. As stated previously, in the standard enclosures the activation of the enclosed commands occur only after all of the involved inputs have arrived. In the eager enclosures, the enclosed commands are activated as soon as the control activates the inputs, without waiting for the data to arrive. This has performance benefits, because the control is given a head start, hence reducing the control overhead. However, any enclosed command that does not depend on the arrival of data may occur before the data arrives and, if not used carefully, this could result in incorrect operation.

The eager variants still guarantee that the command will not complete until input data has also completed. Details on the implementation of the eager enclosure construct were introduced in [89].

To illustrate the use and behaviour of both types of enclosure, let us consider the following examples:

```
a, b -> then
    out1 <- (a + b as byte)
 || out2 <- b
 || out3 <- 10
end -- a,b ->
```

In the previous code active enclosure is used. Writing to the channels `out1`, `out2` and `out3` can only occur after the arrival of inputs `a` and `b`, despite `out2`

being independent of a and out3 being independent of both inputs.

```
a, b ->! then
    out1 <- (a + b as byte)
 || out2 <- b
 || out3 <- 10
end -- a,b ->
```

In this example, eager active enclosure is specified. Here the command that writes to channel out3 starts as soon as the control reaches the enclosure command, without waiting for the arrival of a and b. Furthermore, if b arrives earlier, the command that writes to out2 starts without waiting for input a. However, all commands will complete only after both inputs complete. An example of the use of eager active inputs that results in incorrect operation will be given in section 3.3.12, example 5.

3.3.10 Arbitration

Balsa features the arbitrate command when choice is required among two non-mutually exclusive inputs (or groups of inputs). Its syntax is similar to that of the select command:

```
arbitrate
    groupOfChannels1 then command1
  | groupOfChannels2 then command2
end
```

Upon arrival of every input in one of the groups, the associated command is activated. Similar to the select construct, the command will be enclosed within the handshakes of the inputs and these can be read as described previously. Both of the two groups of inputs may arrive, but the control will be passed only to the command enclosed by the group that arrives first. If the two groups arrive so close in time, in such a way that the first arriving group cannot be discerned, an arbitrary decision is made.

If more than two events require arbitration, an arbiter tree can be constructed using the arbitrate construct. An example of a parameterised arbiter tree can be found in the Balsa Manual.

3.3.11 Permissive Concur

The permissive *Concur* (`|||!`) permits the parallel composition of the potentially unsafe operations described previously. This relaxation can be used when the designer knows that the unsafe conditions will never occur, leading to either smaller or faster circuits and, in some cases, to more compact descriptions. Consider for instance a situation where two concurrent processes *P1* and *P2* write to a common channel `c`. If the operation is such that the writes are guaranteed to be mutually exclusive, there is more than one way to implement the access to channel `c`. The more straightforward implementation would be the use of the `select` command described earlier. Another option would be to use a (previously generated) selection data channel that signals which process is the next to write, and then use it as the guard of a conditional construct that selects the appropriate source to pass to the destination channel. However, because the potential conflict will not occur, *P1* and *P2* can be composed using the permissive *Concur* which will allow them to access the common channel. An example that illustrates its use will be given in section 3.3.12, example 6.

3.3.12 Compilation examples

This section presents some simple program examples and their resulting handshake circuits in order to familiarise the reader with the structures generated by the use of different Balsa constructs and their operation. Details of the compilation of a simple 1-place buffer have already been given in section 1.2. A brief description of the handshake components used in the examples can be found in Appendix B. Extensive details on the compilation process can be found in [108, 29, 89, 82].

Example 1: passive enclosure

The code for a two-input, uncontrolled multiplexer (merge) is shown in figure 3.4. Inputs `a` and `b` must be mutually exclusive. The resulting handshake circuit showing the translation of this construct is shown in figure 3.5. In this and the subsequent handshake circuit figures, regions of different colours show the boundaries of the commands. Control tree elements are embedded in a darker shade of the command area colour. Thick arrow lines connect datapath components and thin lines represent control (dataless) channels. Passive ports are represented by

small unfilled circles, and active ports by small filled circles.

```
1  procedure merge2
2  (
3    parameter DataType: type;
4    input a, b : DataType;
5    output o   : Datatype
6  ) is
7  begin
8      select
9        a then
10         o <- a
11     | b then
12         o <- b
13     end -- select
14 end -- merge2
```

Figure 3.4: An uncontrolled multiplexer (merge).

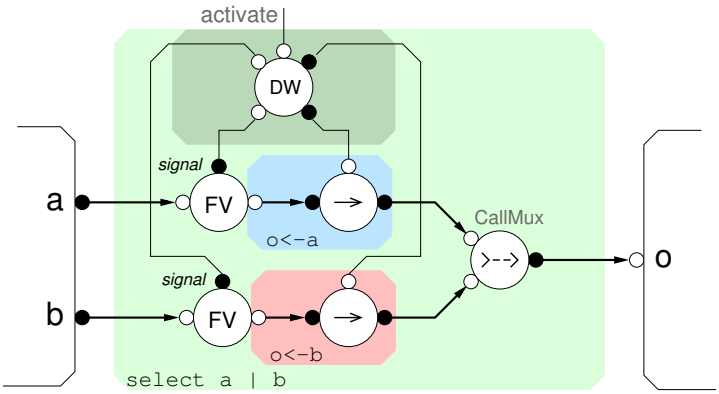

Figure 3.5: Handshake circuit of the uncontrolled multiplexer.

The *DecisionWait* component (*DW*) synchronises the activation signal with one of its inputs coming from the *signal* outputs of the *FalseVariable* components (*FV*), and activates the corresponding decision output. As its name suggests, an *FV* does not have storage: it simply provides passive read ports and a control output *signal* (the active port on the top) to indicate arrival/removal of data. The *FV* activates its *signal* output as soon as the least significant bit (bit 0) of the data input arrives. The reader can refer to [89] and Appendix C for details on the operation and current implementation of this component.

The outputs of the *DW* are used to pull data from the selected data channel, using a *Transferrer*(`->`) component, through the read port of its associated *FalseVariable*. Finally, a *CallMux* (`>-->`) (mixer/merger) component is used to merge the source channels into the output `o`. In this particular example, everything but

the mixer is overhead, as will be explained later in example 6 with the use of the *permissive Concur*.

Example 2: active enclosure and operators

The code for a simple adder using active enclosure is shown in figure 3.6. The resulting handshake circuit showing the translation of the various constructs is shown in figure 3.7. Notice that the circuit features *pull* (active) channels at the I/O data interfaces.

```
1  procedure adder
2  (
3    input a, b : dtype;
4    output o   : dtype;
5  ) is
6  begin
7      a, b -> then
8          o <- (a + b as dtype)
9      end -- a, b ->
10 end -- adder
```

Figure 3.6: The description of a simple two-input adder.

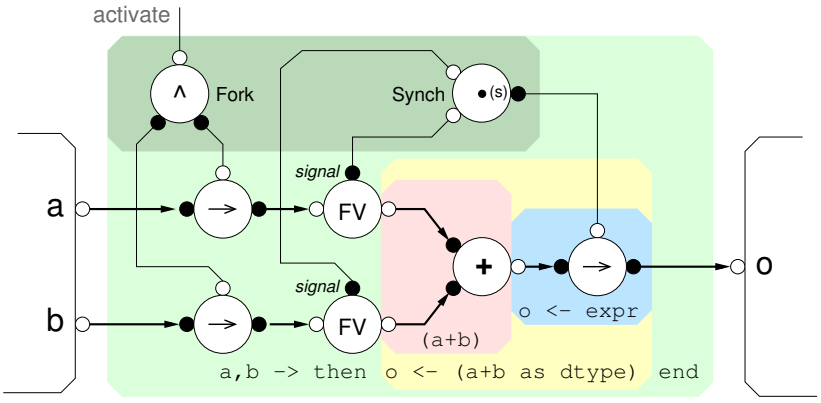

Figure 3.7: Handshake circuit of the adder code in figure 3.6.

On top of figure 3.7, a *Fork* component is used to fork the *activate* signal to the two *Transferrer* components. Upon activation, these transfer the inputs to the two *FalseVariable* components (*FV*). The *signal* outputs of the *FVs* are connected to a *Synch* (synchroniser) component, which activates its output when both input signals indicate the arrival of data. The *Synch* output activates the transfer on channel o through another *Transferrer*, which *pulls* the result from the addition operator (+). This pull action results in the reading of both *FVs*.

Eventually, the environment connected to channel `o` will acknowledge the transfer and this is passed to the *Synch*, which in turns indicates this to the *FVs* through their signal port. Upon receiving the acknowledge, the *FVs* acknowledge the inputs and the *Transferrer* components pass it to the forked activation. The activating control will eventually respond initiating the RTZ phase and a set of RTZ events will propagate in similar fashion to what has been described until the four-phase handshakes complete.

Example 3: conditional execution and active *eager* inputs

Figure 3.8 shows the code for a circuit that reads input channel `i` and, depending on the value of the `s` signal, passes the constant 10 or the value of `i` to the output channel `o`. The resulting circuit is shown in figure 3.9.

```
procedure condInput
(
  input i  : byte;
  input s  : bit;
  output o : byte
) is
begin
    s, i ->! then
        if s then
            o <- i
        else
            o <- 10
        end -- if s
    end -- s, inp ->!
end
```

Figure 3.8: Example of conditional execution.

The description is made using active *eager* inputs, but other descriptions are also possible. Note that on this occasion *activeEagerFalseVariable* (*aeFV*) components are used. An *aeFV* has an active input port and a *trigger* port to activate it. Unlike a *FV*, its *signal* output activates as soon as the trigger is activated, without waiting for data arrival. For details of its operation and current implementation, please refer to Appendix C.

The *Case* (@) component is essentially a decoder that activates only one of its control outputs at a time depending on the value on its input channel, allowing the transfer of either the value of channel `i` (in the bottom *aeFV*) or the value `10` from the *Constant* component. A *CallMux* component is used to merge the

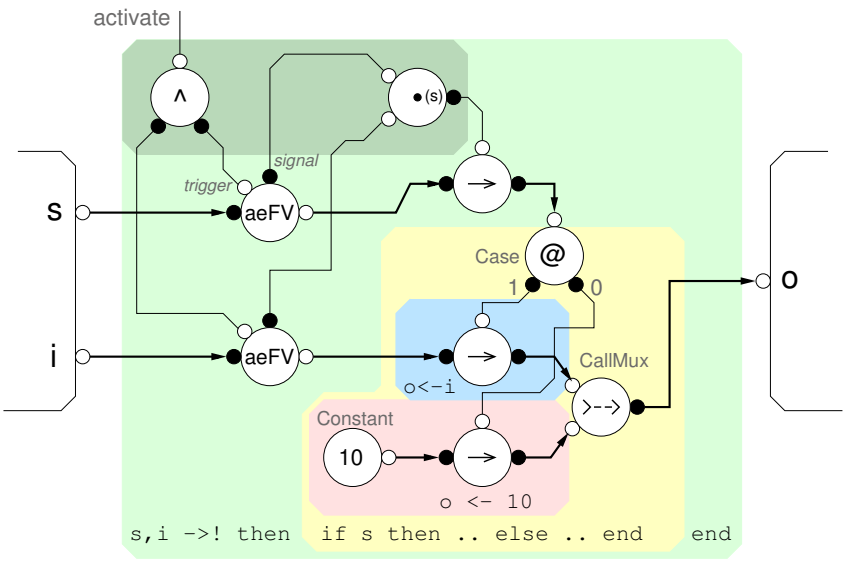

Figure 3.9: Handshake circuit of the code in figure 3.8.

source channels. The *Case* component guarantees the required mutual exclusivity at the inputs of the *CallMux*.

As stated earlier, the use of active eager inputs has the benefit of allowing the control section to proceed without waiting for the data. Thus, when data arrives, control signals are already in place resulting in faster operation [89]. This early start of the control section also allows the outputs that do not depend on all inputs to be generated without waiting for all the inputs to arrive. Its use relies on the assumption that such early data generation will not cause interference further down in the pipeline. In the above example, if `s` = 0, the constant value will be sent to the output even if input `i` has not arrived. This implies that, in the pipeline, it must be safe to send a token to output `o` before receiving tokens from both inputs in the conditional block. Example 5 examines a case when the use of active eager enclosure leads to incorrect operation.

Example 4: control operators, composed commands and finite iteration

The code in this example implements a special kind of one-place buffer that stores and duplicates the data until a *tail* flag located in the MSB (*M*ost *S*ignificant *B*it) of the input data signals the last transfer. When the tail flag is zero, the loop terminates and control is returned to the activating party. Figure 3.10 shows the code and figure 3.11 the resulting handshake circuit. The `#` in line 14 of the code is the *smash* operator: a piece of syntactic sugar that provides the bit-array

casting required to access the MSB bit.

```
1  type hdata is 9 bits -- hdata [8] = tail flag
2  procedure dupbuf
3  (
4    input i       : hdata;
5    output o1, o2 : hdata
6  ) is
7      variable buf : hdata
8  begin
9      loop
10         i -> buf                  -- buffer data
11       ;
12         o1 <- buf || o2 <- buf   -- relay & duplicate
13         -- until tail flag signals the last transfer
14     while (#buf[8] as bit) = 1 then continue
15     end
16 end
```

Figure 3.10: An example of a finite loop and command composition.

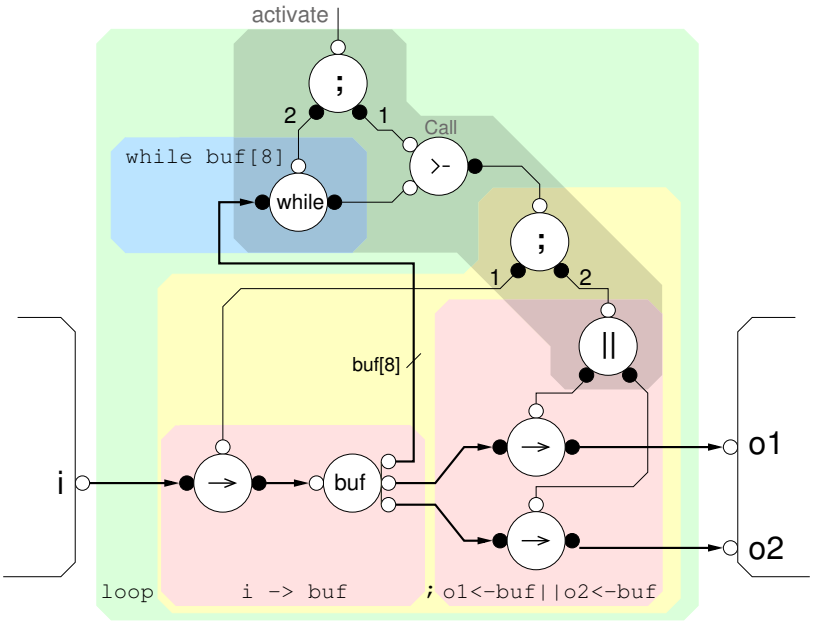

Figure 3.11: Handshake circuit of the code in figure 3.10.

The implementation is effectively a `repeat ... until` loop. As in the previous examples, figure 3.11 shows the different constructs with different shadings. The *Sequencer* (;) component at the top is required to generate the first iteration of the repeat loop before checking the exit condition. The other *Sequencer* corresponds to the operator in line 11 in the code that sequences the writes and reads of the variable `buf`.

Notice that in the figure the *While* component implements the control for the conditional loop. Upon receiving a handshake on its activation port (located at the top), this component holds the activation handshake open and performs two sequenced actions: first it reads the guard value through the active input at its left and, if it is a 1', the next action is a handshake in the passive output port. If the guard is 0, the *While* component completes the activation handshake and control returns to the activating party. Notice how in this example the control tree is relatively more complex because of the composition of *Sequence* and *Concur* operators inside the loop.

Example 5: Pitfalls in the use of active eager inputs

To illustrate a case where incorrect operation may occur as a result of the use of active eager inputs, let us consider the segment of code corresponding to a simplified description of a processor's execution unit, shown in figure 3.12. The code describes the operations involved to generate the value to be written to the channel `registerWrite2`. The operation is as follows:

The instruction type and the result from the ALU are read (line 22) and, depending on the instruction type, either a value is read from memory into channel `memDataIn` (line 25) *or* the ALU result is sent through channel `statusIn` to generate a new status word (line 27). The description of the status word generator is shown in lines 2 - 12. For simplicity, this unit simply appends four zeros to the lower 8 bits of the input and casts the result into a value of type `Datapath`. Notice that active eager enclosures are used to read the inputs in both the status generator (line 8) and inside the loop implementing the condition (line 22).

Because the conditional construct guarantees mutual exclusivity in the generation of the values for channels `memDataIn` and `statusOut`, the `select` construct can be used to merge these channels into channel `registerWrite2`. As illustrated in line 37 of the example code, this could be achieved by using an instantiation of the `merge2` module shown in figure 3.4. However, the mutual exclusivity assumption does not hold in the given description as a consequence of using eager active inputs in the module `genNewStatus`: inside this module, the (constant) lower four bits of channel `statusOut` are eagerly generated, without waiting for the input, as soon as the control activates the module (in parallel with the conditional and merge loops).

As previously explained, the `select` construct uses the arrival of bit 0 of the

```
1  -- new status generation unit definition
2  procedure genNewStatus (
3    input statusIn : Datapath;
4    output statusOut : Datapath
5  ) is
6  constant SUFFIX = 0b0000 : 4 bits
7  begin
8      statusIn ->! then
9          -- new status is {i[7:0], 0000}
10         statusOut <- (#SUFFIX @ #statusIn[7..0] as Datapath)
11     end
12 end
13
14 -- declaration of a merge2 module of type Datapath
15 procedure merge2_Datapath is merge2(Datapath)
16  .
17  .
18 procedure Execute(
19 -- I/O declarations
20 ) is
21 -- some local declarations (not shown)
22 .
23 .
24 -- interesting segment of Execute stage:
25     -- select operation
26     loop
27         aluResult, instrType ->! then
28             case instrType of
29               MEMREAD then
30                 getDataFromMem(aluResult, memDataIn)
31             | SETSTATUS then
32                 statusIn <- aluResult
33             end
34         end
35     end ||
36     -- generate new status word
37     loop
38         genNewStatus(statusIn, statusOut)
39     end ||
40     -- Merge values to write in second register bank port
41     loop
42         merge2_Datapath(memDataIn, statusOut, registerWrite2)
43     end
44     .
45     .
46 end -- Execute
```

Figure 3.12: Example of unsafe use of active eager enclosure.

input channels to determine which channel will be selected. The early arrival of the eagerly generated lower four bits of channel `statusOut` will activate too early its side of the *DW*. If the operation to be executed is a read from memory,

both inputs of the *DW* will end up activated. In this situation, the *DW* will erroneously activate the transfers on the two inputs of the *CallMux* generating interference on its output (the incomplete dual-rail codeword from `statusOut` will be merged (ORed) with the dual-rail codeword from channel `registerWrite2`). This interference will result in a deadlock, either because of the generation of invalid dual-rail codewords or the impossibility of completing the RTZ phase on channel `registerWrite2`.

In summary, within an active eager enclosure, every data generation construct that involves concatenation (like the `@` operator, record construction and casting to unsigned wider data types) can be potentially dangerous. If the use of the result data further down the pipeline relies on a mutual exclusivity assumption and some portions of the concatenated data can be generated unconditionally (as within the `genNewStatus` module of the example) the non-eager active enclosure must be used.

Example 6: permissive *Concur*

If, in the previous example, non-eager active enclosure is used in the `genNewStatus` module, the mutual exclusivity of channels `memDataIn` and `newStatus` will be guaranteed. In this situation, it is possible to use the permissive `Concur` operator (`||!`) between the loop of the conditional construct and the `genNewStatus` instantiation to allow these operations to write to the common channel `registerWrite2`, eliminating the need for a merge module, as shown in figure 3.13, lines 25 and 33. The `||!` operator implicitly introduces a *CallMux* to merge writes to the same channel within the composed commands.

Figure 3.14 shows a simplified handshake circuit for the *corrected* version of the code in figure 3.12 (no active eager enclosure in line 8) and figure 3.15 shows the circuit for the new version. Because all of the parallel-composed commands are unbounded loops, the Balsa compiler inserts a cheaper *WireFork* ($W\hat{}$) component instead of a *Concur*. The *WireFork* simply forks the activation signal to each of the *Loop* components and, just like the *Loop* component themselves, never returns an acknowledgement. *PassivatorPush* ($\bullet$) components are used to connect active inputs and outputs as will be explained in section 3.3.13. In both circuits, only the merge section has been detailed to highlight the benefits of using the permissive *Concur*.

Comparing both circuits, it is clear that the new circuit is simpler: The whole

```
19 -- segment of Execute stage:
20     -- select operation
21     loop
22         aluResult, instrType ->! then
23             case instrType of
24               MEMREAD then
25                 getDataFromMem(aluResult, registerWrite2)
26             | SETSTATUS then
27                 statusIn <- aluResult
28             end
29         end
30     end ||!
31     -- generate new status word
32     loop
33         genNewStatus(statusIn, registerWrite2)
34     end
35     -- Now merge is implicit when using the same channel and ||!
36     .
37     .
38     .
```

Figure 3.13: Using the permissive *Concur* with mutually exclusive writes.

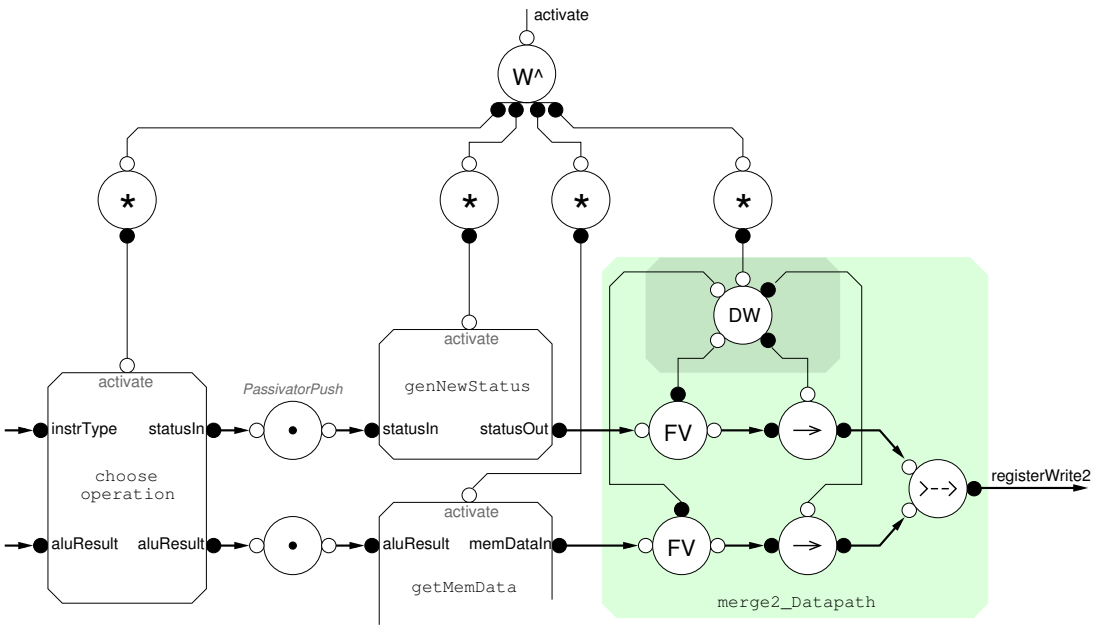

Figure 3.14: Example of merging channels using the `select` construct.

`merge2_Datapath` module has been replaced with a single *CallMux*. The new circuit benefits from having less datapath latency (the *FV*s have been removed and there is no control for the merge section). The reduction in components results in smaller area and lower energy as additional benefits. Finally, the resulting description is simpler.

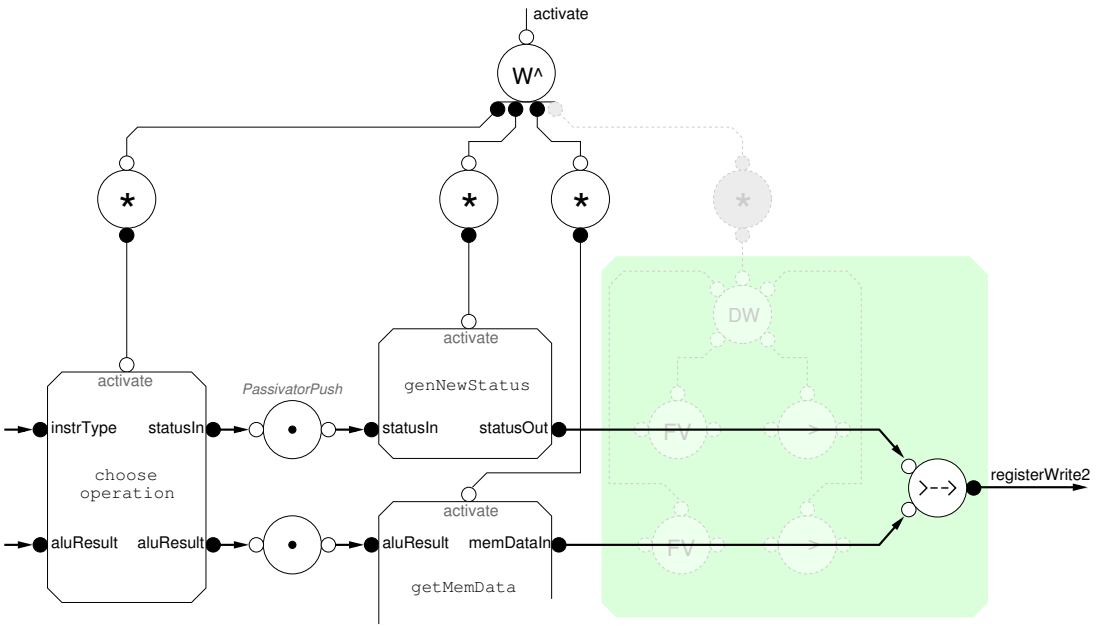

Figure 3.15: Example of merging channels using the permissive *Concur* operator.

The benefits on performance and expressiveness allowed by the (`|||`) operator were exploited in the design of the Forwarding Unit for the nanoSpa processor that will be described in section 7.4.

3.3.13 Interconnecting Balsa modules

Balsa circuits generally have active inputs and outputs, that is, the synthesised modules have *pull-push* input-output interfaces. To connect an active output port with an active input, a component that synchronises requests from both sides before acknowledging them is used: the *Passivator* (*PassivatorPush* in the case of data channels). Figure 3.16 shows the use of this component to connect two Balsa procedures (modules) using one control and two data channels and the implementation of a 1-bit dual-rail *PassivatorPush*.

3.4 Summary

This chapter introduced the Balsa Synthesis System and the Balsa language. Details of the compilation scheme targeting handshake circuits were presented with the aim of highlighting the mapping of the main set of language constructs that will be used in the next chapter. This chapter also presented some previously

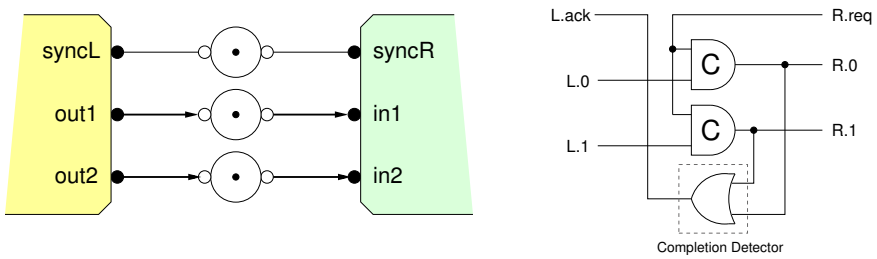

(a) (b)

Figure 3.16: (a) Interfacing of two Balsa modules with active ports using *Passivators*. (b) A 1-bit dual-rail *PassivatorPush*.

undocumented features of the language, namely, the use of active eager enclosure and its implications on the expected operation of the circuit, and the use of the *permissive Concur* operator, illustrating in both cases their potential benefits.

Chapter 4

Optimising Balsa circuits

4.1 Introduction

The syntax-directed synthesis paradigm has been shown to be a powerful synthesis approach. However, its control-driven nature results in significant performance overhead [100, 101]. In an attempt to reduce this overhead, the following circuit-level approaches have been previously reported:

- *Peephole optimisations*: this technique is based on the identification of a pattern of components that can be replaced with a faster alternative [106, 83, 19].
- *Control resynthesis*: this technique consists on clustering sections of control trees and replacing these with an optimised controller that implements the same behaviour [19, 60, 88].
- *Component optimisation*: this is based on finding alternative designs for the handshake components that result in more concurrent, faster operation [85].

An orthogonal alternative to the above is to exploit the *directness* of the synthesis method at the description level. Highly expressive, high-level description languages like Balsa and Haste can result in naïve descriptions with poor performance unless the designer has a good understanding of the underlying compilation process. Furthermore, it is often claimed that in this approach, an experienced designer could make performance/power/area trade-offs. This task would be easier if the designer could have some insight into the impact of a particular construct or coding style.

This chapter explores the effects of directness in the performance of Balsa synthesised circuits and proposes coding techniques and optimisations that result in more concurrent, faster implementations. The chapter begins with the description of a set of language-level techniques for increasing the performance of Balsa circuits. Finally, new peephole optimisation and handshake circuits that further improve the performance of the designs are described.

4.2 Related work

In [85], Plana *et al.* used Balsa to demonstrate the impact on performance of some description-level techniques combined with the introduction of more concurrent handshakes components when applied to the synthesis of a RISC processor. In particular, true asynchronous operation of the processor pipeline, a data-driven coding style and the use of speculation within the execution stage are presented as performance-driven description techniques. In this thesis, those techniques are revisited and further investigated together with new techniques introduced here, using various design examples.

In a recent work, Hansen and Singh [47] describe a series of automated "source-to-source" transformations that optimise syntax-directed descriptions using a variety of concurrency-enhancing optimisations including: automatic parallelisation, automatic pipelining using pipeline variables, arithmetic optimisation and reordering of channel communication. The proposed transformations target Haste descriptions. Although considerable speed-ups are claimed, some of the example designs start with extremely naïve code sequences (with *all* operations initially sequenced), where significant improvements can be easily obtained. The transformations proposed here target both sequential and parallel compositions, make use of explicit buffering as an alternative to pipeline variables and do not use speculation to optimise conditionals.

The approach proposed in the mentioned work is limited to *slack elastic* [64] systems descriptions only (a slack elastic system preserves correct operation even if extra pipeline buffer stages are introduced in any channel). This limitation reduces the usefulness of an "automated" approach as it is frequently necessary for the designer to understand the nature of the transformations to ensure they are safe, which may represent a considerable design effort for the user. Furthermore, automatic code generation frequently needs to be used in conjunction with manual

optimisation because there may be some code that needs to be hand-crafted to meet specific design constraints. In contrast to the ones presented in the mentioned work, the examples used in this thesis are more complex and non-slack elastic: they contain *Merge*s (uncontrolled multiplexers), like the processor and the router.

The approach used here is more general and attempts to give the designer a clearer understanding of the source of performance inefficiencies, the techniques available to reduce it and the trade-offs made. As an additional and important benefit, manual optimisation techniques can be applied to exploit the designer's knowledge about the behaviour of the system. This knowledge is something that is more complex to automate because it cannot be inferred by analysing the code.

This work is complementary to the approaches presented above and to the circuit-level optimisation techniques. The techniques presented here could also serve as a source for optimising compilers or to enhance automated source-to-source transformations.

4.3 The data-driven description style

In Balsa/Haste it is relatively easy for a user to write a working, but most likely low-performance, description of a system due to their similarities with C and Verilog language. One of the major challenges for an asynchronous designer is to learn to think in terms of concurrent processes, instead of the easier to understand sequential processing found in imperative languages. An imperative, sequential description generates a large control tree that directs the flow of data in the datapath. This large control tree results in performance penalties that tends to increase with the complexity of the description.

As an example, consider the simplified description of the *EXECUTE* stage of the SPA processor given in [85], which is reproduced in figure 4.1(a). Here, all actions are explicitly sequenced and in every "step" the control tree activates the *Fetch* components (`->`) to guide the data through the required unit. Due to this lockstep mode, the control tree guarantees mutual exclusivity of the results, allowing the use of a simple *CallMux* (`|`) to write the results into the register write-back. The resulting simplified handshake circuit is shown in figure 4.1(b).

However, it is possible to describe a more concurrent operation by using a *data-driven* description style, that is, a description in which the arrival of data

```
  doRegisterRead
;
  case instruction of
   ADD then
      doShift
     ;
      doAlu
  | MUL then
      doMul
  | LDR, STR then
      doMemAccess
  end
;
  doRegisterWriteBack
```

(a)

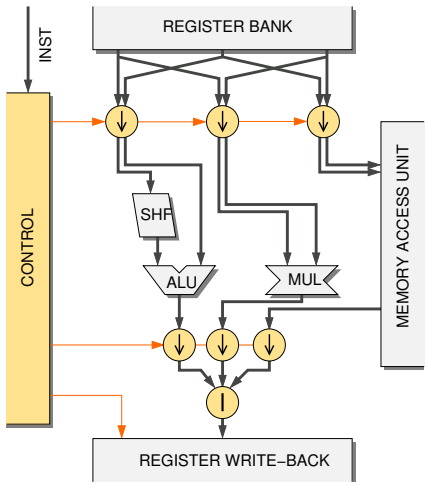

(b)

Figure 4.1: The simplified control-driven SPA *EXECUTE* stage [85].

activates the units. In the data-driven style the description of a circuit is divided into simpler, concurrent actions that communicate using channels. Given the asynchronous nature of the circuits, these actions are activated immediately by the data arriving at their inputs, process the information and generate outputs to activate the next unit.

This strategy is used in the alternative description of the SPA's *EXECUTE* stage shown in figure 4.2(a). Instead of providing an explicit sequencing of actions (with its associated large, slow control tree), the actions are composed concurrently, with incoming data used as the activation. The resulting control tree is generally small and local to the modules implementing the actions. To guide the data, *steer* (demultiplexing with optional multicasting) and *multiplexer* units are added. Control for these units comes directly from the decoder and does not involve any sequencing. Notice that this steering and multiplexing is a specific requirement of the example, not a general feature of data-driven descriptions. The simplified handshake circuit is shown in figure 4.2(b).

Key to implementing data-driven circuits is an adequate partitioning of the circuit into actions/groups of actions that source and consume data. Internal channels will connect these actions. The partitioning also involves determining the group of actions that will necessarily require sequencing, as unnecessary sequencing is a well-known source of overheads. Sequencing is normally associated with the use of variables but also may be required to prevent deadlocks. Every

```
steerRegData ||
doRegisterRead ||
doShift ||
doAlu ||
doMul ||
doMemAccess ||
multiplexResults ||
doRegisterWriteBack
```

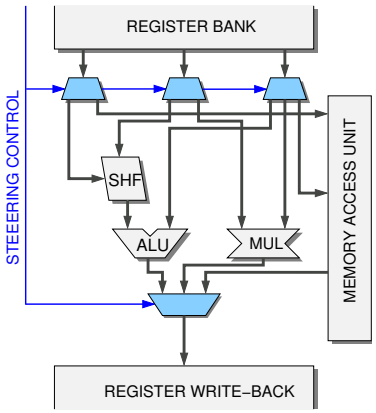

(a) (b)

Figure 4.2: The simplified data-driven SPA *EXECUTE* stage [85].

variable that has a write-then-read access pattern inside each iteration of a group of actions can be substituted by a channel write and an enclosing read (where the value can be read as many times as required). Only variables that store a value required in the next iteration need to be left in the description.

4.3.1 Control driven to data driven example

Consider the description of a branch metric unit (BMU) for a soft-decision-based Viterbi decoder like the one described in [16]. This unit takes two 3-bit quantities (a,c) which are soft-coded representations of the two received bits in a Viterbi decoder. For each input, 000 (0) denotes the reception of a strong zero and 111 (7) indicates a strong 1.

The task of the BMU is to calculate the distance (branch weight) between the received pair and the ideal branch pattern symbols (0,0), (0,7), (7,0), (7,7), as shown in figure 4.3(a). The distance to be calculated is the Manhattan distance, as this turns out to be equivalent to the Euclidean distance squared in this application [91]. The required branch weights are: $d00 = a + c$, $d01 = a + d$, $d10 = b + c$, $d11 = b + d$, where $b = 7 - a$ and $d = 7 - c$.

The linear weights are further minimised (reduced) by subtracting the x and y distance to the nearest ideal point, so the smallest linear metric is always made zero. This can be done by finding the smallest linear metric and then subtracting this value from every metric. Figure 4.3(b) depicts the BMU algorithm.

An almost direct translation of the branch metrics algorithm into Balsa is

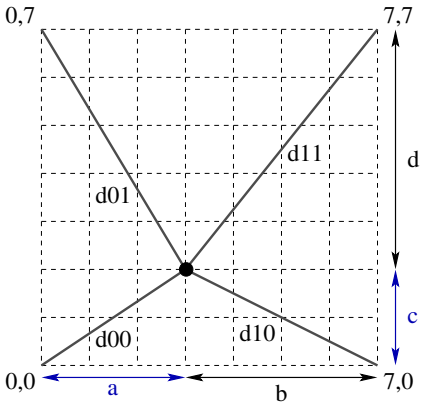

(a)

```
input (a,c) ;
b ← 7 - a ;
d ← 7 - c ;
d00 ← a + c ;
d01 ← a + d ;
d10 ← b + c ;
d11 ← b + d ;
smallestM ← smallest(d00, d01, d10, d11);
bm00 ← d00 - smallestM ;
bm01 ← d01 - smallestM ;
bm10 ← d10 - smallestM ;
bm11 ← d11 - smallestM ;
output(bm00, bm01, bm10, bm11)
```

(b)

Figure 4.3: Branch metric computation for a Viterbi decoder [91].

shown in figure 4.4. This description is very similar to the one that a novice Balsa user wrote for this unit in [42], although it is not a completely fully-sequential naïve description: values for b, d and $d00$ are calculated concurrently, and after that, the remaining metrics are calculated. To find the smallest metric, they are compared in pairs (concurrently) and two are discarded. The process is then repeated to get the final result. The four reduced metrics (outputs) are also calculated in parallel by subtracting this value. Figure 4.5 shows the compiled handshake circuit (the diagram was generated using the `breeze-sim-ctrl` tool).

In the circuit, the highlighted control tree shows the six-way sequencer used to activated each group of concurrent commands labelled (1) to (6) at the right side of the given code. The control tree reflects the use of `;` and `||` commands in the description.

An examination of the algorithm reveals that all variables have a write-then-read pattern, so instead of using variables, we could use channels to pass data directly from sources to the commands that make the processing. The processing commands will use active enclosure to read from channels.

For instance, consider the first three groups of actions in the above description (lines 15 to 23) which are reproduced in figure 4.6(a). The two input reads can be changed into an active input enclosure of the actions (2) and (3) as both actions require the value of the input channels `ia` and `ic`. In this particular case, the enclosure requirements are relaxed (the results can be generated in any order as soon as the inputs are available) and we can use eager active enclosure.

```
1  -- A Branch Metric Unit for soft-decision
2  -- Viterbi decoder with 3-bit quantisation
3  type TInp is 3 bits
4  type TOut is 4 bits
5  procedure BMU(
6    input ia, ic : TInp;
7    output bm00, bm01, bm10, bm11 : TOut
8  ) is
9    variable a, c : TInp
10   variable b, d : TOut
11   variable d00, d01, d10, d11 : TOut
12   variable tempA, tempB, smallestM : TOut
13 begin
14     loop
15         [ ia -> a || ic -> c ] ; -- read inputs (1)
16         -- first batch of calculations          (2)
17         [ b   := (7 - a as TOut)  ||
18           d   := (7 - c as TOut)  ||
19           d00 := (a + c as TOut) ] ;
20         -- compute the other metrics            (3)
21         [ d01 := (a + d as TOut)  ||
22           d10 := (b + c as TOut)  ||
23           d11 := (b + d as TOut) ] ;
24         -- now find the smallest metric         (4)
25         if d00 < d01 then
26             tempA := d00
27         else
28             tempA := d01
29         end ||
30         if d10 < d11 then
31             tempB := d10
32         else
33             tempB := d11
34         end ;
35         -- resolve which is the smallest        (5)
36         if tempA < tempB then
37             smallestM := tempA
38         else
39             smallestM := tempB
40         end ;
41         -- generate the reduced outputs         (6)
42         [ bm00 <- (d00 - smallestM as TOut) ||
43           bm01 <- (d01 - smallestM as TOut) ||
44           bm10 <- (d10 - smallestM as TOut) ||
45           bm11 <- (d11 - smallestM as TOut) ]
46     end
47 end
```

Figure 4.4: Initial BMU description.

Inside the enclosure, variables `b` and `d` are replaced by local channels that are written during action (2) and *concurrently* read during action (3) using another active enclosure. Inside this last enclosure, variables `d01` to `d11` are replaced in a

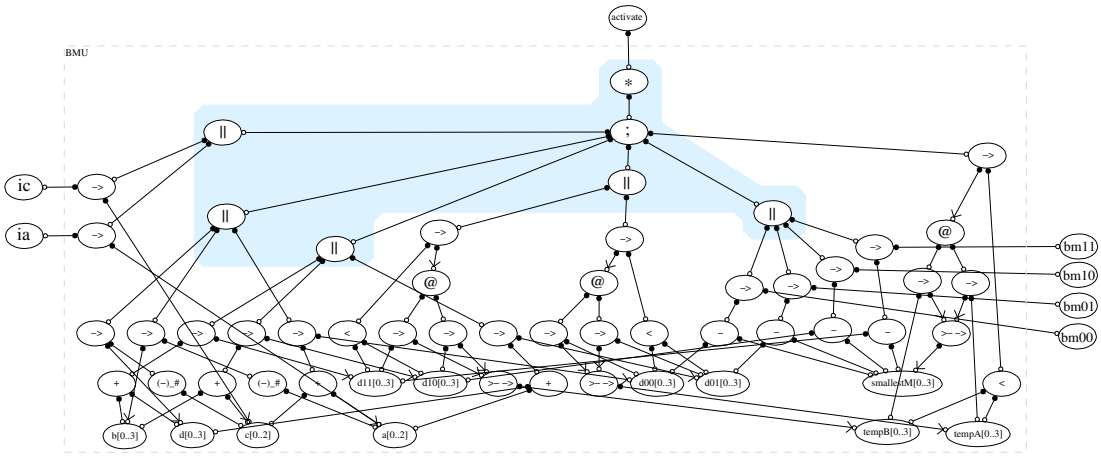

Figure 4.5: Handshake circuit of the BMU.

similar fashion. Because the values are now available in channels, the **;** operators are replaced by **||** operators increasing the concurrency of the actions. These modifications are shown in figure 4.6(b).

```
[ ia -> a || ic -> c ] ; --      (1)
-- first batch of calculations   (2)
[ b   := (7 - a as TOut)  ||
  d   := (7 - c as TOut)  ||
  d00 := (a + c as TOut) ] ;
-- compute the other metrics     (3)
[ d01 := (a + d as TOut)  ||
  d10 := (b + c as TOut)  ||
  d11 := (b + d as TOut) ]
```

(*a*)

```
ia, ic ->! then -- read inputs   (1)
    -- first batch of calcs      (2)
    b   <- (7 - ia as TOut)  ||
    d   <- (7 - ic as TOut)  ||
    d00 <- (ia + ic as TOut) ||
    -- compute the other metrics (3)
    b, d ->! then
        d01 <- (ia + d as TOut) ||
        d10 <- (b + ic as TOut) ||
        d11 <- (b + d as TOut)
    end
end
```

(*b*)

Figure 4.6: First operations of the BMU: (*a*) original, (*b*) Data-driven.

The replacements and active enclosure use described above can be applied to the remaining actions, resulting in the optimised code shown in figure 4.7. The compiled handshake circuit is shown in figure 4.8. The *activeEagerFalseVariable* (`aeFV`) components associated with each enclosure are light coloured, grouped and labelled for illustrative purposes. Notice how the six-way *Sequence* in the initial circuit has been replaced by a two-way *Concur* plus separated small controllers for each group of enclosed actions.

```
1  -- A Branch Metric Unit for soft-decision
2  -- Viterbi decoder with 3-bit quantisation
3  type TInp is 3 bits
4  type TOut is 4 bits
5  procedure BMU(
6    input ia, ic : TInp;
7    output bm00, bm01, bm10, bm11 : TOut
8  ) is
9    channel a, c : TInp
10   channel b, d : TOut
11   channel d00, d01, d10, d11 : TOut
12   channel tempA, tempB, smallestM : TOut
13 begin
14     loop
15         ia, ic ->! then -- read inputs                (1)
16             -- first batch of calculations            (2)
17             b   <- (7 - ia as TOut)  ||
18             d   <- (7 - ic as TOut)  ||
19             d00 <- (ia + ic as TOut) ||
20             -- compute the other metrics              (3)
21             b, d ->! then
22                 d01 <- (ia + d as TOut) ||
23                 d10 <- (b + ic as TOut) ||
24                 d11 <- (b + d as TOut)
25             end
26         end ||
27         d00, d01, d10, d11 ->! then
28         -- now find the smallest metric              (4)
29             if (d00 < d01) then
30                 tempA <- d00
31             else
32                 tempA <- d01
33             end ||
34             if (d10 < d11) then
35                 tempB <- d10
36             else
37                 tempB <- d11
38             end || -- resolve which is the smallest  (5)
39             tempA, tempB ->! then
40                 if (tempA < tempB) then
41                     smallestM <- tempA
42                 else
43                     smallestM <- tempB
44                 end
45             end ||
46             smallestM ->! then
47             -- generate the reduced outputs          (6)
48                 bm00 <- (d00 - smallestM as TOut) ||
49                 bm01 <- (d01 - smallestM as TOut) ||
50                 bm10 <- (d10 - smallestM as TOut) ||
51                 bm11 <- (d11 - smallestM as TOut)
52             end
53         end
54     end
55 end
```

Figure 4.7: Optimised BMU description.

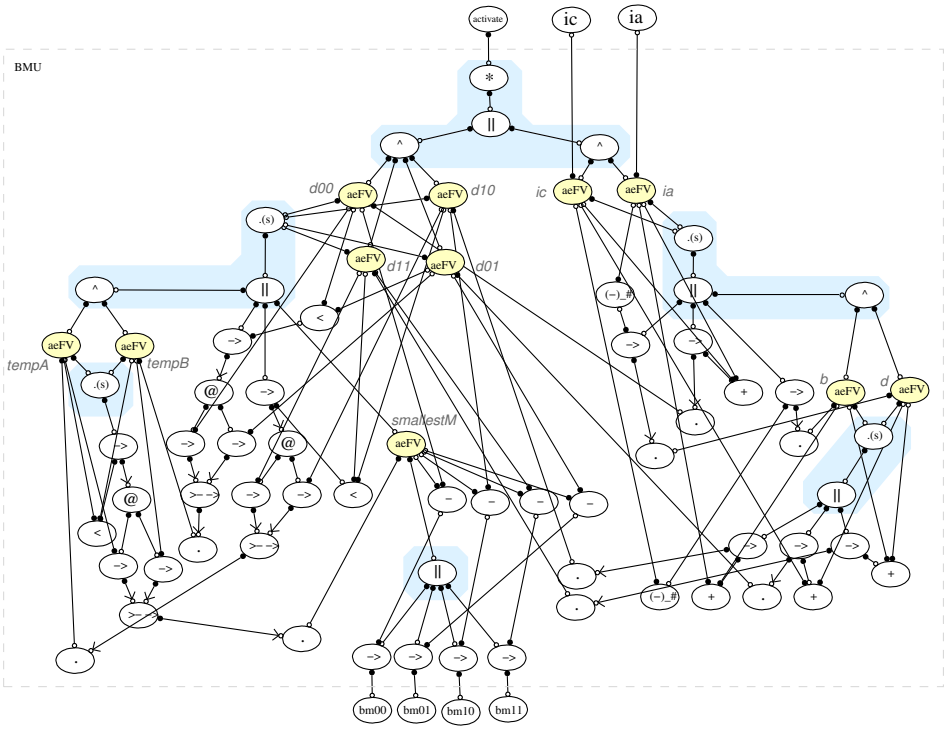

Figure 4.8: Handshake circuit of the optimised BMU.

A quantitative evaluation demonstrates that the smaller, concurrent control trees increase the performance at the cost of some area penalty, as shown in the simulation results presented in table 4.1. The results are from pre-layout, transistor-level simulation using a 180 nm cell library. The energy results presented throughout this thesis correspond to dynamic energy only. The experimental setup consisted on processing 1000 random pairs of soft-coded symbols (a,c) provided by an eager environment. The figure of merit is the average processing time ($t_{process}$) of a symbol pair.

Device	$t_{process}$ (ns)	Relative speed	Area (transistors)	Relative area	Relative energy
BMU Original	9.152	1.00	9663	1.00	1.00
BMU Optimised	6.906	1.33	10898	1.13	1.22

Table 4.1: BMU Simulation results.

Thanks to the directness of the compilation method and the availability of different constructs, there is no a single way of writing data-driven descriptions. Pipelining and paralellising descriptions can be done in different fashions as will be demonstrated in the next sections.

4.4 Optimising data-driven descriptions

In this section different performance-optimised data-driven description techniques will be introduced. To give a clearer idea of the effects in the code, a simplified version of the BMU (without the linear weight minimisation step) will be used here for code and handshake circuit examples. That is, the body of the reference data-driven description will be the code in figure 4.6(b) embedded in a `loop ... end` construct.

As an initial evaluation of the performance gains and trade-offs made, this section also presents pre-layout, transistor-level simulation results for the complete BMU example using the proposed techniques. Results for more complex designs (including the complete Viterbi decoder) will be presented and discussed in chapter 7.

4.4.1 Separating actions into concurrent loops

The example code in figure 4.9(a), which is already split in two groups of actions, can be split into two concurrent enclosed groups instead of having two nested enclosures. Furthermore, the outer unbounded loop can be split into two concurrent unbounded loops, where any value of the original enclosure required in the second loop must be passed using new internal channels. In this example, the values of `ia` and `ic` required in the second group are transferred together with `b` and `d`, as shown in figure 4.9(b). In general, this "splitting" can continue until all grouping possibilities are exhausted, according to the dependencies of the commands. Notice the use of active eager enclosures in the description.

The resulting circuits are shown in figure 4.9(c) and (d). After the splitting process the datapath will be a pipelineable description *without* pipeline registers. On the control side, the control tree in the middle has been split and now the control for the second round of computations runs concurrently with the control of the input section. The new description results in the addition of two extra *aeFV*s (for the copies of `ia` and `ib` passed to the bottom loop). The four *aeFV*s decouple the RTZ phases of the control of the two loops, without adding any latency.

The results for the BMU description that uses this technique are labelled *"Lopt non-eager" "Lopt eager"* in the graphs of figure 4.10. These correspond to the use of normal and eager active enclosures respectively. All results are normalised

to those of the *BMU original* design presented earlier in table 4.1. Let us refer for now to the first group of bars labelled *"no ch. broadcast"* in figure 4.10 (the other groups of results will be introduced later). From the graphs, the performance gain using the technique just introduced is ∼1.5 for the eager version (compare to the previous 1.33 in table 4.1 which also uses eager enclosures), with a relative area and energy of ∼1.3 and ∼1.5 respectively. Notice that the non-eager version does not produce any significant performance improvement, it is included in the results to highlight the benefits of the active eager enclosure.

```
loop
    ia, ic ->! then
        b   <- (7 - ia as TOut)  ||
        d   <- (7 - ic as TOut)  ||
        d00 <- (ia + ic as TOut) ||
        -- compute the other metrics
        b, d ->! then
            d01 <- (ia + d as TOut) ||
            d10 <- (b + ic as TOut) ||
            d11 <- (b + d as TOut)
        end
    end
end
```

(a)

```
loop
    ia, ic ->! then
        b   <- (7 - ia as TOut)  ||
        d   <- (7 - ic as TOut)  ||
        d00 <- (ia + ic as TOut) ||
        ta  <- ia ||
        tc  <- ic
    end
end ||
loop -- compute the other metrics
    ta, tc, b, d ->! then
        d01 <- (ta + d as TOut) ||
        d10 <- (b + tc as TOut) ||
        d11 <- (b + d as TOut)
    end
end
```

(b)

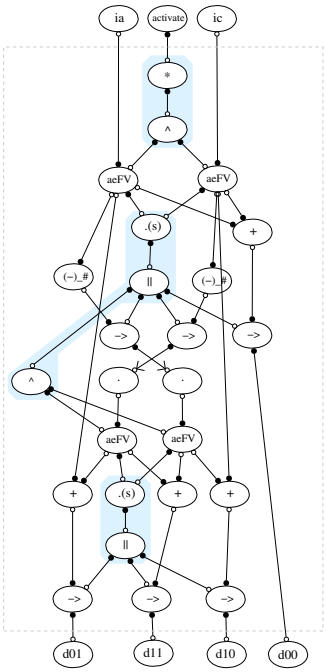

(c)

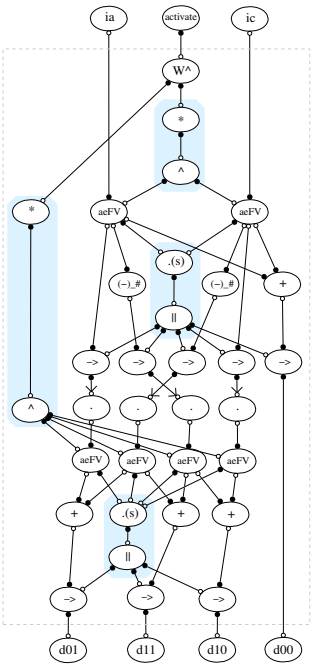

(d)

Figure 4.9: Example of separating actions into concurrent loops (first steps).

An important remark with respect to the level of granularity of this technique is that the throughput will depend on the slowest stage and increasing the pipeline depth will increase the latency. Indiscriminate loop splitting (either manually or automatically) by just analysing precedences and/or dependencies may end up being suboptimal. The designer must take into account the balancing of the pipeline, the nature of the data and the behaviour of the environment among other factors. Being able to express the designer's knowledge about the circuit is an advantage but also a challenge in syntax-directed descriptions.

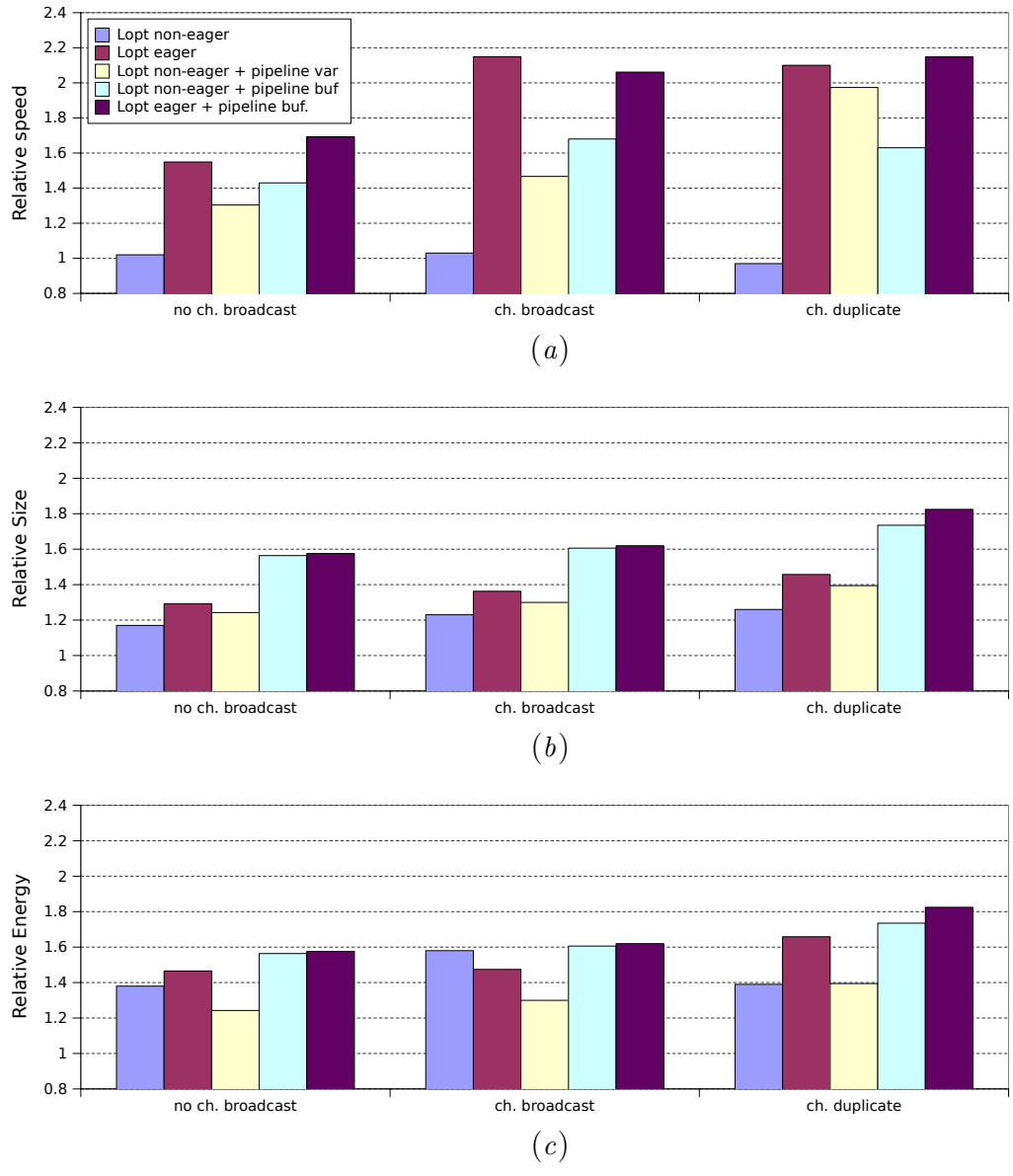

Figure 4.10: Simulation results of different optimisations applied to the BMU.

4.4.2 Broadcasting values

Often within a pipeline, a value from a channel is required unconditionally and concurrently by more than one stage in the pipeline, as noticed previously with `ia` and `ic`. Enclosure provides a means for multicasting values but it may prevent finer grain concurrency and deeper pipelining. For instance, in the code of figure 4.6(a) the groups of actions (2) and (3) are within the same enclosure, hence no new token can be processed by action (2) until action (3) has finished. A solution for this, shown previously in the loop splitting example (figure 4.9(b)), relied on duplicating the values required by the next group of actions inside the active enclosure, but more concurrent solutions for broadcasting are possible. In Balsa, there are two ways of specifying multiple concurrent receivers for the same channel:

i. Using implicit *broadcasting*: In the description, the channel is read in every place that it is required. In this case, the reads are fully synchronised: the data will be available to the reading processes only after every read request has been received. Similarly, data withdrawal will begin only after all reading processes have signalled the consumption of data.

ii. Using explicit *duplication* of the channel by means of enclosure. This method provides more decoupling between processing and the RTZ phases of the reads, as every request will be granted independently of the arrival of the others.

The code in figure 4.11 show these two forms of broadcasting in the simplified BMU example. This technique further improves concurrency, which results in higher performance at the cost of some area and energy penalties. The bins labelled *"ch. duplicate"* and *"ch. broadcast"* in the graphs of figure 4.10 shows the results for the complete BMU design when these techniques are applied. Referring to the *"Lopt eager"* columns, the increase in performance is now ∼2.1 (slightly larger for the broadcast method). The relative area and energy are ∼1.45 and ∼1.65 when using channel duplication and a bit smaller (∼1.35 and ∼1.50) when using implicit broadcasting.

In this particular example, the synchronisation penalty imposed by the implicit broadcasting is not apparent because the design has balanced threads: all four outputs are generated using similar operations and the simulation environment generate inputs and consumes outputs eagerly. In designs with this balanced

```
loop
    ia, ic ->! then
        b <- (7 - ia as TOut) ||
        d <- (7 - ic as TOut)
    end
end ||
-- ia and ic reuse in next loop
-- creates implicit broadcasting
loop
    ia, ic, b, d ->! then
        d00 <- (ia + ic as TOut)||
        d01 <- (ia + d as TOut) ||
        d10 <- (ic + b as TOut) ||
        d11 <- (b + d as TOut)
    end
end
```

(a)

```
loop -- make two copies of ia explicitly
    ia ->! then  a1 <- ia || a2 <- ia end
end ||
loop -- make two copies of ic explicitly
    ic ->! then c1 <- ic || c2 <- ic end
end  ||
loop
    a1, c1 ->! then
        b <- (7 - a1 as TOut) ||
        d <- (7 - c1 as TOut)
    end
end ||
loop
    a2, c2, b, d ->! then
        d00 <- (a2 + c2 as TOut)||
        d01 <- (a2 + d as TOut) ||
        d10 <- (c2 + b as TOut) ||
        d11 <- (b + d as TOut)
    end
end
```

(b)

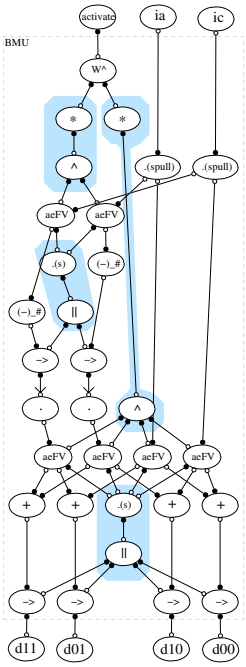

(c)

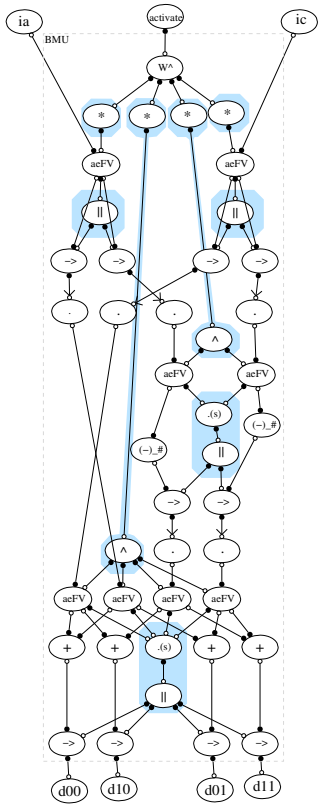

(d)

Figure 4.11: Broadcasting: (*a*,*c*) Implicit broadcasting. (*b*,*d*) Explicit duplication.

behaviour, broadcasting has the advantage of less area and energy penalties. However, in designs with more complex, unbalanced thread execution patterns, like a

processor, thread decoupling provided by explicit duplication allows a head start for some of the threads required to complete an instruction, resulting in fully asynchronous operations and better performance.

In common with the previous technique, it is difficult to predict the places or levels of granularity to apply efficiently this technique by only analysing the operation precedences or data dependencies without input from the designer's knowledge about the system.

4.4.3 Adding pipeline registers

To increase its throughput, a pipelined description requires inter-stage pipeline registers to decouple them. These can be added in two ways:

i. Using *pipeline variables* within the stage instead of the active enclosure, as presented in [47].

ii. Using explicit pipeline buffer modules (like the one described in section 1.2.3) between stages, as presented in [85].

These two styles are shown in the example codes of figure 4.12. Use of pipeline variables adds a *Sequencer* to the control tree and results in lower performance than the use of explicit pipeline buffers. Results in the graphs of figure 4.10 reveal this performance penalty. However, pipelining using variables is cheaper in terms of area and energy because no extra *FalseVariable* and *Passivator* components are required.

Results for the design that uses pipeline variables are labelled *"Lopt non-eager + pipeline var"*. Results for the designs that use explicit buffering are labelled *"Lopt non-eager + pipeline buf."* and *"Lopt eager + pipeline buf."* (with active eager inputs). Notice how in the latter case, the synchronisation imposed by channel broadcasting has limited the effectiveness of the decoupling.

A detailed look at the results in figure 4.10 reveals that adding pipeline registers when using broadcasting or channel duplication has not noticeably increased the performance, but has increased the area and energy penalties. There are two reasons for this: Firstly, the BMU stages are very simple and have low latency (four bit adders/comparators), the extra latency of the pipeline registers reduces their possible benefits. Secondly, as seen in the previous examples (figure 4.9), the use of active inputs requires *PassivatorPush* components to interface with active

```
-- Pipeline variables :
-- va, vc,
-- vta, vtc, vb, vc
loop
    [ ia -> va || ic -> vc ] ;
    [ b <- (7 - va as TOut) ||
      d <- (7 - vc as TOut) ||
      ta <- va || tc <- vc ]
end ||
loop
    [ ta -> vta || tc -> vtc ||
      b -> vb || d -> vd ] ;
    [ d00 <- (vta + vtc as TOut)||
      d01 <- (vta + vd as TOut) ||
      d10 <- (vtc + vb as TOut) ||
      d11 <- (vb + vd as TOut) ]
end
```

(a)

```
-- procedure buf3 is buf(TInp)
-- procedure buf4 is buf(TOut)
buf3(a, pa) || buf3(c, pc) ||
loop
    pa, pc ->! then
        b <- (7 - pa as TOut) ||
        d <- (7 - pc as TOut) ||
        ta <- pa || tc <- pc
    end
end ||
buf3(ta, pta) || buf3(tc, ptc) ||
buf4(b, pb) || buf4(d, pd) ||
loop
    pta, ptc, pb, pd ->! then
        d00 <- (pta + ptc as TOut)||
        d01 <- (pta + pd as TOut) ||
        d10 <- (ptc + pb as TOut) ||
        d11 <- (pb + pd as TOut)
    end
end
```

(b)

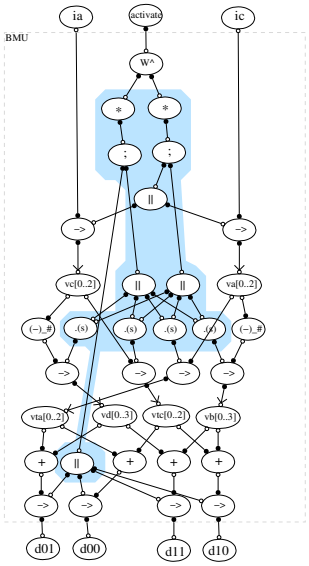

(c)

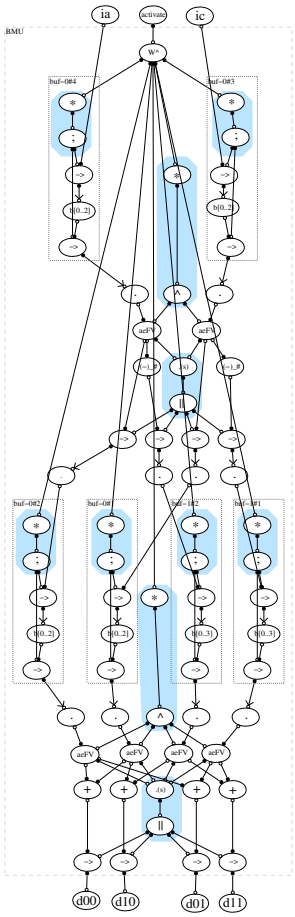

(d)

Figure 4.12: Pipelining: (a,c) using variables. (b,d) using explicit pipeline buffers.

outputs. When using dual-rail or other DI encoding these interface components require storage in the form of C-elements as shown in figure 3.16(b) Hence, the *PassivatorPush* acts as a simple *half latch* [91, 17]. (a half latch allows the active output to withdraw the data after synchronising with the active input request while the other side is in the processing phase). Each time a channel is duplicated using active enclosure, a half latch is added to the pipeline, providing decoupling between stages. Inserting explicit pipeline registers in this case will only contribute to increase the latency and area of the circuit.

In summary, the implicit storage added to the channels when specifying active inputs serves in some cases as a pipeline register which, when combined with the optimised control of the active eager inputs, efficiently implements decoupling between pipeline stages.

4.5 Optimising guards

Another common source of inefficiencies when coding in Balsa is related to the implementation of the guard expressions for conditional loops and for the `case` and `if` constructs. These conditional constructs require the use of handshake circuits that generate control channels from the datapath, like the *Case* component in figure 3.9 and the *While* component in figure 3.11. In many cases, the designer can optimise these datapath-generated control by evaluating the guards before their use in the construct, as will be demonstrated here.

```
input (a, b);
while a ≠ b do
     if a > b  then a ← a − b;
               else b ← b − a;
output (a);
```

Figure 4.13: A pseudo-code specification of GCD [91].

Consider the GCD algorithm example, that computes the greatest common divisor of an integer. Figure 4.13 shows a specification of the GCD algorithm. Figure 4.14(a) shows a direct implementation of the algorithm in Balsa. In the implementation, the two guards (`va /= vb` and `va > vb`) are evaluated only after the control reaches each conditional structure, resulting in an unnecessary delay. The code also exhibits the common "problem" of auto-assignment, which in most cases introduces additional performance penalties (see section 3.3.5).

The performance-optimised description of the GCD shown in figure 4.14(b) illustrates how to solve the above problems: Firstly, to avoid auto-assignment, two additional variables (`tva` and `tvb`) are used as temporary storage. Secondly, the two required guards are evaluated in parallel and stored using 1-bit variables `neq` and `gt`. The resulting handshake circuits are shown below the code.

Notice in the circuit at the left how the body of the `loop ... while` (highlighted) contains four sequenced operations:

i. Evaluate the guard expression for the `loop ... while` construct and proceed accordingly.

ii. Evaluate the guard expression for the `if` construct and make the decision.

iii. Update one of the auxiliary variables (labelled only for variable `b` in the circuit).

iv. Update one of the variables (labelled only for variable `b` in the circuit).

In the optimised circuit at the right the loop has only three sequenced operations:

i. Read the guard expression for the `loop ... while` construct and proceed accordingly.

ii. Read the guard expressions for the `if` construct *and* update one of the auxiliary variables.

iii. Evaluate and store both guards, and update both variables.

Table 4.2 shows the simulation results for the two circuits above. The table compares the average processing time required to calculate the GCD of two 8-bit numbers. Area and energy results are also given.

Device	$t_{process}(ns)$	Relative speed	Area (transistors)	Relative area	Relative energy
GCD Original	181.68	1.00	6856	1.00	1.00
GCD Optimised	133.26	1.36	6991	1.02	1.14

Table 4.2: GCD Simulation results.

```
type dtype is 8 bits
procedure gcd
(
  input a, b : dtype;
  output gcdout : dtype
) is
  variable va, vb : dtype
begin
   loop
      [ a -> va || b -> vb ] ;
      loop
      while va /= vb then
         if va > vb then
            va := (va - vb as dtype)
         else
            vb := (vb - va as dtype)
         end
      end ;
      gcdout <- va
   end
end
```

(a)

```
type dtype is 8 bits
procedure gcd
(
  input a, b : dtype;
  output gcdout : dtype
) is
  variable va, vb, tva, tvb : dtype
  variable neq, gt : bit
begin
   loop
      [ a -> tva || b -> tvb ] ;
      loop
         neq := tva /= tvb ||
         gt := tva > tvb ||
         va := tva ||
         vb := tvb
      while neq then
         if gt then
            tva := (va - vb as dtype)
         else
            tvb := (vb - va as dtype)
         end
      end ;
      gcdout <- va
   end
end
```

(b)

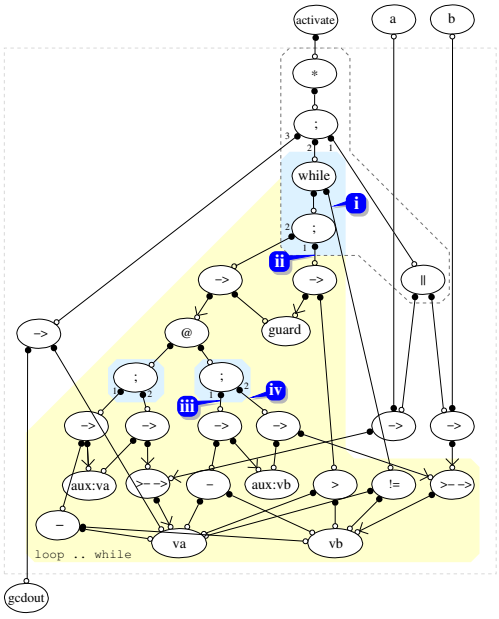

(c)

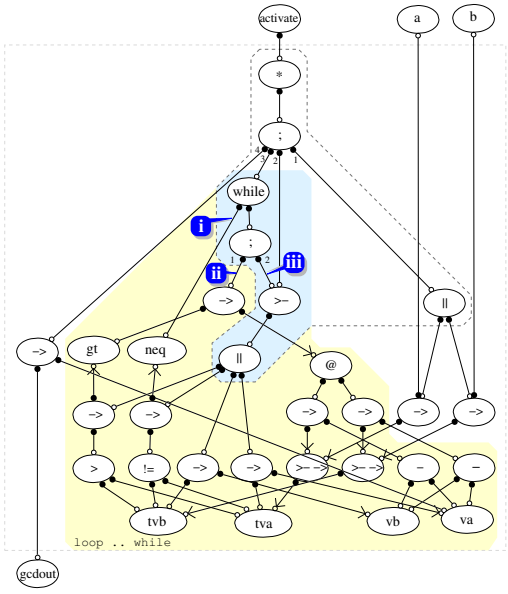

(d)

Figure 4.14: Two implementations of the GCD algorithm in Balsa and their compiled handshake circuits.

As the reader may have already noticed, in this example area and energy are being traded for speed. On each iteration, there is a redundant update operation

of the variable that does not change and two 1-bit variables are used. The design with the optimised guard is 36% faster at the cost of 14% extra energy and negligible area increase.

4.5.1 Encoding multiple guards

In situations where multiple guards are required, it is better to encode the guards into a multi-bit variable and use a `case` construct instead of the more straightforward (but slower) multi-guarded `if` construct. Consider the example code in figure 4.15 adapted from the description of the input buffer of a *sliced-channel* wormhole router designed in Balsa [90]. Each router has five I/O ports, namely, *Local*, *North*, *South*, *East* and *West*. The code shown corresponds to the *South* input buffer and has been simplified for clarity: only the operations over the dataless *sync* channels that generate the request to the destination ports are detailed.

The first value received at input `d_in[0]` is the *header flit*. It contains the XY destination addresses that will be compared with the addresses of the router `addrX` and `addrY`. The destination is chosen accordingly to the comparisons and the order of priority specified in the description. The optimised code is shown in figure 4.16. In this new description, instead of using the `if` construct, all guards are evaluated and stored in parallel with the buffering of the input value within an active enclosure. The four bits generated by these evaluations are then joined and used as the guard expression of a `case` construct. Also, in this new construct the encoding of the guards reflect the priority expressed in the original description.

Simulation results for the wormhole router, which are detailed in section 7.5.3, indicate that the guard encoding technique contributes to an increase of 10% in speed and a reduction of the area to 86% of the original, at the cost of 7% increase in energy consumption.

4.6 New peephole optimisations

The previous sections showed how to write optimised Balsa code targeting high performance. In general, the circuit derived from an optimised data-driven description will consist of small clusters of control components which reduces the possibility of further optimisations using control resynthesis.

```
type Destination is enumeration
  WEST, NORTH, EAST, LOCAL
end

procedure input_buf_south
(
  array 4 of input d_in : 9 bits;
  array 4 of sync req;
  array 16 of output d_out : 9 bits
) is
  variable buf : array 4 of 9 bits
  constant addrX = (2 as 4 bits)
  constant addrY = (2 as 4 bits)

begin
  loop
    d_in[0] -> buf[0];
    -- NOTE: buf[0][4..7] = X, buf[0][0..3] = Y
    if (#(buf[0])[4..7] as 4 bits) < addrX then sync req[NORTH]
        -- data transfer commands ommited
    |  (#(buf[0])[0..3] as 4 bits) > addrY then sync req[EAST]
        -- data transfer commands ommited
    |  (#(buf[0])[0..3] as 4 bits) < addrY then sync req[WEST]
        -- data transfer commands ommited
    else sync req[LOCAL]
    -- data transfer commands ommited
    end
  end
end
```

Figure 4.15: Simplified description of the *South* input buffer of a sliced-channel wormhole router [90].

Part of this research work focused on analysing these optimised circuits and looking for further optimisation opportunities using component substitutions or redesign. This section introduces some new peephole optimisations and components aimed to increase the performance of the synthesised circuits. Datapath optimisations include the removal and substitution of *FalseVariable* components and the use of a more concurrent *Fetch* component. Optimisations for the control of unbounded active input enclosures and unbounded read-then-write actions over a variable are also presented.

The optimisations introduced in this section were manually applied to some of the design examples presented in this thesis, as they are not yet incorporated into the Balsa design flow. Modifying the Balsa compiler to automate these was considered more a time-consuming exercise on compiler development than a contribution to the objectives of this research.

```
type Destination is enumeration
  WEST, NORTH, EAST, LOCAL
end

procedure input_buf_south
(
  array 4 of input d_in : 9 bits;
  array 4 of sync req;
  array 16 of output d_out : 9 bits
) is
  variable buf : array 4 of 9 bits
  constant addrX = (2 as 4 bits)
  constant addrY = (2 as 4 bits)
  channel n, e, w : bit -- guard variables
  channel d_in0 : 9 bits

begin
  loop
  -- NOTE: d_in[0][4..7] = X, d_in[0][0..3] = Y
    d_in[0] ->! then
      n <- (#(d_in[0])[4..7] as 4 bits) < addrX ||
      e <- (#(d_in[0])[0..3] as 4 bits) > addrY ||
      w <- (#(d_in[0])[0..3] as 4 bits) < addrY
      d_in0 <- d_in[0] -- replicate d_in required
    end
  end ||
  loop
    n, e, w ->! then
      case (#w @ #e @ #n as 3 bits) of
       0b1xx then sync req[NORTH]
         -- data transfer commands ommited
      |0b01x then  sync req[EAST]
         -- data transfer commands ommited
      |0b001 then  sync req[WEST]
         -- data transfer commands ommited
      else sync req[LOCAL]
         -- data transfer commands ommited
      end
    end
  end
end
```

Figure 4.16: Optimised, simplified description of the *South* input buffer.

4.6.1 Removing redundant *FalseVariables*

As demonstrated previously in section 3.3.12, active input control can be used in Balsa when there is no input choice. In this case, *Fetch* and *FalseVariable* (or just *activeEagerFalseVariable*) components are used to implement the construct.

In cases when the input channels are *unconditionally* read only once and the control simply transfers the value to a consumer module in the datapath, the

FalseVariable can be removed safely. This can also be done with the *activeEagerFalseVariable* component.

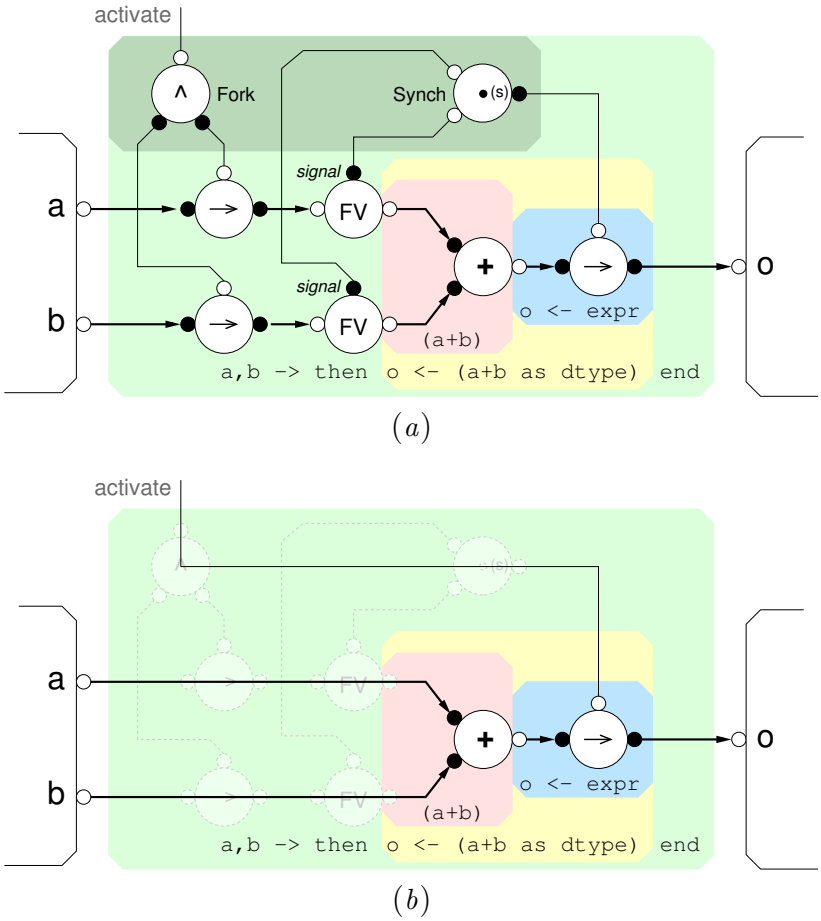

Figure 4.17: Handshake circuit for example in figure 3.6, (*a*) original, (*b*) optimised.

As an example, consider the Balsa code for a simple adder shown previously in figure 3.6 where two input channels, `a` and `b`, are read and then added to produce the output `o`. For convenience, the resulting handshake circuit is reproduced again in figure 4.17(a). In this case, because the two input channels are unconditionally read just once, both *FV*s and the *Synch* are redundant: the control can initiate the read operation by directly triggering the transferrer at the output, which can then immediately start pulling the values from the input channels through the `(+)` operator. Figure 4.17(b) shows the optimised circuit.

The above transformation results in both latency and area reduction, yet preserving the external behaviour of the circuit. The control tree is reduced to

just the activation channel and the two FVs are removed from the datapath. In general, in order to apply this optimisation, the single read of the *FalseVariables* must not be activated through the use of a conditional component (*Case*, *While* or *DW*). For instance, figures 3.5 and 3.9 are examples of circuits where this optimisation cannot be applied.

4.6.2 Control of active enclosures

When two or more channels are used as inputs in an active enclosure, Balsa introduces a *Fork* component to broadcast the activation to the *Fetch* components that push data into the *FalseVariable*s. See for instance figure 4.17(a). With active eager inputs, this signal is passed to the *trigger* inputs of the *activeEagerFalseVariable*s, as shown in figure 3.9.

In both cases, the *signal* control channels of all inputs are synchronised using a *Synch* component, which activates the command that reads from the enclosure once all *signal* requests have been received. Figure 4.18 shows the circuit implementations of the *Fork* and *Synch* components. It can be seen that these components have mirrored circuits. The *Synch* implementation guarantees that, for every input Ii, Ii_{req} occurs before O_{req}. Mathematically, $Ii_{req} \prec O_{req}$. Equivalently in the *Fork*, for every output Oi, $Oi_{ack} \prec I_{ack}$. The *Fork* synchronises all the transferrer/trigger acknowledges before acknowledging the activating party.

Figure 4.18: (*a*) *Fork* implementation. (*b*) *Synch* implementation.

A *Permanent* procedure is a procedure activated using a *Loop* component that is either connected directly or through nothing other than *WireFork*s to the global circuit activation, like the circuit shown in figure 4.19(a). In these cases the synchronisation of acknowledges imposed by the *Fork* is redundant: the *Loop* component does not acknowledge its activation to the caller, hence each *aeFV /Fetch* may be activated independently with separated *Loop*s.

The *Synch* component in the enclosure structure guarantees that only one token from each FV or $aeFV$ is allowed during each execution of the enclosed command. Each *Loop* can issue a new token only after the enclosing command completes. Eliminating the *Fork* reduces the latency of the control and increases the concurrency at the inputs. Figure 4.19(b) shows the optimised circuit. The *WireFork* is required to fork the activation request to all the control loops. Note that the $aeFV$ and its activating *Loop* could be amalgamated into a single component.

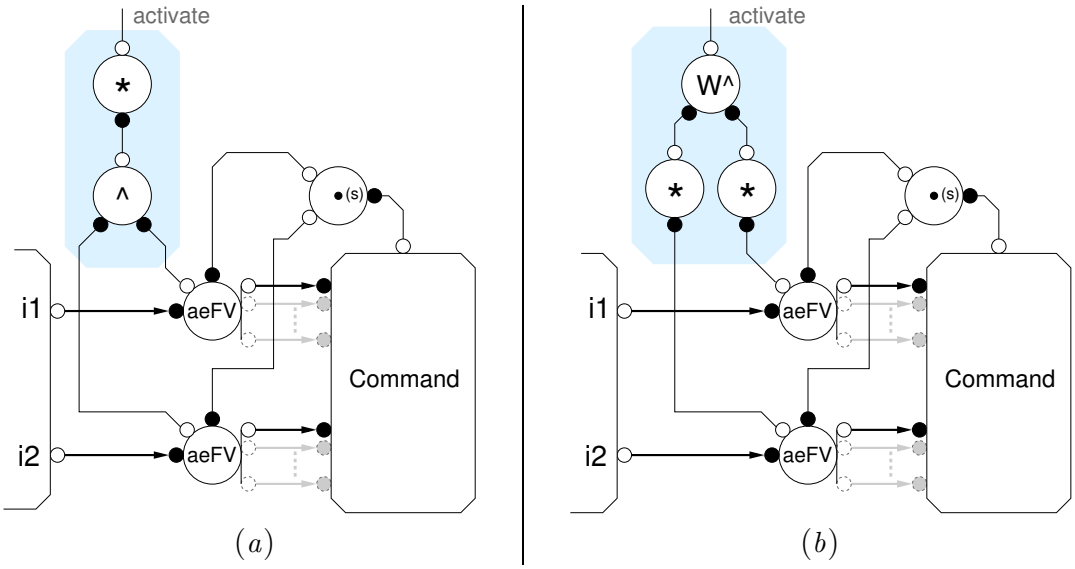

Figure 4.19: Permanent active eager input: (a) original, (b) with optimised control.

4.6.3 Unbounded read-then-write on variables

This section introduces an optimisation of the handshake circuit required to perform unbounded read followed by write actions in variables, based in the unfolding of the first read operation and the use of the optimised sequencer introduced in [89].

Performance of sequenced operations

In synchronous circuits, the sequencing of events is straightforward: event A is sequenced with event B if they occur at different *clocking events*, that is, a full clock pulse, a clock level or a clock transition. In an asynchronous environment,

sequencing is more complicated and generally includes extra control overhead. Sequencing of handshake events must follow the protocol rules in order to avoid data or control hazards that may cause malfunction and deadlock.

Depending on the degree of handshake overlapping allowed, Balsa generates two types of sequencers based on the S-element and T-element respectively [89]. Figure 4.20 presents a block diagram of such components with their respective STGs (see section 2.6.1). Figure 4.21 shows the implementations of the Balsa sequencers and their respective STGs as introduced in [89].

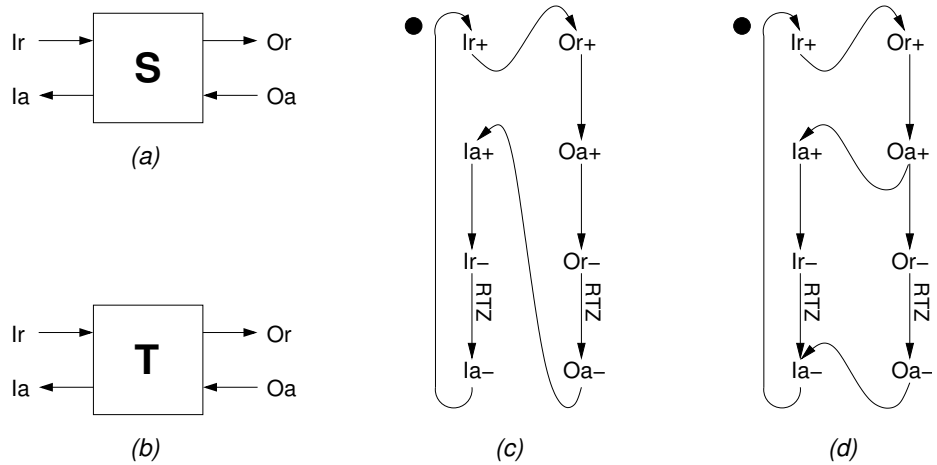

Figure 4.20: (a) S-element. (b) T-element. (c) S-element STG. (d) T-element STG.

Notice that in the sequencer based on the T-element, the RTZ phase of the first command overlaps with the processing phase of the second command and the RTZ of the activation, which results in a more concurrent operation. Unfortunately, it is not always possible to use this type of overlapping due to the possibility of introducing write-after-write (WAW) and write-after-read (WAR) hazards. For a complete discussion of these issues, the interested reader can refer to [89].

A performance penalty occurs in designs where repeated read-then-write operations occur on the same variable. An unbounded repetition of this type can be described in Balsa as shown in the piece of code in figure 4.22(a), where processes `rd_proc()` and `wr_proc()` access the common variable `V`. Figure 4.22(b) shows the resulting handshake circuit. It is necessary in this case the use of a sequencer based on the *S-element* because the use of the T-element based sequencer may introduce a WAR hazard. This hazard is caused by the RTZ phase of the first command trying to close the variable read port concurrently with the second

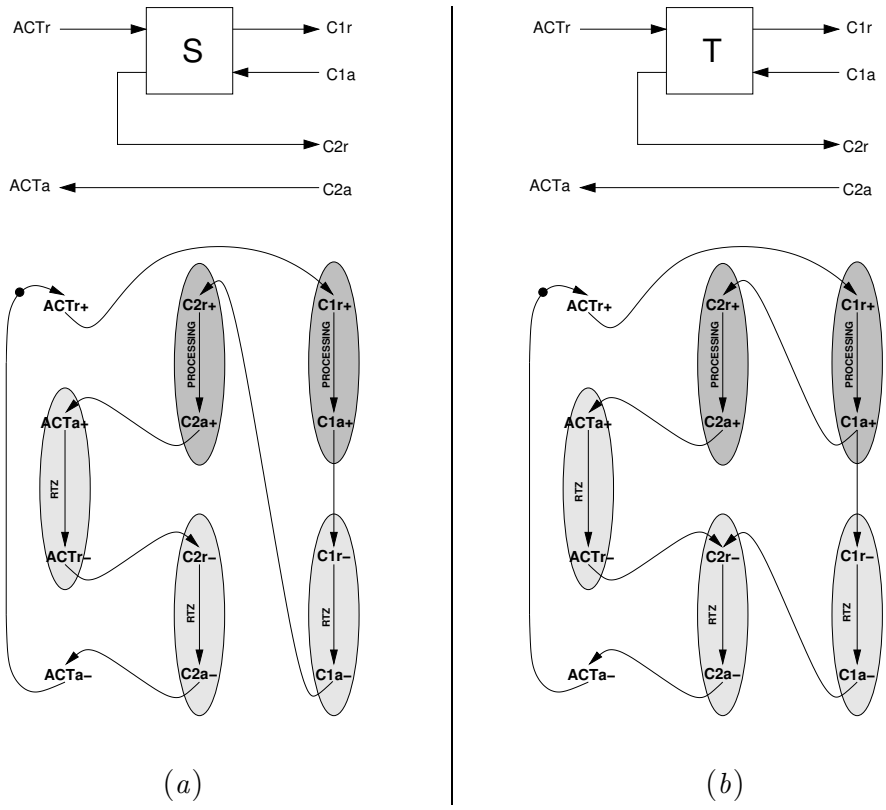

Figure 4.21: Balsa sequencers: (a) based on the S-element, (b) based on the T-element [89].

command trying to write new data. If the new data arrives first it will appear at the output of the read port before it closes, potentially altering the result of the first command [89].

If the first read operation is taken out of the loop construct (the first read operation is *unfolded*), as the code shown in figure 4.23(a), the behaviour will remain the same, but now the operation inside the loop is a write-then-read, which does not have WAR hazards. In Balsa, a write-then-read sequence to a local variable within a procedure will generate a *Sequencer* based in the T-element. However, if the write and read processes reside in separate modules running in parallel, the Balsa compiler is conservative, as the level of allowed overlapping in communications is unknown, and inserts a safe sequencer based on the S-element. Performing this optimisation at the source code level requires the use of multiplexers in the datapath to merge the reads and duplicate blocks (larger area, energy and latency) as shown in the resulting circuit of figure 4.23(b).

```
-- other declarations
variable V : someType
-- other declarations
begin
    loop
       rd_proc(rd_args) ;
       wr_proc(wr_args)
    end
end
```

(a)

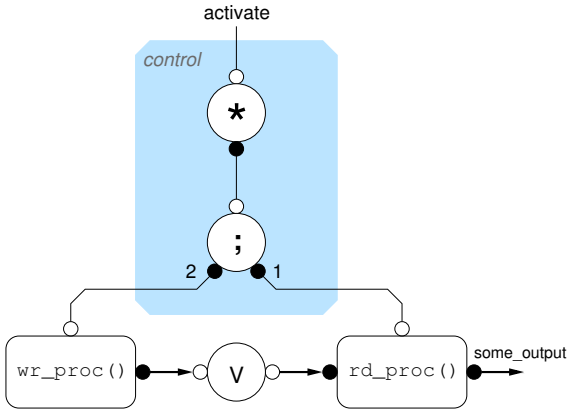

(b)

Figure 4.22: Read-write loop: (a) code, (b) handshake circuit.

```
-- other declarations
variable V : someType
-- other declarations
begin
    rd_proc(rd_args) ;
    loop
       wr_proc(wr_args) ;
       rd_proc(rd_args)
    end
end
```

(a)

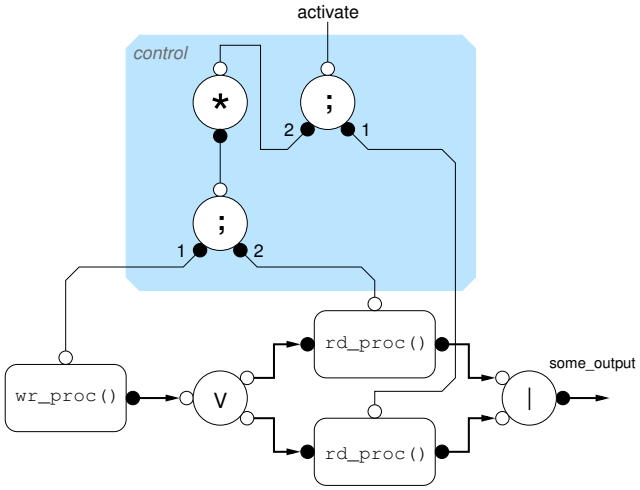

(b)

Figure 4.23: First-read-unfolded version of circuit in figure 4.22.

In order to avoid hardware duplication, Balsa allows the use of *shared procedures* with the limitation that local channels may not be accessed [5]. The proposed solution is to substitute the loop-sequencer control structure obtained for unbounded loop descriptions like the one in figure 4.22(b) by the optimised control shown in figure 4.24(b). This new controller allows write and read RTZ overlapping and does not have local channel accesses restrictions.

In dual-rail circuits, the time required to complete the RTZ phase increases proportionally to the width of the data because the completion detection circuit must check more bits. Table 4.3 shows transistor-level simulation results of first-read-unfolded loops with different data widths. The simulated loop was a simple

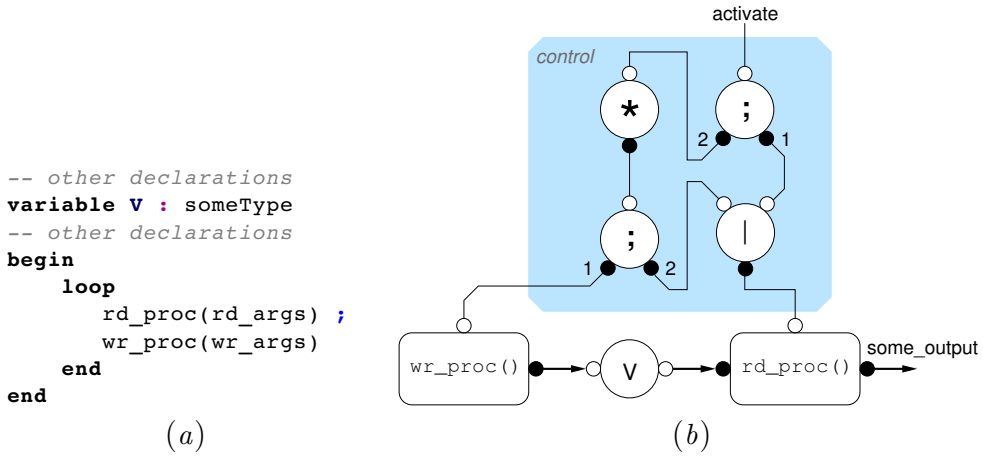

Figure 4.24: Optimised first-read-unfolded read-write loop.

read-then-write to a variable. These figures give an estimated upper bound for the performance gain that can be obtained and show that for datapath widths greater than 3 bits, the speed-up achieved by RTZ overlapping is greater than the overhead of the merge required in the unfolded control tree of figure 4.24. Section 7.4 presents the design of a *Forwarding Unit* that makes use of this optimisation technique.

width (bits)	1	2	3	4	8	16	32	64
speed-up (%)	-11.8	-2.5	-1.0	5.0	7.2	9.0	8.8	11.4

Table 4.3: Influence of data widths in first-read-unfold of read-write unbounded repetitions

4.6.4 Fetch component with concurrent RTZ

The Balsa dual-rail *Fetch* component, shown in figure 4.25(a), consists of wires only, with broad data validity in both data ports. The signal transition graph (STG) in figure 4.25(b) shows how the RTZ phases of the activation, input and output are fully sequenced.

In [81], Peeters described two single-rail transferrers with concurrency in the data channels, the *par-ser* and the *ser-par*, but its implementation in dual-rail would require completion detection inside the *Fetch*. The *Fetch* proposed here, focuses on the concurrency of RTZ phase of data and activation channels: if the handshake on the activation channel is itself enclosed within the handshake

of a wide data channel, the RTZ of that channel will delay unnecessarily the RTZ of the input data channel. In Balsa circuits, this situation occurs when the activation is generated by a *Case* component whose input data port has a considerable number of bits, as found in the implementation of the *Decode* stage of the nanoSpa processor [89, 95] or in the write index for arrayed variables with many entries. A more concurrent operation can allow the RTZ on the activation channel to occur in parallel with the RTZ on the data channels. Figure 4.26 (a) shows the new circuit for the dual-rail fetch and the resulting STG.

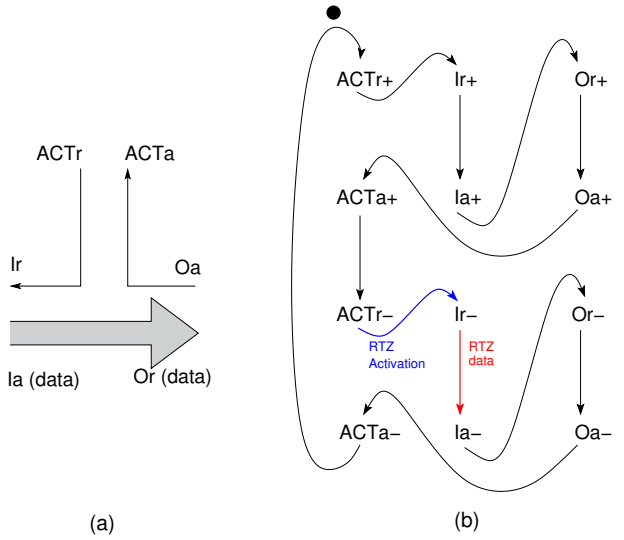

Figure 4.25: Conventional Balsa dual-rail *Fetch*: (*a*) circuit, (*b*) STG.

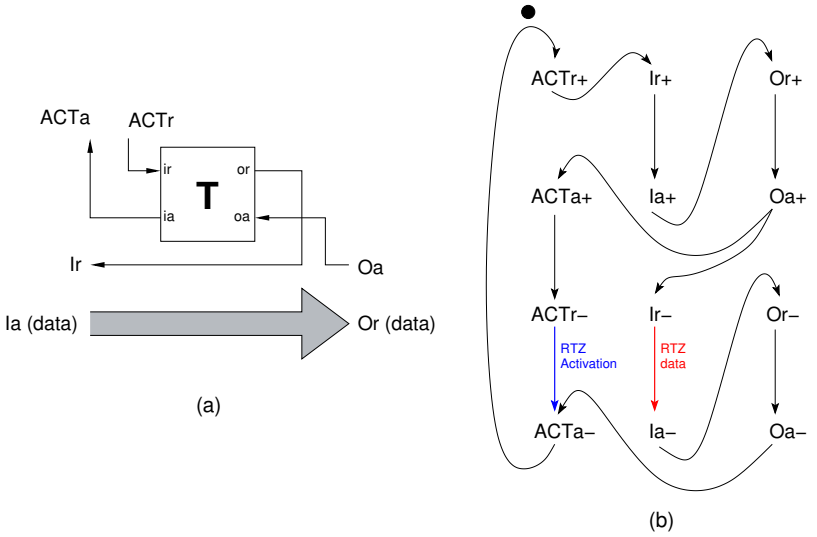

Figure 4.26: Fetch with concurrent RTZ: (*a*) circuit, (*b*) STG.

The new control interface now features a *T-element* which provides the desired decoupling. In order to obtain performance benefits, substitution of the wires-only *Fetch* should only be made when the *Case* component that activates it has a slower RTZ than the delays introduced by the controller in the new *Fetch*, but this threshold can be easily tunable in the compiler. The *nanoSpa* processor and the Viterbi decoder presented in chapter 7 are used as design examples to evaluate this optimisation.

4.6.5 Summary

This chapter has presented a number of description-level optimisations together with their effects in performance, resulting circuit structures and trade-offs made. First, the data-driven description style was introduced as a technique that, using the arrival of data to activate the processing units, results in faster circuits with smaller and localised control sections.

Description level techniques that result in faster data-driven descriptions were introduced and analysed. These included: separation of actions within unbounded loops to increase concurrency, broadcasting styles and stage decoupling techniques. The effects of the use of active eager enclosures with these techniques were also analysed. The reduced control tree achieved with these optimisation techniques combined with the head start of the control provided by the active eager enclosure contribute to the increase in performance of the circuit. The effects on the performance of the circuits clearly depend on the nature of the operations implemented. However, usually there will be some energy and area penalty as shown in the results for the running example.

Early evaluation of guards and encoding of multiple guards for conditional `loop`s and `case` constructs were also presented as a way of increasing the performance. Because the structures that implement the `loop` and `case` constructs generate control signals from the datapath, optimising the decision-making circuit speeds up the control. Finally, some new peephole optimisations for the resulting optimised handshake circuits were proposed. These include the removal of single-write with unconditional single-read *FalseVariables*, the optimisation of the control of the active input structures, the optimised control for unbounded write-then-read operations and a more concurrent version of the *Fetch* component. The techniques and optimisations presented here will evaluated and further discussed in chapter 7 using a number of substantial examples.

Chapter 5

Optimising Token-flow circuits and descriptions

5.1 Introduction

In chapter 3 the Balsa synthesis system was introduced along with examples of handshake circuit implementations of synthesised circuits. The components produced are similar to those produced by the Tangram system, the precursor of Handshake Solutions' TiDE system [23]. Balsa was developed to allow optimisation opportunities in handshake circuit designs to be explored. In particular, the *FalseVariable* component and input-enclosure language construct [5] have allowed pipelined descriptions with alternating latch and combinatorial handshake processing stages to be more naturally described.

The Teak system was proposed by Bardsley [6] as part of his research work within the APT Group at The University of Manchester. The Teak system extends the degree to which the Balsa language can sympathetically be used to describe pipelined systems by proposing a new set of components, synthesis rules and compiler. The aim of the Teak system is to provide a path for future performance increases in Balsa synthesis by exploiting high performance pipelined asynchronous circuit styles. The author of this thesis has contributed to the Teak System with:

i. the optimisations ideas presented in section 5.3 and their automation.

ii. automatic latch insertion strategies presented in section 6.4.

iii. the description-level optimisations presented in section 5.4.2.

iv. the evaluation of Teak using many of the design examples presented in chapter 7.

Some of the contents of this section are based in [6], a paper written by the author and Andrew Bardsley.

5.2 The Teak system

Teak replaces the dataless activation channel (used to enclose the behaviour of program fragments in handshake circuit synthesis) with separate *go* and *done* channels. Control/datapath interactions using components which exploit signal-level event interleaving are replaced by the rendezvous/forking of control and data channels with local handshaking to complete control interactions. This separation of "go" and "done" makes Teak much more like the Macromodules system [93] than handshake circuit systems. However, the ability to merge control and data channels gives the Teak system more flexibility.

Treating control channels in this way allows all the optimisation techniques usable with pipelined asynchronous systems (i.e. those with input-enclosing-output processing stages and decoupling latching stages) to be used on Teak circuits whilst still allowing local sequenced behaviour by using control channels.

Explicit pipeline latch insertion (also referred to as *buffering* in this chapter) is used to decouple one component from another and to introduce the desired degree of token storage to enable the circuit to function and, looking beyond the work presented in this thesis, to allow more transforming synthesis methods to increase circuit parallelism.

5.2.1 Teak components

There are currently eight Teak components (as shown in figure 5.1):

***Steer* (*S*):** conditional steer of input to exactly one output. Parameterised with disjoint match conditions for each output and bit ranges to carry to outputs. With 0 bits carried to outputs, *Steer* works like the Balsa *Case* component.

***Fork* (*F*):** unconditional n-way fork. *Fork* can be parameterised by which (if any) bits of the input are carried to each output. A two-way *Fork* of n and 0 bits can be used to generate a control token from moving data.

***Merge* (*M*):** input on one of the input ports is multiplexed towards the output. Inputs must be mutually exclusive. In some configurations, *Merge* may have to cope with second input arrival during first input activity.

***Arbiter* (*A*):** merge with arbitration between inputs.

***Join* (*J*):** unconditional n-way join. Concatenates data bits of arriving inputs.

***Variable* (*V*):** persistent storage. Separate write and read sections allow arbitrary control ordering/conditionality of reads. *Variables* allow complicated control activity without incurring the cost of always moving data along with control around a circuit. 'wg/wd' and 'rg/rd' (go/done) pairs make all writes data initiated and control token completed, all reads control token initiated and data delivery terminated.

***Operator* (*O*):** any and all data transforming operations. Inputs are formed into a single word. Internally an *Operator* is organised into interconnected terms allowing *Operators* to be amalgamated or separated to allow cheaper implementation or *Latch* insertion.

***Latch* (*L*):** data storage and channel handshake decoupling.

All of the components, except *Latch*, can be implemented with any chosen degree of input to output channel coupling (i.e. concurrency of handshaking events). *Latch* must provide at least some decoupling so that it can be used to separate pipeline tokens. In this way, Teak components resemble the components of other elastic token pipeline systems.

The *Variable* is included in this component set in order to allow sequential, storage-centric descriptions to be mapped directly into hardware. This is in contrast to other token flow approaches to asynchronous synthesis [116] [103] which perform single assignment analysis on the input language to allow variables to be eliminated in favour of pipeline buffers. This decision was made to allow the exploration of the possible power and area implications of retaining 'fixed' variables. Also, pipeline buffer-only approaches find it difficult to handle descriptions of persistent register banks without messy 'register refreshing' loops [100].

Figure 5.2(a) shows the one-place buffer example from Section 1.2.3 constructed from Teak components using synthesis rules from Section 5.2.2. The

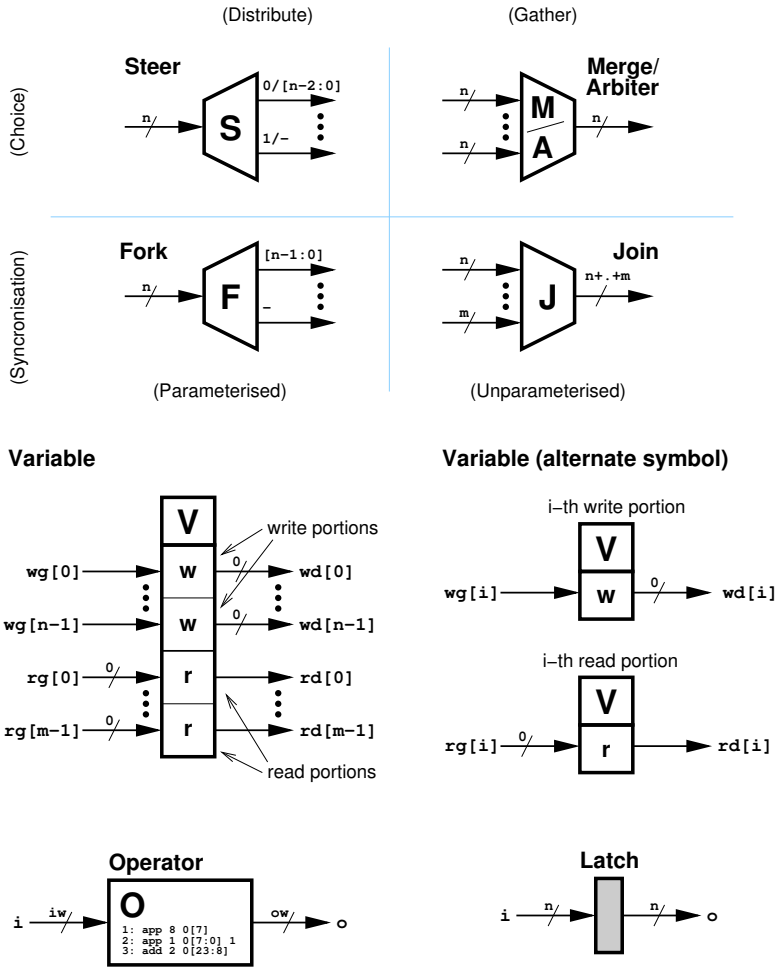

Figure 5.1: Teak components.

handshake circuit for this example is reproduced here in figure 5.2(b) for comparison.

Notice that the *Loop* component has become a loop comprised of a *Merge* (to introduce the 'go' token), a *Join* (to meet incoming data), and a *Fork* (to return a token back around the loop, through the *Merge*, after the output command) rather than a composition of enclosing control components.

5.2.2 Teak synthesis

Teak synthesis is initially syntax directed. Optimisations can then be performed on the generated Teak component netlists (Teak circuits). Each command in a Balsa description is mapped into components with dangling 'go' and 'done' control channels (a few commands never terminate and have no 'done'). Expressions,

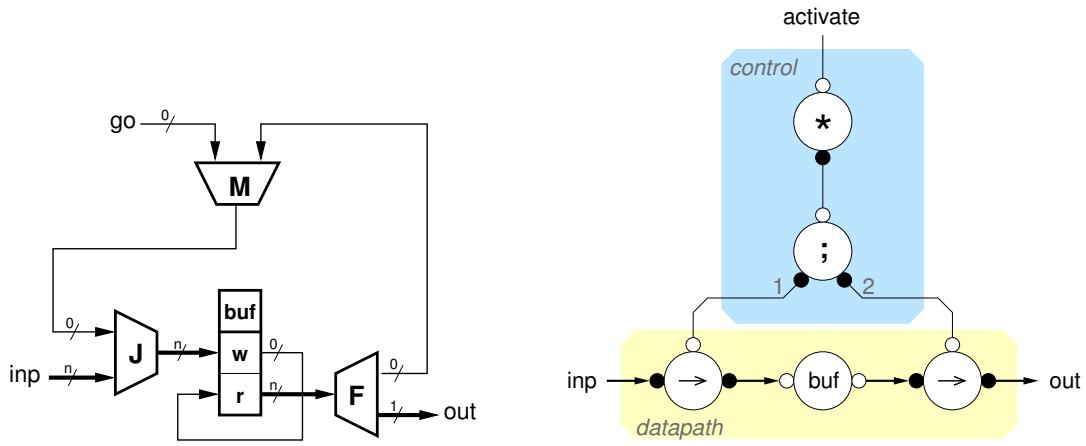

(a) (b)

Figure 5.2: (a) Teak circuit for 1-place buffer, (b) Handshake circuit for 1-place buffer.

channel accesses and assignment left-hand sides similarly have a pair of dangling channels: one bearing data and the other a control initiating/completion channel. Control can be sequenced by joining commands 'done' to 'go' in a chain. Data and control usually meet with *Fork* and *Join* components.

As with Balsa intermediate *Breeze* netlists, there are many possible choices of data encoding and signalling protocols on the channels between components. As Teak deals with the flow of tokens rather than enclosing handshakes, Teak component implementations also have choices of the degree of interleaving between input to output handshakes, the use of weak-condition behaviour and storage within components. The Teak synthesis system consists of a single front-end program called `teak`. There are a number of switches that allow technology mapping to be specified and various plotting options and optimisations.

Channels

Channels in Balsa have no capacity. Inputs and outputs on a channel form a synchronisation where either party can delay the transaction until both are ready for data to be transferred. In Balsa, the `select` command (which allows choice based on order of arrival of data on a number of channels) and the 'enclosed' channel input command can be used to exploit the non-atomic nature of asynchronous channel construction to allow latch-less implementations of data processing stages to be described. In such stages, data processing and outgoing channel outputs

are enclosed within the input handshake, as described in section 3.3.9. Alternating such stages with latch-containing pipelining stages allows push pipeline-like structures to be built.

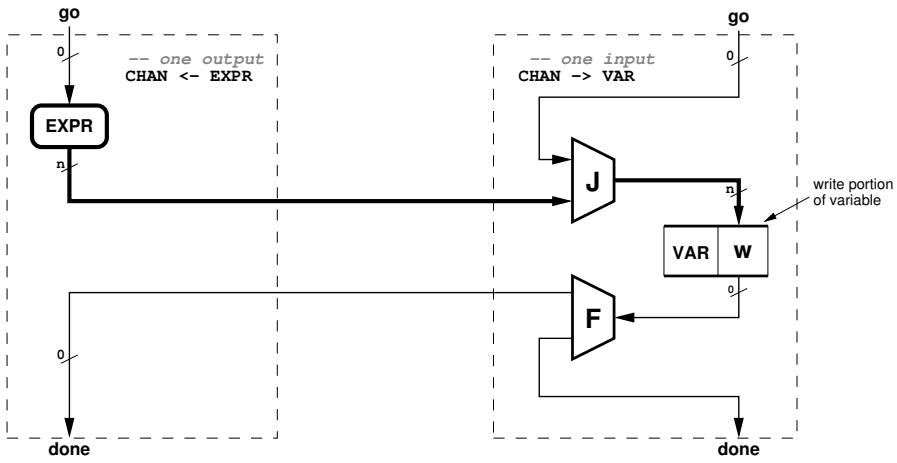

Figure 5.3: Balsa-style channel implementation.

Figure 5.3 shows a single output, single input Balsa-style channel implemented using Teak components. The pair of data and acknowledging ("done") channels between output and input commands form a synchronisation and limit to a single token the capacity of the loop formed from output command (as data), through input command and back to the output command (as an acknowledging "done"). Note the use of *Forks* and *Joins* between data and control.

Unfortunately, Balsa's channel implementation does not allow the capacity of buffered Teak channels to be exploited. Instead, the semantics of Balsa channel has been changed to make writes "fire and forget". Channel outputs and inputs are no longer synchronised and enclosure inside a sending handshake can no longer be relied upon. In practice, this reduces the utility of the `select` language construct but allows descriptions to be formed which exploit (or possibly rely upon) non-zero channel capacity. This introduces an incompatibility with the Balsa system's interpretation of descriptions.

Figure 5.4 shows how channel read and write commands are combined to form a complete Teak style language-level channel. The [i] and [j] constant-valued *Operator* components "tag" the request channels from different input/output commands so that once those requests are merged, with the following *Merge* component, the source of the request is encoded on the *Merge* output. This common request is then *Join*ed to a token *Fork*ed from the outgoing data *Merge* (or,

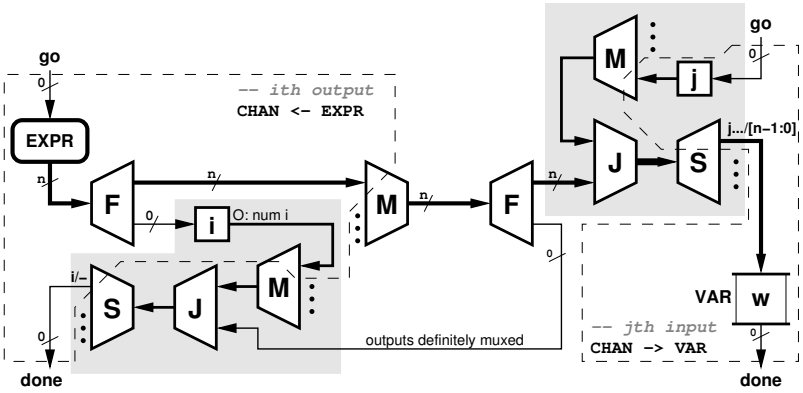

Figure 5.4: Multiple-output channel implementation.

for inputs, the incoming data itself) and *Steer*ed to provide the local command acknowledgements.

The combination of tagging *Operators*, the following *Merge* and the *Join*/*Steer* combination (the two shaded boxes in figure 5.4) plays a similar role to the Balsa *DecisionWait* [3] Handshake Component. This involves steering an incoming token (in this case the acknowledgement from the data-bearing merge) to the correct output based on the arrival of a single token on one of a group of input tokens (in this case, the choice of output command site). In Teak, the component parts of the *DecisionWait* are separated, rather than provided as a single component, to allow for flexibility of *Latch* insertion.

In cases where acknowledgement tokens need not be steered (e.g. where there is only one read or write to a channel in the description) much of the control/data interaction can be optimised away (as shown in figure 5.5). This implementation is similar to that of figure 5.3, but without the sequencing of variable write to the output command's "done".

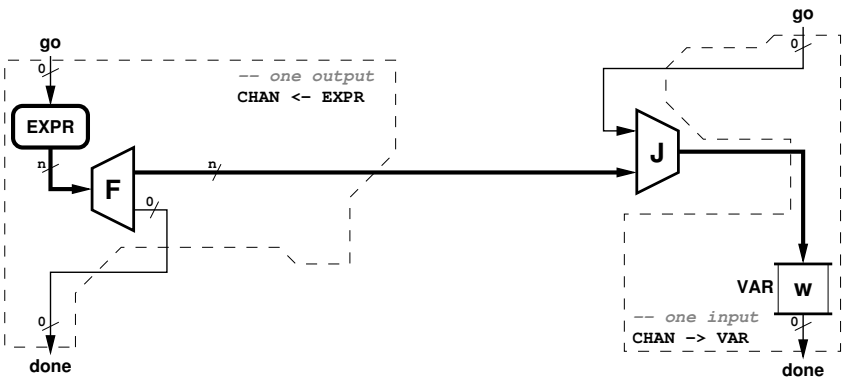

Figure 5.5: Channel component optimisation.

Commands

Figure 5.6 shows sequential and parallel composition of commands. Command "go" and "done" channels can be connected in series to form sequencing, so no explicit *Sequence* component is required. Parallel composition requires two components (*Fork* and *Join*) in contrast to Balsa's *Concur* component which contains both functions in one component. Figure 5.6's presentation of command composition is very similar to that used in non-return-to-zero (2-phase) signalled handshaking, as is illustrated by Brunvand [18]. Note, however, that here we are using handshake **channels** rather than individual wire signals for each of "go" and "done". On a channel, the token recipient can stall a handshake (by denying an acknowledgement) and so the token capacity of a string of commands is not necessarily limited to one (i.e. the strict alternation of "go", "done" events between between all commands). Where resources are not shared between sequentially composed commands, this property allows pipelining to naturally arise.

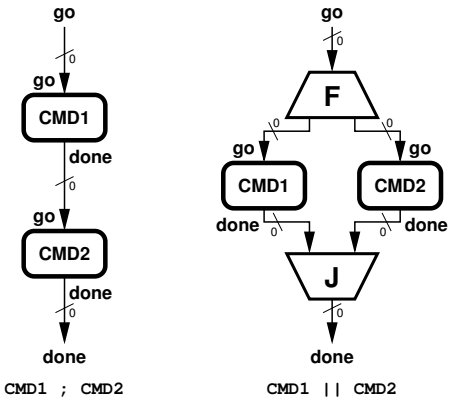

Figure 5.6: Sequential/parallel composition.

Figure 5.7 shows the structure of a `loop ... while` command. The *Steer* component provides the control choice at the top of the loop. Note that the loop formed by the *Merge* and *Steer* components must have at least some buffering to prevent deadlock. Insertion of *Latch*es will, obviously, affect circuit performance. Section 6 discusses different strategies for buffering and presents those currently available in the Teak System.

A non-terminating loop may be implemented by using the "done" of `CMD1` to close the loop and removing the *Steer*, the `COND` and the `CMD2` blocks. This is illustrated in figure 5.2(a).

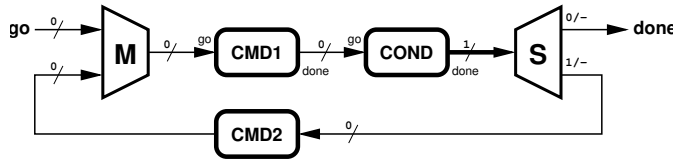


```
loop CMD1 while COND then CMD2 end
```

Figure 5.7: While loop implementation.

Expressions

Expressions are compiled by adding pairs of "rg" (read go) and "rd" (read done) ports on variable components, and *Operator* components to process the read data. Reading from channels within expressions (when within `select` commands or enclosed input commands, e.g. `chan -> then var := chan + 1 end`) is achieved by inserting *Variable* components to capture channel read data, and then using read port pairs on those variables to use that data. These variables can often be removed if data is unconditionally used within the body command.

5.3 Optimising Teak circuits

This section introduces some optimisations for Teak circuits by exploiting the properties of components both individually and in groups. Optimisations are presented using simplified practical descriptions extracted from the design examples used in chapter 7. The plots of all Teak circuits shown in the following sections were generated automatically using the Teak System.

5.3.1 Variables

In cases where reads from a channel occur unconditionally after every write, the *Variable* can be removed (for single-read channels) or replaced by a cheaper and faster *Fork* component (for multiple-read channels), provided the *Variable* components are not used to enforce sequencing. Figure 5.8 shows a single-write followed by unconditional single-read channel structure before and after optimisation.

As an example, consider the Balsa description of an n-bit full adder whose output is separated into sum and carry-out portions shown in figure 5.9. The resulting circuit will contain *Variable* components implementing the inputs on `a` and `b` and the channel `cs` as described in section 5.2.2.

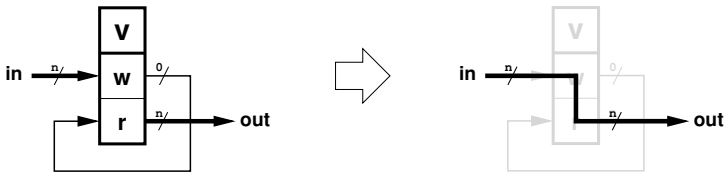

Figure 5.8: Variable single read-after-write optimisation.

```
1  procedure adder (
2    input a, b   : N bits;
3    output sum   : N bits;
4    output carry : bit
5  ) is
6     channel cs : N+1 bits
7  begin
8      loop
9          a, b -> then
10             cs <- (a + b as N+1 bits)
11         end ||
12         cs -> then
13             sum <- (#cs[0..N-1] as N bits) ||
14             carry <- (#cs[N] as bit)
15         end
16     end
17 end
```

Figure 5.9: Balsa code for `n`-bit full adder.

For simplicity, let us consider only the part of the synthesised circuit that provides the `sum` and `carry` outputs as shown in figure 5.10(a), which corresponds to lines 12-15 in the source code.

The *Variable* that implements the channel `cs` has a single write port and two read ports (for `sum` and `carry`). Reads are initiated as soon as the `cs` *Variable* 'wd' (write done) port indicates that new data has been stored. The *Fork* component at the top provides tokens for both read ports. As a write operation is directly followed by a read, this *Variable* can be substituted by a *Fork* that provides 'sum', 'carry' and 'done' results as shown in figure 5.10(d). An additional benefit of this type of optimisation for dual-rail circuits is that the forked channels would only need to wait for the arrival of those input bits that will be carried to the output.

The above optimisation can be viewed as a 3-step process:

i. The *Fork* labelled 1 is displaced 'downstream' in the datapath, after the *Variable* `cs`, leaving a single write, single read *Variable*, as shown in figure 5.10(b).

ii. *Variable cs* can be removed as a write is directly followed by a read and

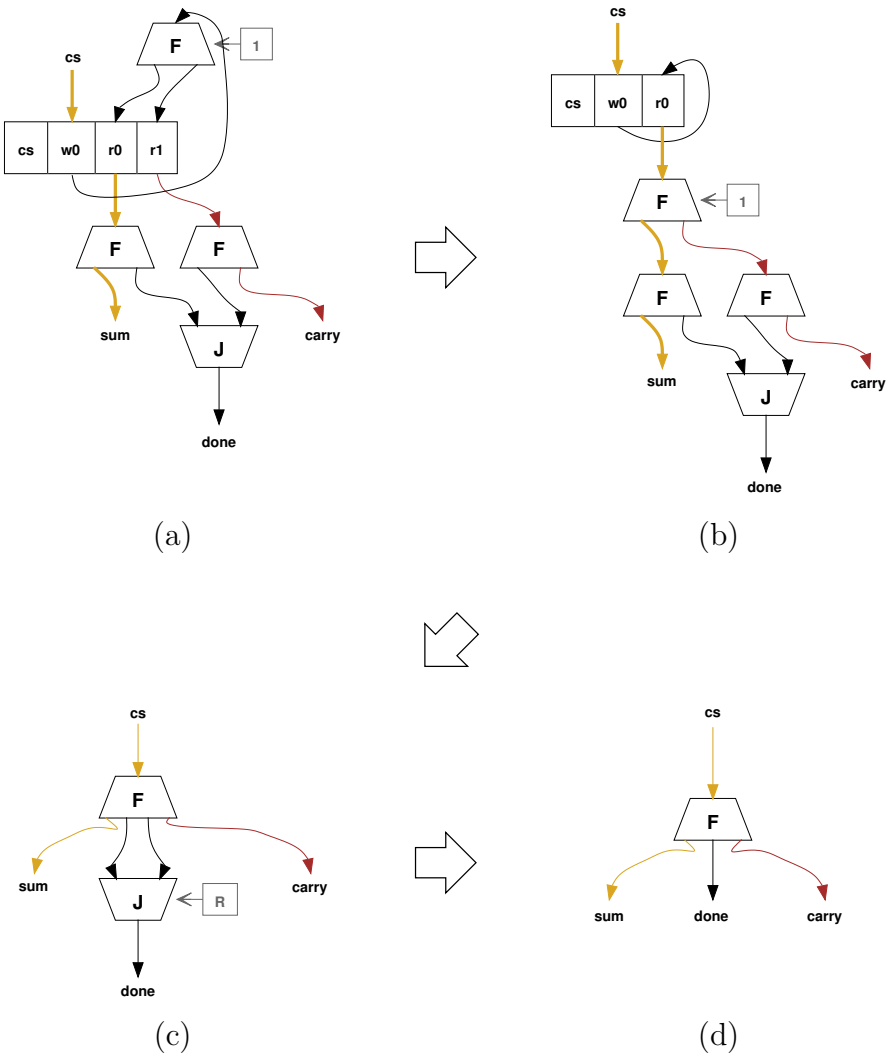

Figure 5.10: Variable substitution example.

the three *Fork*s can be merged into a four-way *Fork*, leading to the circuit in figure 5.10(c).

iii. Now, the *Join* component in figure 5.10(c) is redundant because both inputs come from the same fork. The inputs of the *Join* can be merged and the final circuit is shown in figure 5.10(d)

Similar kinds of optimisations based in component displacement will be presented in the following sections.

5.3.2 Fork displacement

In some circumstances, *Fork* components can also be displaced 'upstream' in a data or control path to allow for more concurrent operation. Consider the segment of code in figure 5.11 where the results generated by the two output commands must be written sequentially to a common channel `out`.

```
1 procedure tenFifteen (
2    output out : 4 bits
3 ) is
4 begin
5    loop
6       out <- 10 ; -- exprA
7       out <- 15   -- exprB
8    end
9 end
```

Figure 5.11: Sequential write to a channel.

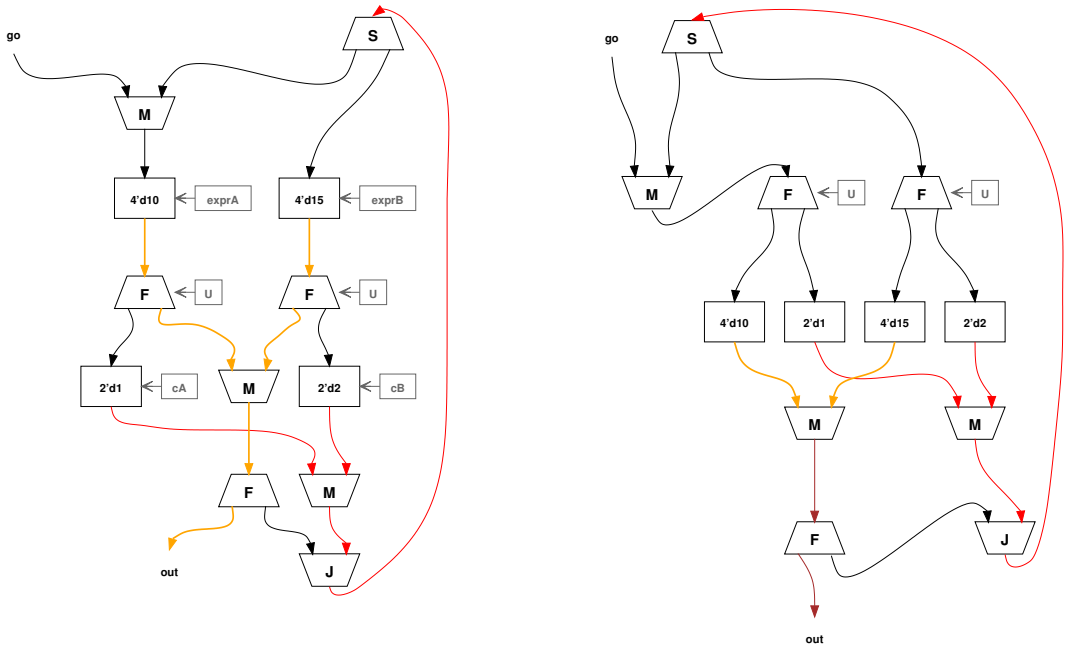

(a) (b)

Figure 5.12: Sequenced channel write example: (*a*) original, (*b*)after *Fork* displacement.

The resulting circuit is shown in figure 5.12(a). Note how the *Fork*s labelled U fork the result of exprA and exprB to generate the output and the "tag" constants (cA and cB). As explained in section 5.2.2, those constants indicate which

of the expressions will be output in the next iteration via the *Steer* component. If those *Fork*s are moved upwards through the expression generators, as in figure 5.12(b), the constant that steers the control for the next iteration will be generated concurrently with the output. This kind of displacement can be done through any data transforming operation or even single-input command blocks.

5.3.3 *Fork-Merge-Join* and *Steer-Merge*

Another target for optimisation are *Fork-Merge-Join* and *Steer-Merge* compositions. In Teak circuits, *Forks* are used in a datapath to generate a control token from a data token, to either synchronise or sequence operations. Sometimes all the *Fork*ed control tokens from a set of mutually exclusive data results need to be *Merge*d into a single token. At some point further down in the pipeline this new control token will rendezvous in a *Join* with a second data or control token. If the second token is derived from the merging of the aforementioned set of mutually exclusive data sources, the *Fork-Merge-Join* composition for the control tokens can be simplified.

Consider the segment of code in figure 5.13(a) which is a simplified version of a "sign adjust" unit for the multiplicand input of the Booth's multiplier in the nanoSpa processor [95]. The circuit takes an N bit input word `b` and, depending of the type of multiplication specified by the `mType` input, either appends M zeroes after the most significant bit of input `b` or sign-extends it to $N + M$ bits to generate the adjusted output `ba`. For clarity, let $N = 8$ and $M = 3$ in this example.

The unoptimised circuit is shown in figure 5.13(b). In this figure, the dotted blocks labelled `inB` and `inM`, contain the implementation of the two input channels reads and writes. The *Fork-Merge-Join* optimisation will be applied to the shaded the block of figure 5.13(b), labelled `BOut`. In this block, the output data from *Operators* `zE` (zeroExtend) and `sE` (signExtend) are forked to produce control (thin lines) and data (wide lines) tokens. The data tokens are merged and then forked again to produce the output `ba` and a new control token (*Merge* and *Fork* labelled `c0`).

The control tokens from the top *Forks* in block `BOut` generate tag values (constant *Operators* `2'd1` and `2d'2`) required to steer the control to the correct source in the next iteration (components labelled `c1`). As both data tokens are

```
1  loop
2    mType, b -> then
3      case mType of
4      MUL, UMULL, UMLAL then
5      -- unsigned, pad with 0s
6        ba <- zeroExtend (8, 11, b)
7      else
8        -- signed, sign-extend
9        ba <- signExtend (8, 11, b)
10     end
11   end
12 end
```

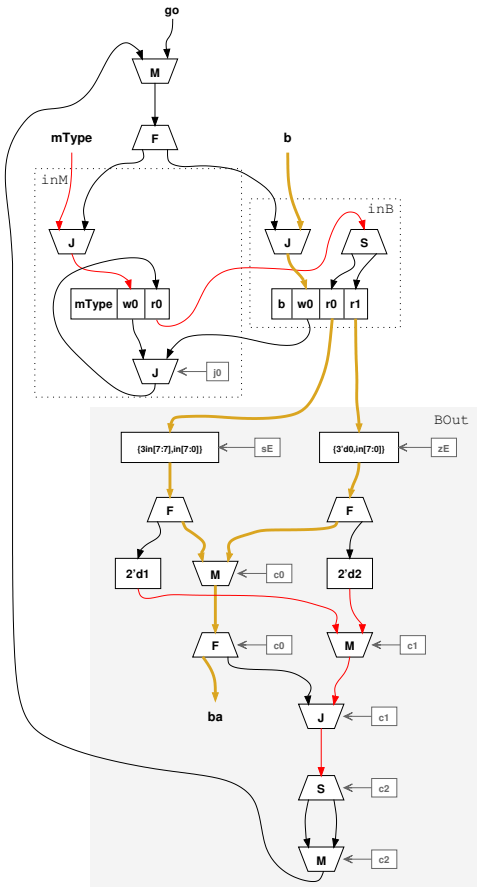

(*a*) (*b*)

Figure 5.13: 'Sign adjust" example.

derived from a common source, the outputs of the *Steer* are the only inputs to the *Merge* that generates the control token for the next iteration (components labelled c2). The simplification steps are:

i. The bottom *Steer-Merge* in figure 5.13(b) can be simplified into a single-output *Fork* which acts as an adaptor that generates a control token from a data token as shown in figure 5.14(a).

ii. As the generation of the control token in the new *Fork* is independent of the data value, the data channels that carry the constants can be simplified into control channels, making the constant blocks redundant. These are simplified in figure 5.14(a).

iii. Now the control tokens forked from the outputs of zE and sE are redundant because each one will always synchronise with its sibling data token at the

Join c1, hence those *Forks* and the *Merge* and *Join* with labels c1 can be reduced. The new single-input *Fork* inserted in step (i) can also be removed. The final circuit is shown in figure 5.14(b).

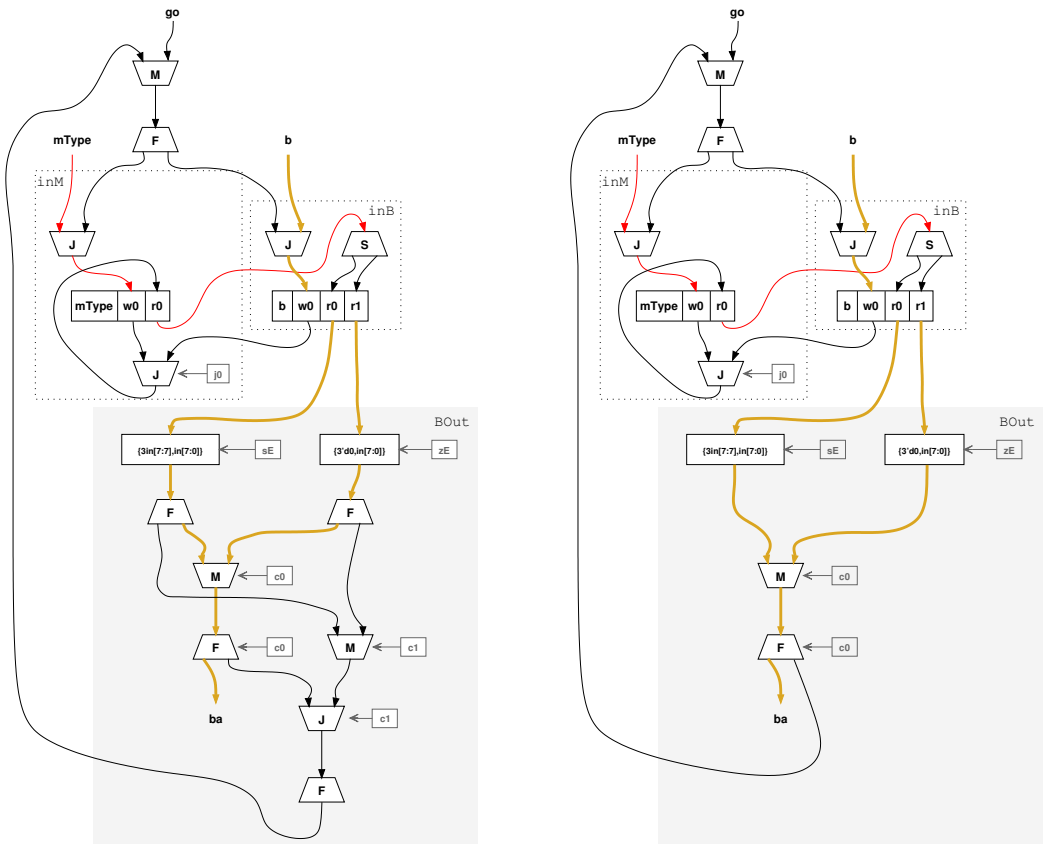

Figure 5.14: "Sign adjust" circuit: (*a*) first optimisation steps, (*b*) final circuit.

5.3.4 Removing "go" cycles

In Teak circuits, "go" cycles (loops) occur when the description specifies `loop` constructs (as in figures 5.2(a), 5.7, 5.12 and 5.13). A single initial "go" control token is introduced through a *Merge* component and the subsequent "go" tokens are locally generated when the circuit produces its outputs.

In the case of unbounded repetition loops, this control cycle can be removed if it does not contain a *Steer-Merge* (conditional) composition. This means that new "go" tokens for the loop are generated unconditionally.

Consider the example of the N-bit full adder introduced in section 5.3.1 whose code is shown in figure 5.9, and its optimised Teak circuit shown in figure 5.15(a). Clearly, the generation of the next "go" token is unconditional in this circuit. The components used to reinsert the "go" token can then be removed safely, leading to the circuit shown in figure 5.15(b). In this particular case, the circuit consist only of data channels. In fact, the optimised circuit ends up having the structure of a fully data-driven pipeline.

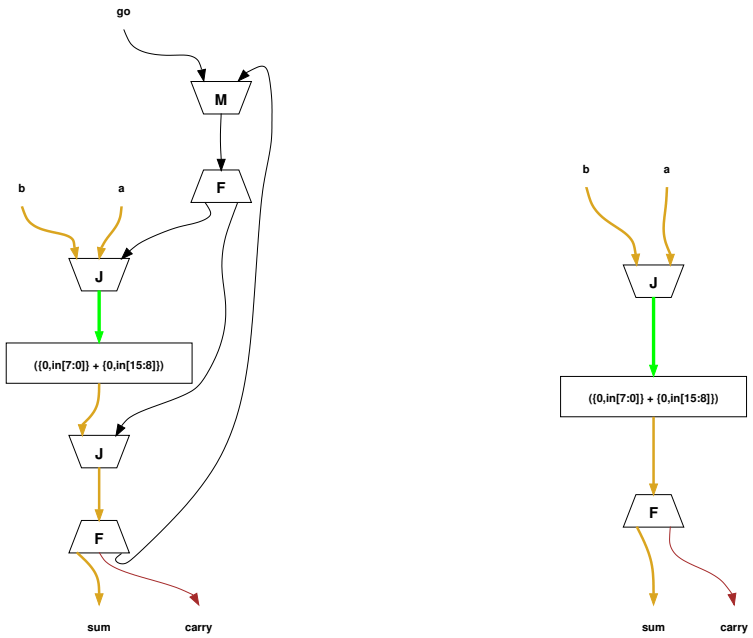

(a) (b)

Figure 5.15: Teak circuit of the N-bit adder: (a) Optimised, (b) With the "go" cycle removed.

If a cycle contains a *Steer-Merge* composition, there is a possibility of inserting tokens in the wrong order through the *Merge* if the number of tokens in the cycle is not limited by the "go" circuitry. This is so because, as explained in section 5.2.1, channels in Teak are allowed to have any amount of storage and components can be implemented with any degree of input to output channel coupling. The circuits with conditionals inside a `loop` construct of the previous sections (e.g. figures 5.12 and 5.13) are examples of circuits with irremovable "go" cycles. In these cases, the number of tokens is limited to one and they are referred to as *single-token cycles* in the rest of this thesis.

5.4 Description-level optimisations

Teak synthesis use a different set of components and composition strategies than those used in Balsa. It is not therefore surprising that not all of the description-level strategies presented in chapter 4 will be as effective in Teak. In this section, Teak-specific optimisations will be introduced and their impact on the resulting circuit will be analysed.

5.4.1 Commonalities with Balsa optimisations

Teak descriptions also benefit from the data-driven style description introduced in section 4.3, and the following optimisations also apply to Teak: separation of actions into concurrent loops, adding pipeline registers, explicit duplication, and guard optimisation. However, the enclosure techniques (based on pull structures) used widely to speed-up Balsa descriptions may result in poor performance when compiled into Teak push-based circuits.

5.4.2 Description techniques to remove *Variables*

Variables in Teak are used for implementing both permanent storage and channels (see section 5.2.2). They are the most complex and expensive component in Teak, but allow sequential, storage-centric descriptions to be mapped directly into hardware, avoiding some of the restrictions of not having such a component, as explained in section 5.2.1.

Variables with unconditional reads can be removed as described in section 5.3.1. However, *Variables* used in the implementation of channels with conditional reads cannot be removed, although in some cases descriptions may be rewritten to avoid conditional reads and therefore allow the variables to be removed.

Avoiding Variables associated with conditional reads

Conditional channel reads occur when a channel access encloses a conditional construct within which the channel's value is used. Figure 5.16(a) shows an example description of a two-output demultiplexer. In the example, the (write) access to channel `i` encloses two conditional reads on this channel. In the resulting Teak circuit, in figure 5.16(c), the write and read sections of channel variable `i` are separated by a *Steer* and cannot be optimised because of the conditional reads.

```
1  procedure dmux (
2    input ctl : bit;
3    input i   : N bits;
4    output z0, z1  : N bits
5  ) is
6  begin
7     loop
8        i, ctl -> then
9           if ctl then
10             z1 <- i
11          else
12             z0 <- i
13          end
14       end
15    end
16 end
```

(a)

```
1  procedure dmux (
2    input ctl : bit;
3    input i   : N bits;
4    output z0, z1  : N bits
5  ) is
6  begin
7     loop
8        ctl -> then
9           if ctl then
10             i -> then z1 <- i end
11          else
12             i -> then z0 <- i end
13          end
14       end
15    end
16 end
```

(b)

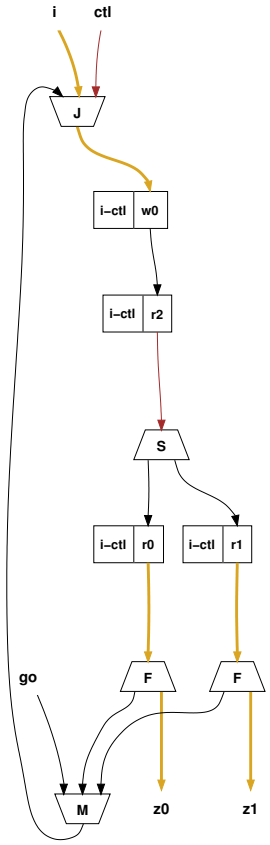

(c)

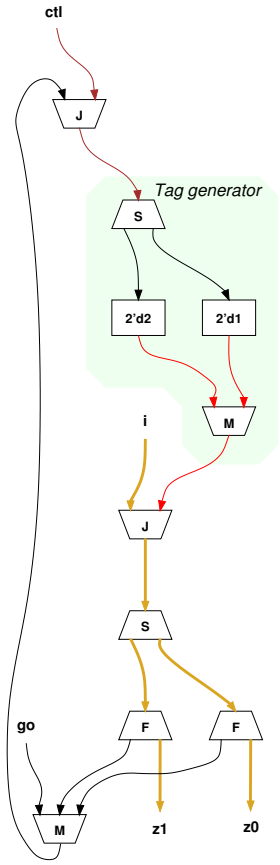

(d)

Figure 5.16: Avoiding *Variables* associated with conditional reads.

If the target were a Balsa handshake circuit, this description would have the advantage of triggering the control to access the *pull* channel `i` early. In Teak *push* channels, the arrival of valid data initiates the handshake and so no early

activation can occur.

In Teak it is more advantageous to access channel `i` *inside* the conditional block, as shown in the code of figure 5.16(b). In this description, paired write and read accesses to channel `i` are not separated by a conditional and the variable implementing `i` can be removed. The Teak circuit is shown in figure 5.16(d). Input i is tagged according to the value of `ctrl` before it is *Steer*ed to the required destination.

The cost associated with this style is the extra *Steer-Operator(constant)-Merge* structure required to generate the tags, but in general the benefits of not having *Variables* compensates this overhead, as will be shown next and in the examples of chapter 7.

Discarding inputs conditionally

A similar situation can occur when inputs need to be conditionally *discarded* (that is, the data token is consumed but not used in any operation). Consider the description of a two-input multiplexer shown in figure 5.17(a). The specification is such that both inputs are always expected and one of them must be discarded. The description in figure 5.17(a) has been optimised to generate optimised Balsa handshake circuits. In the following, this coding style will be referred to as *Balsa-optimised*.

In Balsa handshake circuits, the resulting input structure ensures that all inputs have arrived before completing the enclosing handshake, although the output is generated as soon as the selected input is present. The unused input is implicitly discarded by the input control structure. However, when compiled into Teak circuits as shown in figure 5.17(c), this Balsa-optimised style generates conditional channel reads that prevent the removal of the associated channel *Variables*.

In the description optimised for Teak circuits shown in figure 5.17(b) the inputs are read (and discarded) *inside* the conditional block. This creates channel *Variables* that may be removed. The resulting optimised circuit without channel variables is shown in figure 5.17(d). This style of description targeting the optimisation of Teak circuits will be referred as *Teak-optimised*.

Notice in the Teak-optimised circuits that, because all read accesses to channel `i` are now done inside the conditional construct, it has been necessary to generate steering tags for each input (to tag them with either “pass” or “discard”). Finally,

```
1  procedure mux2 (
2    input ctl : bit;
3    input i0, i1 : N bits;
4    output z  : N bits
5  ) is
6  begin
7     loop
8        i0, i1, ctl ->! then
9           if ctl then
10             z <- i1
11          else
12             z <- i0
13          end
14       end
15    end
16 end
```

(a)

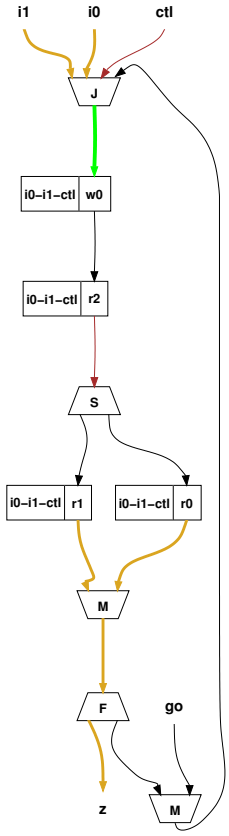

(c)

```
1  procedure mux2 (
2    input ctl : bit;
3    input i0, i1 : N bits;
4    output z  : N bits
5  ) is
6  begin
7     loop
8        ctl -> then
9           if ctl then
10             i1 -> z ||
11             i0 -> then
12                continue
13             end
14          else
15             i0 -> z ||
16             i1 -> then
17                continue
18             end
19          end
20       end
21    end
22 end
```

(b)

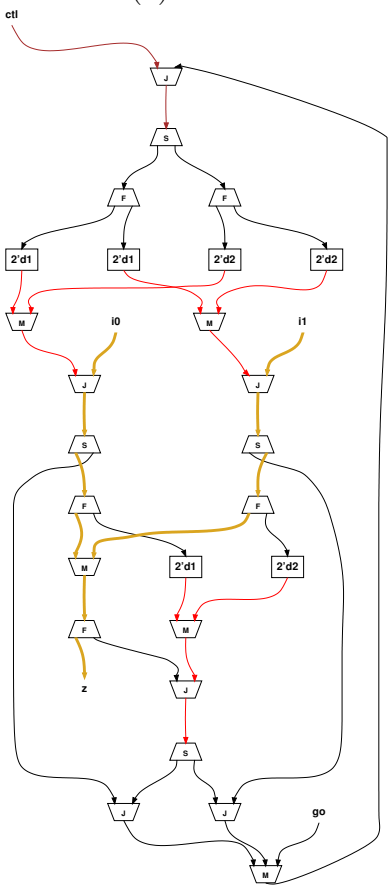

(d)

Figure 5.17: Discarding inputs conditionally in Teak: (*a*, *c*) Balsa-optimised style; (*b*, *d*) Teak-optimised style.

another steering tag is generated from the "passing" value to rendezvous the token from the "discarded" item.

Another possible optimisation is shown in figure 5.18(a): before using the inputs inside the conditional block, they are explicitly joined into the single channel `i01` (lines 8 - 11). Inside the conditional structure and, for each condition, the relevant bits of this channel are passed to the output.

```
1  procedure mux2 (
2    input ctl : bit;
3    input i0, i1 : N bits;
4    output z  : N bits
5  ) is
6    channel i01 : 2*N bits
7  begin
8    loop
9      i0, i1 -> then
10       i01 <- (#i0 @ #i1 as N bits)
11     end
12   end ||
13   loop
14     ctl -> then
15       if ctl then
16         i01 -> then
17           z <- (#i01[0..N-1] as N bits)
18         end
19       else
20         i01 -> then
21           z <- (#i01[N..2*N-1] as N bits)
22         end
23       end
24     end
25   end
26 end
```

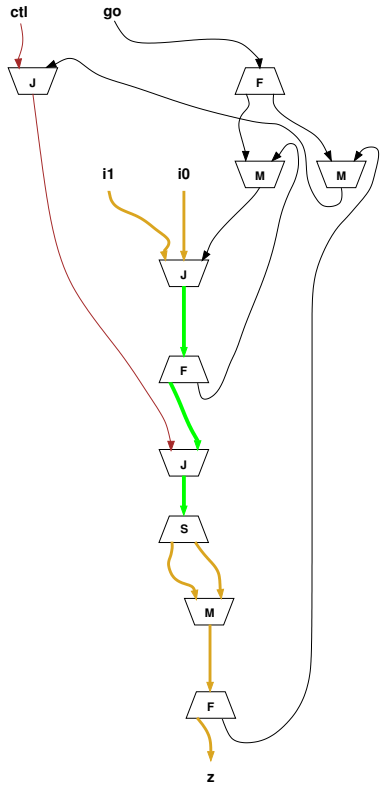

(a) (b)

Figure 5.18: Joining inputs to reduce the tagging circuitry.

Figure 5.19 shows speed (processing time), area and dynamic energy comparisons for the three multiplexer designs presented above, for different data widths (the fourth, dotted bar in each series, labelled *Circuit-level*, will be introduced later in this section). In all the simulation results presented in this section the circuits are connected to an environment that is always ready to provide data in all the inputs simultaneously. Random data values were generated for data inputs whereas select control values were generated such that all options were equally exercised.

The results in the graphs of figure 5.19 show that, for data widths ≥ 4,

the joined-inputs optimisation delivers the fastest speed with area and energy consumption smaller or comparable to that of the Teak-optimised style. The results also show that, compared to the Balsa-optimised, the Teak-optimised style is advantageous for wider datapaths, when the overhead of tagging is smaller compared to the cost of the wider Variables (their associated completion detection circuitry becomes larger and slower as the number of bits increase). For the optimised circuits, the speed-up is directly proportional to the data width whereas area and energy penalties are inversely proportional.

The joined-inputs optimisation is less effective in circuits where there is a large difference in the arrival time of the inputs because in order to generate an output, both inputs must be present. In the first optimisation an output may be produced with only one input present and so input synchronisation is only required for the RTZ phase.

Duplicating values to avoid conditional channel reads

In cases when multiple, non-mutually exclusive conditional reads can occur, it is necessary to explicitly duplicate some of the channels to get rid of the *Variables*. The `SteerAlu` module from the nanoSpa Execute stage is shown in figure 5.20.

This module multicasts the ALU result to a set of destinations depending on the bits of the `ctrl` input. The set of destinations may be empty, in which case the ALU result is discarded. The Balsa-optimised description is shown in figure 5.20(a) and the resulting Teak circuit in figure 5.21.

The Teak-optimised version is shown in figure 5.20(b) and the resulting circuit in figure 5.22. In this case, to avoid the conditional channel reads, the input has been explicitly duplicated (one copy for each condition) and, in a similar way to the demultiplexer example, each copy is either passed or discarded but it is always read.

Figure 5.23 shows speed(processing time), area and dynamic energy comparisons for the two `steerAlu` descriptions, using various data widths. It can be seen in the graphs that the Teak-optimised circuits are $\sim$ 30% to 60% faster, more energy efficient and with an area penalty inversely proportional to the data width. As explained earlier, as the data width increases, the overhead of a wider *Variable* becomes larger compared to that of the tagging circuitry.

It is clear from the examples that the overhead of the *tag-and-steer* mechanism will increase with the number of inputs and conditions involved. In fact, when

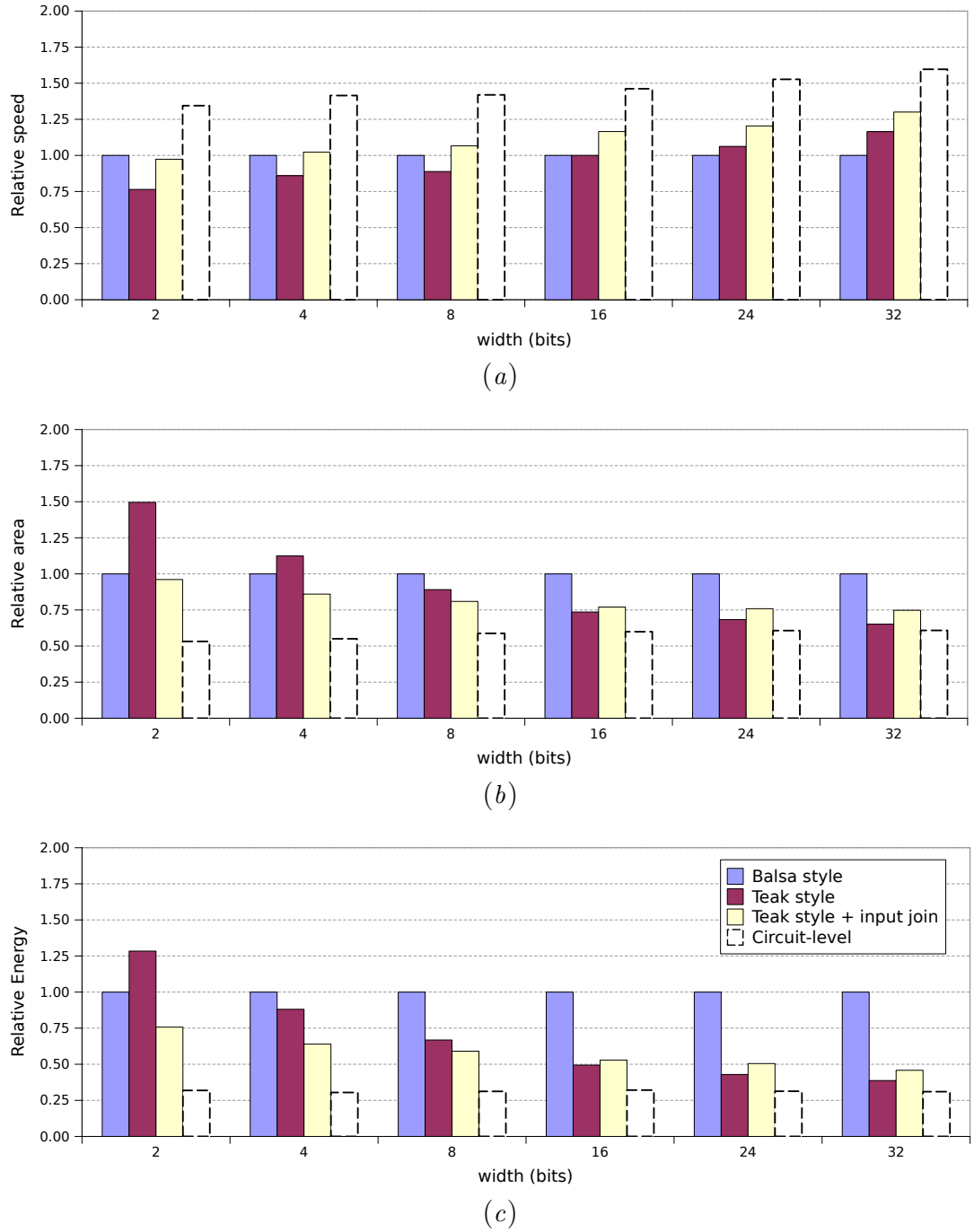

Figure 5.19: Simulation results for different optimised versions of the `mux` example.

complex nested conditions occur, a variable-free description may result in a large, nested tag-and-steer circuitry which will result in area overhead with insignificant speed-ups. In such cases, it is not advisable to apply the above techniques.

```
type Datapath is N bits
type AluSelect is 6 bits

procedure steerAlu (
  input a : Datapath;
  input ctrl : AluSelect;
  array 6 of output o : Datapath
) is
begin
  loop
    ctrl ->! then
      a ->! then
         for || i in 0..5 then
           if (#ctrl[i..i] as bit) then
             o[i] <- a
           end
         end
      end
    end
  end
end
```

(a)

```
type Datapath is N bits
type AluSelect is 6 bits

procedure steerAlu (
  input a : Datapath;
  input ctrl : AluSelect;
  array 6 of output o : Datapath
) is
  array 6 of channel aC : Datapath
begin
  -- generate six duplicates of input
  loop
    a -> then
      for i in 0..5 then
        aC[i] <- a
      end
    end
  end ||
  loop
    ctrl ->! then
      for || i in 0.. 5 then
        if (#ctrl[i..i] as bit) then
          aC[i] -> o[i] -- steer
        else
          aC[i] -> then
            continue  -- discard
          end
        end
      end
    end
  end
end
```

(b)

Figure 5.20: `steerAlu` example: (*a*) original, (*b*) channel duplication to avoid conditional reads.

A circuit-level approach to remove conditional channel reads

The above description-level optimisation examples have shown that in order to remove *Variable*s in conditional structures (*i*) tags derived from the guard token must be added to each data token and (*ii*) copies of each data token must be produced for each non-mutually exclusive conditional read. The result is always a number of tagged data tokens that will be *Steer*ed accordingly.

The optimised structures suggest a new circuit-level optimisation opportunity to get rid of the *Variables* without having recourse to the directness of the compilation. This new optimisation is based on the data steering property of the *Steer* component: *Steer* uses a subset of the input bits as the output selector and it passes a subset of the input bits to the matching output. Instead of appending a tag generated from the guard, it is possible to append the actual guard and modify the *Steer* specification to use directly this value, simplifying the Teak

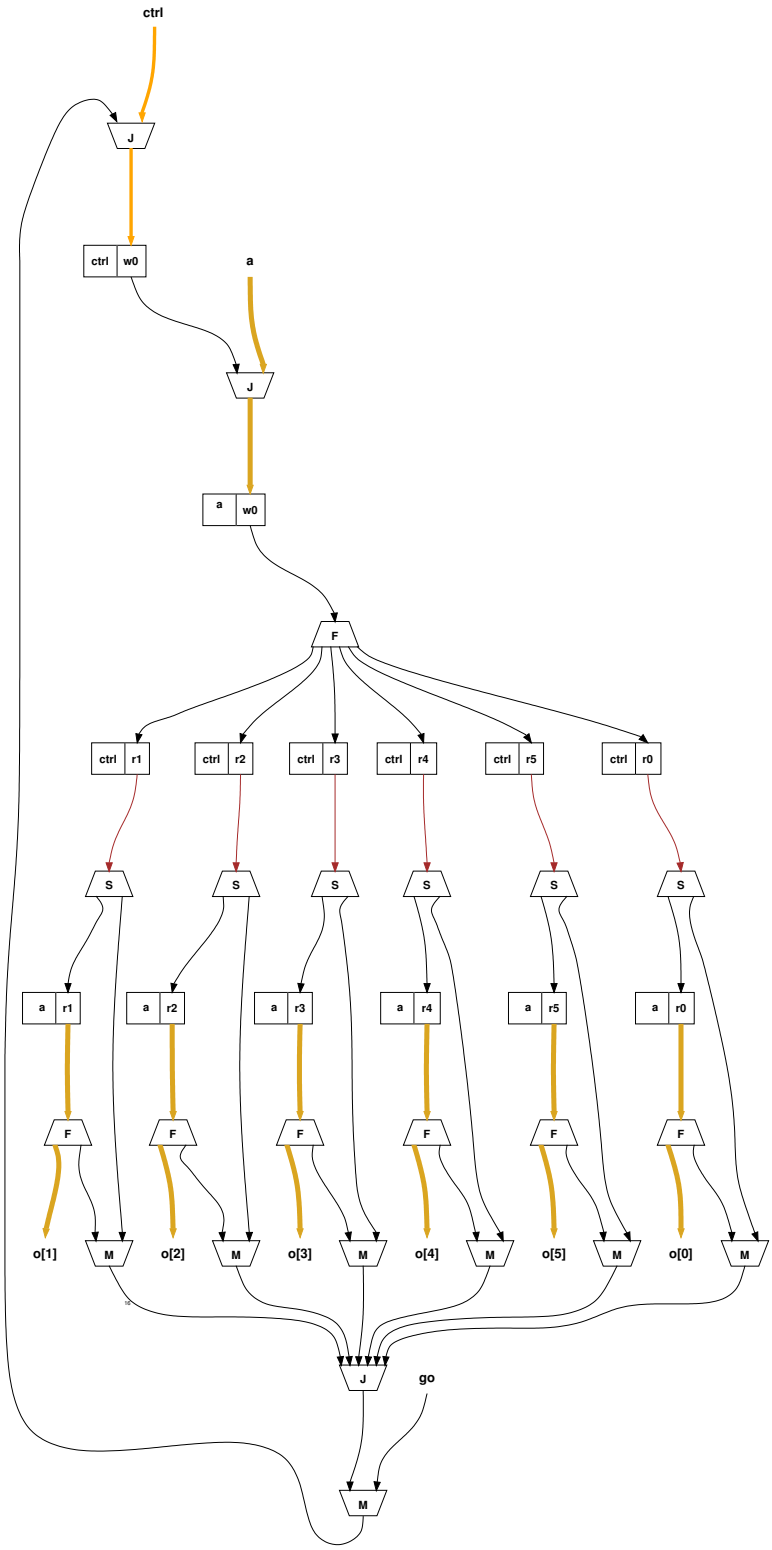

Figure 5.21: `steerAlu` Teak circuit.

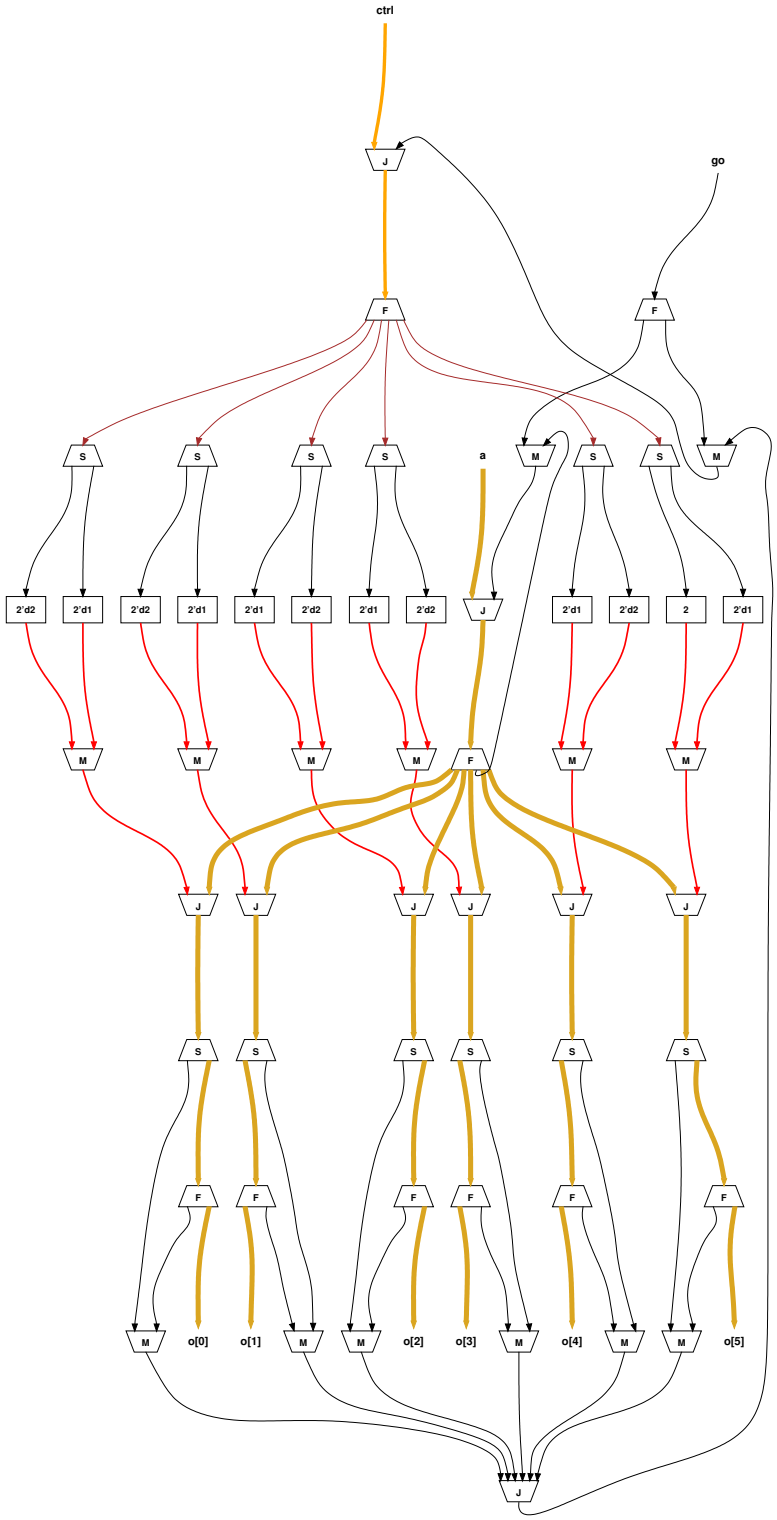

Figure 5.22: Optimised `steerAlu` Teak circuit.

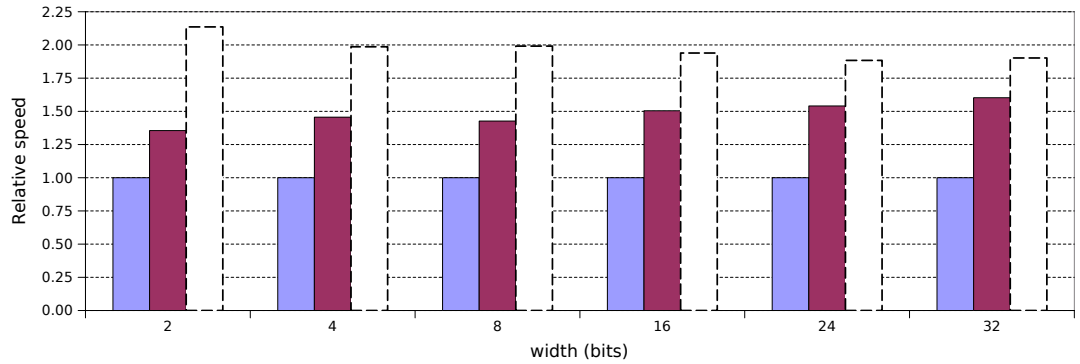

(a)

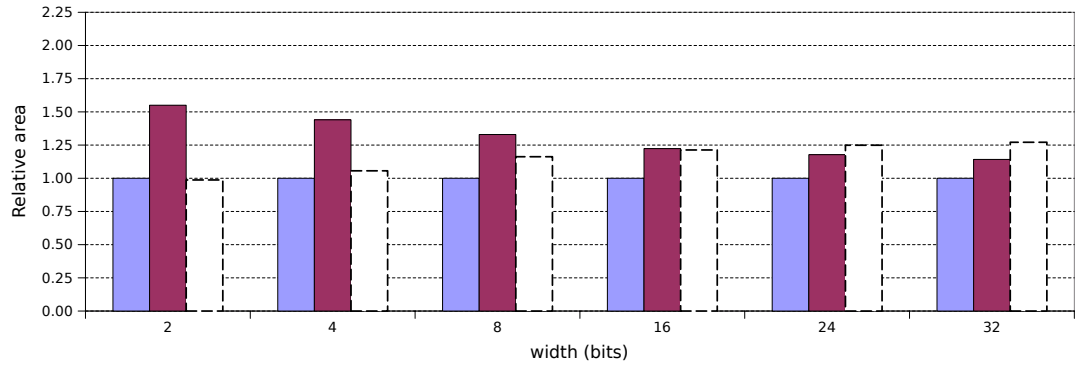

(b)

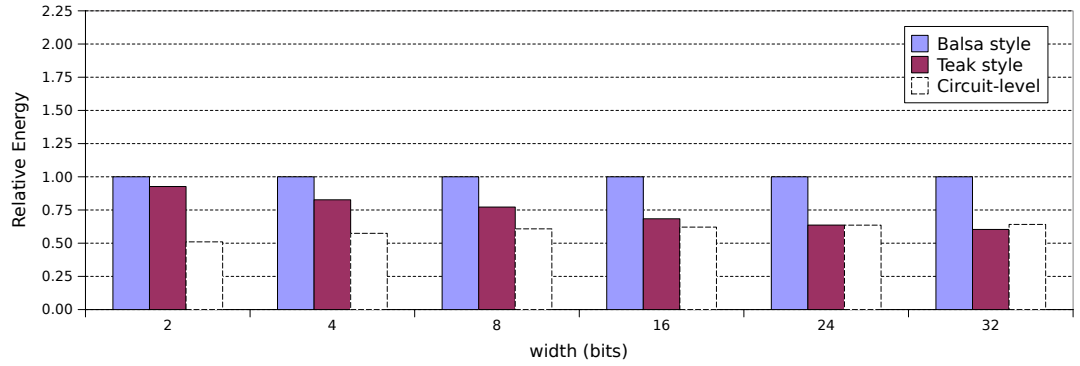

(c)

Figure 5.23: Simulation results for the `steerAlu` example.

network. The cost of this approach is in the increased complexity of the *Steer*s required and in the complexity of the rules to determine situations where the transformation may be applied.

To illustrate the proposed mechanism, let us revisit the circuit for the two-input multiplexer, reproduced again in figure 5.24(a). In this figure, channels `i0,`

`i1` and `ctrl` are joined and stored into the channel *Variable* `i0-i1-ctrl`. The *wd* (write done) token generated by the `w0` portion activates the read portion `r2`, which provides the bits corresponding to the `ctrl` guard only.

The *Steer* that implements the conditional generates zero-width control tokens to activate one of the read portions `r1` or `r0`, which provide the values of `i1` or `i0`, respectively. If these portions are displaced upstream through the *Steer*, they can be combined with portion `r2` into a single read portion that will provide all of the bits of the composite channel `i0-i1-ctrl`. The specification of the *Steer* must be modified accordingly to accept this wider value at its input and to steer the required portions to its outputs.

The above modifications are shown in the circuit of figure 5.24(b). In this circuit, *Variable* `i0-i1-ctrl` is unconditionally read and can be removed, as shown in figure 5.24(c).

Notice that the new optimisation does not require the tagging circuitry, but the specification of the *Steer* will be more complex. In this particular case, the resulting *Steer-Merge* combination cannot be removed because the offsets of the two *Steer* outputs are different (they correspond to the `i0` and `i1` sections in the composite channel `i0-i1-ctrl`).

If the write and read portions of a variable are separated by a *Fork*, as in the `steerAlu` example of figure 5.21, a further combination is required when the individual portions are displaced through the *Fork*, which in turn must also be modified accordingly. This is the equivalent of the duplication mechanism used before at the description level. Figure 5.25 shows the resulting optimised circuit for the `steerAlu` example. Again, no tagging circuitry is required but the *Steer*s will end up being more complex.

Simulation results for these hand-applied transformations on the multiplexer and `steerAlu` examples are shown in figures 5.19 and 5.23 under the key *Circuit-level* (dotted bars). The results show that this optimisation produces circuits that are considerably faster ($\sim$ 30% to 50%) and more energy efficient ($\sim$ 5% to $\sim$ 50%) than the circuits produced with the description-level optimisations.

Notice in figure 5.23(a) how the more complex *Steer*s used in the `steerAlu` example increase the area penalty as the data width increases.

The rules for the above transformations must check a number of conditions of the components surrounding the write and read portions, some of which have been highlighted in the examples:

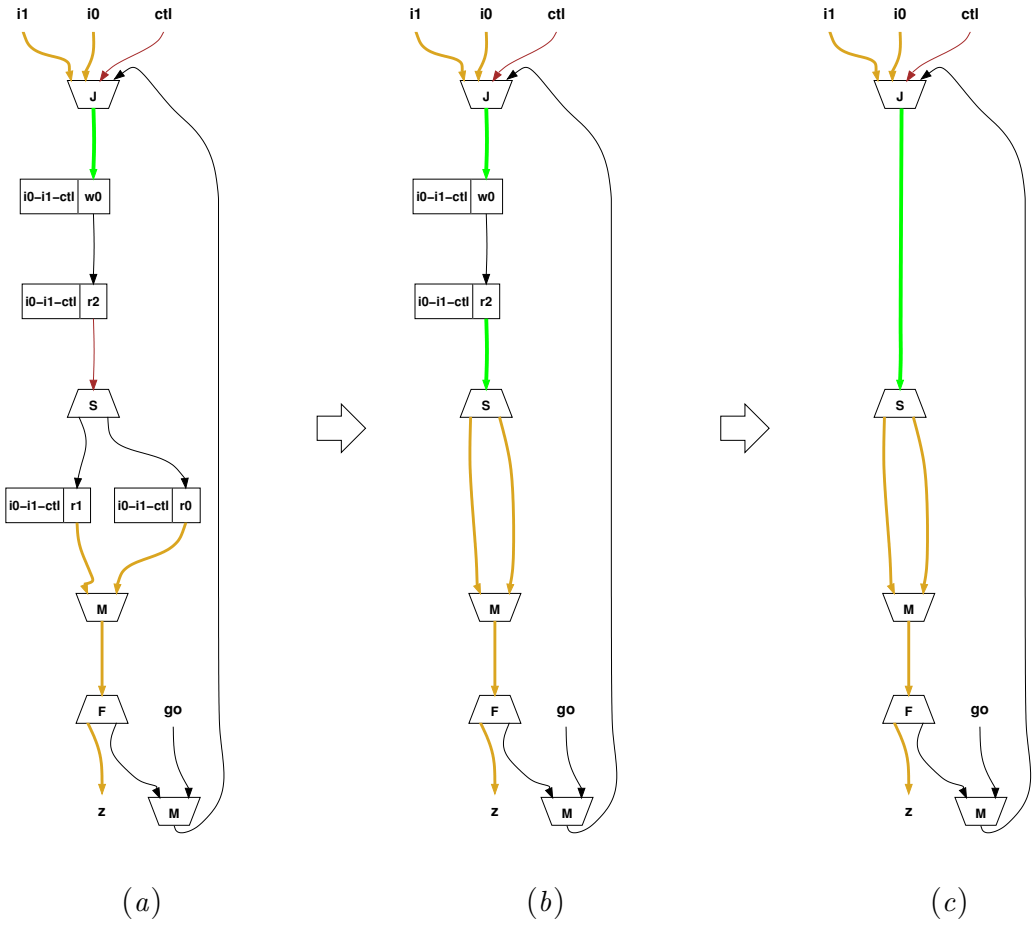

Figure 5.24: Circuit-level conditional reads removal.

- the write portions of two different variables must be separated by a channel or by *Joins*.
- the write and read portions must be separated by a channel or by *Forks*. In the latter case, the *Fork* outputs must be modified accordingly to accommodate the read portions.
- the read portions that provides the selection must be separated from the selected read portions by *Steers*.

*Variable*s with multiple write portions will make the transformation rules even more complex because a larger window of components will need to be checked. Furthermore, it is not always desirable to get rid of variables because they may form part of the specified behaviour. The procedure-level mechanism for passing optimisation options in section 6.5 is useful for this purpose, although a finer,

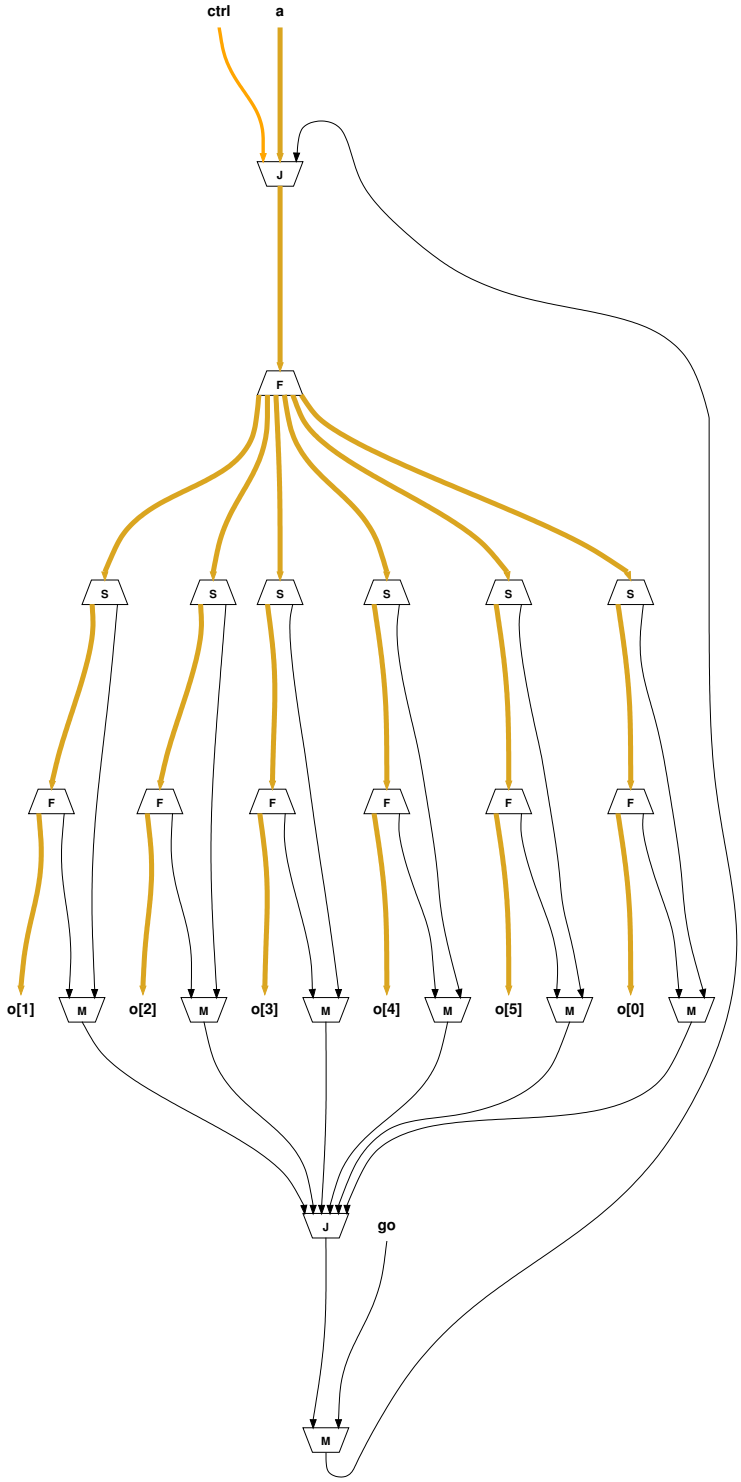

Figure 5.25: Circuit-level optimisation of the `steerAlu` module.

structure-level mechanism is envisaged. The proposed transformations demonstrates that there is still room for further optimisation of Teak networks.

5.4.3 Summary

This chapter has introduced Teak as a novel approach towards the synthesis of asynchronous circuits using a token-flow approach together with a set of optimisation techniques for the resulting networks. The basis of this system is a small set of components that provide basic datapath operations. Teak shares the *push-only* data style of the data-driven style proposed by Taylor [100], although Teak compiles Balsa descriptions and is more similar to the Macromodules system [93] than handshake circuits. Another difference with the data-driven handshake circuits is the availability of "real" Variables as permanent storage elements that permits flexible read and write accesses.

The properties of the Teak components and its compositions were used as the basis for optimisation techniques which are based in (*i*) circuit transformation, like the *Fork*, *Operator* and *Join* displacement, (*ii*) pattern-matching and replacement (like the loop removal and the *Variable* substitution, or (*iii*) a combination of transformation and substitution, like the *Steer-Merge-Join* optimisation.

Description-level techniques aimed specifically to this approach were also presented. In particular, it was noted that the enclosure technique used to optimise Balsa handshake components implementation may introduce performance overhead in Teak circuits. The description-level techniques target the removal of channel *Variables* with conditional accesses. The principle of these techniques were used as the basis to a more efficient circuit-level transformation that exploits the data-steering property of the the *Steer* component.

As will be seen in the chapter 7, for large and complex designs like the nanoSpa processor, implementations of Teak circuits currently have worse performances than those of Balsa circuits. This is unfortunate but not unexpected. The implementations for Teak components are at an early stage of development. However, there is a lot of headroom within the Teak approach as its small, regular component set allows the freedom to merge and split data and control much more naturally than in handshake components.

There is still much work that can be done to improve the optimisation of Teak-generated circuits. This includes: improved component implementations, the implementation of components with different data encodings (e.g. one-hot

codes running up to *Steer* inputs) as well as extensions to the current optimisation and automation of the optimisation described in section 5.4.2. The important optimisation issue of latch insertion in Teak circuits is considered in the next chapter.

Chapter 6

Latch insertion in Teak circuits

6.1 Introduction

Teak channels can be buffered to decouple components and to introduce the desired degree of token storage. In the Teak system, *Latch* components are used for buffering purposes. The *Latch* components used in the circuits presented in this thesis are implemented as half latches [91, 17]. Although other implementations are possible, the half latch implementation was selected for its simplicity.

The Teak synthesis algorithm does not introduce any buffering initially, this allows optimisation techniques to explore different buffer placement strategies. When the network contain *cycles* (also referred to as *rings* or *loops* in the related literature) buffers must be inserted in order to prevent deadlock. Latches may be inserted into any circuit to decouple processes and increase throughput.

A simple insertion strategy is to add a *Latch* to every channel. This will add enough token storage to prevent any circuit from deadlock but has a high penalty. To optimise the circuit's latency and throughput more elaborate buffer insertion strategies must be used. In [115, 114], Williams and Horowitz introduced some basic concepts and metrics to characterise the performance of asynchronous pipelines and rings. Based on their work, some approaches have been proposed to increase the performance of pipelined asynchronous circuits through latch insertion and *slack matching* [7, 45, 46]. Those approaches target iterative circuits with cycles that may contain more than one token and that can benefit from pipelining inside the cycle.

This chapter introduces a range of latching strategies currently implemented in the Teak system. The strategies target cycle structures that can hold a maximum

of one token (single-token cycles) commonly present in Teak circuits and that do not benefit from cycle pipelining. The aim of the strategies proposed here is solely to provide a more efficient alternative to the exhaustive insertion mechanism, although some analysis on the complexity and resulting performance is presented. The strategies are based on:

i. the identification and minimum latching of cycles.

ii. separation of tokens to avoid WAR hazards between portions of *Variable* components.

iii. the correct decoupling of control tokens in parallel and sequential compositions.

Optimal latch insertion targeting area/speed and pipeline slack matching is outside of the scope of this work.

6.2 Buffering cycles

Cycles in Teak circuits occur when the description specifies `loop` constructs, but also when modules are connected together in a ring fashion. In order to allow the circuit to progress, each cycle must have always enough buffering for a lead token to move forward and leave space for the following token. This translates into having a minimum of three half latches in a cycle [114, 91].

The most common single-token cycle structure in Teak circuits is the *Merge - Logic Block - Fork* circuit shown in figure 6.1, which can be clearly seen in some of the previous examples. Often, within the logic block of such structures there will be some latches required to separate the read and write tokens of *Variable* components.

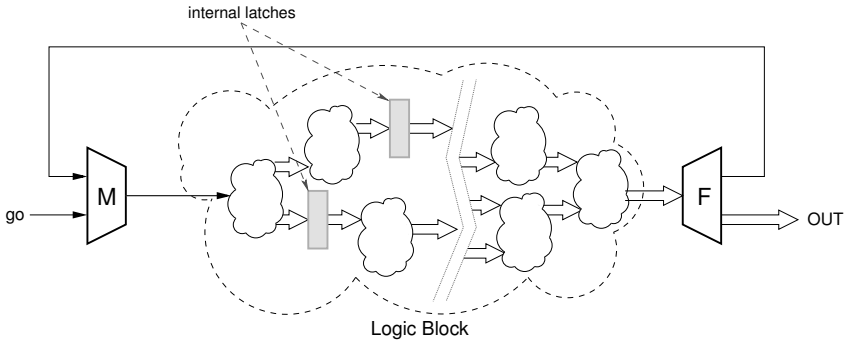

Figure 6.1: The Teak single-token loop *Merge - Logic block - Fork* structure.

6.2.1 Detecting cycles

In the first step of the analysis the circuit is mapped into a *directed graph*, where the edges are ordered pairs (s, d), connecting a source vertex to a destination vertex, as in figure 6.2(a). Within the graph each Teak component is mapped into a vertex and each channel into an edge. For *Variable* components, write and read sections are mapped into separate vertices.

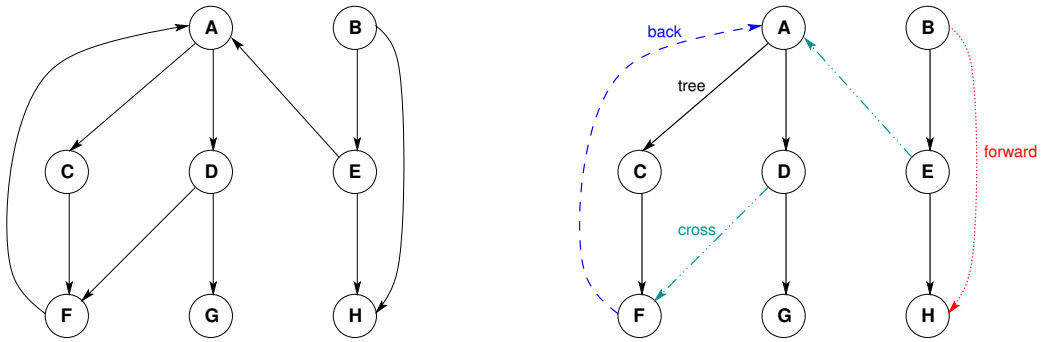

(a) (b)

Figure 6.2: (a) A directed graph and (b) a depth-first forest of the graph.

The resulting graph is then analysed using techniques based on depth-first search (DFS) [59, 98, 24] to obtain a classification of the edges. Initially all of the vertices of the graph are set to "unvisited". The DFS algorithm begins by choosing one unvisited vertex (a *root*) and exploring an edge leading to a new vertex. The algorithm continues in this fashion until it reaches a vertex which has no edges leading to unvisited vertices. The algorithm will then backtrack to the previous vertex and continue from the latest vertex that does lead to new unvisited vertices.

After DFS has visited all the reachable vertices from a particular root vertex, it chooses one of the remaining unvisited vertices as a new root and continues the search. The DFS process creates a set of *depth-first trees* that constitute a *depth-first forest*. The edges of the resulting forest are classified as *tree edges* (edges which lead to unvisited vertices), *forward edges* (edges which connect ancestors with descendants in a particular tree), *back edges* (the ones that connect descendants with ancestors), and *cross-edges* (which connect vertices across the forest). Figure 6.2(b) shows one possible DFS forest and the different classes of edges of the directed graph at its left.

The interesting class of edges for cycle detection are the *back edges*, because each back edge closes one or more cycles. Typically there are many valid depth-first forests for a given graph, depending on the (arbitrary) selection of the initial root and subsequent unvisited root vertices. There are therefore many different (and equally valid) resulting classifications for the edges. In Teak networks, the best candidates for root vertices are the components connected to the "go" and input ports, in that order of priority. This selection and priority is based in the following observations derived from compiled circuits:

i. A Teak network with a "go" port will always map into a *connected graph* (a graph such that there exists at least one path between all pairs of vertices). Using the component connected to "go" as a root vertex will ensure that all vertices are visited. It also ensures that the channel that returns the control token for the next iteration will be classified as a back edge. This is the most "natural" classification for such channel and also prevents the selection of a wider data channel as the back edge of the cycle, which would be more expensive to buffer.

ii. An optimised Teak network without a "go" port may map into a *disconnected* graph, consisting of two or more connected sub-graphs. Selecting vertices connected to input ports as root vertices will ensure that all vertices will be visited.

iii. If the description contains explicit ring structures, selecting the modules connected to the input ports as root vertices will ensure that the outputs that feed back and complete the ring will be classified as back edges.

Figure 6.3 shows the Teak circuit of figure 5.12(b) and its mapping into a directed graph. Notice that input and output channels are not included in the graph, but they are used in the selection of vertices as explained above.

Figure 6.4 shows the forest that results from applying a DFS analysis to the graph in figure 6.3. The graph has three back edges, {(L,A), (G,I), (J,K)}. These generate four cycles, namely, {A, B, D, H, J, K, L}, {A, B, E, I, K, L}, {C, F, H, J, K, L} and {C, G, I, K, L}. Each cycle c comprising v_c vertices has $e_c = v_c + 1$ edges. In this example, the cycles have 7, 6, 6 and 5 edges, respectively.

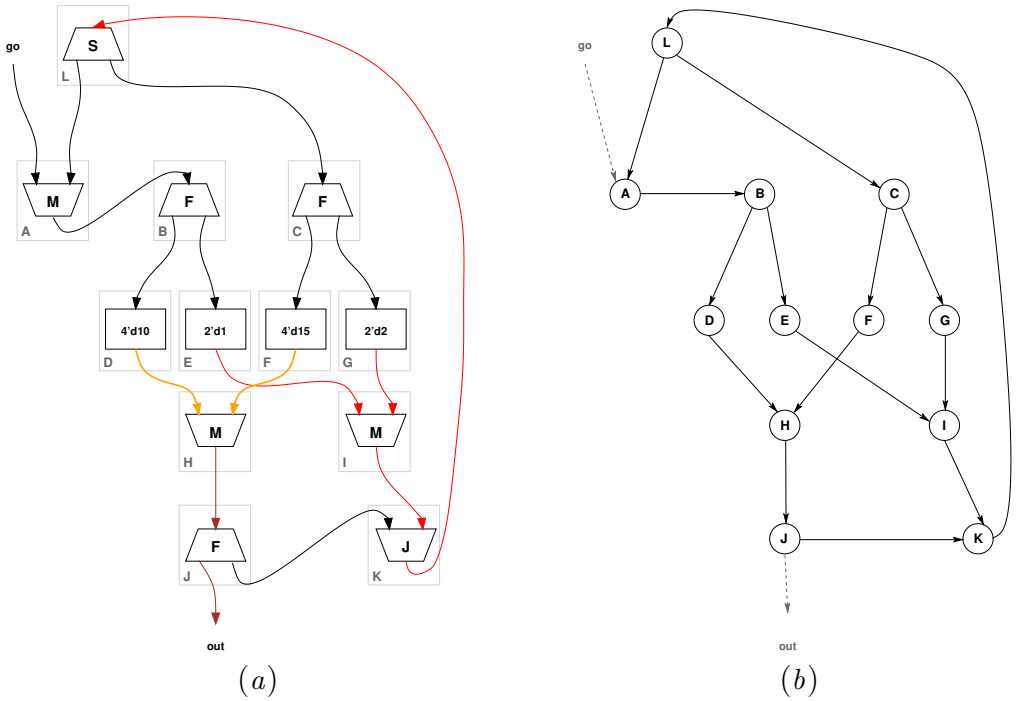

Figure 6.3: Mapping of a Teak circuit into a directed graph.

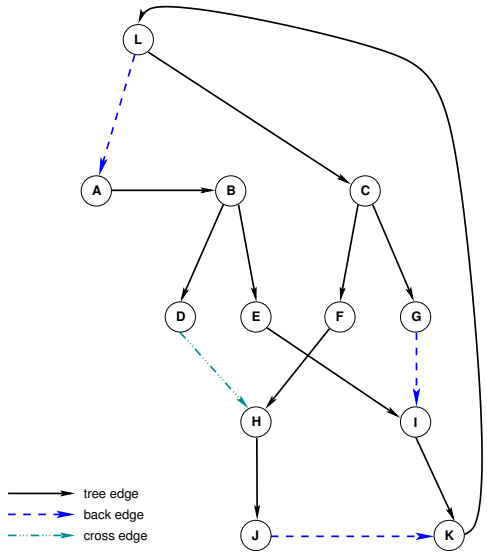

Figure 6.4: DFS forest of graph in figure 6.3(b).

6.2.2 Complexity of finding the optimum latch insertion points

For the simple example above it is not difficult to find by observation that the minimum set of edges that guarantees at least three latches within each cycle is:

{(L, A), (L, C), (I,K), (J,K), (K,L)}. However, in order to obtain the best possible location of the latches (targeting either minimum area or latency) each edge of the graph must be assigned a cost function depending on the type of components connected by the edge and the channel width. All possible arrangements of three latches within each cycle must then be enumerated and a cost assigned to each.

The number of possible arrangements for three latches in a cycle is given by the combinatorial number $l_c = \binom{v_c}{3}$. For the previous example, the total number C of different arrangements to be examined would be:

$$C = \binom{7}{3}\binom{6}{3}\binom{6}{3}\binom{5}{3} = 140\,000$$

In practice, for medium or large circuits, the number of components and cycles in a circuit makes an exhaustive analysis to find the optimum insertion points infeasible. Added to the complexity of finding all possible arrangements for the three latches, is that of finding all the cycles. In [99], Tarjan demonstrated that the complexity of finding all the cycles (referred to as *elementary circuits* in his work) in a graph with v vertices, e edges and c cycles is $O(v{\cdot}\, e(c+1))$. An optimised algorithm [53] reduces this complexity to $O((v+e)(c+1))$. However, the optimisation excludes cases that may occur in Teak circuits, like self-loops (edges of the form (v, v)) and multiple edges between the same vertices.

As it can be seen in the previous examples, Teak circuits normally comprise *Fork-Join* and *Steer-Merge* "diamonds". Each n-branch diamond located inside a cycle multiplies the number of possible cycles by n. This implies that for large circuits, the complexity of finding all cycles is too high, not to mention the combinatorial explosion of finding all possible latch placements. Consider for instance the optimised Teak circuit for the GCD shown in figure 6.5, derived from the description previously shown in figure 4.14(b). The directed graph from this circuit will have 41 vertices, 51 edges and 36 cycles, resulting in a complexity of $\mathbb{O}(77\,367)$ for finding cycles, which appears manageable. However, determining the best latch placements is more complex.

The GCD circuit has 8 cycles with 15 edges, 16 cycles with 16 edges and 8 cycles with 17 edges, hence, the number of possible combinations for latch placement is:

$$C = \binom{15}{3}^{8}\binom{16}{3}^{16}\binom{17}{3}^{8} \simeq 7.85 \times 10^{87}$$

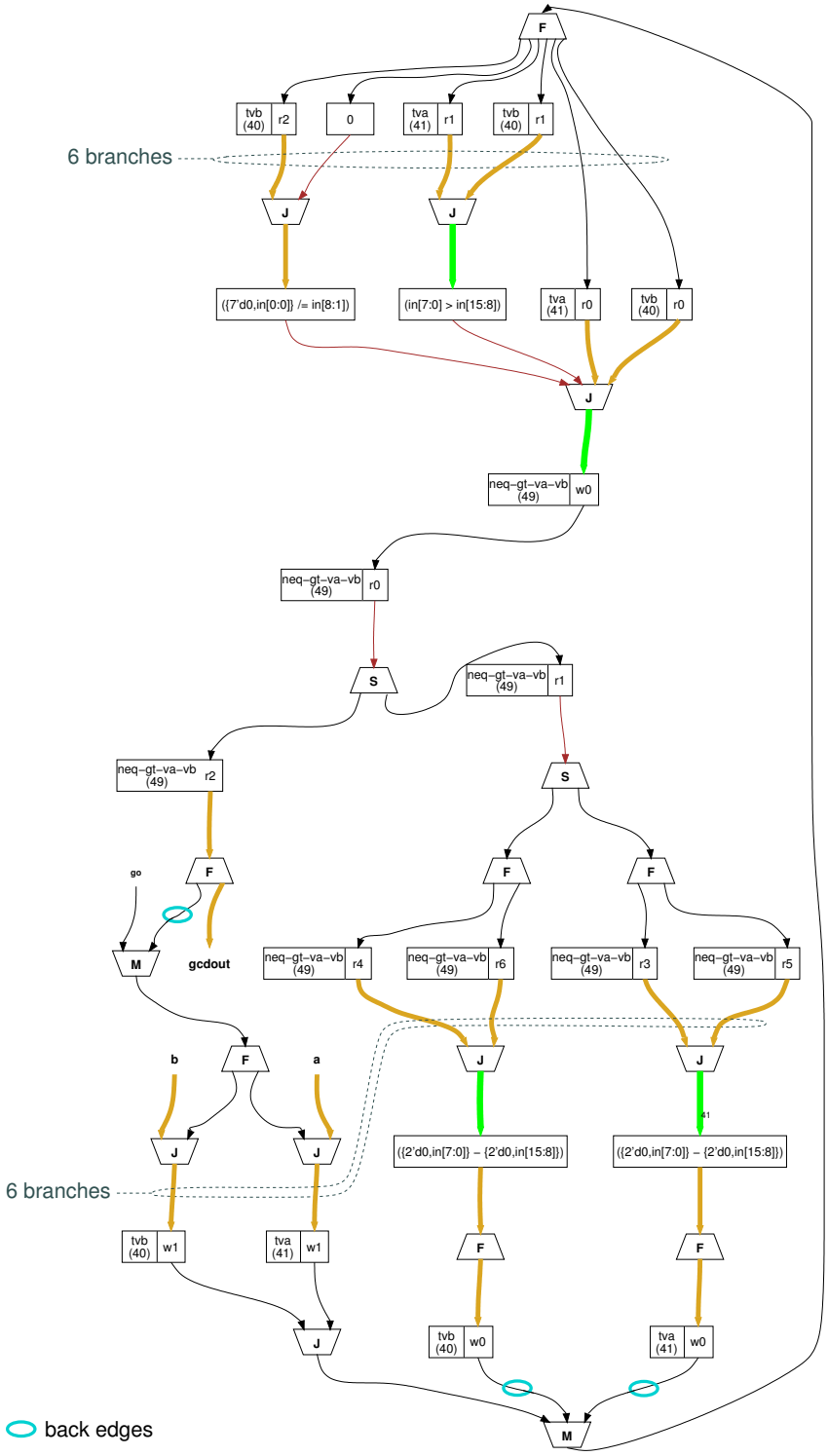

Figure 6.5: Optimised Teak circuit for the GCD description in figure 4.14(b)

In order to efficiently determine latch placements, heuristics are required to reduce the complexity of the problem. At present, the approach implemented in Teak is to use simpler strategies to latch token-limited cycles with the minimum three latches located in places that guarantee a deadlock-free cycle and a fast decoupling of the cycle outputs.

In the current implementation of Teak, as well as the insertion of three latches in every cycle, the user can specify the insertion of an arbitrary number of latches to decouple *Operators*, read sections of *Variables*, placed in forked control tokens, or placed in every channel. These latching strategies can be specified for the whole design or in a module-by-module basis. The next section will discuss issues related to the strategy used to automatically latch token-limited cycles.

6.3 Buffering single-token cycles

Using the DFS analysis together with the root selection rules described in section 6.2 ensures that the channel used to return the control token in a cycle is classified as a back edge. This is the result of selecting the vertex connected to the "go" (a *Merge*) as the first root. Because every cycle contains at least one back edge, inserting one latch in the following places will ensure that all the cycles containing the back edge (s_i, d_i) will have *at least* three latches:

- every back edge (s_i, d_i)
- every edge ending at s_i
- every edge beginning at d_i

The insertion is optimised to avoid inserting multiple latches in the same edge. This strategy is illustrated in figure 6.6 using the circuit for the GCD. The above heuristics reduce the complexity of the latching to the complexity of the DFS used to find the back edges, which is $O(v + e)$ [59], plus the processing of each back edge, resulting in a complexity of $O(v + e + b)$, where b is the number of back edges in the graph.

This approach efficiently solves the problem of combinatorial explosion, but it does not guarantee the optimal placement for performance or minimum area. Depending on the topology of the circuit, some extra latches may be added and

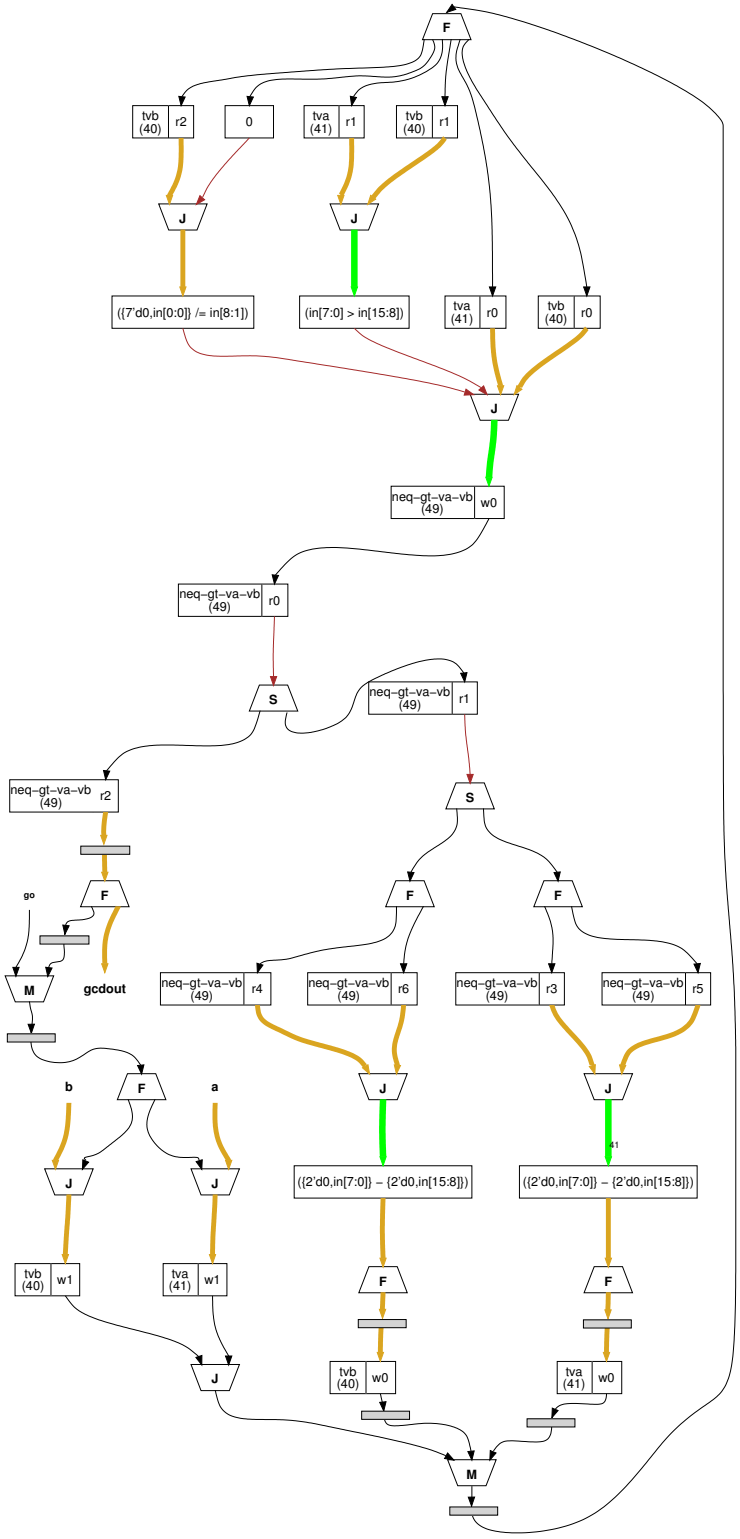

Figure 6.6: Strategy for latching all cycles of the GCD circuit of figure 6.5 based in latching back edges.

some cycles may end up having more than three latches, as shown in figure 6.6. However, some of the additional latches can be used to fulfil other latching requirements, such as the token separation latches for read and write sections of *Variables*.

Two variants of this approach will be analysed in the next section. Although the strategies target single-token cycles (those generated by *loop* constructs), they also serve to guarantee deadlock-free operation for multi-token cycles. In any case, the most important parameter is the time elapsed between iterations (the cycle time).

6.4 Two simple latching strategies for Teak circuits

This section analyses and compares two strategies to arrange three latches in single-token cycles. The strategies use the heuristics of attempting to place the latches as close as possible to the inputs and outputs to provide them with fast decoupling. These two strategies are:

i. placing a latch in the back link and after each back link successor, and before each predecessor. This arrangement is shown in figure 6.7(a). This strategy will be called "A".

ii. distributing the three latches so that the delay of the logic block is evenly split among smaller blocks, as shown in figure 6.8(a). This is strategy "B".

The figure of merit to evaluate each strategy is the cycle time, which will be determined by using a *dependency graph* analysis [91, 114]. A dependency graph represents the dependencies between signal transitions in a circuit. The vertices of such a graph represent rising or falling transitions and the edges represent dependencies between the signal transitions. In the analysis presented here, dependencies are represented as directed arcs and transitions are represented with boxes annotated with an internal label denoting the transition name and an external label denoting the delay associated with the transition.

Figure 6.7(b) and (c) shows the logic circuit and the corresponding dependency graph for the strategy "A". Similarly, figure 6.8(b) and (c) shows the logic circuit and the corresponding dependency graph for the strategy "B". In the diagrams, t_i, t_c and t_{cd} represent the latencies of an inverter, a C element and an

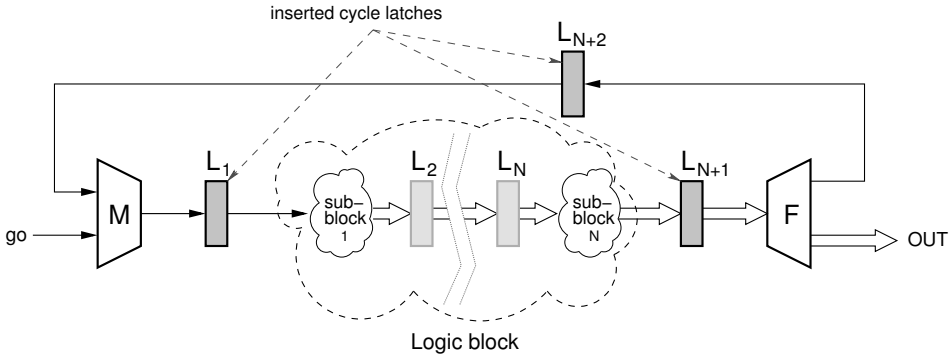

(a)

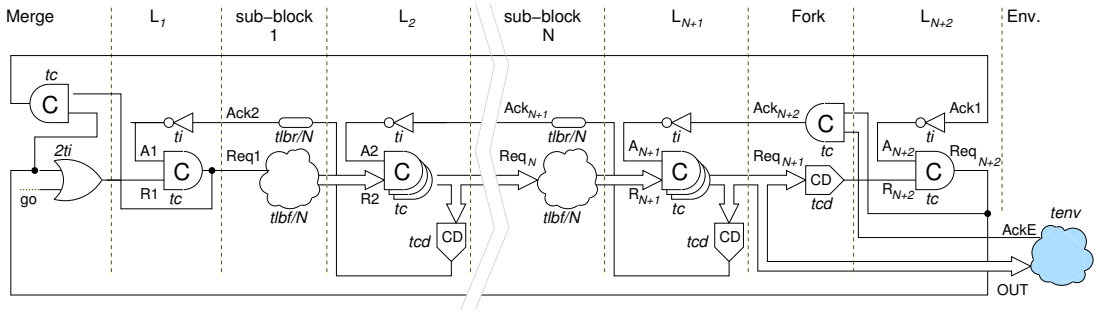

(b)

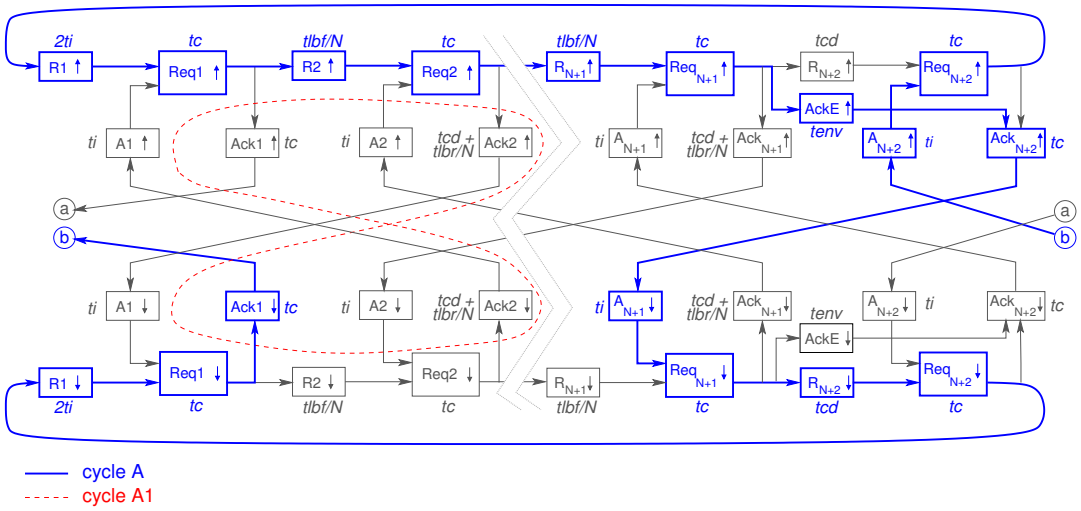

(c)

Figure 6.7: Latching strategy "A" for single-token *M-LB-F* blocks: (*a*) Teak circuit, (*b*) logic circuit, (*c*) dependency graph.

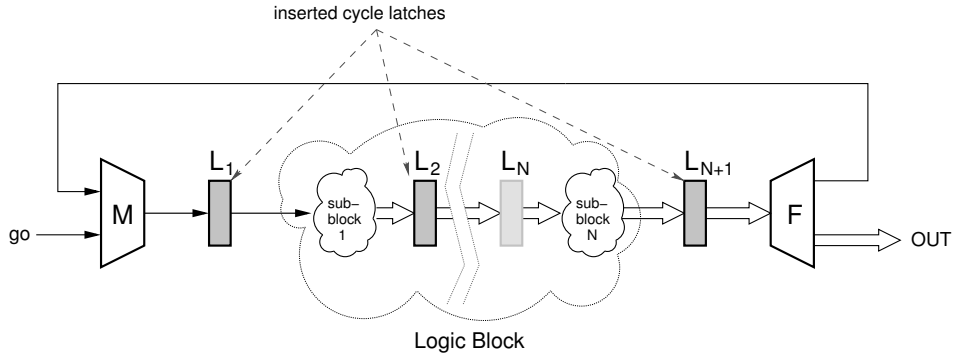

(a)

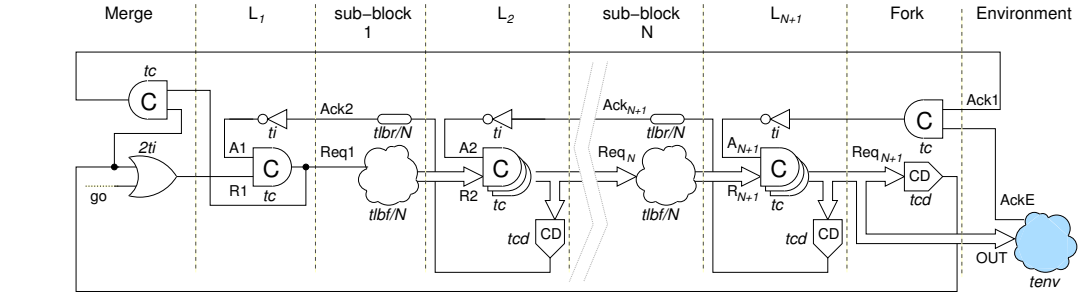

(b)

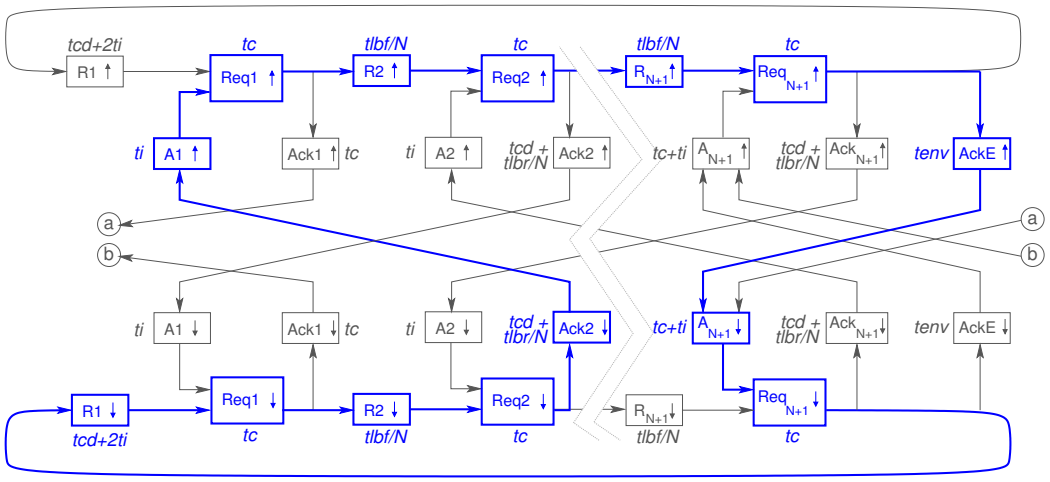

(c)

Figure 6.8: Latching strategy "B" for single-token *M-LB-F* blocks: (*a*) Teak circuit, (*b*) logic circuit, (*c*) dependency graph.

n-bit completion detector respectively. To simplify the analysis, the following assumptions have been made:

i. all circuit components have symmetric delays for rising and falling transitions.

ii. there are $N-1$ latches inside the logic block which evenly split the delay of the block by N. These are the latches associated with the read and write decoupling of *Variable* components inside the block.

In the current dual-rail implementation, *Operator* components have zero *backward latency* (the latency for the acknowledge), whereas other Teak components have some backward latency depending on the data width (*Merge*) or the number of outputs (*Steer, Fork*). The forward and backward latency of the logic blocks are labelled t_{lbf} and t_{lbr} respectively. The latency of the environment (typically another Teak circuit connected to the outputs) has been included in the circuits and graphs and is denoted as t_{env}.

6.4.1 Analysis of the latching strategies

The longest simple cycle for the latching strategy "A" has been highlighted in the dependency graph of figure 6.7(c). Starting from transition $R1\uparrow$ at the left of the graph, and following the highlighted path, the cycle time is:

$$\begin{aligned} t_{cycleA} &= 2t_i + (N+1)t_c + N(\frac{t_{lbf}}{N}) + t_{env} + 6t_c + 4t_i + t_{cd} \\ t_{cycleA} &= 6t_i + (N+7)t_c + t_{cd} + t_{env} + t_{lbf} \end{aligned} \tag{6.1}$$

Assuming that the latency t_c of a C-element is equivalent to two inversions,

$$t_{cycleA} = (N+10)t_c + t_{cd} + t_{env} + t_{lbf} \tag{6.2}$$

Similarly, for strategy "B", starting from transition $Req1\uparrow$ at the left of the graph in figure 6.8(c), the cycle time is:

$$\begin{aligned} t_{cycleB} &= (N+1)t_c + N(\frac{t_{lbf}}{N}) + t_{env} + 4t_c + 4t_i + 2t_{cd} + \tfrac{1}{N})t_{lbf} + \tfrac{1}{N}t_{lbr} \\ t_{cycleB} &= 4t_i + (N+5)t_c + 2t_{cd} + t_{env} + (1+\tfrac{1}{N})t_{lbf} + \tfrac{1}{N}t_{lbr} \end{aligned}$$

Assuming that the latency of a C-element is equivalent to two inversions,

$$t_{cycleB} = (N+7)t_c + 2t_{cd} + +t_{env} + (1+\tfrac{1}{N})t_{lbf} + \tfrac{1}{N}t_{lbr} \quad (6.3)$$

For t_{cycleA} to be the shortest, $t_{cycleB} - t_{cycleA} > 0$. From Eqs. 6.2 and 6.3,

$$\begin{aligned}(N+7)t_c + 2t_{cd} + +t_{env} + (1+\tfrac{1}{N})t_{lbf} + \tfrac{1}{N}t_{lbr} & \\ -((N+10)t_c + t_{cd} + t_{env} + t_{lbf}) &> 0 \\ -3t_c + t_{cd} + \tfrac{1}{N}t_{lbf} + \tfrac{1}{N}t_{lbr} &> 0 \\ t_{cd} + \tfrac{1}{N}(t_{lbf} + t_{lbr}) &> 3t_c \end{aligned} \quad (6.4)$$

The inequality 6.4 will hold for all cases where there is at least one latch inside the logic block. The inequality is independent of the environment latency. Looking closely at the path in figure 6.7(c), it can be noticed that the latch in the back edge decouples the logic block during the RTZ phase (the path does not go through the logic block), reducing the cycle time.

In cases when the logic block contains no internal latches (that is, no variables), inequality 6.4 no longer holds. In these cases, if the strategy "B" is used, the second inserted latch (*L2* in figure 6.8) will split the logic block into two halves, forcing $N = 2$ in equation 6.3. However, for strategy "A", N will be equal to 1 because the inserted latches are always outside the logic block. With these conditions, there will be another longest cycle candidate for strategy "A" (the "eight" shaped dotted line in figure 6.7). Starting from transition $Req1\uparrow$ and following this new path,

$$\begin{aligned} t_{cycleA1} &= 5t_c + 2t_{cd} + \tfrac{2}{N}t_{lbf} + \tfrac{2}{N}t_{lbr} \\ t_{cycleA1} &= 5t_c + 2t_{cd} + 2t_{lbf} + 2t_{lbr} \end{aligned} \quad (6.5)$$

Substituting $N = 2$ in equation 6.3 and performing the required operations (again, assuming t_{cycleA} to be the shortest):

$$t_{env} > \tfrac{1}{2}t_{lbf} + \tfrac{3}{2}t_{lbr} - 5t_c \quad (6.6)$$

In this case, strategy "A" will produce a faster circuit unless inequality 6.6 does not hold, that is, when the environment is faster than the delay through the

logic block. As an example, let us consider the situation when the logic block has the equivalent latency of two adders (addition is the slowest operation in Teak). Substituting $t_{env} = t_{cd}$, $t_lbf = 2t_{adder}$ and $t_lbr = 0$ in Eq. 6.6, the condition for strategy "A" delivering the faster circuit is:

$$t_{cd} > t_{adder} - 5t_c \tag{6.7}$$

Figure 6.9 shows a plot of both sides of inequality 6.7 as a function of the data width. The values shown are based on a worst-case longest carry chain of $width/2$. This is a conservative scenario, as in practice, the average carry chain length is less than $width/2$ [41, 62]. Figure 6.9 compares the left and right sides of inequality 6.7. The results are for a library with 2 and 3-inputs C-elements. The plot shows that, in this scenario, the inequality 6.7 will hold for $width > 16$ bits.

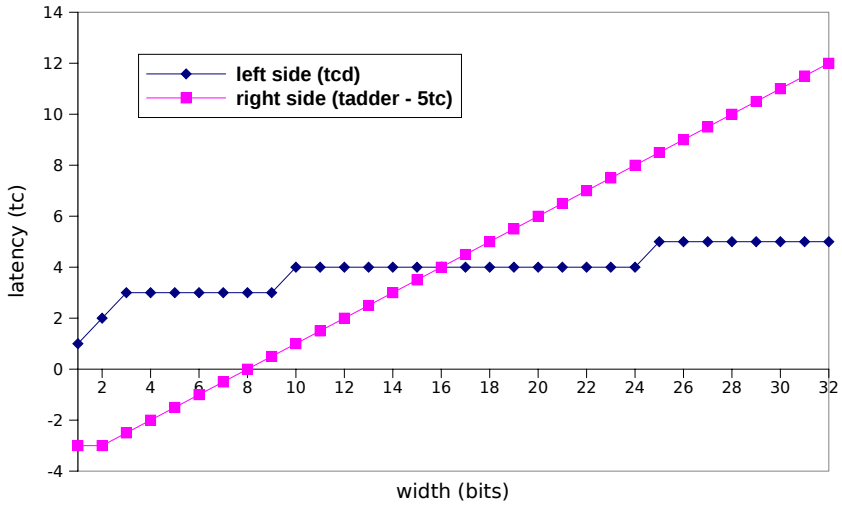

Figure 6.9: Comparison of both sides of inequality 6.6 for different data widths.

Experience with medium and large design examples used in this thesis have shown that complex, slow logic blocks with no variables are uncommon. In summary, the analysis presented in this section shows that, for practical cases, it is safe to assume that strategy "A" will produce a circuit with smaller cycle time. This is the strategy currently used in Teak. An additional benefit of using this strategy is that decomposition of the logic blocks into two equal parts when it contains no latches is not required.

6.5 Specifying latching and optimisation options in Teak

The Teak system provides two mechanisms to specify latching and optimisation options: (*i*) a command-line mechanism to specify the global, default options and (*ii*) a coarse-grained mechanism to specify local optimisations, at procedure-level, that overrides the global options. These mechanisms provide a flexible way of specifying and exploring the optimum set of options for a design.

The current implementation of the procedure-level mechanism is an extension to the Balsa language. If desired, local options can be passed enclosed in the `(* *)` pair, after the port declarations, as illustrated in line 5, figure 6.10. The `opts` label is used to pass optimisation options and the `latches` label is used for latching options. Options are separated by a colon (`:`). In figure 6.10, `trim-vars` specifies *Variable* removal and `move-fork-tos` is a *Fork* displacement optimisation. The latching option `l1` specifies the insertion of three single latches on each cycle of the circuit.

```
1 procedure adder (
2   input a, b   : N bits;
3   output sum   : N bits;
4   output carry : bit
5 ) (* opts="trim-vars:move-fork-tos" latches="l1" *)
6 is
7    channel cs : N+1 bits
8 begin
```

Figure 6.10: Example of passing options at procedure-level.

6.6 Summary

The problem of inserting latches in Teak circuits has been introduced in this chapter. An estimation of the complexity of efficiently buffering circuits to avoid deadlock was presented. The estimation was based on the number of cycles presented in the circuit, which require at least three half-buffers to allow the circuit to progress. In order to find the cycles, the Teak circuits are mapped into directed graphs and then analysed using a depth-first search technique that makes use of some properties of the Teak networks.

Two techniques that implement a minimum latching scheme for the single-token cycles (that results from the synthesis of the `loop` construct) were introduced and analysed. The techniques are presented as a more efficient alternative to the exhaustive latch insertion. The techniques make use of simple heuristics (fast decoupling of input and output ports) in order to reduce the complexity of the latch placement problem. The described techniques are the basis of the automatic latching insertion available in the Teak system.

Efficient buffering of Teak circuits targeting performance remains an open issue, as more heuristics based on the structure of Teak networks are required. The aim of the work presented in this chapter was solely to provide the Teak system with a minimum latching strategy to allow the circuits to operate. Latching insertion targeting performance or area/energy efficiency are considered future work.

Chapter 7

Design Examples and Evaluation

This chapter presents the descriptions and simulation results of a series of substantial design examples that were used to evaluate the different techniques presented in this work. The examples include:

- A 32-bit processor core: Nan's.
- A Viterbi decoder.
- A 32×32 radix-8 Booth multiply-accumulate (MAC) unit.
- A new result forwarding unit for the nanoSpa processor.
- A sliced-channel wormhole router.

All of the above designs were evaluated using the Balsa synthesis system. In Teak, the nanoSpa processor, the Viterbi decoder and the multiplier were used as evaluation examples. The forwarding unit and the router were not used as Teak examples because they rely on constructs and operations based on sequencers whose timing assumptions are not easily translatable into the Teak approach without a complete rewrite of the most complex parts of their descriptions.

All results given in this chapter were obtained using pre-layout, transistor-level simulations, using a 180 nm technology.

7.1 The nanoSpa processor

The nanoSpa processor [85] is an updated specification of the SPA processor [84], an asynchronous implementation of the 32-bit ARM v5T ISA [51] fully synthesisable using the Balsa system. The nanoSpa uses highly optimised Balsa code

targeting higher performance as opposed to SPA, whose description focused on security.

The initial version of nanoSpa [85] shares the same architecture organisation as SPA: an ARM-style 3-stage Fetch-Decode-Execute pipeline with a Harvard-style memory interface. The initial version had the following functional differences with respect to SPA:

- no support for Thumb instructions, interrupts, memory aborts or coprocessors.
- only the *supervisor* and *user* operation modes were available.
- no support for multiply operations.
- no support for half-word data transfers.

The new nanoSpa specification includes major changes in the organisation of the Decode and Execute pipeline stages, oriented to achieve its performance goal. These new features will be described in the next sections. The author has contributed to develop this new version with the following enhancements:

- implementation of the modified Decode stage.
- support for all ARM multiply instructions with the 32x32 MAC unit described in section 7.3.
- support for all ARM modes of operation.
- support for half-word data transfers.
- a branch control mechanism to reduce branch *shadow* penalties.
- the result forwarding unit described in section 7.4

Figure 7.1 shows a diagram of the 3-stage nanoSpa pipeline.

7.1.1 The Fetch stage

The Fetch stage fetches instructions from memory and implements the changes to instruction address flow generated by branches. This unit is very similar to the SPA fetch unit and has not had major changes. Like in SPA, the origin of the

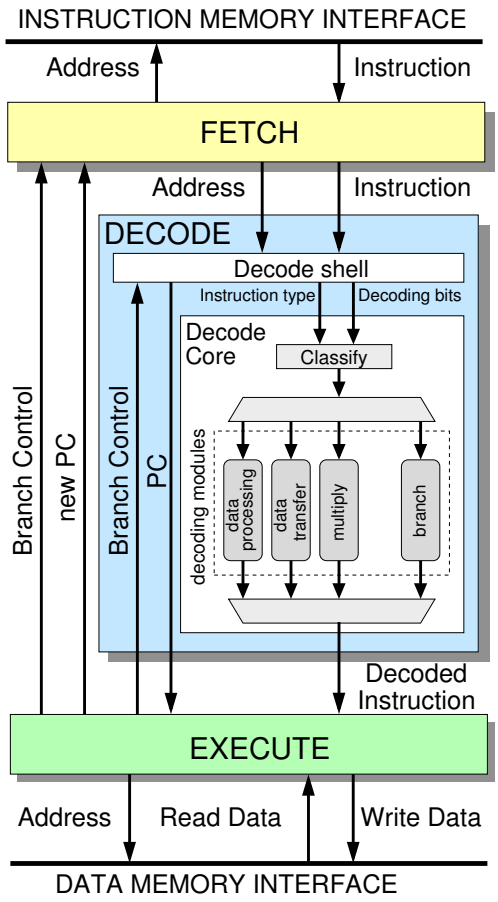

Figure 7.1: The 3-stage nanoSpa pipeline showing details of the *Decode* stage.

fetch address must be arbitrated between the local generated sequential address and the branch target address. This is the only place where arbitration is required in nanoSpa.

7.1.2 The Decode stage

The Decode has been redesigned as a two-level modular decoder as shown in figure 7.1.

Decode shell

This module receives the fetched instruction and performs an initial decoding of the instruction, generating the control signals which are common to all instruction types. It also selects the appropriated fields from the instruction to be used by the next level: the *decode core*.

Decode core and decoding modules

The decode core classifies the instruction according to its type and activates the related decoding module. There is one decoding module for each instruction type. These modules expand the instruction into the control and register selects required by the execute stage. The modules for multi-cycle instructions (such as load and store of multiple registers) unroll the instructions and issue all the required signals multiple times to the execute unit. In Balsa, each decoding module is described as an individual procedure. This modular approach makes it easier to either modify the decoding modules or add new ones, as any additions or changes are almost transparent to the rest of the already decoded signals.

Branch control counter-flow

The decoder receives branch control information from the execute unit, allowing it to discard any fetched instructions that are not within the new instruction flow established by the execution of a branch (those instructions are said to be in the *shadow* of a branch). The branch control from the Execute to the Decode unit is especially important in this design because the execute unit features speculative operation. In this way, instructions already in the pipeline that would be discarded after execution because they are in the shadow of a branch are now discarded earlier, increasing the performance and saving power.

7.1.3 The Execute stage

This stage has been redesigned to implement both data-driven and speculative operation, which has improved significantly its performance. The multiplier unit has also been redesigned and it is implemented using a modified radix-8 Booth algorithm customised to support signed and unsigned operands. A complete description is given in section 7.3. Figure 7.2 shows a simplified version of the nanoSpa execute stage. Data-driven and speculative operation in nanoSpa has been presented previously [85]. A brief description of these is given below.

Data-driven operation

In nanoSpa, all units inside the execution stage are activated in parallel: they wait until data arrives, process it and sends the result out without explicit sequencing. Steering and multiplexing units are added to guide the data and are

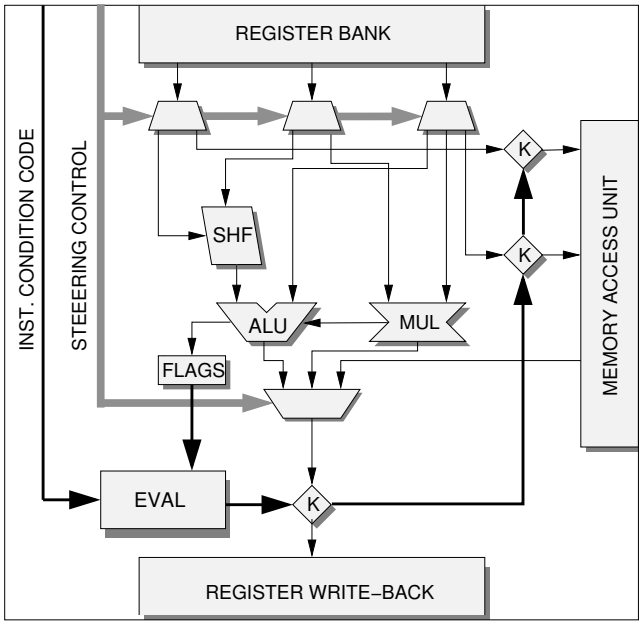

Figure 7.2: Simplified nanoSpa Execute stage.

controlled directly by control signals from the decoder, without any sequencing or synchronisation with data.

Speculative operation

In the ARM instruction set all instructions are conditional, i.e., they can be executed or skipped depending on the condition codes. In nanoSpa, the evaluation of the condition codes and the execution of the instruction are carried out concurrently to allow an early start of the instruction. If the condition code fails, the instruction is discarded at strategically located checkpoints without any result being written back, but ensuring that handshaking on all channels is completed Figure 7.2 shows how kill modules (labelled "K") are used to implement these checkpoints. In nanoSpa, data-processing instructions are started speculatively whereas data memory instructions are not, because of the extremely high penalties in power and performance that could derive from them. Speculative execution will only increase performance if the percentage of executed instructions is high, but this is usually the case.

7.1.4 Results

This section presents the simulation results for the nanoSpa processor using both the Balsa and Teak synthesis systems. The source description used with both synthesis tools was practically the same, apart from some minor modifications because of the "fire and forget" behaviour of Teak channels explained in section 5.2.2. All simulations results were obtained by running the *Dhrystone* benchmark.

Balsa

Table 7.1 shows the performance, area and energy results of different versions of the nanoSpa processor. The original version is called *nanoSpa0* in table 7.1. The device *nanoSpa1* includes the redesigned Decoder stage described in section 7.1.2 with the branch control counter-flow mechanism. The device *nanoSpaRef (DD)* is a description-level optimised and enhanced version of the *nanoSpa1* with added support for all the ARM modes, half-word and byte memory transfers, and the `MSR` and `MRS` instructions, which read and write the current and saved status registers. A finer grained separation of actions in concurrent loops and explicit duplication optimisation techniques were applied to this description.

The results in table 7.1 serve to differentiate the sources of performance improvement. From the table, the architectural enhancements have improved the performance by 8.92%. The description level optimisations improves the performance close to 27%. Therefore, the description level optimisations have increased the performance of the *nanoSpa1* design by 16%.

nanoSpa	*DMIPS*[†]		*Area*		*Energy*[‡]	
device	*absolute*	*Δ (%)*	*elements*	*ratio*	*nJ*	*ratio*
nanoSpa0	57.98	—	485 108	1.00	460	1.00
nanoSpa1	63.15	8.92	622 884	1.28	358	0.78
nanoSpaRef (DD)	73.54	26.84	662 734	1.37	361	0.79

[†] Dhrystone MIPS

[‡] per Dhrystone loop

Table 7.1: Performance, area and energy for three different versions of nanoSpa.

An interesting side-effect of the optimised architecture of the *nanoSpa1* is the reduction in energy consumption. The sources of this reduction are the more efficient design of the decoder and the branch control counterflow mechanism

which discards instructions that fall in a branch shadow at the decoder stage. Area penalties are the result of the enhanced features.

Table 7.2 shows the performance, area and energy results of different source-code and peephole optimisations presented earlier in chapter 4. The following is a key to the devices included:

- *DD*: the reference design. Corresponds to the *nanoSpaRef (DD)* optimised data-driven description presented in table 7.1.
- *DDO*: description-level optimisation of the *DD* design, with optimised guards and the addition of explicit duplication in some modules of the Execute unit.
- *DD/DDO + CF*: the *DD/DDO* description with the use of the concurrent *Fetch* component in the register bank.
- *DD/DDO + nRFV*: the *DD/DDO* description with removal of redundant *FalseVariable*s applied.
- *DDO + nRFV + CF*: the *DDO* description with the use of the concurrent *Fetch* component in the register bank and the removal of redundant *FalseVariable*s applied.
- *DDP (Taylor)*: the results for the original *nanoSpa0* architecture presented in [101] using the *push-only* data-driven synthesis methodology. The description is written in the new input language proposed by Taylor in his PhD thesis [100].

The results show that the different optimisations increased the performance between 2.6% to 6% when applied individually, and more than 11% when combined. Also notice that the description-level optimisations are the largest contributor to the performance increase, at 6%. Comparing the DDO results with the nanoSpa1 in table 7.1, the description-level optimisation increased the performance by around 24%. The results also show that, apart for the negligible area increase when using the concurrent *Fetch*, the optimisations result in area and energy reductions o less than 10%.

The *DDP* device was included to compare the trade-offs of having a full data-driven synthesis against the optimisations techniques proposed here. The description used in this thesis is an enhanced implementation of the one used by Taylor. Despite the differences in architecture, the larger overheads in area and energy

Optimisation applied	*DMIPS* † *absolute*	*Δ (%)*	*Area elements*	*ratio*	*Energy* ‡ *nJ*	*ratio*
DD	73.54	—	662 734	1.00	361	1.00
DD+nRFV	75.45	2.60	661 651	1.00	361	1.00
DD+CF	75.99	3.34	664 006	1.00	359	0.99
DDO	77.96	6.00	611 793	0.92	355	0.98
DDO+nRFV	79.47	8.06	610 361	0.92	356	0.99
DDO+CF	80.30	9.18	612 337	0.92	352	0.98
DDO+nRFV+CF	81.74	11.14	609 817	0.92	339	0.94
DDP (Taylor)	85.21	15.87	956 753	1.44	824	2.28

† Dhrystone MIPS

‡ per Dhrystone loop

Table 7.2: Balsa nanoSpa performance, area and energy results.

of the push-only data-driven implementation is clear from the results. Also, the push-only implementation is only 4% faster than the optimised description-level implementation. It can be argued that using the improved architecture, a *push*-only implementation will achieve even higher performance, however, the added complexity of the new description will also increase the area and energy overheads. The performance-oriented techniques (based in a *pull-push* style) proposed here offer better performance trade-offs.

Teak

The nanoSpa processor is the largest and most complex design synthesised by Teak to date. The source description was practically the same as used to synthesise the *nanoSpaRef* design. The only source of incompatibility was the use of the `select` construct in some small modules, but the construct was relatively easy to replace, maintaining the original architecture. Table 7.3 shows the performance, area and energy results when the following optimisations were applied to the description:

- *VFJ*: removal of redundant *Variables*, and *Fork* and *Join* consolidation and displacement (used in this work as the basic set of optimisations).
- *VFJ+SMJ*: the above plus the optimisation of *Steer-Merge-Join* compositions.

- *VFJ+SMJ+DL*: the above plus the description-level optimisation techniques to remove channel variables as described in section 5.4.2.

All of the above designs used the three-latches per cycle insertion technique described in section 6.4 to allow the circuit to progress.

Optimisation applied	*DMIPS*†		*Area*		*Energy*‡	
	absolute	*Δ (%)*	*elements*	*ratio*	*nJ*	*ratio*
VFJ	24.78	—	2 096 953	1.00	1 365	1.00
VFJ+SMJ	27.87	12.46	1 619 302	0.77	803	0.59
VFJ+SMJ+DL	41.08	65.79	1 674 134	0.80	777	0.57

† Dhrystone MIPS

‡ per Dhrystone loop

Table 7.3: Teak nanoSpa performance, area and energy results.

The results shows that the optimisation of *Steer-Merge-Join* compositions has improved the speed by 12.46% and significantly reduced the area and energy overheads. Adding the description-level optimisations to remove channel variables increases the performance close to 66% with a small increase in area and decrease in energy. These optimisations target conditional constructs.

These results highlight the potential headroom for optimisation that still exist in Teak circuits as conditional structures can be identified as one of the main targets for future optimisations. The results of the circuit-level optimisation technique proposed in section 5.4.2 (shown in figure 5.23) demonstrate that the overhead of the conditional structures in speed, area and energy may be reduced even further.

Table 7.4 shows the comparative performance, area and energy results for the best Balsa and Teak implementations of nanoSpa. The Balsa nanoSpa is 87% faster than its Teak counterpart, which is also 150% larger and consumes 115% more energy.

One potential source of improvement still to be exploited is the circuit-level optimisation presented in section 5.4.2. which targets conditional structures commonly found in all three stages of the nanoSpa pipeline. This optimisation is not yet automated and its manual application was infeasible due to the complexity of the nanoSpa design. It is expected that by applying this optimisation together with a better design of the components and better latching insertion mechanism,

Teak will reach its goal of providing mechanisms to exploit high performance pipelined asynchronous circuit styles using the Balsa language.

The Balsa Synthesis System is a more mature system that has gone through a series of iterations, whereas Teak is in its initial stages of development. The contribution of this work to the development of Teak is twofold: (*i*) a proof of concept for the synthesis methodology through the use of a highly complex demonstrator, and (*ii*) a means to evaluate the performance of the resulting circuits and identify potential sources for their improvement.

Decoder	*DMIPS*[†]		*Area*		*Energy*[‡]	
device	*absolute*	*ovh*	*elements*	*ovh*	*nJ*	*ovh*
Balsa	73.54	—	662 734	—	361	—
Teak	41.08	1.79x	1 674 134	2.52x	777	2.15x

[†] Dhrystone MIPS

[‡] per Dhrystone loop

Table 7.4: Comparison of the Balsa and Teak nanoSpa implementations.

7.2 An asynchronous Viterbi decoder

The design presented here is based in an initial description written by Gavant [42]. The description was optimised using the techniques presented in previous chapters and synthesised with the Balsa and Teak synthesis systems.

7.2.1 Introduction

Viterbi decoders [111] are used today in many digital communication applications to decode convolutional codes as part of a forward error correction (FEC) mechanism. The design of the decoder presented here is largely based in the architecture proposed by Brackenbury et. al [15] for an asynchronous Viterbi decoder aimed at a low power implementation.

Unlike the full-custom reference design, the approach in Gavant's work was to create a synthesisable decoder using the Balsa language to facilitate the exploration of different approaches to reduce the power consumption. However, in line with the objectives of this thesis, the original description was optimised for performance and no considerations were made to the resulting power consumption.

7.2.2 Viterbi decoder algorithm

Convolutional encoding

A convolutional encoder takes the last k bits of data arriving from a v-bit input stream and generates a n-bit output codeword ($n \geq v$) for each new v-bit input data word. The codeword is generated by combining the k bits using modulo-2 (XOR) operations. The number k is called the *constraint length* of the code. The *ratio* of the code is the fraction v/n. Figure 7.3 shows a convolutional encoder with $k = 3, v = 1$ and $n = 2$ (ratio $= 1/2$).

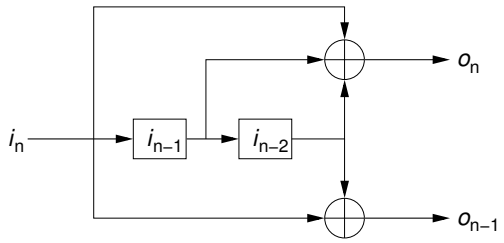

Figure 7.3: A convolutional encoder with $k = 3$ and code ratio $= 1/2$.

A convolutional encoder is a finite state machine with 2^{k-1} states. All possible transitions of the encoder can be represented using a *trellis diagram*. Figure 7.4 shows the trellis diagram for the encoder in figure 7.3. In this figure the circles represent states, a solid arrow indicates a transition when the input is 1 and a dashed arrow a transition when the input is 0. Each arrow is labelled with the output of the encoder. The highlighted path represents the state transitions for the input stream 1101, starting at state "00".

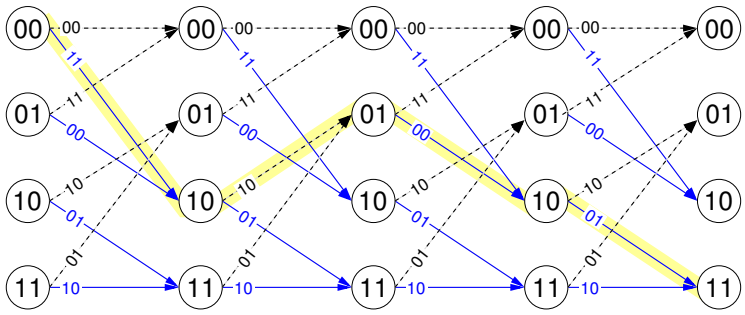

Figure 7.4: Trellis diagram for the encoder in figure 7.3.

Decoding process

The Viterbi decoding algorithm is based on finding the most likely sequence of states (path) in the decoder that would have generated the received data. This is done by calculating, for each possible state the decoder can be in, a *branch metric* (BM) that reflects how close is the received data from the error-free data that the decoder would generate. These measures are combined with a *state metric* (SM) (based on previous observations) that represents the likelihood the encoder was in each state. The combinations of state and branch metrics are called *path metrics* (PM).

The higher of the PMs for each state represents the most likely starting point for the next decoding cycle. This PM is saved and becomes the new SM for that state in the next cycle. The identity of the path that has the highest PM (called the *local winner*) is also saved for use later in the reconstruction of the path the encoder took through the trellis. This process is called *backtracing*.

When the received voltage for each bit is quantised using more than 2 levels, the decoder is said to use *soft-decision* decoding.

7.2.3 Architecture of the asynchronous Viterbi decoder

The decoder consist of three units as shown in the block diagram of figure 7.5: the The Branch Metric Unit (BMU), the Path Metric Unit (PMU) and the History Unit (HU). The parameters of the decoder are the following: code rate = $\frac{1}{2}$, constraint length $k = 3$ (four states), 3-bit soft-decision decoding and 16 slots of backtracing memory. A brief description of the units in the decoder follows. Extensive details about the principle of operation and the architecture can be found in [111, 15, 16].

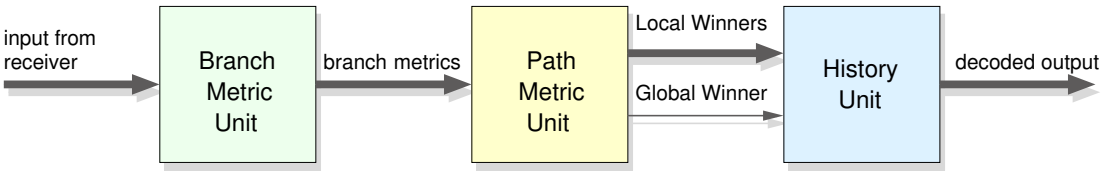

Figure 7.5: Architecture of the asynchronous Viterbi decoder.

The Branch Metric Unit

The Branch Metric Unit (BMU) receives the error-containing data from the receiver and computes the distances between the ideal branch pattern symbols and the received data (branch weights). The distance to be calculated is the Manhattan distance, as this is equivalent to the Euclidean distance squared in this application [15]. The branch weights are then passed to the Path Metric Unit. Details of the BMU implementation can be found in section 4.3.1.

The Path Metric Unit

The Path Metric Unit (PMU) is the core of the Viterbi decoder. Here accumulative weight information relating to each possible encoder state (or node) is maintained.

The PMU, shown in figure 7.6, is composed of 3 main parts:

- the Add-Compare-Select (ACS) units, which compute the weight additions and determine the lowest weight between two previous states. This gives the direction (local winner) for the next branch, upper or lower.
- the PMU Memory, where the weights are stored.
- the Global Winner Generator, which determines the lowest weight of all the states already selected. The global winner is valid when the lowest weight is unique.

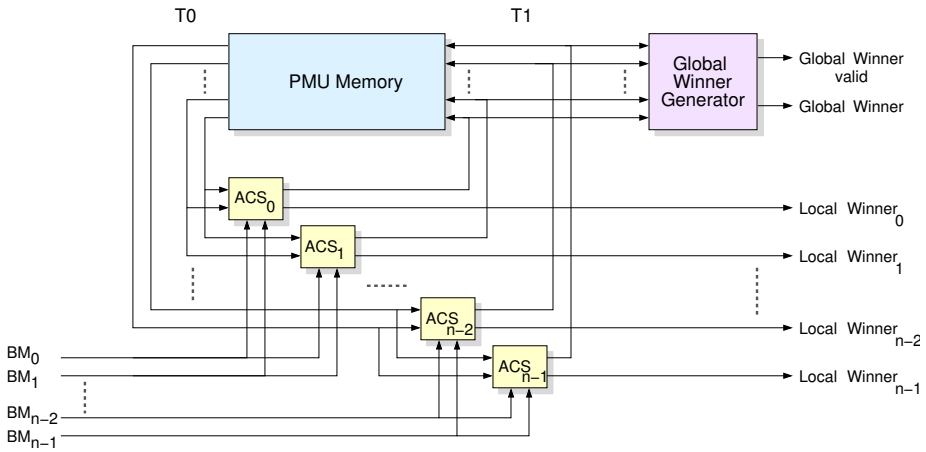

Figure 7.6: The Path Metric Unit.

The History Unit

The History Unit (HU) performs the backtracing. This is done only when a valid global winner is transmitted. With the local winner information, the previous state is computed and updated in the Global Winner Memory (GWM). This operation is repeated until the global winner computed is the same as in the GWM, which indicates that the backtracing has already been at that point. There are two memories, one the local winner (upper or lower) and one to store the global winner. The oldest state in the GWM is the current output of the decoder. Figure 7.7 shows a block diagram of the HU.

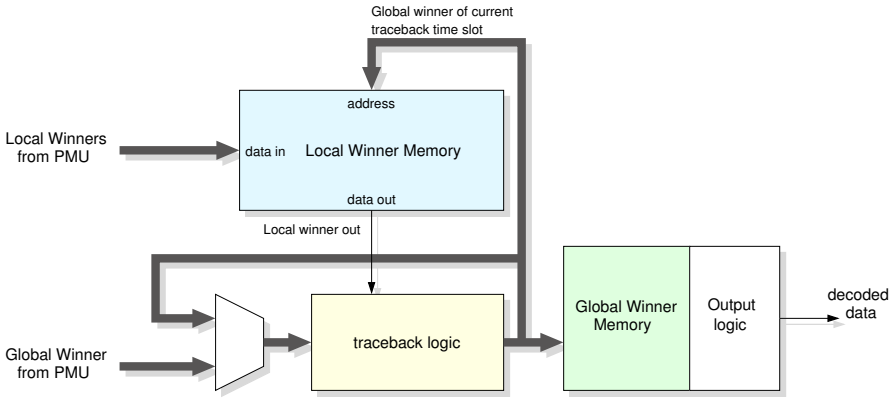

Figure 7.7: The History Unit.

Each unit in the architecture of the Viterbi decoder presents particular pipeline features. The BMU is a linear pipeline, the PMU is composed of a set of single-token rings and the HU is a single-token ring that performs multiple iterations over a token (a repeat-until loop). This unit is heavily control-dominated. As opposed to the nanoSpa pipeline, The Viterbi decoder pipeline has a fixed input-to-output token ratio.

7.2.4 Results

Balsa

The BMU was used as one of the running examples in chapter 4 of this thesis to demonstrate many of the description-level optimisations proposed here and some performance results were given. In this section performance results for the whole decoder will be given. The experimental set-up for the decoder consisted of decoding a stream of 1000 symbols with additive Gaussian white noise (AGWN)

and a signal-to-noise ratio $Eb/No = 2dB$. The parameter used to measure the performance is the average output data rate. Table 7.5 shows the performance, area and energy results for the following versions of the decoder:

- *VD*: the original unoptimised description.
- *VDO*: the description-level optimised version of *VD*.
- *VDO+CF+nRFV*: the *VDO* description with the use of the concurrent *Fetch* component and the removal of redundant *FalseVariable*s optimisations.

Decoder	*data rate*		*Area*		*Energy*	
device	*Msps*	Δ *(%)*	*elements*	*ratio*	*nJ*	*ratio*
VD	31.59	—	58 815	1.00	145	1.00
VDO	64.75	200.5	80 640	1.37	218	1.50
VDO+CF+nRFN	66.98	212.0	68 595	1.17	159	1.10

Table 7.5: Performance, area and energy results for the Viterbi decoder in Balsa.

The results indicate that fully description-level optimised version (*VDO*) achieves more than twice the performance of the original description. It is worth comparing this result with the 16% obtained by the more complex nanoSpa description in section 7.1.4. There are two reasons for this difference: firstly, the base design was written by a less experienced Balsa user and secondly the difference in complexity between the designs makes it easier to improve the critical path with the applied optimisations.

After applying the peephole optimisations to the optimised design (*VDO+CF+nRFN*), there is an extra increase in performance of 12%, (which translates into 3% when compared to the *VDO* version). In this case, the results are similar to those obtained with nanoSpa. As in the case of nanoSpa, the peephole optimisations target only small parts of the whole design, possibly not all belonging to the critical path, hence the smaller increments in speed.

Teak

The Viterbi decoder was directly compiled in Teak from the optimised source code used for the Balsa synthesis. Table 7.6 shows the performance, area and energy results when the following optimisations were applied to the description:

- *VFJ+SMJ (1L)*: removal of redundant *Variables*, *Fork* and *Join* consolidation and displacement and *Steer-Merge-Join* optimisation. A simple, one-latch per link latching strategy was used here.
- *VFJ+SMJ*: The above optimisations but with the used of three-latches per cycle insertion technique.
- *VFJ+SMJ+JI*: the above design plus the input-join description-level optimisation described in section 5.4.2 applied inside the BMU and PMU.
- *VFJ+SMJ+JI+DL*: the above plus the description-level optimisation techniques to remove channel variables described in section 5.4.2.

Decoder	*data rate*		*Area*		*Energy*	
device	*Msps*	Δ *(%)*	*elements*	*ratio*	*nJ*	*ratio*
VFJ+SMJ (1L)	52.30	—	124 656	1.00	269	1.00
VFJ+SMJ	60.76	16.18	106 462	0.85	207	0.77
VFJ+SMJ+JI	62.22	19.97	104 880	0.84	197	0.73
VFJ+SMJ+JI+DL	54.02	3.30	108 744	0.87	215	0.80

Table 7.6: Performance, area and energy results for the Viterbi decoder in Teak.

The results in table 7.6 show that the more elaborate three-latches per cycle strategy improves the performance by 16% and reduces area an energy consumption by 15% and 23%, respectively, for this example.

The technique of joining inputs takes the performance improvement to 19% with further reductions in area and energy. Finally, notice that including the removal of channel *Variables* results in performance, area and energy penalties in this case. These results further support the observations of section 5.4.2. In the Viterbi decoder, the datapaths are narrow (3 to 6 bits) and the overhead of the tagging circuitry generated by the coding style overshadows the potential benefit of removing the *Variables*. In contrast, this technique was very effective in the nanoSpa design because of the widths of the datapaths within the design.

Table 7.7 compares the best Teak and Balsa implementations of the Viterbi decoder. The results shows a small performance overhead for the Teak implementation. However, the Teak implementation could be further optimised using the circuit-level optimisation of section 5.4.2, whereas the Balsa counterpart has already been fully optimised at both the description and circuit levels.

Decoder	*data rate*		*Area*		*Energy*	
device	*Msps*	*ovh %*	*elements*	*ovh %*	*nJ*	*ovh %*
Balsa	66.98	—	68 595	—	159	—
Teak	62.22	7.65	104 880	52.90	197	34.52

Table 7.7: Comparison of the Viterbi decoder in Balsa and Teak.

7.3 A 32×32-bit radix-8 Booth MAC

The Booth algorithm [13] is an efficient multiplication algorithm that is commonly used to implement the multiplication of two signed binary numbers in hardware. A number of bundled-data asynchronous multiplier have been described that implement the *modified* Booth algorithm, in which the number of iterations is fixed [54, 55, 94]. A bundled-data implementation of the *original* Booth algorithm, which skips consecutive chains of zeroes and ones leading to a number of iterations that depends on the operands, is described in [31].

The multiply-accumulate unit described here was designed to support all the variations of the ARM multiply instructions in the nanoSpa core, replacing the shift-and-add multiplier used in the SPA processor. Figure 7.8 shows the architecture of the nanoSpa multiplier.

The unit is a 32×32 multiplier with 32-bit accumulation. It is implemented as a radix-8 (Booth-3) modified Booth's algorithm [13, 27]. This implementation was selected after comparing it with a radix-4 (Booth-2) implementation as a good performance-area trade-off: for an increase of 2.5% in the total nanoSpa processor area, the multiplier performance increases by 25% [95].

In figure 7.8, A and B are the multiplicands, and C is the optional 32-bit accumulate. The result is delivered as one or two 32-bits words (depending on the type of multiplication), H being the most-significant 32 bits and L the least significant 32 bits. The unit also calculates the zero (Z) and negative (N) flags. The multiplier consists of the following units:

Bypass and Merge: To support the speculative operation of the nanoSpa Execute stage, the multiplier is wrapped within the *Bypass* and Merge units. These units facilitate the early termination of the multiplication when the condition code of the instruction fails. If this is the case, the *Bypass* section generates a constant result of zero and discards the operands. In this way, the handshake is completed in the operand channels, the Booth loop is not

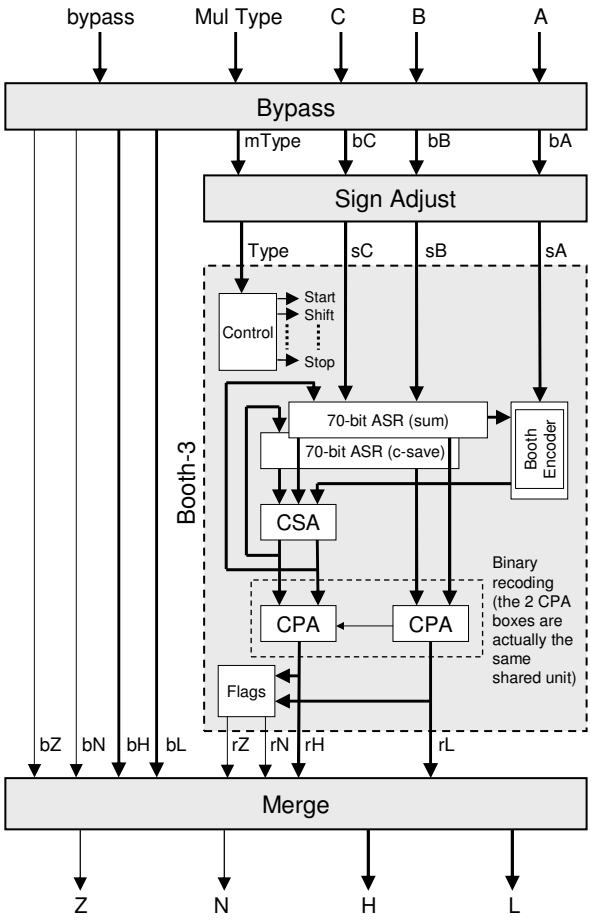

Figure 7.8: Architecture of the nanoSpa multiplier unit.

executed, and a result data is sent down the datapath to be discarded and to quickly finish the instruction. The *Merge* section passes either the zero results generated by *Bypass* or the actual multiplication and flags results to the output channel.

Sign Adjust: In order to accommodate the algorithm requirements, and the signed and unsigned operations specified in the ARM instruction set, this unit either sign-extend or zero-fill the operands A, C. For operand B, a zero is added at the least significant position (to complete the bit encoder bit grouping) and two bits are added at the most-significant positions (to save the carry out and to set the unsigned operands as positive numbers). This unit also passes the accumulate operand or zero if no accumulation is required.

Booth-3: This unit carries out the actual multiply-accumulate (MAC)

operation This block consists of a Booth-3 decoder that selects the partial product to be added to the multiplicand, two arithmetic 70-bit shifters (one for the Carry-Save bits and one for the sum bits), a 32-bit Carry-Save Adder (CSA) to speed up the addition in the loop, a controller unit, and a 32-bit Carry-Propagate Adder (CPA). Together, the decoder, the shifters, the controller, and the CSA implement the Booth iteration. The shifter is initialised with the sign-extended multiplicand sB in its lower 35 bits and with the value of the accumulate, sC in its upper 35 bits (to add it on the first iteration). The sign-extended multiplier operand sA is passed to the Booth encoder to generate the required partial products to be added. The controller initiates and stops the iterations and, after the last iteration, steers the CSA output and the 32 bits of the shifter containing the lower 32 bits of the result of the loop to the CPA. The CPA recodes the lower 32 bits by adding the lower halves of the two shift registers. It also recodes the upper 32 bits by adding the outputs of the CSA. In order to save hardware, these two recoding operation use the same CPA sequentially.

7.3.1 32-bit Multiply with 64-bit accumulation

Given that MAC operations with 64-bit accumulation are not very common, in order to perform a full 64-bit accumulation, nanoSpa executes any long multiply-and-accumulate in two cycles: the first cycle executes a MAC with 32 bit accumulation and then executes an ADD operation with the upper 32 bits of the MAC result and the upper 32 bits of the accumulate register. This architectural decision contributes to reducing the area overhead of the multiplier.

7.3.2 Results

The Booth-3 unit (the core of the multiplier) is a control-dominated circuit as can be seen in the "X-ray" picture of its Handshake Circuit, show in figure 7.9. The parameter used to measure the performance was the average cycle time of signed multiply-and-accumulate operations. The design was synthesised in Balsa and Teak from an already optimised source, however some of the new optimisations were also applied. This design was used to further compare Balsa and Teak synthesis styles using a medium-complexity control-dominated example.

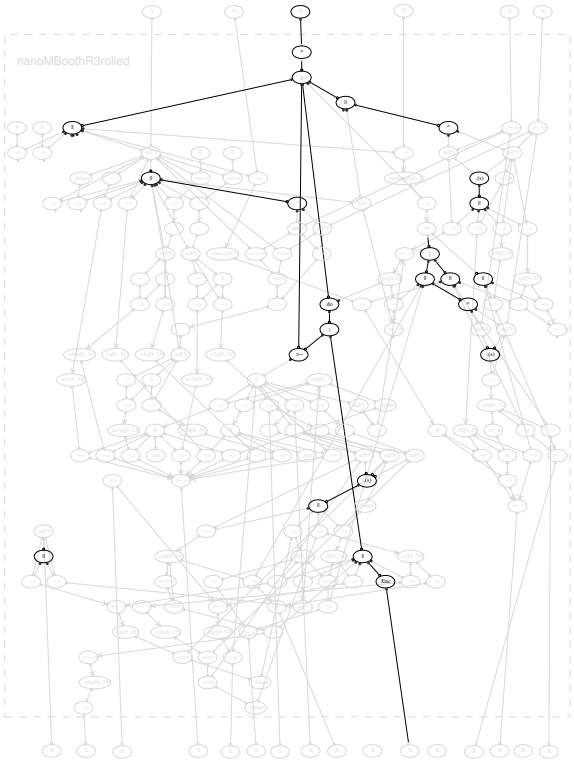

Figure 7.9: An "X-ray" picture of the Booth-3 Handshake Circuit revealing its control tree.

Balsa

Table 7.8 shows the performance (average delay time of 32-bit multiply and accumulate operations), area and energy results for the following versions of the multiplier:

- *MAC*: the original description.
- *MAC+DL* : the *MAC*. with description-level optimised `case` guards and explicit duplication in the *Booth encoder* block.
- *MAC+DL+AEC*: the above plus the optimisation of the control of active enclosures described in section 4.6.2.

The results show that, despite the small room available in this very optimised control-dominated design, some performance increase can be achieved with the new optimisations: The description-level optimisations delivered 2.35% performance increase, which together with the optimised control results in an extra 3.57% with a 5% of area overhead.

Multiplier	*delay*		*Area*		*Energy*	
device	*ns*	Δ *(%)*	*elements*	*ratio*	*nJ*	*ratio*
MAC	90.60	—	115 680	1.00	80	1.00
MAC+DL	88.60	2.36	120 900	1.05	78	0.98
MAC+DL+AEC	87.48	3.57	120 961	1.05	80	1.00

Table 7.8: Performance, area and energy results for the MAC unit in Balsa.

Teak

Table 7.9 shows the performance, area and energy results when the following optimisations were applied to the MAC description:

- *VFJ+SMJ (1L)*: removal of redundant *Variables*, *Fork* and *Join* consolidation and displacement, and *Steer-Merge-Join* optimisation. A simple, one latch per link latching strategy was used here.
- *VFJ+SMJ*: The above optimisations but with the use of three latches per cycle insertion technique.
- *VFJ+SMJ+JI*: the above design plus the input-join description-level optimisation described in section 5.4.2.

Multiplier	*delay*		*Area*		*Energy*	
device	*ns*	Δ *(%)*	*elements*	*ratio*	*nJ*	*ratio*
VFJ+SMJ (1L)	147.88	—	249 070	1.00	153	1.00
VFJ+SMJ	133.66	10.64	179 242	0.72	98	0.64
VFJ+SMJ+JI	129.34	14.33	180 972	0.73	93	0.61

Table 7.9: Performance, area and energy results for the MAC unit in Teak.

The results in table 7.9 show that the three-latches per cycle strategy has improved the performance by 10% and has reduced the area by 30% and the energy consumption by 36%. These results are similar to those obtained for the Viterbi decoder.

The technique of joining inputs improves the MAC performance by 14% with a small increase in area, but smaller energy consumption. In this design it was impractical to use the description-level technique to remove the channel *Variables* due to its heavily sequenced and iterative architecture.

Finally, table 7.10 compares the best Teak and Balsa implementations of the MAC unit. In this control-dominated case, the Teak overhead in performance is larger, mainly because the design heavily relies on the use of variables.

Multiplier	*delay*		*Area*		*Energy*	
device	*ns*	*ovh %*	*elements*	*ovh %*	*nJ*	*ovh %*
Balsa	87.48	—	120 961	—	80	—
Teak	129.34	47.85	180 972	49.61	93	16.15

Table 7.10: Comparison of the MAC implementations using Balsa and Teak.

7.4 The nanoSpa Forwarding Unit

This section presents the description of a synthesisable result forwarding unit for the nanoSpa asynchronous microprocessor, using the syntax-directed synthesis approach and targeting a robust QDI implementation. The author has published a paper based on this work [96].

7.4.1 Introduction

Result forwarding [49] is a method used in pipelined microprocessors to reduce the penalty caused by inter-instruction data dependencies. The forwarding mechanism can also be used to allow partial overtaking of (normally slow) memory operations by faster instructions, whilst making sure that the instructions complete in the same order as they appear in the instruction stream. Figure 7.10 depicts some potential performance benefits of the result forwarding mechanism.

In synchronous systems, the problem of result forwarding can be easily solved because the clock signal serves as a reference that allows synchronisation between result producing and consuming units. In an asynchronous environment, the problem of implementing a result forwarding mechanism is more complicated due to the lack of synchronisation between producers and consumers. In this case, one cannot rely on a control signal that indicates which cycle an instruction is in as this requires a lockstep operation of the pipeline that would heavily penalise the performance.

An efficient, full-custom solution to the problem of result forwarding within an asynchronous environment was proposed and implemented in the Amulet3

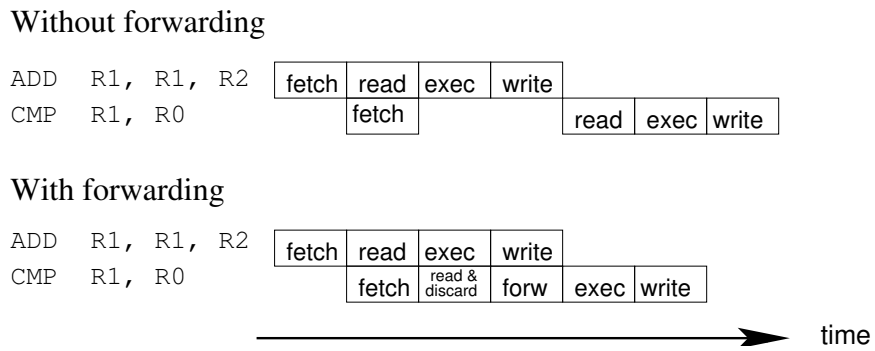

Figure 7.10: Potential performance benefits of result forwarding in a 4-stage pipeline.

asynchronous processor [43, 44, 36], targeting a bundled-data implementation, with the consequent limitations on design-space exploration, technology portability due to its full custom design, and with similar timing closure problem as synchronous designs. In order to overcome such limitations and reduce the impact of increasingly difficult timing closure within modern fabrication process variability, it is desirable to have a synthesisable asynchronous description which can be mapped into a quasi-delay-insensitive implementation.

The following sections introduce relevant related work and discusses the implementation of a forwarding mechanism designed to be used in the nanoSpa processor described earlier in section 7.1.

7.4.2 Related work

Earlier asynchronous techniques for resolving dependencies include: the register locking mechanism for the Amulet1 processor [80, 35], register locking plus "last result" register used in the Amulet2 processor [37, 112], the last result bypass mechanism of the Caltech asynchronous MIPS [69], the scoreboard-like Data Hazard Detection Table (DHDT) of the SAMIPS processor [118], the CounterFlow Pipeline Processor architecture (CFPP) proposed in [92] and the asynchronous "queue" FIFO [43] for the Amulet3 processor [38]. The ARM996HS processor by Handshake Solutions is a commercially-available synthesisable asynchronous 32-bit CPU that was implemented using the TiDE tools [23]. The processor ARM996HS core is a five-stage asynchronous pipeline and so may benefit from result forwarding but no information has been published about the dependency

avoidance technique used. As with Amulet3, its implementation uses bundled-data encoding.

The Amulet3 asynchronous "queue" FIFO (AQF from herein) was used as the reference model for the nanoSpa forwarding unit (nFU). The AQF is a circular buffer that acts both as a forwarding unit and a reorder buffer. The AQF stores the results and their register destinations from previous instructions. Figure 7.11 shows a diagram of the AQF process model. The queue operation consist of 5 processes: *Lookup*, *Allocation*, *Forward*, *Arrival* and *Writeout* [44, 43].

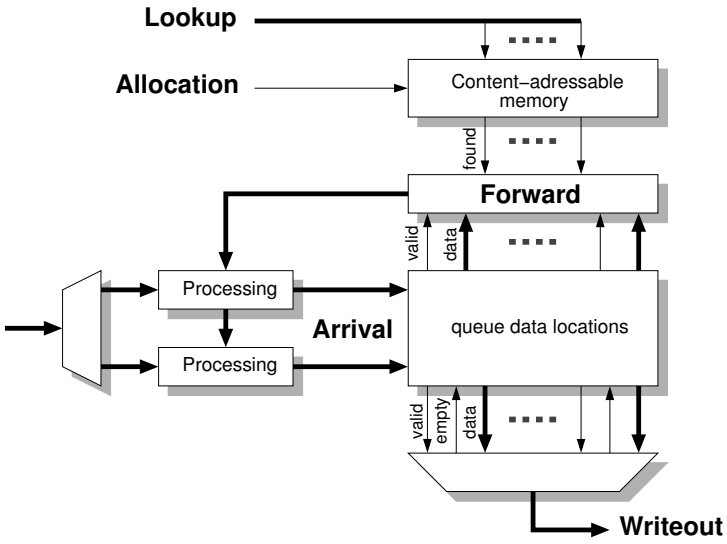

Figure 7.11: AQF process model.

Lookup: This process receives the source register names for instruction operands from the decoder, examines the queue to see if they are present, and returns a bit mask indicating the possible data source positions in the queue. This is performed using a CAM (Content Addressable Memory) that holds the previously allocated destination registers.

Allocation: After obtaining the lookup source mask, the instruction's own destination address can be written into the CAM. The writing position is allocated cyclically within the circular buffer structure.

Forward: Concurrently with Allocation, this process receives the mask generated during Lookup, examines each of the possible sources (starting at the most recent), waits until the data is present and then checks for

validity. Valid data is forwarded to the required places, otherwise the process examines the next most recent possibility. If all the possibilities are exhausted (or if there were no data sources) the forwarding process gives up and the default value, read from the register bank, is used.

Arrival: Results arriving at the queue carry their allocated queue address. The allocation process guarantees non-conflicting allocations even in the event of multiple writes. When the data allocated to a particular slot arrives, the previous data in the slot will have been written back to the register and so can be overwritten without conflict. If the instruction was abandoned due to conditional execution then the result will be marked as invalid.

Writeout: This process copies valid results back to the register bank. It examines the queue locations cyclically and waits until the valid result arrives then copies the data to the register bank and marks the location as "empty" so it can be reallocated.

In order to improve the speed of the Lookup process, the Amulet3 AQF uses a small CAM to hold the information about the registers written in the buffer. Speculative read of the default value from the register bank is also performed in case the source operand is not present in the buffer. The AQF has a centralised, token-passing asynchronous control and features three read ports for forwarding and two write ports for arrival.

7.4.3 The target processor: nanoSpa

In a new experimental description of nanoSpa, the pipeline depth has been increased to enhance the performance. Figure 7.12 shows a simplified version of the new 5-stage nanoSpa pipeline.

7.4.4 Architecture of the nanoForward Unit

The nFU has the same number of read ports (3) and write ports (2) as the AQF, but as the current nanoSpa architecture does not execute instructions out of order, the nFU is not used as a reorder buffer.

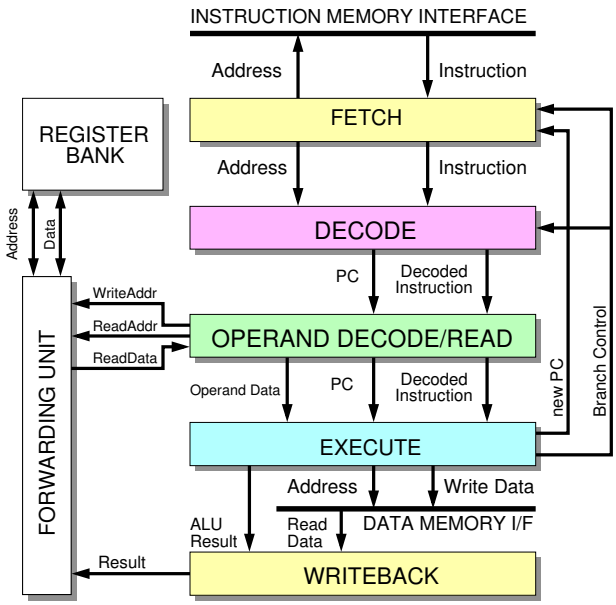

Figure 7.12: The 5-stage nanoSpa pipeline.

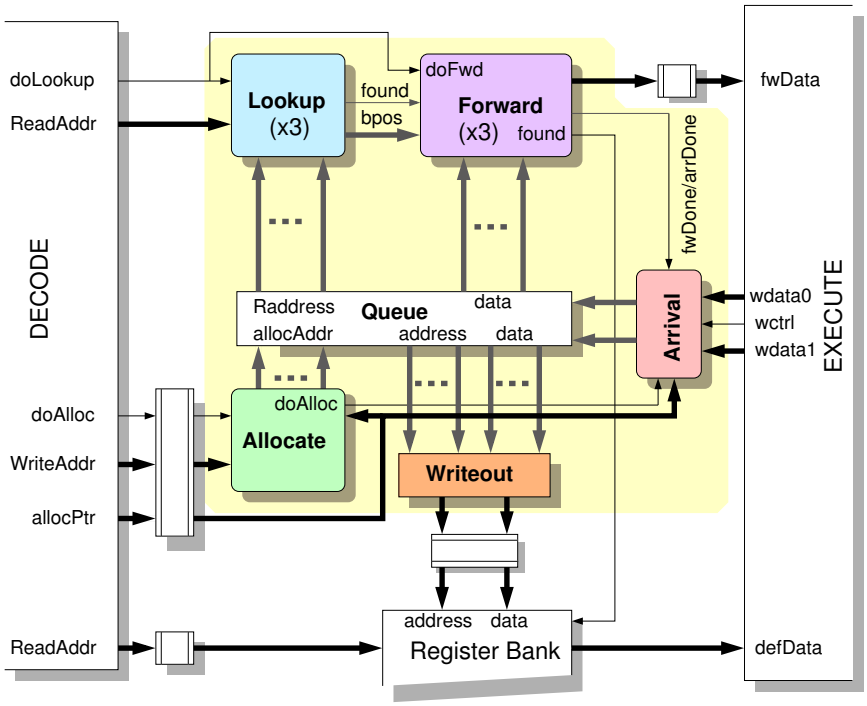

Figure 7.13: The nanoForward Unit architecture

Figure 7.13 shows the architecture of the nFU and its location within the new nanoSpa pipeline. The figure shows details of the communication interface between the various processes, the queue and the processor units.

The decode stage generates sequenced values of allocation pointers (*allocPtr*)

that steer the allocation and arrival data and guarantee mutual exclusivity in the allocation of queue cells. There are two allocation pointers, because some instructions can generate up to two results. The queue cells communicate using a token-passing mechanism to avoid cell reallocation when successive two-result instructions appear in the pipeline. Also, each queue cell handles its communication with the other processes independently.

7.4.5 Implementation issues

In ARM processors any instruction can be executed conditionally, which adds extra complexity to the result forwarding mechanism. In order to improve the efficiency of the pipeline in both the AQF and the nFU, allocation is done regardless of whether the instruction is conditional. If a conditional instruction fails its condition code tests, a token is sent through the pipeline to indicate that the instruction has been processed and the allocated queue slots are marked as invalid. This introduces some wasted slots in the queue, however, figures reported in [43] give 90% of queue utilisation for typical ARM programs by using this unconditional allocation strategy.

Synchronisation between processes

To guarantee correct operation, on each instruction the nFU must perform several operations sequentially as shown in figure 7.14. An initial nFU description was based on the use of *sync* channels as a token-passing mechanism to synchronise the processes but this caused a large performance penalty due to its reliance on the use of *Sequencers* so alternatives were looked for.

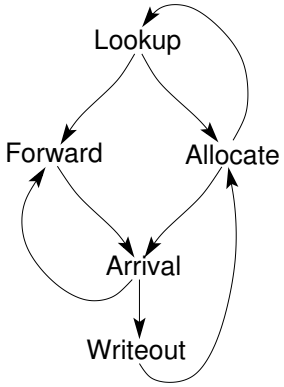

Figure 7.14: Inter-process dependencies in the nFU.

A solution that dramatically reduced this penalty was to perform synchronisation using data instead of sync tokens: to decouple Forward from Arrival, the queue contents are read speculatively and sent through data channels to the Forward process. Lookup and Allocation were decoupled using an "allocation mask" that blocks the reading of the queue locations that are about to be modified by the allocation/arrival process during the current instruction. This masking mechanism has two drawbacks: (*i*) the effective length of the queue is reduced in one or two locations, depending on the number of results to be written (one or two), and (*ii*) it dissipates more power and requires larger area.

Another alternative is to implement a less concurrent operation by grouping the processes according to the information that they read or write: Lookup;Allocate are sequenced as they read;write the register names and the *valid* flag. Similarly, Forward;Arrival are sequenced because they read;write results. In this way, Lookup;Allocation can now run concurrently with Forward;Arrival. Synchronisation between Lookup and Forward is done with data tokens carrying the lookup result. Allocation and Arrival completion must be synchronised and this information triggers the Writeout process.

Optimising sequenced operations

One performance problem that arises with the grouping scheme presented earlier is that, as explained in section 4.6.3, read-then-write operations require the use of non-RTZ-overlapped sequencers based on the *S-element* in order to avoid the risk of WAR hazards. To allow a more concurrent operation with decoupled RTZ phases, the processes can be rearranged as Allocation;Lookup and Arrival;Forward. This write-then-read operation permits the safe use of a sequencer based on the *T-element* but requires an initial empty token to be sent to Allocate and Arrival before the nFU begins to process instructions.

In Balsa, a write-then-read sequence to a variable inside a procedure generates a sequencer based on the *T-element*. However, because in the nFU the write and read processes reside in separate modules (with multiplexed/demultiplexed accesses to a global variable) the Balsa compiler inserts a safe non-RTZ-overlapped sequencer. An improvement to the above solution is to take advantage of the unbounded repetition of read-then-write actions over common variables and use the read-then-write optimisation describe in section 4.6.3.

Lookup CAM and forward process implementation

In the Amulet3 AQF, the Lookup process uses a small, very fast custom CAM to determine if the source registers of the decoded instruction are written or have been allocated in the buffer. Balsa does not provide a way to describe a CAM and generate an efficient circuit structure. The Balsa synthesised circuit used to replace the CAM consists of a number of logic comparators that, despite being relatively simple, do not perform as well as an optimised CAM, resulting in some performance penalty for the Lookup process.

In the Amulet3 AQF the Forward process iteratively examines the possible data sources until valid data is found or, if all possibilities are exhausted, the default value read form the register bank is used. This operation was efficiently implemented at the signal-level. As Balsa is a behavioural language, no signal-level operations can be described and attempting to replicate this behaviour in the nFU would require extensive use of sequenced operations that penalise performance.

The implemented solution is to wait for the data validity flag during the allocation process and to attach this information to the register number before writing it to the nFU CAM substitute. In this way the CAM substitute will report nothing or the single most recent valid source to the forwarding process, avoiding the need for iteration.

7.4.6 Use of the permissive *Concur*

The composition of concurrent actions in the nFU allows the use of the permissive concur to enhance the performance. The operations in the nFU were grouped into two concurrent groups of actions: (Lookup`;`Allocate) and (Forward`;`Arrival). These actions read and write from the same set of variables (the *Queue* buffer). The allocation pointer and token passing mechanism guarantees mutual exclusivity of these read and write actions allowing the use of the permissive concur. Outputs of these processes can be merged without the use of the `select` construct acting as a data driven merge.

For the case of the queue, the guaranteed mutual exclusivity allows the Allocation and Arrival processes of each cell to be composed with permissive concurs leading to similar benefits. Figure 7.15 shows the composition of the different

processes using the permissive concur inside the description of the nFU. For clarity, the I/O signals have been removed in the code. The complete source code can be found in Appendix G.

```
-- Lookup/Allocate group
loop
    -- Lookup (one for each read port)
    for || i in 0..READPORTS-1 then
        lookup(i, ...)
        )
    end
  ;
    -- steer Allocate information to allocation subcells
    steerAlloc_1(...) ||!
    steerAlloc_2(...)
    )
end ||!
-- Forward/Arrival group
loop
    -- forward (one for each read port)
    for || i in 0..READPORTS-1 then
        forward (i, ...)
    end
  ;
    -- Steer arrival requests
    steerArrival_1(...)
    ) ||!
    steerArrival(...)
    )
end ||!
-- Cell allocation subprocesses
for || i in 0..ROBSIZE-1 then
    allocCell( i, ...)
    )
end ||!
-- Cell arrival & writeout subprocesses
for ||! i in 0..ROBSIZE-1 then
    arrCell( i, ...)
end
```

Figure 7.15: Composition of actions with the permissive *Concur* inside the nFU.

7.4.7 Results

After a series of pre-layout, transistor level simulations it was found that the optimum queue size is 4. Different architectures of the nFU were tested and compared running the Dhrystone benchmark program. Tables 7.11 and 7.12 show that performance increases were 10%, with area and energy overheads of 13%. These results also show that the techniques used for desynchronising the

processes achieve close to 40% increase in performance relative to the use of sync channels. Results show that the first-read-unfold technique described in section 4.6.3 is a key factor for the performance gain in the nFU, contributing more than 50% of the speed-up.

nanoSpa device	*DMIPS*	*speed-up (%)*	*area overhead (%)*
no nFU	78.37	0.00	0.00
nFU (sync signals)	61.22	-28.80	5.20
nFU (allocation mask)	82.03	4.67	15.71
nFU (grouping)	81.86	5.86	11.20
nFU (grouping + unfolding)	86.27	10.08	11.21

Table 7.11: Performance results for nanoSpa using the nFU

nanoSpa device	*Energy for a Dhrystone loop(μJ)*	*overhead* (%)
no nFU	0.360	0.00
nFU (allocation mask)	0.491	36.23
nFU (grouping)	0.393	8.90
nFU (grouping + unfolding)	0.408	13.33

Table 7.12: Energy results for nanoSpa using the nFU

Unfortunately, it is not possible to make a relative comparison of the performance gain with respect to the Amulet3 AQF, because there are no published figures with and without the AQF. Pre-implementation, simulation results in [44] suggest that the AQF in Amulet3 would increase its performance by 22.5% when running the Dhrystone benchmark. Notice also that the Amulet3 pipeline has a decoupled memory stage and this feature is not currently present in nanoSpa.

7.5 A sliced-channel wormhole router

This section presents the architecture of a novel sliced-channel wormhole router proposed by Wei Song [90] and the results of some optimisations applied to its Balsa description. Details of the implementation and operation can be found in the reference given.

7.5.1 Introduction

Network-on-chip (NoC) is new on-chip communication paradigm. Asynchronous NoCs are attractive because they are power efficient and robust to process variation. As opposed to the *store-and-forward* routing scheme used in macronetworks, in NoC the prevailing scheme is *wormhole routing* [12]. In store-and-forward routing the node stores the complete packet and forwards it based on the information within its header. In wormhole routing, the packet is decomposed into into smaller units called *flits* (*fl*ow control dig*its*). The network node looks at the header of the packet to determine its next hop and immediately forwards it. The subsequent flits are forwarded as they arrive, causing the packet to *worm* its way through the network possibly spanning a number of nodes. The advantages of wormhole routing are low latency and the avoidance of area costly buffering queues [12].

In wormhole routing each packet is decomposed into three types of flits: (*i*) the *head* flit, which conveys the routing information (destination address) for the subsequent flits; (*ii*) a variable number of *data* flits, which carry the payload and (*iii*) the *tail* flit, which is used to close the connection.

7.5.2 Architecture of the sliced-channel wormhole router

In order to meet bandwidth requirement, state-of-the-art asynchronous routers broaden their channels by synchronising multiple sub-channels [12, 2, 86]. The new router architecture proposed in [90] and described here uses multiple independent sub-channels to transmit data. Since some synchronization is removed, the cycle period of all sub-channels are reduced, speeding up the network.

Figure 7.16(a) shows the simplified datapath of a wormhole NoC using synchronized channels. If, for instance, the asynchronous channel between routers is formed by four sub-channels, a four input C-element tree is required to generate the *ack* signal on each port. All sub-channels are merged into one channel and traverse the router through the multiplexer controlled by an arbiter. To remove the C-element tree, the data path could be restructured as shown in figure 7.16(b). The four sub-channels still go through the multiplexer together but each of them has its own *ack* line and can run independently.

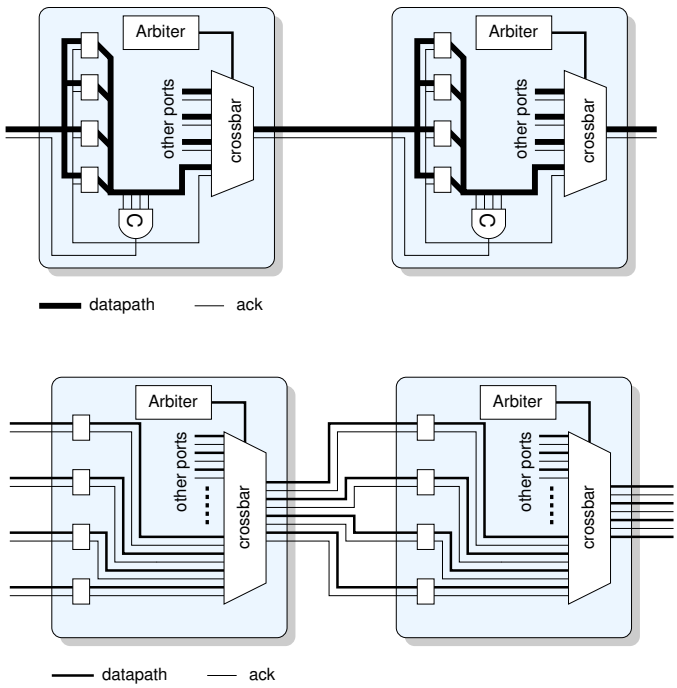

Figure 7.16: Wormhole NoC datapath [90].

The sliced-channel wormhole router

The implemented sliced-channel wormhole router has five 32-bit ports. To avoid separating the address in the head flit, the data width of a sub-channel in the router is set to 8 bits, allowing the header to address a 16×16 mesh. Consequently, the 32-bit channel is divided into four 8 bit sub-channels. The wire count is increased to 76 because the sub-channels now have their own set of end-of-frame and *ack* wires. In contrast, a conventional router having the same number of channels requires 67 wires: 64 data wires, two wires for the end-of-frame bit and one *ack* wire.

The architecture of the new router is shown in figure 7.17. The router comprises five input buffers, five output buffers and five multiplexers controlled by five arbiters. The depth of all buffers is one bit.

In this design example the dominating structures in the Balsa description are the data-dependant conditional structures that implements the input buffers and crossbar (multiplexers and demultiplexers). The control consists of the arbiters that select the routes and iterative `loop .. while` structures (localised at each input and output buffer) that detect the end (tail) of the packets entering/leaving the router.

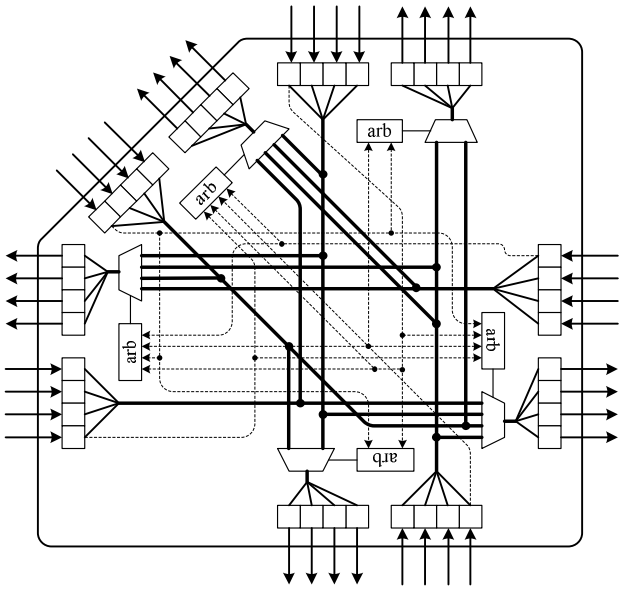

Figure 7.17: Sliced-channel wormhole router with four sub-channels [90].

7.5.3 Results

The experimental set-up consisted of sending packets of random lengths from every port to randomly selected port/destination and measuring the average throughput of the whole router (sum of the throughput of all ports). Random lengths and destinations were pre-generated and the same set was used for all designs. Table 7.13 shows the performance, area and energy results for the following versions of the router:

- *WR*: the original unoptimised description.
- *WR+DL*: the description-level optimised version of *WR*. In particular, the guard optimisation and guard grouping were used in the input buffers and crossbar.
- *WR+DL+AEC*: the above plus the optimisation of the control of active enclosures described in section 4.6.2.
- *WR+B+DL*: the *WR+DL* plus data broadcasting in the output buffers.
- *WR+B+DL+AEC*: the above plus the optimisation of the control of active enclosures

Results show that the description-level optimisation of guards has increased the performance by 7.3% with a reduction in area of 14% of the original and a

Router device	*Throughput* *Mflits/s*	*Δ (%)*	*Area* *elements*	*ratio*	*Energy* *pJ/flit*	*ratio*
WR	712	—	103 251	1.00	11.64	1.00
WR+DL	764	7.3	88 762	0.86	12.49	1.07
WR+DL+AEC	784	10.1	88 768	0.86	12.51	1.08
WR+DL+B	786	10.4	117 850	1.14	15.51	1.33
WR+DL+B+AEC	836	17.4	117 856	1.14	15.40	1.32

Table 7.13: Balsa wormhole router simulation results.

penalty of 7% in energy. Adding the peephole optimisation of the active eager inputs increases the performance by 10% with negligible penalties. Applying a more aggressive optimisation in the output buffers increases the performance by 17.4% at the expense of larger area and energy penalties.

7.6 Summary

This chapter has presented the evaluation of the performance-oriented techniques introduced in this thesis on a set of medium-to-large complexity designs described in the Balsa language. The impact on performance for the different techniques varies depending of the operational complexity of the circuit, with control-dominated circuits having smaller performance increases.

7.6.1 Balsa

The combined use of description-level optimisations obtained performance gains that range in percentage from 5-10% for the control-dominated MAC to 200% for the Viterbi decoder. The Viterbi example is interesting because the source description was written by an inexperienced Balsa user, highlighting the fact that the expressiveness of the language can lead to functional but poor implementations. In contrast, the source description of the nanoSpa processor (by far the most complex example investigated) was written by a highly experienced user, leaving less room for improvement.

New peephole optimisations were applied to highly optimised code where they can be more effective. However, as they target more localised sections of a circuit, the performance increase obtained is limited.

In general, the description-level optimisations result in small area and energy penalties. However, some of the large speed-ups are associated with larger overheads. The combined use of the two types of optimisations compares very favourably to a more aggressive push-only data-driven style, achieving similar levels of performance increases at relatively very low cost in overheads. This result suggests that a combination of push-only data-driven style and the optimisations introduce here might yield larger improvements at lower overhead costs.

7.6.2 Teak

Three designs were used as evaluation for Teak: the nanoSpa, the Viterbi decoder and the MAC unit. The circuit-level optimisations proposed for Teak corresponds to the initial set of optimisations derived for Teak circuits and, in contrast to the Balsa examples, a reference design was not available. In spite of this, some sets of the optimisations were applied separately to highlight the potential optimisation headroom available. In particular, the optimisation of conditional structures that results in compositions of *Steer-Merge-Join* components were evaluated, showing these structures as an excellent target for optimisation. The other optimisation highlighted in the examples was the latch insertion mechanism proposed in section 6.4. The results demonstrate its effectiveness in speeding up the circuit, saving area and energy as a side effect.

The proposed description level optimisations targeting the elimination of channel variables effectively improved the performance of the designs, resulting in speed-ups directly proportional to the width of the datapaths involved.

The evaluation examples demonstrated that the Teak methodology is capable of synthesising large complex circuits that operate correctly, but currently the performance overhead of Teak circuits for complex designs (like nanoSpa) or for control-dominated circuits (like the multiplier) is too large. The structures used to provide conditional access to channels and the sequencing of operations were identified as one the main sources of overhead. For the conditional access to channels, the circuit-level optimisation described in section 5.4.2 appear to be a promising source of improvement but is yet to be automated.

Chapter 8

Conclusions and future work

8.1 Balsa

The syntax-directed synthesis approach targeting handshake circuits used in Balsa is a flexible method that allows the synthesis of complex asynchronous VLSI circuits. The flexibility for making design trade-offs at the description-level has been claimed to be one of its major advantages. The major drawback of the method is the poor performance of the synthesised circuits and different techniques have been proposed to optimise them.

This thesis has proposed and evaluated a series of description-level and peephole optimisations to increase the performance of circuits synthesised using the syntax-directed approach. The synthesis and the optimisations presented here target dual-rail, quasi-delay-insensitive implementation as this is a robust approach that helps to reduce the impact of increasingly difficult timing closure within modern fabrication process variability.

This work has contributed to the knowledge of the asynchronous design methodologies by proposing and analysing a set of description-level techniques that result in faster compositions of the target structures used in the handshake circuits approach. The techniques are based on the data-driven style of description in which the arrival of data activates the operations of the circuits, as opposed to the more traditional and straightforward control-driven style. The overall effect of the proposed description techniques is the splitting of the tree of control elements of the synthesised circuits into smaller clusters, resulting in a reduction of the associated overhead.

Another contribution is a new set of peephole optimisations targeting Balsa

handshake circuits that further increase the performance of the synthesised circuits. In general, the description-level optimisations result in small area and energy penalties and in some cases, they even improve area and energy consumption. However, large speed-ups are associated with increased area and energy overheads. The peephole optimisations presented here have negligible overheads.

The performance gains obtained by using the different optimisations depends on the original input source code. For sources written by experienced designers, performance increases of 15-24% were achieved with area and energy penalties of less than 17% in most cases. The peephole optimisations achieved limited performance increases (of the order of 5-10% for the examples analysed) because they target smaller sections of the system.

The combined use of the two types of optimisations compares very favourably to a more aggressive push-only data-driven style, achieving similar levels of performance increases at relatively very low cost in overheads. This was demonstrated using a large and complex design example. The result suggests that it may be possible to obtain higher performances at a lower cost with an adequate mixture of both techniques. This will be discussed in the future work section.

A final contribution of this work is a varied set of highly optimised designs (and their corresponding simulation results) that can be used in further investigations.

8.2 Teak

This work has also evaluated a novel token flow-based asynchronous synthesis approach and techniques for increasing the performance of the resulting circuits were proposed and analysed. Although sharing the same input language as Balsa, the synthesis method is different to both Balsa and Haste, hence different optimisation methods had to be devised. Three designs were used as evaluation for this novel token-flow approach: the nanoSpa, the Viterbi decoder and the MAC unit.

The proposed optimisations for Teak fall into circuit-level and description-level categories. Circuit-level optimisation rely on the properties of the Teak components and its compositions and comprise circuit transformations, pattern-matching and substitution, or a combination of transformation and substitution. Description-level techniques target the removal of channel *Variables* with conditional accesses.

Two main targets for optimisation were identified: *Steer-Merge-Join* compositions and conditional read accesses to channels. The optimisation of *Steer-Merge-Join* compositions is achieved using circuit transformations and substitutions whilst conditional read accesses to channels were optimised using description-level techniques. Furthermore, a circuit-level optimisation was proposed for conditional read accesses that could further improve the performance of Teak circuits.

Teak circuits need latch insertion to prevent deadlock within circuits with cycles. An automatic latch insertion mechanism based on the minimum token storage required in a cycle was proposed, analysed and incorporated in the synthesis system.

The evaluation examples demonstrated that the Teak methodology is capable of synthesising large complex circuits. However, further optimisations are necessary to obtain competitive levels of performance with Balsa circuits.

8.3 Future work

The optimisations presented here can contribute in several ways to further improve existing tools used in the synthesis of asynchronous circuits and to create new ones. The work conducted on the Teak synthesis is just one of the first steps towards the implementation of a mature synthesis tool for this novel synthesis approach.

8.3.1 Description-level optimisations

The circuit structures that result from the optimised descriptions can serve as a reference to create the mappings in an optimisation step of the compiler or can be incorporated as rules for automated source-to-source transformation tools. As an example, the optimisations of the guards evaluation and the encoding of multiple guards look like excellent candidates for automation.

8.3.2 Peephole optimisations

The peephole optimisations proposed for the Balsa handshake circuits can be incorporated into the Balsa compiler and further evaluations performed on them. With some of the more complicated situations which are difficult to match with

a template, such as the read-then-write sequencing, the optimisation could be incorporated as a "pragma" in the source code.

8.3.3 Synthesis using hybrid style

Balsa normally generates modules with active input ports (*pull* inputs) and active output ports (*push* outputs) with a mixture of active and passive inputs at the handshake component level. In contrast the data-driven synthesis proposed in [101], which uses *push*-only handshake components (passive inputs and active outputs), provide faster performance but poorer area and energy consumption. The fact that the description-level optimisations have closed the gap between Balsa and the *push*-only style suggests that there may be inefficiencies with the *push*-only approach that could be exploited by using *pull* structures in key places of the handshake circuits. Clearly there will be more than one way of mixing these styles, either importing push-style modules to replace slower Balsa mixed-style modules or incorporating the more efficient push-style components in Balsa or vice versa. Investigating these inefficiencies and the best way of implementing this hybrid style is a challenging future research topic.

8.3.4 Teak

Teak is still a project under development. The evaluation carried out during this work was part of the initial proof of concept for the methodology, and this work has opened a series of paths to continue its development.

The automation of the proposed circuit-level approach to remove *Variables* associated with conditional channel reads is required to provide further enhancements in the performance, area and energy of the synthesised circuits.

The optimisation of the three latches per cycle is necessary to reduce the number of redundant latches due to the overlapping of cycles. This is an NP, non-trivial problem that opens a good research opportunity. The use of heuristics based on the structure of the Teak networks could serve as the basis for an optimised latch insertion mechanism.

At the component-level there is much to do on the design of optimised versions of Teak components, and some work on this has already started. The methodology allows the components to be designed with any chosen degree of channel

coupling, and there are good research opportunities in investigating better degrees of channel decoupling that can be embedded inside each component. It is even possible to have different versions for each component and select the one that provides the best performance depending on the construct, the neighbour components or datapath width.

Circuit transformations and peephole optimisations for Teak circuits can be described in a language external to the compiler to facilitate its description, composition and application to the circuits. There is already some work in progress within the APT group to develop this idea.

References

[1] S. Anellal and B. Kaminska. Scheduling of a control and data flow graph. pages 1666–1669, May 1993.

[2] J. Bainbridge and S.Furber. Chain: a delay-insensitive chip area interconnect. *IEEE Micro*, 22(5):16–23, Sep./Oct. 2002.

[3] A. Bardsley. Balsa: an asynchronous circuit synthesis system. Master's thesis, Department of Computer Science, University of Manchester, 1998.

[4] A. Bardsley. The balsa web pages. *http://www.cs.man.ac.uk/amulet/balsa/projects/balsa*, 2000.

[5] A. Bardsley. *Implementing Balsa Handshake Circuits*. PhD thesis, Department of Computer Science, University of Manchester, 2000.

[6] A. Bardsley, L. Tarazona, and D. A. Edwards. Teak: a token-flow implementation for the balsa language. In *Proc. International Conference on Application of Concurrency to System Design*, pages 23–31, July 2009.

[7] Peter A. Beerel, Nam-Hoon Kim, Andrew Lines, and Mike Davies. Slack matching asynchronous designs. In *Proc. International Symposium on Asynchronous Circuits and Systems*, pages 184–194. IEEE Computer Society Press, March 2006.

[8] C. H. (Kees) van Berkel, Cees Niessen, Martin Rem, and Ronald W. J. J. Saeijs. VLSI programming and silicon compilation. In *Proc. International Conf. Computer Design (ICCD)*, pages 150–166, Rye Brook, New York, 1988. IEEE Computer Society Press.

[9] Kees van Berkel, Ronan Burgess, Joep Kessels, Ad Peeters, Marly Roncken, and Frits Schalij. A fully-asynchronous low-power error corrector for the

DCC player. In *International Solid State Circuits Conference*, pages 88–89, February 1994.

[10] Kees van Berkel, Joep Kessels, Marly Roncken, Ronald Saeijs, and Frits Schalij. The VLSI-programming language Tangram and its translation into handshake circuits. In *Proc. European Conference on Design Automation (EDAC)*, pages 384–389, 1991.

[11] A. Bink and R. York. ARM996HS: the first licensable, clockless 32-bit processor core. *IEEE Micro*, 27(2):58–68, March 2007.

[12] T. Bjerregaard and J. Sparso. Implementation of guaranteed services in the MANGO clockless network-on-chip. *IEE Proc. in Computers and Digital Techniques*, 153(4):217–229, July 2006.

[13] A.D. Booth. A signed binary multiplication technique. *Quarterly Journal of Mechanics Applied Mathematics*, 4:236–240, 1951.

[14] S. Borkar, T. Karnik, S. Narendra, J. Tschanz, A. Keshavarzi, and V. De. Parameter variations and impact on circuits and microarchitecture. In *Proc. ACM/IEEE Design Automation Conference*, pages 338–342, June 2003.

[15] L. Brackenbury, M. Cumpstey, S. Furber, and P. Riocreux. An asynchronous Viterbi decoder. In Rene van Leuken, Reinder Nouta, and Alexander de Graaf, editors, *European Low Power Initiative for Electronic System Design*, pages 8–21. Delft Institute of Microelectronics and Submicron Technology, July 2000.

[16] Linda E. M. Brackenbury. *Principles of Asynchronous Circuit Design: A Systems Perspective*, chapter An Asynchronous Viterbi Decoder, pages 240–272. Kluwer Academic Publishers, 2001.

[17] C. Brej. *Early-output logig and anti-tokens*. PhD thesis, Department of Computer Science, University of Manchester, 2005.

[18] E. Brunvand. *Translating Concurrent Communicating Programs into Asynchronous Circuits*. PhD thesis, Carnegie Mellon University, 1991.

[19] Tiberiu Chelcea, Andrew Bardsley, Doug Edwards, and Steven M. Nowick. A burst-mode oriented back-end for the Balsa synthesis system. In *Proc.*

Design, Automation and Test in Europe (DATE), pages 330–337, March 2002.

[20] T.-A. Chu, C. K. C. Leung, and T. S. Wanuga. A design methodology for concurrent VLSI systems. In *Proc. International Conf. Computer Design (ICCD)*, pages 407–410. IEEE Computer Society Press, 1985.

[21] Tam-Anh Chu. *Synthesis of Self-Timed VLSI Circuits from Graph-Theoretic Specifications*. PhD thesis, MIT Laboratory for Computer Science, June 1987.

[22] Wesley A. Clark. Macromodular computer systems. In *AFIPS Conference Proceedings: 1967 Spring Joint Computer Conference*, volume 30, pages 335–336, Atlantic City, NJ, 1967. Academic Press.

[23] Handshake Solutions company website. *http://www.handshakesolutions.com/Technology/Haste*.

[24] Thomas H. Cormen, Charles E. Leiserson, Ronald L. Rivest, and Clifford Stein. *Introduction to algorithms*. MIT Press, Cambridge, MA, USA, 2001.

[25] J. Cortadella, M. Kishinevsky, A. Kondratyev, L. Lavagno, and A. Yakovlev. Petrify: a tool for manipulating concurrent specifications and synthesis of asynchronous controllers. *IEICE Transactions on Information and Systems*, E80-D(3):315–325, March 1997.

[26] J. Cortadella, A. Kondratyev, L. Lavagno, and C.P. Sotiriou. Desynchronization: Synthesis of asynchronous circuits from synchronous specifications. *IEEE Trans. on Computer-Aided Design*, 25(10):1904–1921, October 2006.

[27] D.S. Dawoud. Modified booth algorithm for higher radix fixed-point multiplication. In *Proc. of the 1997 South African Symposium on Communications and Signal Processing, Grahamstown, South Africa, September, 1997*, pages 95–100, 1997.

[28] SA.V. Dinh Duc, J.-B. Rigaud, A. Rezzag, A. Sirianni, J. Fragoso, L. Fesquet, and M. Renaudin. Tast CAD tools. In *Proc. Second ACiD-WG Workshop*, volume I, pages 28–29, January 2002.

[29] D. Edwards and A. Bardsley. Balsa: An asynchronous hardware synthesis language. *Computing Journal*, 45(1):12–18, 2002.

[30] Doug Edwards, Andrew Bardsley, Lilian Janin, Luis Plana, and Will Toms. *Balsa: A Tutorial Guide*. The University of Manchester, 2006.

[31] A. Efthymiou, W. Suntiamorntut, J. Garside, and L. Brackenbury. An asynchronous, iterative implementation of the original Booth multiplication algorithm. In *Proc. International Symposium on Asynchronous Circuits and Systems*, pages 207–215. IEEE Computer Society Press, April 2004.

[32] Karl M. Fant and Scott A. Brandt. NULL conventional logic: A complete and consistent logic for asynchronous digital circuit synthesis. In *International Conference on Application-specific Systems, Architectures, and Processors*, pages 261–273, 1996.

[33] R. M. Fuhrer, S. M. Nowick, M. Theobald, N. K. Jha, B. Lin, and L. Plana. Minimalist: An environment for the synthesis, verification and testability of burst-mode asynchronous machines. Technical Report TR CUCS-020-99, Columbia University, NY, July 1999.

[34] R. M. Fuhrer, S. M. Nowick, M. Theobald, N. K. Jha, and L. A. Plana. MINIMALIST: An environment for the synthesis and verification of burst-mode asynchronous machines. In *Proc. International Workshop on Logic Synthesis*, June 1998.

[35] S. B. Furber, P. Day, J. D. Garside, N. C. Paver, and J. V. Woods. AMULET1: A micropipelined ARM. In *Proceedings IEEE Computer Conference (COMPCON)*, pages 476–485, March 1994.

[36] S. B. Furber, D. A. Edwards, and J. D. Garside. AMULET3: a 100 MIPS asynchronous embedded processor. In *Proc. International Conf. Computer Design (ICCD)*, September 2000.

[37] S. B. Furber, J. D. Garside, P. Riocreux, S. Temple, P. Day, J. Liu, and N. C. Paver. AMULET2e: an asynchronous embedded controller. *Proceedings of the IEEE*, 87(2):243–256, February 1999.

[38] Stephen B. Furber, James D. Garside, and David A. Gilbert. AMULET3: A high-performance self-timed ARM microprocessor. In *Proc. International Conf. Computer Design (ICCD)*, October 1998.

[39] Hans van Gageldonk, Daniel Baumann, Kees van Berkel, Daniel Gloor, Ad Peeters, and Gerhard Stegmann. An asynchronous low-power 80c51 microcontroller. In *Proc. International Symposium on Asynchronous Circuits and Systems*, pages 96–107, 1998.

[40] J. D. Garside, W. J. Bainbridge, A. Bardsley, D. A. Edwards, S. B. Furber, J. Liu, D. W. Lloyd, S. Mohammadi, J. S. Pepper, O. Petlin, S. Temple, and J. V. Woods. AMULET3i — an asynchronous system-on-chip. In *Proc. International Symposium on Asynchronous Circuits and Systems*, pages 162–175. IEEE Computer Society Press, April 2000.

[41] Jim D. Garside. A CMOS VLSI implementation of an asynchronous ALU. In S. Furber and M. Edwards, editors, *Proc. Working Conf. on Asynchronous Design Methodologies*, volume A-28 of *IFIP Transactions*, pages 181–207. Elsevier Science Publishers, 1993.

[42] Fabien Gavant. Asynchronous viterbi decoder described in balsa language (internal report). Technical report, September 2008.

[43] D. A. Gilbert and J. D. Garside. A result forwarding mechanism for asynchronous pipelined systems. In *Proc. International Symposium on Asynchronous Circuits and Systems*, pages 2–11. IEEE Computer Society Press, April 1997.

[44] David Alan Gilbert. *Dependency and Exception Handling in an Asynchronous Microprocessor*. PhD thesis, Department of Computer Science, University of Manchester, 1997.

[45] Gennette Gill, Vishal Gupta, and Montek Singh. Performance estimation and slack matching for pipelined asynchronous architectures with choice. In *Proc. International Conf. Computer-Aided Design (ICCAD)*, pages 449–456. IEEE Computer Society Press, November 2008.

[46] Gennette Gill and Montek Singh. Bottleneck analysis and alleviation in pipelined systems: A fast hierarchical approach. In *Proc. International*

Symposium on Asynchronous Circuits and Systems, pages 195–205. IEEE Computer Society Press, May 2009.

[47] J. Hansen and M. Singh. Concurrency-enhancing transformations for asynchronous behavioral specifications: A data-driven approach. In *Proc. International Symposium on Asynchronous Circuits and Systems*, pages 15–25. IEEE Computer Society Press, April 2008.

[48] Scott Hauck. Asynchronous design methodologies: An overview. *Proceedings of the IEEE*, 83(1):69–93, January 1995.

[49] J.L. Hennessy and D.A. Patterson. *Computer Architecture: a Quantitative Approach (2nd edition)*. Morgan Kaufmann, 1996.

[50] C. A. R. Hoare. Communicating sequential processes. *Communications of the ACM*, 21(8):666–677, August 1978.

[51] D. Jaggar and D. Seal. *ARM Architecture Reference Manual*. Addison-Wesley, 2000.

[52] Cheoljoo Jeong and S.M. Nowick. Block-level relaxation for timing-robust asynchronous circuits based on eager evaluation. In *Proc. International Symposium on Asynchronous Circuits and Systems*, pages 95 –104, April 2008.

[53] Donald B. Johnson. Finding all the elementary circuits of a directed graph. *SIAM Journal on Computing*, 4(1):77–84, 1975.

[54] Tin-Chak Johnson-Pang, Chiu-Sing Choy, Cheong-Fat Chan, and Wai-Kuen Cham. Self-timed Booth's multiplier. In *Proceedings of 2nd International Conference on ASIC*, pages 280–283, Shanghai, China, October 1996.

[55] David Kearney and Neil W. Bergmann. Bundled data asynchronous multipliers with data dependant computation times. In *Proc. International Symposium on Asynchronous Circuits and Systems*, pages 186–197. IEEE Computer Society Press, April 1997.

[56] Robert M. Keller. Towards a theory of universal speed-independent modules. *IEEE Transactions on Computers*, C-23(1):21–33, January 1974.

[57] J. Kessels. Register-communication between mutually asynchronous domains. In *Proc. International Symposium on Asynchronous Circuits and Systems*, pages 66–75. IEEE Computer Society Press, March 2005.

[58] Joep Kessels, Torsten Kramer, Ad Peeters, and Volker Timm. DESCALE: a design experiment for a smart card application consuming low energy. In Rene van Leuken, Reinder Nouta, and Alexander de Graaf, editors, *European Low Power Initiative for Electronic System Design*, pages 247–262. Delft Institute of Microelectronics and Submicron Technology, July 2000.

[59] David J. King and John Launchbury. Structuring depth-first search algorithms in Haskell. In *Proceedings of the 22nd ACM SIGPLAN-SIGACT symposium on Principles of programming languages*, pages 344–354. ACM Press, 1995.

[60] Tilman Kolks, Steven Vercauteren, and Bill Lin. Control resynthesis for control-dominated asynchronous designs. In *Proc. International Symposium on Asynchronous Circuits and Systems*, March 1996.

[61] Alex Kondratyev and Kelvin Lwin. Design of asynchronous circuits by synchronous CAD tools. In *Proc. ACM/IEEE Design Automation Conference*, June 2002.

[62] Yijun Liu and Stephen B. Furber. The design of an asynchronous carry-lookahead adder based on data characteristics. In *15th International Workshop of Integrated Circuit and System Design, Power and Timing Modeling,Optimization and Simulation (PATMOS)*, pages 647–656, 2005.

[63] INMOS Ltd. *Occam 2 programming Manual*. Series in Computer Science. Prentice-Hall International, 1989.

[64] Rajit Manohar and Alain J. Martin. Slack elasticity in concurrent computing. In J. Jeuring, editor, *Proc. 4th International Conference on the Mathematics of Program Construction*, volume 1422 of *Lecture Notes in Computer Science*, pages 272–285, 1998.

[65] A. J. Martin. Programming in VLSI: From communicating processes to

delay-insensitive circuits. In C.A.R. Hoare, editor, *Developments in Concurrency and Communication*, UT Year of Programming Series, pages 1–64, Addison-Wesley, Reading MA, 1990.

[66] Alain J. Martin. Compiling communicating processes into delay-insensitive VLSI circuits. *Distributed Computing*, 1(4):226–234, 1986.

[67] Alain J. Martin. The limitations to delay-insensitivity in asynchronous circuits. In William J. Dally, editor, *Sixth MIT Conference on Advanced Research in VLSI*, pages 263–278. MIT Press, 1990.

[68] Alain J. Martin, Steven M. Burns, T. K. Lee, Drazen Borkovic, and Pieter J. Hazewindus. The first asynchronous microprocessor: the test results. *Computer Architecture News*, 17(4):95–110, June 1989.

[69] Alain J. Martin, Andrew Lines, Rajit Manohar, Mika Nyström, Paul Pénzes, Robert Southworth, and Uri Cummings. The design of an asynchronous MIPS R3000 microprocessor. In *Advanced Research in VLSI*, pages 164–181, September 1997.

[70] Alain J. Martin, Mika Nyström, Karl Papadantonakis, Paul I. Pénzes, Piyush Prakash, Catherine G. Wong, Jonathan Chang, Kevin S. Ko, Benjamin Lee, Elaine Ou, James Pugh, Eino-Ville Talvala, James T. Tong, and Ahmet Tura. The lutonium: A sub-nanojoule asynchronous 8051 microcontroller. In *Proc. International Symposium on Asynchronous Circuits and Systems*, pages 14–23. IEEE Computer Society Press, May 2003.

[71] David E. Muller. Asynchronous logics and application to information processing. In *Symposium on the Application of Switching Theory to Space Technology*, pages 289–297. Stanford University Press, 1962.

[72] T. Murata. Petri nets: Properties, analysis and applications. *Proceedings of the IEEE*, 77(4):541–574, April 1989.

[73] Takashi Nanya, Yoichiro Ueno, Hiroto Kagotani, Masashi Kuwako, and Akihiro Takamura. TITAC: Design of a quasi-delay-insensitive microprocessor. *IEEE Design & Test of Computers*, 11(2):50–63, Summer 1994.

[74] L. S. Nielsen, C. Niessen, J. Sparsø, and K. van Berkel. Low-power operation using self-timed circuits and adaptive scaling of the supply voltage. *IEEE Transactions on VLSI Systems*, 2(4):391–397, December 1994.

[75] S.F. Nielsen, J. Sparso, J.B. Jensen, and J.S.R. Nielsen. A behavioral synthesis frontend to the haste/TiDE design flow. In *Proc. International Symposium on Asynchronous Circuits and Systems*, pages 185–194, May 2009.

[76] S.F. Nielsen, J. Sparso, and J. Madsen. Behavioral synthesis of asynchronous circuits using syntax directed translation as backend. *IEEE Transactions on VLSI Systems*, 17(2):248–261, February 2009.

[77] Steven M. Nowick and David L. Dill. Automatic synthesis of locally-clocked asynchronous state machines. In *Proc. International Conf. Computer-Aided Design (ICCAD)*, pages 318–321. IEEE Computer Society Press, November 1991.

[78] Steven M. Nowick and David L. Dill. Synthesis of asynchronous state machines using a local clock. In *Proc. International Conf. Computer Design (ICCD)*, pages 192–197. IEEE Computer Society Press, October 1991.

[79] N. C. Paver, P. Day, C. Farnsworth, D. L. Jackson, W. A. Lien, and J. Liu. A low-power, low-noise configurable self-timed DSP. In *Proc. International Symposium on Asynchronous Circuits and Systems*, pages 32–42, 1998.

[80] N. C. Paver, P. Day, S. B. Furber, J. D. Garside, and J. V. Woods. Register locking in an asynchronous microprocessor. In *Proc. International Conf. Computer Design (ICCD)*, pages 351–355. IEEE Computer Society Press, October 1992.

[81] A. Peeters. *Single-Rail Handshake Circuits*. PhD thesis, Eindhoven University of Technology, June 1996.

[82] A. Peeters. Implementation of handshake components. In C. B. Jones A. E. Abdallah and J. W. Sanders, editors, *Communicating Sequential Processes, the first 25 years*, volume 3525 of *Lecture Notes in Computer Science*, pages 98–132. Springer-Verlag, January 2005.

[83] A. Peeters and K. van Berkel. Single-rail handshake circuits. In *Proc. Working Conf. on Asynchronous Design Methodologies*, pages 53–62, May 1995.

[84] L. A. Plana, P. A. Riocreux, W.J. Bainbridge, A. Bardsley, J. D. Garside, and S. Temple. SPA – a synthesisable Amulet core for smartcard applications. In *Proc. International Symposium on Asynchronous Circuits and Systems*, pages 201–210. IEEE Computer Society Press, April 2002.

[85] L.A. Plana, D. Edwards, S. Taylor, L. Tarazona, and A. Bardsley. Performance-driven syntax directed synthesis of asynchronous processors. In *Proc. International Conference on Compiles, Architecture & Synthesis for Embedded Systems*, pages 43–47, September 2007.

[86] L.A Plana, S.B. Furber, S. Temple, M. Khan, Y. Shi, J. Wu, and S. Yang. A globally asynchronous, locally synchronous infrastructure for a massively parallel multiprocessor. *IEEE Design and Test of Computers*, 24:454–463, sep 2007.

[87] Luis A. Plana. *Contributions to the Design of Asynchronous Macromodular Systems*. PhD thesis, Department of Computer Science, Columbia University, January 1998.

[88] Luis A. Plana and Steven M. Nowick. Architectural optimization for low-power non-pipelined asynchronous systems. *IEEE Transactions on VLSI Systems*, 6(1):56–65, March 1998.

[89] Luis A. Plana, Sam Taylor, and Doug Edwards. Attacking control overhead to improve synthesised asynchronous circuit performance. In *Proc. International Conf. Computer Design (ICCD)*, pages 703–710. IEEE Computer Society Press, October 2005.

[90] Wei Song and Doug Edwards. Building asynchronous routers with independent sub-channels. In *Proc. International Symposium on System-on-Chip 2009*, October 2009.

[91] Jens Sparsø and Steve Furber, editors. *Principles of Asynchronous Circuit Design: A Systems Perspective*. Kluwer Academic Publishers, 2001.

[92] Robert F. Sproull, Ivan E. Sutherland, and Charles E. Molnar. The counterflow pipeline processor architecture. *IEEE Design & Test of Computers*, 11(3):48–59, Fall 1994.

[93] Mishell J. Stucki, Severo M. Ornstein, and Wesley A. Clark. Logical design of macromodules. In *AFIPS Conference Proceedings: 1967 Spring Joint Computer Conference*, volume 30, pages 357–364, Atlantic City, NJ, 1967. Academic Press.

[94] Tin-Yau Tang, Chiu-Sing Choy, Pui-Lam Siu, and Cheon-Fat Chan. Design of self-timed asynchronous Booth's multiplier. In *Proc. of Asia and South Pacific Design Automation Conference*, pages 15–16, 2000.

[95] L. A. Tarazona, L. A. Plana, and D. A. Edwards. Architecture enhancements for a synthesised self-timed processor. In *Proceedings of the UK Asynchronous Forum*, September 2007.

[96] L. A. Tarazona, L. A. Plana, and D. A. Edwards. A synthesisable quasi-delay insensitive result forwarding unit for an asynchronous processor. In *Proceedings of 12 Euromicro Conference on Digital System Design (DSD)*, pages 627–634, August 2009.

[97] Luis A. Tarazona, Doug A Edwards, Andrew Bardsley, and Luis A. Plana. Description-level optimisation of synthesisable asynchronous circuits. In *Proceedings of 13 Euromicro Conference on Digital System Design (DSD) (to appear)*, September 2010.

[98] Robert Tarjan. Depth-first search and linear graph algorithms. *SIAM Journal on Computing*, 1(2):146–160, 1972.

[99] Robert Endre Tarjan. Enumeration of the elementary circuits of a directed graph. *SIAM Journal on Computing*, 2(3):211–216, 1973.

[100] S. Taylor. *Data-driven handshake circuit synthesis*. PhD thesis, Department of Computer Science, University of Manchester, 2007.

[101] S. Taylor, D. Edwards, and L. Plana. Data-driven asynchronous circuits. In *Proc. International Symposium on Asynchronous Circuits and Systems*, pages 3–14. IEEE Computer Society Press, April 2008.

[102] Sam Taylor, Doug Edwards, Luis A. Plana, and Luis A. Tarazona. Asynchronous data-driven circuit synthesis. *IEEE Transactions on VLSI Systems*, 18(7):1093–1106, 2010.

[103] John Teifel and Rajit Manohar. Static tokens: Using dataflow to automate concurrent pipeline synthesis. In *Proc. International Symposium on Asynchronous Circuits and Systems*, pages 17–27. IEEE Computer Society Press, April 2004.

[104] TIMA Laboratory, Concurrent Integrated Systems Group. TAST: Tool for asynchronous circuit synthesis. *http://tima.imag.fr/cis/Tast/tast.html*, 2002.

[105] K. van Berkel, R. Burgess, J. Kessels, A. Peeters, M. Roncken, and F. Schalij. Asynchronous circuits for low power: A DCC error corrector. *IEEE Design & Test of Computers*, 11(2):22–32, Summer 1994.

[106] K. van Berkel and M. Rem. VLSI programming of asynchronous circuits for low power. In G. Birtwistle and A. Davis, editors, *Asynchronous Digital Circuit Design*, pages 152–210. Springer-Verlag, 1995.

[107] Kees van Berkel. Beware the isochronic fork. *Integration, the VLSI journal*, 13(2):103–128, June 1992.

[108] Kees van Berkel. *Handshake Circuits: an Asynchronous Architecture for VLSI Programming*. Cambridge University Press, 1993.

[109] Kees van Berkel, Ferry Huberts, and Ad Peeters. Stretching quasi delay insensitivity by means of extended isochronic forks. In *Proc. Working Conf. on Asynchronous Design Methodologies*, pages 99–106. IEEE Computer Society Press, May 1995.

[110] Tom Verhoeff. Delay-insensitive codes—an overview. *Distributed Computing*, 3(1):1–8, 1988.

[111] A. J. Viterbi. Error-bounds for convolutional codes and an asymptotically optimum decoding algorithm. In *IEEE Transactions in Information Theory*, volume 13, pages 260–269, 1967.

[112] Amulet webpages. *http://intranet.cs.man.ac.uk/apt/projects/processors/amulet/*.

[113] Ted Williams, Niteen Patkar, and Gene Shen. SPARC64: A 64-b 64-active-instruction out-of-order-execution MCM processor. *IEEE J. of Solid-State Circuits*, 30(11):1215–1226, November 1995.

[114] Ted E. Williams. Performance of iterative computation in self-timed rings. *Journal of VLSI Signal Processing*, 7(1/2):17–31, February 1994.

[115] Ted E. Williams and Mark A. Horowitz. A zero-overhead self-timed 160ns 54b CMOS divider. *IEEE J. of Solid-State Circuits*, 26(11):1651–1661, November 1991.

[116] Catherine G. Wong and Alain J. Martin. Data-driven process decomposition for the synthesis of asynchronous circuits. In *IEEE International Conference on Electronics, Circuits and Systems*, 2001.

[117] K. Y. Yun and D. L. Dill. Automatic synthesis of 3D asynchronous state machines. In *Proc. International Conf. Computer-Aided Design (ICCAD)*, pages 576–580. IEEE Computer Society Press, November 1992.

[118] Q.Y. Zhang and G. Theodoropoulos. Towards an asynchronous MIPS processor. In *Cryptographic Hardware and Embedded Systems (CHES 2003)*, volume 2779 of *Lecture Notes in Computer Science*, pages 137–150. Springer-Verlag, 2003.

Appendix A

List of Balsa operators

The following table show the operators available in Balsa, in order of decreasing precedence:

Symbol	Operation	Valid types	Notes
`.`	record indexing	record	
`#`	smash	any	takes value from any type and reduces it to an array of bits
`[]`	array indexing	array	non-constant index possible, can generate lots of hardware
`^`	exponentiation	numeric	only constants
`not, log, - (unary)`	unary operators	numeric	log only works on constants, returns the ceiling: e.g. log 15 returns 4. - returns a result 1 bit wider than the argument
`*, /, %`	multiply, divide, remainder	numeric	only applicable to constants
`+, -`	add, subtract	numeric	results are 1 or 2 bits longer than the largest argument
`@`	concatenation	arrays	
`<,>,<=,>=`	inequalities	numeric enumerations	
`=, /=`	equals, not equals	all	comparison is by sign extended values for signed numeric types
`and`	bitwise and	numeric	Balsa uses type `1 bits` for `if/while` guards so bitwise and logical operators are the same
`or, xor`	bitwise or, xor	numeric	

Table A.1: Balsa binary/unary operators [30].

Appendix B

Balsa handshake components

This appendix provides a brief description of the handshake components available in the Balsa Synthesis System that appear in the example circuits of this thesis. For details on the implementation and formal description, the reader can refer to [5] and the Balsa Manual [30].

Balsa handshake components can be divided into three categories, according to its interaction with data and control signals.

Control components use only sync (dataless) ports. Their operation is triggered through the *activate* port. Their output sync channels are connected to the activation ports of other components.

Datapath components have only data channels. They are used for storing, processing, merging and splitting data channels.

Control to datapath interface components control the movement of data through the datapath. They have one or more sync ports used to communicate with control components as well as data channel ports. Some of them initiate handshakes on data channels in response to activation. Others generate an activation in response to the arrival of data.

B.1 Control components

B.1.1 Loop

Loop implements unbounded repetition. After receiving an activation on its passive port, it produces an infinite number of activations on its active port.

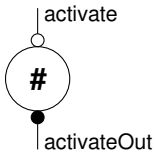

B.1.2 Concur

Produces an activation on all of its output ports following an input activation. All the output activations are begun at the same time but then operate independently.

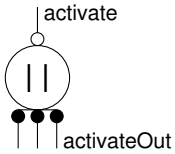

B.1.3 Fork

Produces an activation on all of its output ports following an activation on its input. All outputs synchronise between the processing and RTZ phases.

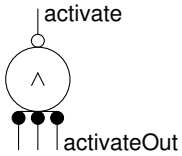

B.1.4 WireFork

Produces an activation on all of its output ports following an activation on its input, but never returns an acknowledgement. *WireFork* effectively forks the activation request to all of its outputs.

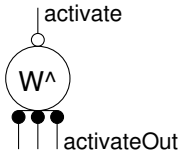

B.1.5 Sequence

Upon receiving and activation, its output activations are produced one at at time in sequence.

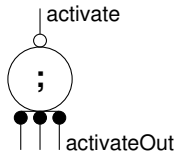

B.1.6 Call

Call passes a handshake on one of its input ports to the output port. The inputs must not occur concurrently.

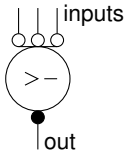

B.1.7 Sync

Synchronises the request on all of its inputs before passing these handshakes to the output.

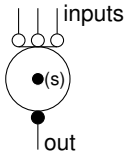

B.1.8 Arbitrate

Passes handshake on inA to outA or a handshake on inB to outB. If both inA and inB are activated concurrently it makes a non-deterministic decision as to which to pass first.

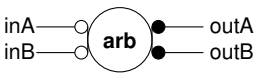

B.1.9 DecisionWait

Synchronises an activation with one of its inputs and then passes this handshake to the corresponding output. The inputs must be mutually exclusive.

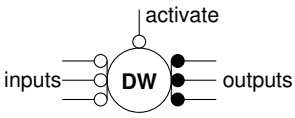

B.2 Datapath components

B.2.1 Unary function

Implements single-operand operations such as invert. The The handshake is simply passed through the component with the modified data.

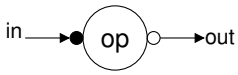

B.2.2 Binary function

Implements two-operand operations such as addition, subtraction, comparisons and bit-wise boolean functions. The output request is forked to both inputs. The input acknowledges are synchronised and passed to the output.

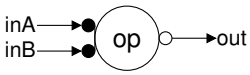

B.2.3 CallMux

CallMux is used as a merge element in datapaths. Multiple push input channels can are merged onto a single output channel. The inputs must be mutually exclusive.

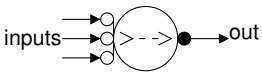

B.2.4 SplitEqual

Splits the data on its input port to multiple chunks of the same width, one chunk being sent on each output.

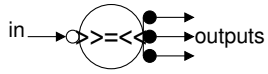

B.2.5 CaseFetch

When CaseFetch receives a request on its output, it pulls an index and uses this to decide which of its input ports to pull data on and then passes this data to the output port.

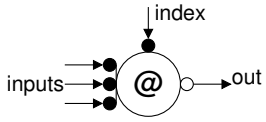

B.2.6 PassivatorPush

Used to connect an active output port from one process to the active input port of another process. See also section 3.3.13.

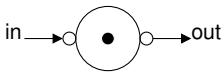

B.2.7 Variable

The Variable component has a single write port and multiple read ports. It stores data that it receives on the write port and provides it to the read ports on request. Reads and writes must not occur concurrently.

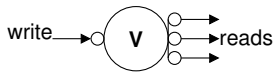

B.3 Control to datapth interface components

B.3.1 Fetch

Upon activation, the Fetch component pulls data on its input port and then pushes it on the output.

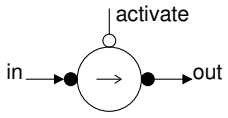

B.3.2 While

Implements the guarded loop language construct. When it is activated the While component pulls a single bit data item from its *guard* port. If the guard is true then While produces an output activation. When this activation has been acknowledged, While pulls another guard and repeats the process until a guard that is false is received.

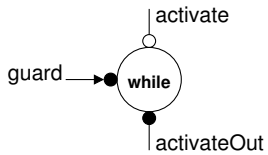

B.3.3 Case

Upon activation, the Case component pulls a guard on its data port. It then activates one of its outputs based on the data that was received. Multiple values can be mapped to each output. If some values are not mapped to an output they will result in no output activation.

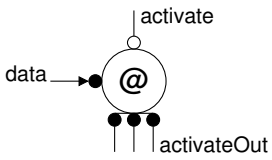

B.3.4 FalseVariable

Upon activation, the FalseVariable pulls data on its write port. It then holds this handshake open and activates the *signal* port. The FalseVariable acts as a Variable component, supplying, on request, the data from the write port to a set of read ports. When the *signal* handshake is completed (by the activated command), the write data is released.

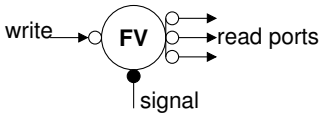

B.3.5 activeEagerFalseVariable

The activeEagerFalseVariable has an active input port and a trigger port to activate it. As opposed to a FalseVariable, its *signal* output activates as soon as the trigger is activated, without waiting for data arrival.

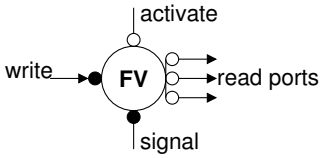

Appendix C

FV and *aeFV* implementations

The following pages show the implementation and STG of the *FalseVariable* (FV) and *activeEagerFalseVariable* ($aeFV$) components.

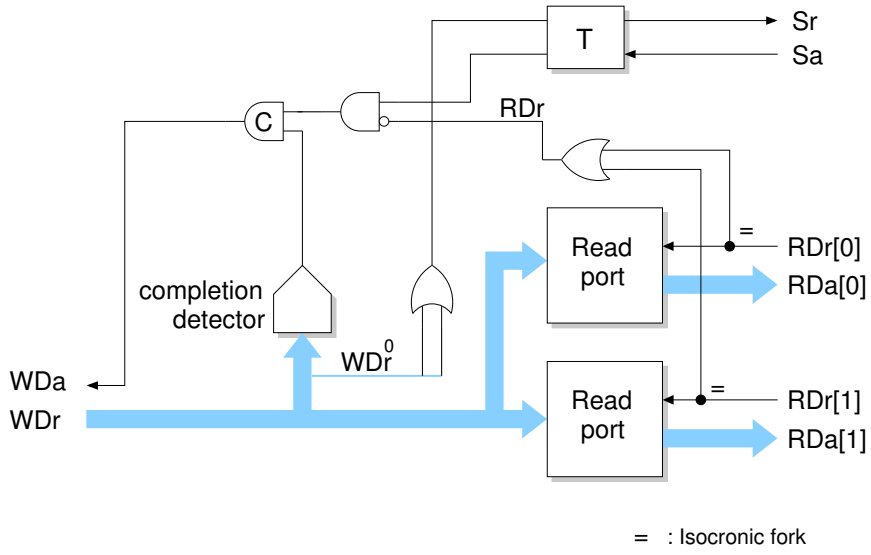

(a)

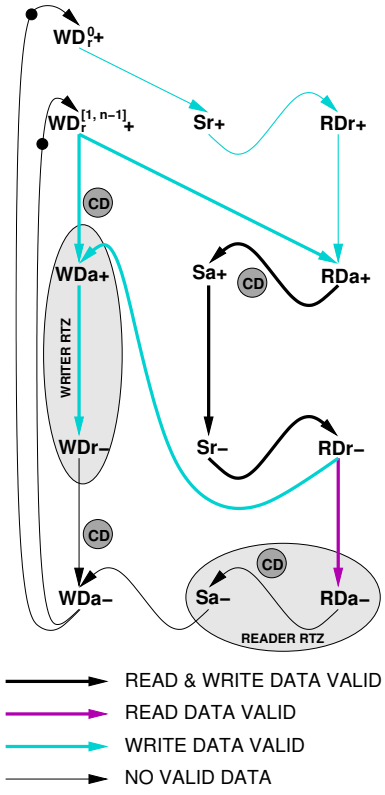

(b)

Figure C.1: *FalseVariable*: (a) Implementation, (b) STG.

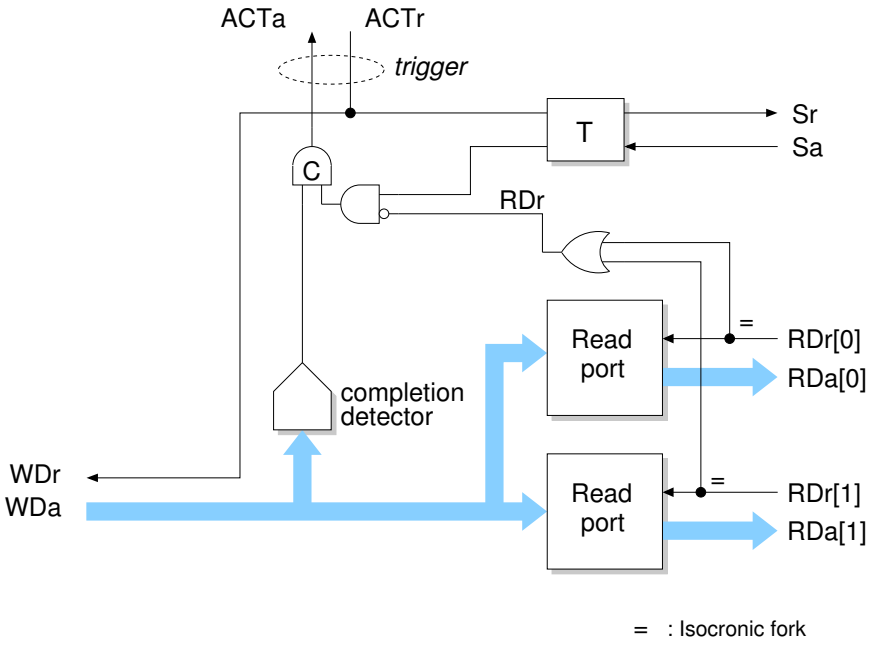

(a)

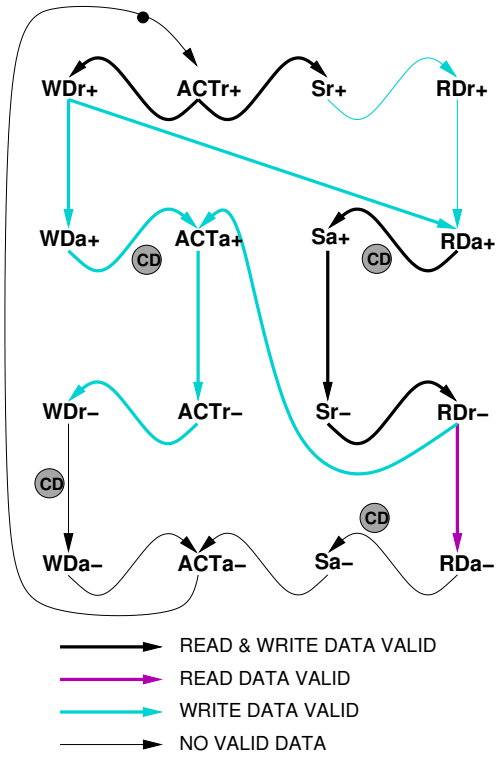

(b)

Figure C.2: *activeEagerFalseVariable*: (a) Implementation, (b) STG.

Appendix D

Optimised Viterbi decoder Balsa description

The following pages show the Balsa source files for this design.

VD.balsa 1

```
1  -- The University of Manchester
2  -- School of Computer Science
3  -- Advanced Processors Technology (APT) group
4  --
5  -- Asynchronous Viterbi Decoder r=1/2, k=3 (4 states)
6  -- Author: Luis Tarazona (based on original description by Fabien Gavant)
7  -- 10/09/2008
8  -- Viterbi decoder top level
9
10 import[balsa.types.basic]
11 import[BMU] -- name of the file
12 import[PMU]
13 import[HU]
14 import[def_2]
15
16 procedure ViterbiDecoder_k2(
17   input in_a : 3 bits;
18   input in_c : 3 bits;
19   output Out_state : State;
20   output out_o : 1 bits
21 )is
22
23 array 0..3 of channel data_BMU_PMU : nibble
24 channel data_PMU_HU : Bundle_PMU_HU
25
26 begin
27     BMU (
28         -- Input
29         in_a,
30         in_c,
31         -- Output
32         data_BMU_PMU ) ||
33     PathMetricUnit (
34         -- Input
35         data_BMU_PMU,
36         -- Output
37         data_PMU_HU ) ||
38     HistoryHunit (
39         -- Input
40         data_PMU_HU,
41         -- Output
42         Out_state,
43         out_o )
44 end -- ViterbiDecoder_k2
```

def_2.balsa 1

```
1  -- The University of Manchester
2  -- School of Computer Science
3  -- Advanced Processors Technology (APT) group
4  --
5  -- Asynchronous Viterbi Decoder r=1/2, k=3 (4 states)
6  -- Author: Luis Tarazona (based on original description by Fabien Gavant)
7  -- 10/09/2008
8  -- data types
9
10 import[balsa.types.basic]
11
12 type bit3 is 3 bits -- new type for the input: 0 to 7
13
14 type State is enumeration
15     S0, S1, S2, S3
16 end
17 type trellisState is enumeration
18     LS0, LS1, LS2, LS3,
19     US0, US1, US2, US3
20 end
21
22 type Bundle_BMU_PMU is record
23 a_c : nibble; -- 4 bits
24 a_d : nibble;
25 b_c : nibble;
26 b_d : nibble
27 end
28
29 type Bundle_PMU_HU is record
30 Global_winner_found : 1 bits;
31 Global_winner : State;
32 dir_S0 : 1 bits;
33 dir_S1 : 1 bits;
34 dir_S2 : 1 bits;
35 dir_S3 : 1 bits
36 end
37
38
39
```

BMU.balsa 1

```
1  -- The University of Manchester
2  -- School of Computer Science
3  -- Advanced Processors Technology (APT) group
4  --
5  -- Asynchronous Viterbi Decoder r=1/2, k=3 (4 states)
6  -- Author: Luis Tarazona (based on original description by Fabien Gavant)
7  -- 10/09/2008
8  --  Branch Metric Unit
9
10 import[balsa.types.basic]
11 import[def_2]
12
13 procedure smaller (
14   input  x : nibble;
15   input  y : nibble;
16   output o : nibble
17 ) is
18 begin
19     x, y ->! then
20         if (x < y) then
21             o <- x
22         else
23             o <- y
24         end -- if
25     end -- x,y ->!
26 end -- procedure smaller
27
28 procedure BMU(
29   input a : bit3; -- 3bits
30   input c : bit3;
31   array 0..3 of output Out_BMU : nibble -- Bundle_BMU_PMU
32 --output a_c : nibble; -- 4bits
33 --output a_d : nibble;
34 --output b_c : nibble;
35 --output b_d : nibble
36 ) is
37     constant a_c = 0 : 2 bits
38     constant a_d = 1 : 2 bits
39     constant b_c = 2
40     constant b_d = 3
41
42 --local
43     channel b : nibble
44     channel d : nibble
45 -- temp values
46     channel ta_c : nibble
47     channel ta_d : nibble
48     channel tc_b : nibble
49     channel tb_d : nibble
50 -- copy of temp values
51     channel ta_c1 : nibble
52     channel ta_d1 : nibble
53     channel tc_b1 : nibble
54     channel tb_d1 : nibble
55 -- comparators outputs
56     channel c0 : nibble
57     channel c1 : nibble
58     channel smallest : nibble
59
60 begin
61     loop
62         a, c ->! then
63             b <- (7 - a as nibble) ||
64             d <- (7 - c as nibble) ||
65             b,d ->! then
```

BMU.balsa 2

```
66                ta_c <- (a + c as nibble) ||
67                ta_d <- (a + d as nibble) ||
68                tc_b <- (c + b as nibble) ||
69                tb_d <- (b + d as nibble)
70            end -- b, d ->! then
71        end -- a,c ->!
72    end || -- loop
73    loop
74        ta_c, ta_d, tc_b, tb_d ->! then
75            ta_c1 <- ta_c ||
76            ta_d1 <- ta_d ||
77            tc_b1 <- tc_b ||
78            tb_d1 <- tb_d ||
79            smaller(ta_c1, ta_d1, c0) ||
80            smaller(tc_b1, tb_d1, c1) ||
81            smaller(c0, c1, smallest) ||
82            smallest ->! then
83                Out_BMU[a_c] <- (ta_c - smallest as nibble) ||
84                Out_BMU[a_d] <- (ta_d - smallest as nibble) ||
85                Out_BMU[b_c] <- (tc_b - smallest as nibble) ||
86                Out_BMU[b_d] <- (tb_d - smallest as nibble)
87            end -- smallest ->!
88        end -- ta_c ... tb_d ->!
89    end -- loop
90 end -- procedure BMU
91
```

PMU.balsa 1

```
1  -- The University of Manchester
2  -- School of Computer Science
3  -- Advanced Processors Technology (APT) group
4  --
5  -- Asynchronous Viterbi Decoder r=1/2, k=3 (4 states)
6  -- Author: Luis Tarazona (based on original description by Fabien Gavant)
7  -- 10/09/2008
8  -- Viterbi decoder four-state Path Metric Unit (PMU unit)
9
10 import[balsa.types.basic]
11 import[def_2]
12
13 type word32 is 32 bits
14 type word5 is 5 bits -- 0 to 31
15 type word6 is 6 bits -- 0 to 63
16
17 constant lower=0
18 constant upper=1
19
20 procedure smaller6 (
21   input  x : word6;
22   input  y : word6;
23   output o : word6
24 ) is
25 begin
26     loop
27         x, y ->! then
28             if (x < y) then
29                 o <- x
30             else
31                 o <- y
32             end -- if (x < y)
33         end -- x,y ->!
34     end -- loop
35 end -- procedure smaller
36
37 procedure ACSUnit (
38     input WState_A : word6;
39     input BMU_A : nibble;
40     input WState_B : word6;
41     input BMU_B : nibble;
42     output WState_O : word6;
43     output direction : bit;
44     output isZero    : bit
45 )is
46
47 channel WA : word6 -- Weight result A
48 channel WB : word6 -- Weigt result B
49
50 begin
51     loop
52         WState_A, BMU_A, WState_B, BMU_B -> then
53             WA <- (WState_A + BMU_A as word6) ||
54             WB <- (WState_B + BMU_B as word6) ||
55             WA, WB ->! then
56                 if(WA <= WB) then
57                     WState_O <- WA     ||
58                     direction <- lower ||
59                     isZero <- (WA = 0)
60                 else
61                     WState_O <- WB     ||
62                     direction <- upper ||
63                     isZero <- (WB = 0)
64                 end -- if(WA < WB)
65             end -- WA, WB -> then
```

PMU.balsa 2

```
66          end -- WState_A, BMU_A, WState_B, BMU_B -> then
67      end -- loop
68  end -- procedure ACSUnit
69
70  procedure reduction(
71      array 0..3 of input WMSa   : word6;
72      array 0..3 of input WMSb   : word6;
73      array 0..3 of output NWMS : word6
74  ) is
75
76  local
77      channel smallest, smallest1, smallest2  : word6
78
79  begin
80      smaller6(WMSa[0], WMSa[1], smallest1)    ||
81      smaller6(WMSa[2], WMSa[3], smallest2)    ||
82      smaller6(smallest1, smallest2, smallest) ||
83      loop
84          smallest, WMSb[0], WMSb[1], WMSb[2], WMSb[3] ->! then
85              for || i in 0..3 then
86                  NWMS[i] <- (WMSb[i] - smallest as word6)
87              end -- for || i
88          end -- smallest ... WMSb[3] ->!
89      end -- loop
90  end -- procedure reduction
91
92  procedure trellis (
93  (--     input WMS0 : word6 -- Weight MemState 0
94      input WMS1 : word6 -- Weight MemState 1
95      input WMS2 : word6 -- Weight MemState 2
96      input WMS3 : word6 -- Weight MemState 3
97  --)
98    array 0..3 of input wMS : word6;
99  (--
100     input a_c : nibble
101     input a_d : nibble
102     input b_c : nibble
103     input b_d : nibble
104 --)
105   array 0..3 of input bM : nibble;
106
107   array 0..3 of output wmA : word6;
108   array 0..3 of output wmB : word6;
109   array 0..3 of output bmA : nibble;
110   array 0..3 of output bmB : nibble
111 )is
112
113 begin
114     loop
115         wMS[0] ->! then
116             wmA[0]  <- wMS[0] ||
117             wmA[1]  <- wMS[0]
118         end
119     end ||
120     loop
121         wMS[1] ->! then
122             wmA[2]  <- wMS[1] ||
123             wmA[3]  <- wMS[1]
124         end
125     end ||
126     loop
127         wMS[2] ->! then
128             wmB[0]  <- wMS[2] ||
129             wmB[1]  <- wMS[2]
130         end
```

PMU.balsa 3

```
131     end ||
132     loop
133         wMS[3] ->! then
134             wmB[2] <- wMS[3] ||
135             wmB[3] <- wMS[3]
136         end
137     end ||
138     loop
139         bM[0] ->! then -- a_c
140             bmA[0]  <- bM[0] ||
141             bmB[1]  <- bM[0]
142         end
143     end ||
144     loop
145         bM[1] ->! then -- a_d
146             bmA[2]  <- bM[1] ||
147             bmB[3]  <- bM[1]
148         end
149     end ||
150     loop
151         bM[2] ->! then  -- b_c
152             bmB[2]  <- bM[2] ||
153             bmA[3]  <- bM[2]
154         end
155     end ||
156     loop
157         bM[3] ->! then -- b_d
158             bmB[0]  <- bM[3] ||
159             bmA[1]  <- bM[3]
160         end
161     end
162 end -- procedure trellis
163
164 procedure pmBuff(
165   input  i  : word6;
166   output oa : word6;
167   output ob : word6
168 ) is
169   variable b : word6
170 begin
171     oa <- 0 || -- initial value
172     ob <- 0 ;   -- initial value
173     loop
174         i -> b  ;
175         oa <- b ||
176         ob <- b
177     end
178 end -- procedure pmBuff
179
180 procedure globalWinner(
181   array 0..3 of input isZero : bit;
182   output globalWinner : State;
183   output globalWinner_found : bit
184 ) is
185 begin
186     loop
187         isZero[0], isZero[1], isZero[2], isZero[3] ->! then
188             case (#(isZero[0]) @ #(isZero[1]) @
189                   #(isZero[2]) @ #(isZero[3]) as 4 bits) of
190             0b0001 then
191                 globalWinner <- S0      ||
192                 globalWinner_found <- 1
193             |0b0010 then
194                 globalWinner <- S1      ||
195                 globalWinner_found <- 1
```

PMU.balsa 4

```
196             |0b0100 then
197                 globalWinner <- S2      ||
198                 globalWinner_found <- 1
199             |0b1000 then
200                 globalWinner <- S3      ||
201                 globalWinner_found <- 1
202             else
203                 globalWinner <- S0      ||
204                 globalWinner_found <- 0
205             end -- case
206         end -- isZero ->!
207     end -- loop
208 end -- procedure GlobalWinner
209
210 procedure PathMetricUnit(
211   array 0..3 of input Out_BMU : nibble;
212   output Out_PMU : Bundle_PMU_HU
213 )is
214     -- trellis to ACS i/f
215   array 0..3 of channel wmA : word6
216   array 0..3 of channel wmB : word6
217   array 0..3 of channel bmA : nibble
218   array 0..3 of channel bmB : nibble
219   -- ACS to output i/f
220   array 0..3 of channel direction : bit
221   -- ACS to buffer i/f
222   array 0..3 of channel WState_O : word6
223  -- ACS to globalWinner i/f
224   array 0..3 of channel isZero : bit --for global winner check
225  -- buffer to reduction i/f
226   array 0..3 of channel WState_Oa : word6
227   array 0..3 of channel WState_Ob : word6
228  -- reduction to trellis i/f
229   array 0..3 of channel WState : word6
230
231   channel globalWinner : State
232   channel globalWinner_found : bit
233
234 begin
235     trellis(WState, Out_BMU, wmA, wmB, bmA, bmB) ||
236     for || i in 0..3 then
237         ACSUnit(wmA[i], bmA[i], wmB[i], bmB[i],
238                 WState_O[i], direction[i], isZero[i])
239     end ||
240     globalWinner(isZero, globalWinner, globalWinner_found) ||
241     for || i in 0..3 then
242         pmBuff(WState_O[i], WState_Oa[i], WState_Ob[i])
243     end ||
244     reduction(WState_Oa, WState_Ob, WState) ||
245     loop
246         globalWinner, globalWinner_found,
247         direction[0],
248         direction[1],
249         direction[2],
250         direction[3] ->! then
251             Out_PMU <- {globalWinner_found,
252                         globalWinner,
253                         direction[0],
254                         direction[1],
255                         direction[2],
256                         direction[3]}
257         end -- globalWinner ->!
258     end -- loop
259 end -- procedure PathMetricUnit
```

HU.balsa 1

```
1  -- The University of Manchester
2  -- School of Computer Science
3  -- Advanced Processors Technology (APT) group
4  --
5  -- Asynchronous Viterbi Decoder r=1/2, k=3 (4 states)
6  -- Author: Luis Tarazona (based on original description by Fabien Gavant)
7  -- 10/09/2008
8  -- Viterbi decoder History Unit (HU unit)
9
10 import[balsa.types.basic]
11 import[def_2]
12
13 type A4_t is array 4 of bit
14 type testbit is bit
15
16
17 procedure HistoryHunit(
18     input In_HU : Bundle_PMU_HU;
19
20     output Out_state : State;
21     output Data_out : bit
22 )is
23
24 variable Temp: Bundle_PMU_HU
25
26 variable Global_Winner_Valid : array 0..15 of bit
27 variable Global_Winner : array 0..15 of State
28 variable Global_Winner_Head : State
29 variable DL_Winner : array 0..15 of 4 bits -- Direction_Local_Winner
30
31 variable Head, pHead, nHead : 4 bits -- Head of the current time slot
32 variable Child, pChild   : 4 bits -- for the reconstruction of the path
33 variable Parent, pParent : 4 bits -- for the reconstruction of the path
34 channel GW_single : 2 bits -- State 2 bits S0=00, S1=01, S2=10, S3=11
35 variable Temp_state : State
36 variable Token : bit
37 channel Return_direction : array 0..3 of bit
38
39 variable Var_div1 : State
40 channel  Var_div2 : State
41 -- for start with valid value
42 variable Start, doLoop : bit
43
44 variable Safeguard, nSafeguard : 4 bits  -- for the begining
45 variable i : 4 bits
46
47
48 begin
49     -- initialisation
50     Head := 0
51  ||
52     pHead := (0 - 1 as 4 bits)
53  ||
54     Start := 0
55  ;
56     loop
57         Child := pHead
58      ||
59         Parent := Head
60      ||
61         Token := 0
62      ||
63         i := (0 - 1 as 4 bits)
64      ||
65         -- generates the output state when start is ready
```

HU.balsa 2

```
66          --- (good value to release)
67          if Start then
68              Out_state <- Global_Winner_Head
69           ||
70              Data_out <- ((Global_Winner_Head as array 2 of bit)[0]
71                           as testbit)
72          else
73              Safeguard := Head
74          end
75       ||
76          In_HU ->! then -- read data & control
77              -- store data on the memory
78              DL_Winner[Head] := (A4_t {In_HU.dir_S0,
79                                       In_HU.dir_S1,
80                                       In_HU.dir_S2,
81                                       In_HU.dir_S3} as 4 bits)
82           ||
83              -- I update all the data
84              Global_Winner[Head]:= In_HU.Global_winner
85           ||
86              Global_Winner_Valid[Head] := In_HU.Global_winner_found
87           ||
88              doLoop := In_HU.Global_winner_found
89          end
90       ;
91          if doLoop then
92              loop -- reconstruction of the path
93                  -- save the GW
94                  GW_single <- (Global_Winner[Parent] as 2 bits)
95               || -- load the direction of the Local_Winner
96                  Return_direction <- ((DL_Winner[Parent]
97                                       as array 4 of bit))
98               ||
99                  GW_single, Return_direction ->! then
100                     case (#GW_single @ #(Return_direction[GW_single])
101                           as trellisState) of
102                      LS0, LS1 then
103                         Var_div2 <- S0
104                     |LS2, LS3 then
105                         Var_div2 <- S1
106                     |US0, US1 then
107                         Var_div2 <- S2
108                     |US2, US3 then
109                         Var_div2 <- S3
110                     end
111                 end
112              ||
113                 Var_div2 ->! then
114                     if (Var_div2 = Global_Winner[Child]
115                                    and Global_Winner_Valid[Child] = 1
116                                    or Child = Head) then
117                         Token := 1
118                     else
119                         Var_div1 := Var_div2
120                     end
121                 end
122              ||
123                 pParent := Child
124              ||
125                 pChild := (Child - 1 as 4 bits)
126             while (Token = 0 and Safeguard /= i) then   -- Condition
127                 i := (i + 1 as 4 bits)
128              ||
129                 Child := pChild
130              ||
```

HU.balsa 3

```
131                 Parent := pParent
132               ||
133                 if not Token then
134                     Global_Winner[pParent] := Var_div1
135                 end
136             end --loop while
137         end -- if doLoop
138       ||
139         pHead := Head
140       ||
141         nHead := (Head + 1 as 4 bits)
142       ;
143         Head := nHead
144       ||
145         if nHead = 15 then
146             Start := 1
147         end --if Head=15
148       ||
149         Global_Winner_Head := Global_Winner[nHead]
150     end --loop
151 end -- HistoryHunit
```

Appendix E

Optimised 32x32 bit Booth multiplier Balsa description

The following pages show the Balsa source files for this design.

nanoMultiplier.balsa 1

```
1  -- The University of Manchester
2  -- School of Computer Science
3  -- Advanced Processors Technology (APT) group
4  --
5  -- Radix-3 Booth's multiplier for nanoSpa/aviSpa processor in Balsa
6  --
7  -- Author: Luis Tarazona tarazonl@cs.man.ac.uk
8  -- v1.0 20/04/2007 -tarazonl
9  --
10
11 import [balsa.types.basic]
12 import [nanoMulTypes]
13 import [nanoMultSupport]
14 import [nanoMBoothR3rolled]
15
16 procedure CSAdder_DP2 is CSAdder(Datapath_2)
17 procedure CPadder  is fullCPadder(Datapath)
18
19 procedure nanoMultiplier
20 (
21   input bypass  : bit;
22   input bypassH : bit;
23   input mType : MulType;
24   input a    : Datapath;
25   input b    : Datapath;
26   input c    : Datapath;
27   output mpH: Datapath;
28   output mpL: Datapath;
29   output mZ : bit;
30   output mN : bit
31 ) is
32     -- length and multiply-acummulate control words
33     channel mlength : bit
34     channel macc    : bit
35     -- sign adjust I/F input
36     channel ba  : Datapath
37     channel bb  : Datapath
38     channel bc  : Datapath
39     channel bmType : MulType
40     -- sign adjust I/F input
41     channel sa  : Datapath_2
42     channel sb  : Datapath_3
43     channel sc  : Datapath_2
44     -- CS adder I/F
45     channel opA  : Datapath_2
46     channel opB  : Datapath_2
47     channel cs   : Datapath_2
48     channel cin : Datapath_2
49     channel res : Datapath_2
50     -- CP adder I/F
51     channel raA  : Datapath
52     channel raB  : Datapath
53     channel rac0 : bit
54     channel raS  : Datapath
55     channel racN : bit
56     -- multiplier iteration control
57     channel load : bit
58     channel done : bit
59
60     -- bypass interface
61     channel pH  : Datapath
62     channel pL  : Datapath
63     channel z   : bit
64     channel n  : bit
65     channel bpH  : Datapath
```

nanoMultiplier.balsa 2

```
66      channel bpL  : Datapath
67      channel bz   : bit
68      channel bn   : bit
69      channel bH, bL : bit
70  begin
71      CSAdder_DP2(opA,opB,cs,cin,res)
72    ||CPadder(raA,raB,rac0,raS,racN)
73    ||nanoMBoothR3rolled(cin,res, sa, sb, sc, mlength, macc,
74                         load,done,opA,opB,cs,raA,raB,rac0,raS,racN,pH,pL,z,n)
75    ||mControl(10,load,done)
76    ||signAdj(bmType, ba, bb, bc, sa, sb, sc, mlength, macc)
77    ||bypassMul(bypass, bypassH, a, b, c, mType, ba, bb, bc, bmType, bH, bL)
78    ||doByPass(bH, bL, pH, pL, z, n, mpH, mpL, mZ, mN)
79  end
```

nanoMulTypes.balsa 1

```
1  -- The University of Manchester
2  -- School of Computer Science
3  -- Advanced Processors Technology (APT) group
4  --
5  -- Radix-3 Booth's multiplier for nanoSpa/aviSpa processor in Balsa
6  --
7  -- Author: Luis Tarazona tarazonl@cs.man.ac.uk
8  -- v1.0 20/04/2007 -tarazonl
9  --
10 -- reduced nanoSpaTypes file for nanoMultiplier only
11
12 type signedByte is 8 signed bits
13 type HalfWord is 16 bits
14 type signedHalfWord is 16 signed bits
15 type Address is 32 bits
16 type Datapath is 32 bits
17 type signedDatapath is 32 signed bits
18
19 type Flags is record
20     V : bit;
21     C : bit;
22     Z : bit;
23     N : bit
24 end -- type Flags
25
26 -- multiplier types
27 type MulType is enumeration
28     MUL=0,    -- multiply (32-bit result)
29     MLA=1,    -- multiply-accumulate (32-bit result)
30     MUND2=2,  -- undefined code
31     MUND3=3,  -- undefined code
32     UMULL=4, -- unsigned multiply long
33     UMLAL=5, -- unsigned multiply-accumulate long
34     SMULL=6, -- signed multiply long
35     SMLAL=7  -- signed multiply-accumulate long
36 over 3 bits
37 constant length = sizeof Datapath
38 constant xlength = sizeof Datapath + 3
39 constant tbits = log (sizeof Datapath)
40 type cntType is tbits bits
41 type Datapath_1 is length+1 bits
42 type Datapath_2 is xlength bits
43 type Datapath_3 is xlength+1 bits
44
45 type sDatapath is length signed bits
46 type sDatapath_1 is length+1 signed bits
47 type sDatapath_2 is xlength signed bits
48 type sDatapath_3 is xlength+1 signed bits
```

nanoMultSupport.balsa 1

```
1  -- The University of Manchester
2  -- School of Computer Science
3  -- Advanced Processors Technology (APT) group
4  --
5  -- Radix-3 Booth's multiplier for nanoSpa/aviSpa processor in Balsa
6  --
7  -- Author: Luis Tarazona tarazonl@cs.man.ac.uk
8  -- v1.0 20/04/2007 -tarazonl
9  --
10 -- support modules for multiplier
11
12 import [balsa.types.basic]
13 import [nanoMulTypes]
14
15 procedure signAdj
16 (
17   input mType : MulType;
18   input a    : Datapath;
19   input b    : Datapath;
20   input c    : Datapath;
21   output aa : Datapath_2;
22   output ba : Datapath_3;
23   output ca : Datapath_2;
24   output mlength : bit;
25   output macc    : bit
26 ) is
27 begin
28     loop
29         mType,a,b,c ->! then
30             -- Handle signed/unsigned in a,b operands,
31             -- also add 0 to lsb of multiplier (b operand)
32             case mType of MUL,UMULL,UMLAL then
33             -- unsigned, always fill with zeroes
34                 aa <- (a as Datapath_2)
35              ||
36                 ba <- (#0b0[0..0] @ #b[0 .. length-1] as Datapath_3)
37             else  -- signed, extend sign
38                 aa <- (((a as sDatapath) as sDatapath_2) as Datapath_2)
39               ||
40                 ba <- (((#0b0[0..0] @ #b[0 .. length-1]
41                         as sDatapath_1) as sDatapath_3) as Datapath_3)
42             end -- case mCode
43             -- Handle accumulate.
44             -- `c' operand does not need sign extension, fill with zeroes
45           ||
46             ca <- (c as Datapath_2)
47           ||
48             mlength <- (#mType[2..2] as bit) -- long = 1 / short = 0
49           ||
50             macc    <- (#mType[0..0] as bit) -- acc = 1
51         end -- mType ->
52     end -- loop
53 end -- procedure signAdj
54
55 procedure doByPass(
56     input  bH        : bit;
57     input  bL        : bit;
58     input  bpH          : Datapath;
59     input  bpL          : Datapath;
60     input  bmZ          : bit;
61     input  bmN         : bit;
62     output mpH          : Datapath;
63     output mpL          : Datapath;
64     output mZ          : bit;
65     output mN         : bit
```

nanoMultSupport.balsa 2

```
66 ) is
67 begin
68     loop
69         bH, bL ->! then
70             if bL then
71                 mpL <- 0
72              ||
73                 mZ <- 0
74              ||
75                 mN <- 0
76              ||
77                 if bH then
78                     mpH <- 0
79                 end -- if bypassH
80             else
81                 bpL -> mpL
82              ||
83                 bmZ -> mZ
84              ||
85                 bmN -> mN
86              ||
87                 if bH then
88                     bpH -> mpH
89                 end -- if bypassH
90             end
91         end
92     end
93 end
94
95 -- bypasses multiplier if kill order is sent
96 procedure bypassMul(
97     input  bypass          : bit;
98     input  bypassH         : bit;
99     input  mulOpA          : Datapath;
100    input  mulOpB          : Datapath;
101    input  mulOpC          : Datapath;
102    input  mulType         : MulType;
103    output  mulOpAo        : Datapath;
104    output  mulOpBo        : Datapath;
105    output  mulOpCo        : Datapath;
106    output  mulTypeo       : MulType;
107    output  bH             : bit;
108    output  bL             : bit
109 ) is
110 begin
111     loop
112         bypass, bypassH, mulType ->! then
113             mulOpA, mulOpB ->! then
114                 if bypass then
115                     case mulType of MLA, UMLAL, SMLAL  then -- accumulate
116                         mulOpC ->! then
117                             continue
118                         end
119                     else
120                         continue
121                     end
122                 else
123                     mulOpAo <- mulOpA
124                  ||
125                     mulOpBo <- mulOpB
126                  ||
127                     mulTypeo <- mulType
128                  ||
129                     case mulType of MLA, UMLAL, SMLAL  then -- accumulate
130                         mulOpC ->! then
```

nanoMultSupport.balsa 3

```
131                             mulOpCo <- mulOpC
132                         end
133                     else
134                         mulOpCo <- 0
135                     end
136                 end -- if bypass
137             end --  mulOpA mulOpB ->!
138          ||
139             bL <- bypass
140          ||
141             bH <- bypassH
142         end -- bypass, bypassH, mulType ->!
143     end --loop
144 end -- procedure bypassMul
145
146
147 -- carry save adder
148
149 procedure CSAdder
150 ( parameter DataType : type;
151   input     a : DataType;
152   input     b : DataType;
153   input     cs : DataType;
154   output    cout: DataType;
155   output    s : DataType
156 ) is
157 local
158  begin
159     loop
160         a,b,cs ->! then
161             s  <- a xor b xor cs
162           ||
163             cout <- (a and b) or (cs and a) or (cs and b)
164         end
165     end
166 end -- procedure CSAdder
167
168 -- carry propagate adder
169
170 procedure fullCPadder
171 ( parameter DataType : type;
172   input a   : DataType;
173   input b   : DataType;
174   input c0  : bit;
175   output s  : DataType;
176   output cN : bit
177 ) is
178 local
179   constant DTLength = sizeof DataType
180   type eDataType  is DTLength + 1 bits
181   type eeDataType is DTLength + 2 bits
182   channel ea, eb : eDataType
183   channel es : eeDataType
184
185 begin
186     loop
187         a,b,c0 ->! then
188         ea <- (#c0[0..0] @ #a[0..DTLength-1] as eDataType)
189       ||
190         eb <- (#c0[0..0] @ #b[0..DTLength-1] as eDataType)
191         end
192       ||
193         ea,eb ->! then
194             es <- (ea + eb as eeDataType)
195         end -- ea,eb ->!
```

```
196       ||
197         es ->! then
198             s <- (#es[1..DTLength] as DataType)
199           ||
200             cN<- (#es[DTLength+1 .. DTLength+1] as bit)
201         end -- es ->!
202     end --loop
203 end -- procedure fullCPadder
204
205 -- shift register that controls iteration
206 procedure mControl
207 ( parameter cLength : cardinal;
208   input  load : bit;
209   output done : bit
210 ) is
211
212 variable t   :  bit
213 variable c0  :  cLength bits
214 variable c1  :  cLength bits
215
216 begin
217     loop
218         load ->! then
219             t := load
220         end -- load ->
221       ;
222         if t then
223             c0 := (2^(cLength-1) - 1 as cLength bits)
224           ||
225             done <- 1
226         else
227             done  <- (#c0[0..0] as bit)
228           ||
229             c1    := (#c0[1..cLength-1] as cLength bits)
230           ;
231             c0 := c1
232         end --if t
233     end -- loop
234 end  -- procedure mControl
235
236 procedure mControl10 is mControl(10)
```

nanoMBoothR3rolled.balsa 1

```
1  -- The University of Manchester
2  -- School of Computer Science
3  -- Advanced Processors Technology (APT) group
4  --
5  -- Radix-3 Booth's multiplier for nanoSpa/aviSpa processor in Balsa
6  --
7  -- Author: Luis Tarazona tarazonl@cs.man.ac.uk
8  -- v1.0 20/04/2007 -tarazonl
9  --
10 --    Rolled Radix-3 Booth's algorithm (11 iteration cycles)
11
12 import [balsa.types.basic]
13 import [nanoMulTypes]
14
15 procedure nanoMBoothR3rolled
16 (
17   input cin      : Datapath_2;
18   input res      : Datapath_2;
19
20   input a        : Datapath_2;
21   input b        : Datapath_3;
22   input c        : Datapath_2;
23   input mlength  : bit;
24   input macc     : bit;
25
26   output load    : bit;
27   input  done    : bit;
28
29   output opA     : Datapath_2;
30   output opB     : Datapath_2;
31   output cs      : Datapath_2;
32
33   output raA     : Datapath;
34   output raB     : Datapath;
35   output rac0    : bit;
36   input  raS     : Datapath;
37   input  racN    : bit;
38
39   output pH      : Datapath;
40   output pL      : Datapath;
41   output z       : bit;
42   output n       : bit
43 ) is
44 local
45     channel sout     : Datapath_2
46     channel csout    : Datapath_2
47     channel c0       : bit
48
49     variable ctrl    : 4 bits
50     variable  vph    : Datapath
51     variable  vpl    : Datapath
52     variable va      : Datapath_2
53     variable v2a     : Datapath_2
54     variable v3a     : Datapath_2
55     variable v4a     : Datapath_2
56     variable nva     : Datapath_2
57     variable nv2a    : Datapath_2
58     variable nv3a    : Datapath_2
59     variable nv4a    : Datapath_2
60     variable crh     : Datapath_2
61     variable crl     : Datapath_3
62     variable rh      : Datapath_2
63     variable rl      : Datapath_3
64     variable rhp     : Datapath_2
65     variable crhp    : Datapath_2
```

nanoMBoothR3rolled.balsa 2

```
66      variable crlp   : Datapath_3
67      variable rlp    : Datapath_3
68      variable go     : 1 bits
69      variable vmlength : bit
70      variable vmacc    : bit
71      variable vZ       : bit
72      variable vN       : bit
73
74  begin
75      loop --main
76
77          a,b,c,mlength, macc ->! then
78              vmlength := mlength
79            ||
80              vmacc := macc
81            ||
82              va  := a
83            ||
84              v2a := (#0b0[0..0] @ #a[0 .. xlength-2] as Datapath_2)
85            ||
86              v4a :=  (#(0b00 as 2 bits)[0..1] @
87                       #a[0 .. xlength-3] as Datapath_2)
88              -- calculate 3A= 2A + A
89            ||
90              raA <- (#a[1 .. length] as Datapath)  -- a without b0
91            ||
92              raB <- (a as Datapath) -- 2a without b0
93            ||
94              rac0<- 0
95            ||
96              raS,racN ->! then
97                   v3a := (#a[0..0] @#raS[0..length-1] @
98                           #racN[0..0] @ #a[length..length]  as Datapath_2)
99              end
100           ||
101             rlp := b
102           ||
103             rhp := c
104           ||
105             ctrl:= (#b[0..3] as 4 bits)
106           ||
107             crhp := (0b0 as Datapath_2)
108           ||
109             crlp := (0b0 as Datapath_3)
110       end -- a,b,c,mlength ->
111     ;
112           nva := not va
113         ||
114           nv2a := not v2a
115         ||
116           nv3a := not v3a
117         ||
118           nv4a := not v4a
119     ||
120       load <- 1
121     ;
122       loop --iterate
123           opA <- rhp
124         ||
125           cs  <- crhp
126         ||
127           res -> sout
128         ||
129           cin -> csout
130         ||
```

nanoMBoothR3rolled.balsa 3

```
131             c0 <- (#ctrl[3..3] as bit)
132           ||
133             case ctrl of
134             0b0001,0b0010 then --sout <- (rhp + va as Datapath_2)
135                 opB <- va
136             | 0b0011,0b0100 then --  sout <- (rhp + v2a as Datapath_2)
137                 opB <- v2a
138             | 0b101,0b0110 then --  sout <- (rhp +  v3a  as Datapath_2)
139                 opB <- v3a
140             | 0b0111 then --  sout <- (rhp + v4a as Datapath_2)
141                 opB <- v4a
142             | 0b1000 then --  sout <- (rhp + nv4a + 1 as Datapath_2)
143                 opB <- nv4a
144             | 0b1001,0b1010 then -- sout <- (rhp + nv3a + 1 as Datapath_2)
145                 opB <- nv3a
146             | 0b1011,0b1100 then -- sout <- (rhp + nv2a + 1 as Datapath_2)
147                 opB <- nv2a
148             | 0b1101,0b1110 then -- sout <- (rhp + nva + 1 as Datapath_2)
149                 opB <- nva
150             else
151                 opB <- (((ctrl as 4 signed bits)
152                           as sDatapath_2) as Datapath_2)
153             end -- case 2
154             -- shifter:
155           ||
156             sout,csout,c0 ->! then
157                 --shift 2 times (rh arithmetic, but rl logic)
158                 crh := csout
159               ||
160                 crl := (#crlp[3..xlength-1] @
161                          #c0[0..0] @ #csout[0..1] as Datapath_3)
162               ||
163                 rh := (((#sout[3..xlength-1] as xlength-3 signed bits)
164                           as sDatapath_2) as Datapath_2)
165               ||
166                 rl := (#rlp[3..xlength-1] @ #sout[0..2] as Datapath_3)
167             end -- sout ->
168           ||
169             done ->! then
170                go := done
171             end
172         while go then-- while counter /= (length/2 + 1 as tbits bits)
173             crhp := (#crh[2..xlength-1] @ #crh[xlength-1..xlength-1] @
174                      #crh[xlength-1..xlength-1] as Datapath_2)
175           ||
176             crlp := crl
177           ||
178             rhp  := rh
179           ||
180             rlp  := rl
181           ||
182             ctrl := (#rl[0..3] as 4 bits)
183           ||load <- 0
184         end --loop iterate
185       ; -- calculate pL
186         raA <- (#rl[2..length+1] as Datapath)
187       ||
188         raB <- (#crl[2..length+1] as Datapath)
189       ||
190         rac0 <- 0
191       ||
192         raS,racN ->! then
193             vpl:= raS
194           ||
195             go := racN  -- save carry for pH
```

```
196           ||
197             vN := (#raS[31] as bit)
198           ||
199             vZ := (raS = 0 as bit)
200         end
201       ;
202         if vmlength then -- calculate pH and produce two results + flags
203             raA <- (#rl[length + 2..length+2] @
204                     #rh[0..length-2] as Datapath)
205           ||
206             raB <- (#crh[1..length] as Datapath)
207           ||
208             rac0 <- go
209           ||
210             raS,racN ->! then
211                 vph := raS --(#raS[0..length-1] as Datapath)
212             end -- raS, raN ->!
213           ;
214             pH <- vph
215           ||
216             pL <- vpl
217           ||
218             if vmacc then
219                 z <- vZ
220             else
221                 z  <- (vph = 0 as bit) and vZ
222             end
223           ||
224             n  <- (#vph[31]as bit)
225         else -- only produce pL & flags
226             pL <- vpl
227           ||
228             z   <- vZ
229           ||
230             n   <- vN
231         end -- if vmlength
232     end --loop main
233 end
```

Appendix F

Optimised sliced-channel wormhole router Balsa description

The following pages show the Balsa source files for this design.

router.balsa 1

```
1  -- The University of Manchester
2  -- School of Computer Science
3  -- Advanced Processors Technology (APT) group
4  --
5  -- Asynchronous Wormhole router
6  -- Author: Luis Tarazona
7  -- (based on original description by Wei Song songw@cs.man.ac.uk)
8  -- 10/09/2009
9  -- Router top level
10
11 import [balsa.types.basic]
12 import [arbiter]
13 import [input_buf]
14 import [crossbar]
15
16 procedure router (
17     array 20 of input d_in : 9 bits;
18     array 20 of output d_out : 9 bits
19 ) is
20
21 array 64 of channel data_m : 9 bits
22 array 16 of sync req
23 array 3 of channel cfg_lwe : 2 bits
24 array 2 of channel cfg_sn : 1 bits
25 begin
26         input_buf_south(d_in[0..3], req[0..3], data_m[0..15])
27     ||  input_buf_west(d_in[4..7], req[4..5], data_m[16..23])
28     ||  input_buf_north(d_in[8..11], req[6..9], data_m[24..39])
29     ||  input_buf_east(d_in[12..15], req[10..11], data_m[40..47])
30     ||  input_buf_loc(d_in[16..19], req[12..15], data_m[48..63])
31     ||  arbiter_sn({req[6], req[12]}, cfg_sn[0])
32     ||  arbiter_lwe({req[0], req[7], req[10], req[13]}, cfg_lwe[0])
33     ||  arbiter_sn({req[1], req[14]}, cfg_sn[1])
34     ||  arbiter_lwe({req[2], req[4], req[8], req[15]}, cfg_lwe[1])
35     ||  arbiter_lwe({req[3], req[5], req[9], req[11]}, cfg_lwe[2])
36     ||  crossbar(data_m, cfg_lwe, cfg_sn, d_out)
37 end
38
```

arbiter.balsa 1

```
1  -- The University of Manchester
2  -- School of Computer Science
3  -- Advanced Processors Technology (APT) group
4  --
5  -- Asynchronous Wormhole router
6  -- Author: Luis Tarazona
7  -- (based on original description by Wei Song songw@cs.man.ac.uk)
8  -- 10/09/2009
9  -- Arbiters
10
11 import [balsa.types.basic]
12
13 procedure sub_arb_low (
14     array 2 of sync req;
15     output winner : 1 bits
16 ) is
17 begin
18     loop
19         arbitrate req[0] then winner <- 0
20         |         req[1] then winner <- 1
21     end
22 end
23 end
24
25 procedure sub_arb (
26     array 2 of input req : 1 bits;
27     output winner : 2 bits
28 ) is
29 constant one = (1 as 1 bits)
30 begin
31     loop
32         arbitrate req[0] then winner <- (req[0] as 2 bits)
33         |         req[1] then winner <- ((#(req[1]) @ #one) as 2 bits)
34         end
35     end
36 end
37
38 procedure sub_arb_sync (
39     parameter Wi : byte;
40     parameter Wo : byte;
41     parameter Ds : byte;     -- the data when sync is selected
42     input in0 : Wi bits;
43     sync in1;
44     output cfg : Wo bits
45     ) is
46 begin
47     loop
48         arbitrate in0 then cfg <- (in0 as Wo bits)
49         |         in1 then cfg <- (Ds as Wo bits)
50         end
51     end
52 end
53
54 procedure arbiter_lwe (
55     array 4 of sync req;
56     output cfg : 2 bits
57 ) is
58
59 array 2 of channel arb_dir_sub : 1 bits
60
61 begin
62         sub_arb_low(req[0..1], arb_dir_sub[0])
63     ||  sub_arb_low(req[2..3], arb_dir_sub[1])
64     ||  sub_arb(arb_dir_sub, cfg)
65 end
```

input_bufv2.balsa 1

```
1  -- The University of Manchester
2  -- School of Computer Science
3  -- Advanced Processors Technology (APT) group
4  --
5  -- Asynchronous Wormhole router
6  -- Author: Luis Tarazona
7  -- (based on original description by Wei Song songw@cs.man.ac.uk)
8  -- 10/09/2009
9  -- Input buffers
10
11 import [balsa.types.basic]
12
13 procedure input_buf_south (
14     array 4 of input data_in : 9 bits;
15     array 4 of sync req;
16     array 16 of output data_out : 9 bits
17 ) is
18     variable buf : array 4 of 9 bits
19     constant addrx = (2 as 4 bits)
20     constant addry = (2 as 4 bits)
21
22     procedure ibuf_demux (
23         parameter X : byte;
24         input data_in : 9 bits;
25         input steer   : 3 bits;
26         array 4 of output data_out : 9 bits
27     ) is
28     variable steerV : 3 bits
29     begin
30         loop
31             steer -> steerV;
32             loop
33                 data_in -> buf[X];
34                 case steerV of
35                 0b1xx then
36                     data_out[0] <- buf[X]
37                 | 0b01x then
38                     data_out[1] <- buf[X]
39                 | 0b001 then
40                     data_out[2] <- buf[X]
41                 else
42                     data_out[3] <- buf[X]
43                 end
44             while (#(buf[X])[8] as 1 bits) /= (1 as 1 bits)
45             end
46         end
47     end
48
49     array 4 of channel steer : 3 bits
50     channel n,e,w : bit
51     channel data_in0 : 9 bits
52     variable isTail : bit
53
54 begin
55     loop
56         data_in[0] ->! then
57             n <- (#(data_in[0])[4..7] as 4 bits) < addrx
58           || e <- (#(data_in[0])[0..3] as 4 bits) > addry
59           || w <- (#(data_in[0])[0..3] as 4 bits) < addry
60           || data_in0 <- data_in[0]
61         end ;
62         loop
63             data_in[0] ->! then
64                 data_in0 <- data_in[0]
65              || isTail := #(data_in[0])[8]
```

input_bufv2.balsa 2

```
66              end
67          while not isTail
68          end
69      end
70   ||
71      loop
72          n,e,w ->! then
73              for || i in 0..3 then
74                  steer[i] <- (#w @ #e @ #n as 3 bits)
75              end
76           || case (#w @ #e @ #n as 3 bits) of
77               0b1xx then sync req[1]
78              |0b01x then sync req[2]
79              |0b001 then sync req[0]
80              else
81                  sync req[3]
82              end
83          end
84      end
85   ||
86      for || i in 1..3 then
87          ibuf_demux(i, data_in[i],steer[i],
88                        {data_out[i+4], data_out[i+8],
89                         data_out[i],data_out[i+12]})
90      end
91   ||
92      ibuf_demux(0, data_in0, steer[0],
93                    {data_out[4], data_out[8],
94                     data_out[0],data_out[12]})
95  end
96
97  procedure input_buf_west (
98      array 4 of input data_in : 9 bits;
99      array 2 of sync req;
100     array 8 of output data_out : 9 bits
101 ) is
102     variable buf : array 4 of 9 bits
103     constant addrx = (2 as 4 bits)
104     constant addry = (2 as 4 bits)
105
106     procedure ibuf_demux (
107         parameter X : byte;
108         input data_in : 9 bits;
109         input steer   : 1 bits;
110         array 2 of output data_out : 9 bits
111     ) is
112     variable steerV : 1 bits
113     begin
114         loop
115             steer -> steerV;
116             loop
117                 data_in -> buf[X];
118                 case steerV of
119                 0b1 then
120                     data_out[0] <- buf[X]
121                 else
122                     data_out[1] <- buf[X]
123                 end
124             while (#(buf[X])[8] as 1 bits) /= (1 as 1 bits)
125             end
126         end
127     end
128
129     array 4 of channel steer : bit
130     channel e : bit
```

input_bufv2.balsa 3

```
131     channel data_in0 : 9 bits
132     variable isTail : bit
133
134 begin
135     loop
136         data_in[0] ->! then
137             e <- (#(data_in[0])[0..3] as 4 bits) > addry
138          || data_in0 <- data_in[0]
139         end ;
140         loop
141             data_in[0] ->! then
142                 data_in0 <- data_in[0]
143              || isTail := #(data_in[0])[8]
144             end
145         while not isTail
146         end
147     end
148  ||
149     loop
150         e ->! then
151             for || i in 0..3 then
152                 steer[i] <- e
153             end
154          || case e of
155              0b1 then sync req[0]
156             else
157                 sync req[1]
158             end
159         end
160     end
161  ||
162     for || i in 1..3 then
163         ibuf_demux(i,data_in[i],steer[i], {data_out[i], data_out[i+4]})
164     end
165  ||
166     ibuf_demux(0, data_in0, steer[0], {data_out[0], data_out[4]})
167 end
168
169 procedure input_buf_north (
170     array 4 of input data_in : 9 bits;
171     array 4 of sync req;
172     array 16 of output data_out : 9 bits
173 ) is
174     variable buf : array 4 of 9 bits
175     constant addrx = (2 as 4 bits)
176     constant addry = (2 as 4 bits)
177
178     procedure ibuf_demux (
179         parameter X : byte;
180         input data_in : 9 bits;
181         input steer   : 3 bits;
182         array 4 of output data_out : 9 bits
183     ) is
184     variable steerV : 3 bits
185     begin
186         loop
187             steer -> steerV;
188             loop
189                 data_in -> buf[X];
190                 case steerV of
191                 0b1xx then
192                     data_out[0] <- buf[X]
193                 | 0b01x then
194                     data_out[1] <- buf[X]
195                 | 0b001 then
```

input_bufv2.balsa 4

```
196                     data_out[2] <- buf[X]
197                 else
198                     data_out[3] <- buf[X]
199                 end
200             while (#(buf[X])[8] as 1 bits) /= (1 as 1 bits)
201             end
202         end
203     end
204
205     array 4 of channel steer : 3 bits
206     channel s,e,w : bit
207     channel data_in0 : 9 bits
208     variable isTail : bit
209
210 begin
211     loop
212         data_in[0] ->! then
213             s <- (#(data_in[0])[4..7] as 4 bits) > addrx
214          || e <- (#(data_in[0])[0..3] as 4 bits) > addry
215          || w <- (#(data_in[0])[0..3] as 4 bits) < addry
216          || data_in0 <- data_in[0]
217         end ;
218         loop
219             data_in[0] ->! then
220                 data_in0 <- data_in[0]
221              || isTail := #(data_in[0])[8]
222             end
223         while not isTail
224         end
225     end
226  ||
227     loop
228         s,e,w ->! then
229             for || i in 0..3 then
230                 steer[i] <- (#w @ #e @ #s as 3 bits)
231             end
232          || case (#w @ #e @ #s as 3 bits) of
233              0b1xx then sync req[0]
234             |0b01x then sync req[2]
235             |0b001 then sync req[1]
236             else
237                 sync req[3]
238             end
239         end
240     end
241  ||
242     for || i in 1..3 then
243         ibuf_demux(i,data_in[i],steer[i], {data_out[i], data_out[i+8],
    data_out[i+4],data_out[i+12]})
244     end
245  ||
246     ibuf_demux(0, data_in0, steer[0], {data_out[0], data_out[8],
    data_out[4],data_out[12]})
247 end
248
249 procedure input_buf_east (
250     array 4 of input data_in : 9 bits;
251     array 2 of sync req;
252     array 8 of output data_out : 9 bits
253 ) is
254     variable buf : array 4 of 9 bits
255     constant addrx = (2 as 4 bits)
256     constant addry = (2 as 4 bits)
257
258     procedure ibuf_demux (
```

input_bufv2.balsa 5

```
259         parameter X : byte;
260         input data_in : 9 bits;
261         input steer   : 1 bits;
262         array 2 of output data_out : 9 bits
263     ) is
264     variable steerV : 1 bits
265     begin
266         loop
267             steer -> steerV;
268             loop
269                 data_in -> buf[X];
270                 case steerV of
271                 0b1 then
272                     data_out[0] <- buf[X]
273                 else
274                     data_out[1] <- buf[X]
275                 end
276             while (#(buf[X])[8] as 1 bits) /= (1 as 1 bits)
277             end
278         end
279     end
280
281     array 4 of channel steer : bit
282     channel w : bit
283     channel data_in0 : 9 bits
284     variable isTail : bit
285
286 begin
287     loop
288         data_in[0] ->! then
289             w <- (#(data_in[0])[0..3] as 4 bits) < addry
290          || data_in0 <- data_in[0]
291         end ;
292         loop
293             data_in[0] ->! then
294                 data_in0 <- data_in[0]
295              || isTail := #(data_in[0])[8]
296             end
297         while not isTail
298         end
299     end
300  ||
301     loop
302         w ->! then
303             for || i in 0..3 then
304                 steer[i] <- w
305             end
306          || case w of
307              0b1 then sync req[0]
308             else
309                 sync req[1]
310             end
311         end
312     end
313  ||
314     for || i in 1..3 then
315         ibuf_demux(i,data_in[i],steer[i], {data_out[i], data_out[i+4]})
316     end
317  ||
318     ibuf_demux(0, data_in0, steer[0], {data_out[0], data_out[4]})
319 end
320
321 procedure input_buf_loc (
322     array 4 of input data_in : 9 bits;
323     array 4 of sync req;
```

input_bufv2.balsa 6

```
324     array 16 of output data_out : 9 bits
325 ) is
326
327     variable buf : array 4 of 9 bits
328     constant addrx = (2 as 4 bits)
329     constant addry = (2 as 4 bits)
330
331     procedure ibuf_demux (
332         parameter X : byte;
333         input data_in : 9 bits;
334         input steer   : 3 bits;
335         array 4 of output data_out : 9 bits
336     ) is
337     variable steerV : 3 bits
338     begin
339         loop
340             steer -> steerV;
341             loop
342                 data_in -> buf[X];
343                 case steerV of
344                 0b1xx then
345                     data_out[0] <- buf[X]
346                 | 0b01x then
347                     data_out[1] <- buf[X]
348                 | 0b001 then
349                     data_out[2] <- buf[X]
350                 else
351                     data_out[3] <- buf[X]
352                 end
353             while (#(buf[X])[8] as 1 bits) /= (1 as 1 bits)
354             end
355         end
356     end
357
358     array 4 of channel steer : 3 bits
359     channel s,n,e : bit
360     channel data_in0 : 9 bits
361     variable isTail : bit
362
363 begin
364     loop
365         data_in[0] ->! then
366             s <- (#(data_in[0])[4..7] as 4 bits) > addrx
367          || n <- (#(data_in[0])[4..7] as 4 bits) < addrx
368          || e <- (#(data_in[0])[0..3] as 4 bits) > addry
369          || data_in0 <- data_in[0]
370         end ;
371         loop
372             data_in[0] ->! then
373                 data_in0 <- data_in[0]
374              || isTail := #(data_in[0])[8]
375             end
376         while not isTail
377         end
378     end
379  ||
380     loop
381         s,n,e ->! then
382             for || i in 0..3 then
383                 steer[i] <- (#e @ #n @ #s as 3 bits)
384             end
385          || case (#e @ #n @ #s as 3 bits) of
386              0b1xx then sync req[0]
387             |0b01x then sync req[2]
388             |0b001 then sync req[3]
```

input_bufv2.balsa 7

```
389             else
390                 sync req[1]
391             end
392         end
393     end
394  ||
395     for || i in 1..3 then
396         ibuf_demux(i, data_in[i],steer[i],
397                       {data_out[i], data_out[i+8],
398                        data_out[i+12],data_out[i+4]})
399     end
400  ||
401     ibuf_demux(0, data_in0, steer[0],
402                   {data_out[0], data_out[8], data_out[12],data_out[4]})
403 end
```

crossbarv2.balsa 1

```
1  -- The University of Manchester
2  -- School of Computer Science
3  -- Advanced Processors Technology (APT) group
4  --
5  -- Asynchronous Wormhole router
6  -- Author: Luis Tarazona
7  -- (based on original description by Wei Song songw@cs.man.ac.uk)
8  -- 10/09/2009
9  -- Crossbars & output buffers
10
11 import [balsa.types.basic]
12
13 procedure obuf_mux2 (
14     array 2 of input data_in : 9 bits;
15     array 2 of input tail : bit;
16     input steer   :  bit;
17     output data_out : 9 bits
18 ) is
19 variable steerV : bit
20 variable buf : 9 bits
21 variable isTail : array 0..1 of bit
22 begin
23     loop
24         steer -> steerV;
25         case steerV of
26          for i in 0..1 then
27             loop
28                 tail[i] -> isTail [i]
29              || data_in[i] -> data_out
30             while not isTail[i] end
31         end
32     end
33 end
34
35 procedure obuf_mux4 (
36     array 4 of input data_in : 9 bits;
37     array 4 of input tail : bit;
38     input steer   : 2 bits;
39     output data_out : 9 bits
40 ) is
41 variable steerV : 2 bits
42 variable buf : 9 bits
43 variable isTail : array 0..3 of bit
44 begin
45     loop
46         steer -> steerV;
47         case steerV of
48          for i in 0..3 then
49             loop
50                 tail[i] -> isTail [i]
51              || data_in[i] -> data_out
52             while not isTail[i] end
53         end
54     end
55 end
56
57 procedure outbuffer (
58     input data_in : 9 bits;
59     output tail : bit;
60     output data_out : 9 bits
61 ) is
62     variable buf : 9 bits
63 begin
64     loop
65         data_in -> buf;
```

crossbarv2.balsa 2

```
66          data_out <- buf || tail <- (#buf[8] as bit)
67      end
68  end
69
70  procedure sub_crossbar_lwe (
71      array 16 of input data_in : 9 bits;
72      input cfg : 2 bits;
73      array 4 of output data_out : 9 bits
74  ) is
75      -- variable cfg_m : 2 bits
76      array 4 of channel cfg_m : 2 bits
77      array 16 of channel tail : bit
78      array 16 of channel bdata_in : 9 bits
79  begin
80      loop
81          cfg ->! then
82              for || i in 0..3 then
83                  cfg_m[i] <- cfg
84              end
85          end
86      end
87   || for || i in 0..3 then
88          obuf_mux4(
89              { bdata_in[i], bdata_in[i+4], bdata_in[i+8], bdata_in[i+12] },
90              { tail[i], tail[i+4], tail[i+8], tail[i+12]},
91              cfg_m[i],
92              data_out[i]
93          )
94      end
95   || for || i in 0..15 then
96          outbuffer(data_in[i], tail[i], bdata_in[i])
97      end
98  end
99
100 procedure sub_crossbar_sn (
101     array 8 of input data_in : 9 bits;
102     input cfg : bit;
103     array 4 of output data_out : 9 bits
104 ) is
105     -- variable cfg_m :  bit
106     array 4 of channel cfg_m : bit
107     array 8 of channel tail : bit
108     array 8 of channel bdata_in : 9 bits
109 begin
110     loop
111         cfg ->! then
112             for || i in 0..3 then
113                 cfg_m[i] <- cfg
114             end
115         end
116     end
117  || for || i in 0..3 then
118         obuf_mux2(
119             { bdata_in[i], bdata_in[i+4]},
120             { tail[i], tail[i+4]},
121             cfg_m[i],
122             data_out[i]
123         )
124     end
125  || for || i in 0..7 then
126         outbuffer(data_in[i], tail[i], bdata_in[i])
127     end
128 end
129
130 procedure crossbar (
```

```
131     array 64 of input data_in : 9 bits;
132     array 3 of input cfg_lwe : 2 bits;
133     array 2 of input cfg_sn : 1 bits;
134     array 20 of output data_out : 9 bits
135     ) is
136
137 begin
138         sub_crossbar_sn(data_in[24..27]
139                         @ data_in[48..51], cfg_sn[0], data_out[0..3])
140     ||  sub_crossbar_lwe(data_in[0..3] @ data_in[28..31]
141                          @ data_in[40..43] @ data_in[52..55],
142                            cfg_lwe[0], data_out[4..7])
143     ||  sub_crossbar_sn(data_in[4..7]
144                         @ data_in[56..59], cfg_sn[1], data_out[8..11])
145     ||  sub_crossbar_lwe(data_in[8..11] @ data_in[16..19]
146                          @ data_in[32..35] @ data_in[60..63],
147                            cfg_lwe[1], data_out[12..15])
148     ||  sub_crossbar_lwe(data_in[12..15] @ data_in[20..23]
149                          @ data_in[36..39] @ data_in[44..47],
150                            cfg_lwe[2], data_out[16..19])
151 end
```

Appendix G

Optimised nanoSpa forwarding unit Balsa description

The following pages show the Balsa source files for this design.

nanoForwadUnit.balsa 1

```
1  -- The University of Manchester
2  -- School of Computer Science
3  -- Advanced Processors Technology (APT) group
4  --
5  -- Forwarding unit fo the nanoSpa processor
6  -- NOTE : requires substitution of `;' by unfolded ';' in the
7  --        [Lookup ; Allocate] & [Forward ; Arrival ] groups
8  --
9  -- Author: Luis Tarazona
10 --
11 -- 24/01/2009
12 --
13
14 import [balsa.types.basic]
15 import [nanoSpaTypes]
16
17 procedure nanoForwardUnit
18 (
19   -- Allocation pointers
20   input allocPtr1 : allocPtrType;
21   input allocPtr2 : allocPtrType;
22   input arrPtr1  : WROBSIZE bits;
23   input arrPtr2 : WROBSIZE bits;
24   -- allocatio/arrival control
25   array 2 of input doAlloc   : bit;
26   array 2 of input doArrival : bit;
27   array 2 of input invalidIn : bit;
28   -- results from Execute
29   input wrdata0  : Datapath;
30   input wrdata1  : Datapath;
31   -- destination
32   array 2 of input wraddr  : RegSpec;
33   -- lookup interface
34   array READPORTS of input readIn : bit;
35   array READPORTS of input raddr  : RegSpec;
36 -- register read interface
37   array READPORTS of output readReg  : bit;
38 -- forward interface
39   array READPORTS of output fwfound  : bit;
40   array READPORTS of output fwdata : Datapath;
41 -- writeback interface
42   output wbaddr  : RegSpec;
43   output wbdata  : Datapath
44 ) is
45     -- the buffer cells
46     -- the buffer data structure
47     variable bvaddr   : array ROBSIZE of RegSpecExt
48     variable bdata    : array ROBSIZE of Datapath
49     variable bpos     : array ROBSIZE of bit
50     -- extended reg addresses for lookup
51     array READPORTS of channel addr : RegSpecExt
52     -- lookup-forward i/f
53     array READPORTS of channel posMask : 4 bits
54     array READPORTS of channel foundMask : 4 bits
55     --
56     -- steerAlloc - mux allocCells i/f
57     array ROBSIZE of channel  age1   : bit
58     array ROBSIZE of channel  aAddr1 : RegSpec
59     -- steerAllocX - mux allocCells i/f
60     array ROBSIZE of channel  age2   : bit
61     array ROBSIZE of channel  aAddr2 : RegSpec
62     array ROBSIZE of channel  invalid2 : bit
63     --
64     -- mux allocCells - allocCells i/f
65     array ROBSIZE of channel  ageM   : bit
```

```
66      array ROBSIZE of channel  aAddrM : RegSpec
67      array ROBSIZE of channel  invalidM : bit
68      --
69      --- mux arriveCells - arriveCells i/f
70      array ROBSIZE of channel  wbdataM   : Datapath
71      -- arriveCells network i/f
72      array ROBSIZE+1 of channel Tin   : bit
73      array ROBSIZE+1 of channel Tout  : bit
74      -- arriveCells - mux writeback i/f
75      array ROBSIZE of channel  wbdataC : Datapath
76      array ROBSIZE of channel  wbaddrC : RegSpec
77      --
78      -- writeback network
79      array ROBSIZE+1 of channel wbToken : bit
80      array ROBSIZE+1 of channel allocToken : bit
81      array ROBSIZE of channel allocT : bit
82      -- internal forward & register read control
83      array READPORTS of channel doFwd : bit
84      array READPORTS of channel read : bit
85
86  procedure forward (
87    input  doFwd     : bit;
88    input  foundMask : 4 bits;
89    input  posMask   : 4 bits;
90    output fwfound   : bit;
91    output readReg   : bit;
92    output fdata     : Datapath
93  ) is
94  begin
95      -- do the comparison and generate outputs
96      doFwd ->! then
97          if doFwd then
98          foundMask, posMask ->! then
99              case (#posMask @ #foundMask as 2*ROBSIZE bits) of
100             0b0000_xxxx then -- nothing found
101                 continue -- fdata <- 0
102             | 0bxxx1_0001, 0bxxx1_1110,
103               0bxx01_001x, 0bxx01_110x,
104               0bx001_01xx, 0bx001_10xx,
105               0b0001_0000, 0b0001_1111 then
106                 fdata <- bdata[0]
107             | 0bxx1x_001x, 0bxx1x_110x,
108               0bx01x_01xx, 0bx01x_10xx,
109               0b001x_0000, 0b001x_1111,
110               0b0010_0001, 0b0010_1110 then
111                 fdata <- bdata[1]
112             | 0bx1xx_01xx, 0bx1xx_10xx,
113               0b01xx_0000, 0b01xx_1111,
114               0b01x0_0001, 0b01x0_1110,
115               0b0100_001x, 0b0100_110x then
116                 fdata <- bdata[2]
117             | 0b1xxx_0000, 0b1xxx_1111,
118               0b1xx0_0001, 0b1xx0_1110,
119               0b1x00_001x, 0b1x00_110x,
120               0b1000_01xx, 0b1000_10xx then
121                 fdata <- bdata[3]
122             end -- case (#posMask @ #foundMask as 2*ROBSIZE bits)
123         ||
124             readReg <- (foundMask /= 0)
125         ||
126             fwfound <- (foundMask /= 0)
127         end -- foundMask, posMask ->! then
128         end --if doFwd
129     end -- doFwd ->!
130 end -- proceudure
```

nanoForwadUnit.balsa 3

```
131
132 -- Lookup unit, returns position (age) mask and found mask
133 procedure lookup(
134   input  read : bit;
135   input  addr : RegSpecExt;
136   output posMask : 4 bits;
137   output foundMask : 4 bits
138 ) is
139 begin
140     read ->! then
141         if read then
142             addr ->! then
143                 foundMask <- (maskArray {(bvaddr[0] = addr),
144                                          (bvaddr[1] = addr),
145                                          (bvaddr[2] = addr),
146                                          (bvaddr[3] = addr)
147                                        } as 4 bits
148                              ) ||
149                 posMask <- (maskArray { bpos[0], bpos[1], bpos[2],bpos[3] }
    as 4 bits)
150             end
151         end
152     end
153 end
154
155 -- Cell's allocation interface module
156 procedure allocCellT(
157   parameter N  : cardinal;
158   input  Tin : bit;
159   input  age1   : bit;
160   input  waddr : RegSpec;
161   input  invalid : bit;
162   output Tout  : bit;
163   output allocT : bit
164 ) is
165   variable vallocT : bit
166   constant INVALID_BIT = sizeof RegSpec
167 begin
168     Tin ->! then continue end ||
169     age1, waddr, invalid ->! then
170         bvaddr[N] := (#waddr @ #invalid as RegSpecExt) ||
171         bpos[N]   := age1
172     end;
173     allocT <- 1 ||
174     Tout <- 1
175 end
176
177 -- steers the allocation info to destination cell
178 procedure steerAlloc(
179   input doAlloc : bit;
180   input allocPtr1 : allocPtrType;
181   input addrIn : RegSpec;
182   input invalidIn : bit;
183   array ROBSIZE of output age1 : bit;
184   array ROBSIZE of output aAddr1 : RegSpec;
185   array ROBSIZE of output invalid : bit
186 ) is
187 begin
188     addrIn, invalidIn, allocPtr1, doAlloc ->! then
189         if doAlloc then
190             case (allocPtr1.index as WROBSIZE bits) of
191              0b00 then
192                 age1[0]   <- allocPtr1.cy ||
193                 aAddr1[0]  <- addrIn ||
194                 invalid[0] <- invalidIn
```

```
195             |0b01 then
196                 age1[1]   <- allocPtr1.cy ||
197                 aAddr1[1]  <- addrIn ||
198                 invalid[1] <- invalidIn
199             |0b10 then
200                 age1[2]   <- allocPtr1.cy ||
201                 aAddr1[2]  <- addrIn ||
202                 invalid[2] <- invalidIn
203             |0b11 then
204                 age1[3]   <- allocPtr1.cy ||
205                 aAddr1[3]  <- addrIn ||
206                 invalid[3] <- invalidIn
207             end
208         end -- if doAlloc
209     end -- ->!
210 end --procedure steerAlloc
211
212 -- steers the arrival information to cells
213 procedure steerArrival(
214   input doAlloc : bit;
215   input arrPtr1  : WROBSIZE bits;
216   input data     : Datapath;
217   --input fwDone  : bit;
218   array ROBSIZE of output wdata : Datapath
219 ) is
220 begin
221     doAlloc, arrPtr1 ->! then
222         if doAlloc then
223             case arrPtr1 of
224              0b00 then
225                 data -> wdata[0]
226             |0b01 then
227                 data -> wdata[1]
228             |0b10 then
229                 data -> wdata[2]
230             |0b11 then
231                 data -> wdata[3]
232             end
233         end -- if doAlloc
234     end -- ->!
235 --end --loop
236 end --procedure steerArrival
237
238 -- arrival interface to cells
239 procedure arrCellNAA2(
240   parameter N  : cardinal;
241   input  allocT  : bit;
242   input  Tin    : bit;
243   input  data   : Datapath;
244   output Tout   : bit;
245   output wdata : Datapath;
246   output waddr : RegSpec
247 ) is
248   constant INVALID_BIT = sizeof RegSpec
249 begin
250     loop
251         allocT ->! then
252             continue
253         end ||
254         data ->! then
255                 bdata[N] := data
256         end ;
257         Tin -> then -- no active eager (->!) allowed here !!!!!
258             if (not (#(bvaddr[N])[INVALID_BIT] as bit)) then
259                 wdata <- bdata[N] ||
```

nanoForwadUnit.balsa 5

```
260                 waddr <- (#(bvaddr[N])[0..INVALID_BIT-1] as RegSpec)
261             end
262         end;
263         Tout <- 1
264     end
265 end
266
267 -- allocation/arrival initiator
268 procedure arrCellH(
269   input  Tin    : bit;
270   output Tout   : bit
271 ) is
272 begin
273     Tout <- 1 ;
274     loop
275         Tin -> Tout
276     end
277 end
278
279 begin --nanoForwardUnit
280     -- initialise buffer
281     for || i in 0..ROBSIZE-1 then
282         bpos[i] := 0b0
283       ||
284         bvaddr[i] := 0b1_00000 -- invalidate all entries
285     end
286   ;
287     -- Lookup i/f
288     for ||! i in 0..READPORTS-1 then
289         loop
290             raddr[i] ->! then
291                 addr[i] <- (#(raddr[i]) @ #0b0 as RegSpecExt) -- invalid = 1
292             end
293         end ||
294         loop
295             readIn[i] ->! then
296                 read[i]  <- readIn[i] ||
297                 doFwd[i] <- readIn[i]
298             end
299         end
300     end ||
301     -- [Lookup ; Allocate] group
302     loop
303         for ||! i in 0..READPORTS-1 then
304             lookup( read[i],
305                     addr[i],
306                     posMask[i],
307                     foundMask[i]
308             )
309         end ; -- This `;' MUST be substituted by unfolded ';'
310         -- Allocate
311         steerAlloc( doAlloc[0],
312                     allocPtr1,
313                     wraddr[0],
314                     invalidIn[0],
315                     ageM,
316                     aAddrM,
317                     invalidM
318         ) ||!
319         steerAlloc( doAlloc[1],
320                     allocPtr2,
321                     wraddr[1],
322                     invalidIn[1],
323                     ageM,
324                     aAddrM,
```

```
325                     invalidM
326         )
327     end ||!
328     for ||! i in 0..ROBSIZE-1 then
329         loop
330             allocCell( i,
331                        allocToken[i],
332                        ageM[i],
333                        aAddrM[i],
334                        --wbaddr,
335                        invalidM[i],
336                        allocToken[i+1],
337                        allocT[i])
338         end
339     end ||!
340     -- [Forward ; Arrival] Group
341     loop
342         for ||! i in 0..READPORTS-1 then
343             forward ( doFwd[i],
344                       foundMask[i],
345                       posMask[i],
346                       fwfound[i],
347                       readReg[i],
348                       fwdata[i]
349             )
350         end ; -- This `;' MUST be substituted by unfolded ';
351         -- arrival
352         -- Steer arrival requests
353         steerArrival( doArrival[0],
354                       arrPtr1,
355                       wrdata0,
356                       wbdataM
357                 ) ||!
358         steerArrival( doArrival[1],
359                       arrPtr2,
360                       wrdata1,
361                       wbdataM
362                     )
363     end ||!
364     -- arrival cells
365     for ||! i in 0..ROBSIZE-1 then
366         arrCellNAA2( i,
367                      allocT[i],
368                      wbToken[i],
369                      wbdataM[i],
370                      wbToken[i+1],
371                      wbdata,
372                      wbaddr
373         )
374     end ||!
375     -- arrive cell initiators
376     arrCellH(wbToken[ROBSIZE], wbToken[0]) ||!
377     arrCellH(allocToken[ROBSIZE], allocToken[0])
378 end
```